A Molecular and Biochemical Study of Two Recombinant Mammalian Pyroglutamyl Peptidases Type 1.

Thesis submitted for the degree of
Doctor of Philosophy

by

Zelda Kilbane, B.Sc.

Supervised by

Dr. Brendan O'Connor

School of Biotechnology
Dublin City University
Ireland

September 2006

Declaration

I hereby certify that this material, which I now submit for assessment on the programme of study leading to the award of Doctor of Philosophy, is entirely my own work and has not been taken from the work of others save and to the extent that such work has been cited and acknowledged within the text of my work.

Signed: Zelda Kilbane

ID No.: 99097664

Date: 27/09/06

Dedications

First and foremost thanks are due to my supervisor Dr Brendan O'Connor for introducing me into the world of PAP1 For your enthusiasm, support, guidance and encouragement and for you many words of wisdom throughout this project – for this I will always be grateful

To Dr Paul-Roman Vaas for showing me the ropes during the first few months of this project – it helped enormously! For displaying the highest degree of expertise whilst demonstrating the many biochemical and molecular techniques – I learnt from the best!

To Dr John Gallagher for all his help both in DCU and Canada with the crystallisation study To Prof Lynne Howell in the Hospital of Sick Children, Toronto, Canada for allowing me to visit her lab for a month in 2005 To the Benson family who provided funding to enable me to go to Canada – thank you

To Pam – my lab partner of three years! Thanks for all your help, advice and company in the lab To Vinny – the newcomer! Thank you both for the entertainment and for making life in the lab so enjoyable

For financial support, I thank Prof Oliver Dolly

To Catherine, my great Monaghan friend who has journeyed from BT1 to intra to Ph D with me Thanks for the support, the sound advice and for never being too busy for a chat To all my friends in both DCU and Achill especially Eva, Helen and Trish

To Isobel, Clair and Conor – for all the laughs, chats and advice Thanks to Clair for use of the autoclave and to Isobel for the use of the scanner

To everyone in Dr Michael O'Connell's lab, especially Dr Paraic O Cuiv – thanks for never being too busy to answer my many many ceisteanna and for always explaining them in such depth

To my sister Ann, brothers Michael, Martin, James and Joe and my Uncle Sean for their constant support, advice and encouragement

My fiance Tom, my knight in shining armour! Thank you for always being there for me in both good times and bad For believing in me and for always showing an interest in everything I do You will always share my triumphs and disasters Thanks for the many nights you collected me from college For your outstanding support and constant encouragement I am truly grateful X

Finally, I wish to thank my parents Michael and Bridget for their constant support and faith in me throughout this project, it has not gone un-noticed They bore me, raised me, supported me and taught me To them I dedicate this thesis

Published Papers

Kılbane, Z , Vaas, P-R , O Cuiv, P and O'Connor, B (2006) *Cloning and heterlogous expression of bovine pyroglutamyl peptidase type-1 (PAP 1) in Escherichia coli purification, biochemical and kinetic characterisation* (Molecular and Cellular Biochemistry In press)

Vaas, P-R , Kılbane, Z , O'Connor, B and Ryan, T (2006) *Biochemical properties of purified human pyroglutamyl peptidase (type I), recombinantly expressed in E coli* (Ready For Submission)

Vaas, P-R , Kılbane, Z , O'Connor, B and Ryan, T (2006) *Structure-activity relationship studies of recombinant human pyroglutamyl peptidase (type I)* (Manuscript in preparation)

Vaas, P-R , Kılbane, Z , O'Connor, B and Ryan, T (2006) *Pyroglutamyl peptidase (types I & II) A review* (Manuscript in preparation)

Presentations

Kılbane, Z , O'Connor, B *Crystallisation, Mutagenesis and Analysis of Recombinant Human Pyroglutamyl Peptidase Type 1 (PAP1)*, Structural Biology and Biochemistry Department, Faculty of Medicine, University of Toronto, Canada June 2005

Kılbane, Z , O'Connor, B *Cloning and heterlogous expression of bovine pyroglutamyl peptidase type-1 (PAP1) in Escherichia coli purification, biochemical and kinetic characterisation* BMS Group 5 Seminar Series, Dublin City University, Ireland March 2006

Abbreviations

2-ME	2-mercaptoethanol
3D	Three-dimensional
A_{600}	Absorbance at 600 nm
AA	Amino acid (see Appendix D)
AMC	7-amino-4-methylcoumarin
BCA	Bicinchoninic acid
bp	Base-pair
BSA	Bovine serum albumin
cDNA	complementary DNA
cv	Column volume
Conc	Concentration
DFP	Diisopropyl fluorophosphate
dH_2O	Deionised water
DMSO	Dimethyl sulphoxide
DNA	Deoxyribonucleic acid
DTT	Dithiothreitol
EC	Enzyme commission
EDTA	Ethylenediaminetetra acetic acid
IC_{50}	Inhibitor conc resulting in 50% loss of enzymatic activity
IEF	Isoelectric focusing
IMAC	Immobilised metal affinity chromatography
IPTG	Isopropyl-β-$_D$-thiogalactopyranoside
K_{cat}	Turnover number
K_i	Dissociation constant
K_m	Michaelis constant
K_m^{app}	Apparent K_m
LB	Luria Bertani
LHRH	Luteinising hormone-releasing hormone
Log	Logarithm
MCS	Multiple cloning site
MOPS	3-(N-Morpholino)propanesulfonic acid
mRNA	Messenger RNA

NTA	Nitrilotriacetic acid
OD	Optical density
ORF	Open reading frame
PAGE	Polyacrylamide gel electrophoresis
PAP	Pyroglutamyl peptidase
p-CMB	*p*-chloromercurybenzoate
PCR	Polymerase Chain Reaction
pGlu	Pyroglutamic acid
PIPES	Piperazine-1,4-bis(2-ethanesulfonic acid)
PMSF	Phenylmethylsulphonyl fluoride
RBS	Ribosome binding site
RNA	Ribonucleic acid
rRNA	Ribosomal RNA
RT-PCR	Reverse transcription PCR
SDS	Sodium dodecyl sulphate
TEMED	N, N, N, N'-tetramethyl ethylenediamine
TRH	Thyrotropin-releasing hormone
Tris	Tris (hydroxymethyl) amino methane
UV	Ultraviolet light
v/v	Volume per volume
V_e	Elution volume
V_{max}	Maximal enzyme velocity
V_o	Void volume
w/v	Weight per volume
X-Gal	5-bromo-4-chloro-3-indolyl-β-$_D$-galactopyranoside
β-NA	β-naphthylamide

Units

Da	Dalton
g	Gram
g	g-force (relative centrifugal force - rcf)
hr	Hour
L	Litre
m	Metre
M	Molar
min	Minute
sec	Second
pH	Logarithm of reciprocal hydrogen-ion concentration
pI	Isoelectric point
°C	Degrees celcius
K	Kelvin
Å	Angstrom (1.0×10^{-10} metres)
rpm	Revolutions per minute
kb	Kilo base
V	Volts
A	Ampere
Hz	Hertz

Prefixes

k	kilo (10^{3})
c	centi (10^{-2})
m	milli (10^{-3})
μ	micro (10^{-6})
n	nano (10^{-9})
p	pico (10^{-12})

Table of Contents

List of Figures

Chapter 1

Chapter 2

Chapter 3

List of Tables

Chapter 2

Chapter 3

Chapter 4

Chapter 5

Abstract

Pyroglutamyl Peptidase I (PAP1, EC 3 4 19 3) hydrolytically cleaves pyroglutamic acid (pGlu) from the N-terminal of most pGlu-peptides In higher organisms Thyrothropin Releasing Hormone is a notable biologically active substrate of PAP1 The sequence of bovine PAP1 (Accession No XM_866409) was obtained from GenBank at NCBI (www ncbi nlm nih gov) Using suitable primers cDNA was synthesised using RNA extracted from bovine brain tissue Following expression of recombinant bovine PAP1 in Escherichia coli, the protein was purified using immobilised nickel affinity chromatography resulting in a yield of 2 6 mg of PAP1 per litre culture The Michaelis-Menten constant (K_m) for the fluorometric substrate pGlu-7-amino-4-methyl coumarin was determined as 59 μM and the turnover constant (K_{cat}) was determined as 3 5 s^{-1} Optimal enzyme activity was observed at pH range 9 0-9 5 and temperature range 30-37 °C A comparative study carried out with the human and bovine recombinant forms of the enzyme has highlighted interesting differences at amino acid, expression and enzymatic activity levels Site-directed mutagenesis of human PAP1 has revealed that an acidic residue is required for catalytic activity A series of active mutants were generated for human PAP1 using a random mutagenesis approach Biochemical and kinetic analysis of the mutant PAP1 enzymes has shown that methionine residues could potentially have an important role in PAP1 protein expression An attempt to crystallise human PAP1 was carried out However, this proved to be unsuccessful although it is believed that the C-terminal His-tag is causing interference and thus preventing proper crystallisation of human PAP1

CHAPTER ONE

Introduction

1 1 Pyroglutamyl Peptidase

Pyroglutamyl peptidase (PAP) hydrolytically removes pyroglutamic acid (pGlu residue) from the N-terminus of pGlu containing peptides To date, two classes of PAP have been characterised which include Type I (PAP1) and Type II (PAP2) PAP1 is a widely distributed cytosolic peptidase with a broad substrate specificity for pGlu-peptides and is found in a wide range of prokaryotic and eukaryotic organisms, including *Homo sapiens* and *Bos taurus* PAP1 is the subject of this study and is reviewed in detail in Section 1 3 PAP2 (see Section 1 4) is a membrane bound zinc-dependent metallopeptidase of high molecular mass with a narrow substrate specificity cleaving the pGlu-His bond of Thyrotropin-Releasing Hormone (TRH) or very closely related tripeptides A serum form of PAP2 also exists and has been termed Thyroliberinase (Bauer *et al*, 1981)

1 2 pGlu-Peptides

pGlu is a cyclised derivative of glutamic acid (see Figure 1 1) which was first described by Haitinger (1882) who reported that when glutamic acid was heated to 190°C it transformed into a different compound having lost a molecule of water There are numerous reports of the enzymatic synthesis of pGlu from glutamic acid and glutaminyl peptides (Orlowski and Meister, 1971) The enzymatic formation of pGlu suggests that this residue may possess important biological and physiological functions This theory is supported by the observation that many bioactive peptides (e g neuropeptides) exhibit an N-terminal pGlu residue (see Table 1 1)

Table 1 1 Peptides With an N-terminal pGlu Residue

Peptide[a]	Sequence
Thyrotropin-Releasing Hormone	pGlu-His-Pro-NH_2
Luteinizing Hormone-Releasing Hormone	pGlu-His-Trp-Ser-Tyr-
Bombesin	pGlu-Gln-Arg-Leu-Gly-
Neurotensin	pGlu-Leu-Tyr-Glu-Asn-
Gastrin	pGlu-Gly-Pro-Trp-Leu-
Eledoisin	pGlu-Pro-Ser-Lys-
Human Gastrin	pGlu-Gly-Pro-trp-Leu-
Anorexigenic Peptide	pGlu-His-Gly

[a] Further examples are given by Awade *et al* (1994)

Neuropeptides released into the autocrine, paracrine and endocrine systems allow intercellular communications to occur which are required to integrate and regulate the basic processes of life such as metabolic activity, cell differentiation and growth. Structurally, neuropeptides are usually short polypeptide chains with specific modifications to individual residues, such as an N-terminal pGlu residue. Such modifications can govern the distinctive biological activity of each individual neuropeptide. An N-terminal pGlu residue can determine highly specific biological properties of neuropeptides, such as their ability to recognize and bind to cell surfaces and their susceptibility to inactivation by neuropeptidases. For example, TRH binds to its receptor via specific interactions between the pGlu ring and certain residues of the trans-membrane TRH receptor (Perlman *et al.*, 1994a; 1994b). Slight structural substitution in the pGlu ring results in an almost complete loss of receptor binding ability. TRH is one of the most widely documented biologically active pGlu-peptides. It was initially defined as a hormone for its ability to stimulate the release of Thyrotropin Stimulating Hormone (TSH) from the anterior pituitary gland and prolactin from the pituitary gland (Jackson, 1982). It has features that also qualify it as a neurotransmitter and/or neuromodulator. These include its extrahypothalamic distribution in the brain , its localisation and release at the synaptic level as well as its attachment to high affinity receptors, which show remarkable degree of anatomical localisation. It exhibits specific effects on neuronal activity and stimulates a wide range of centrally mediated behavioural effects.

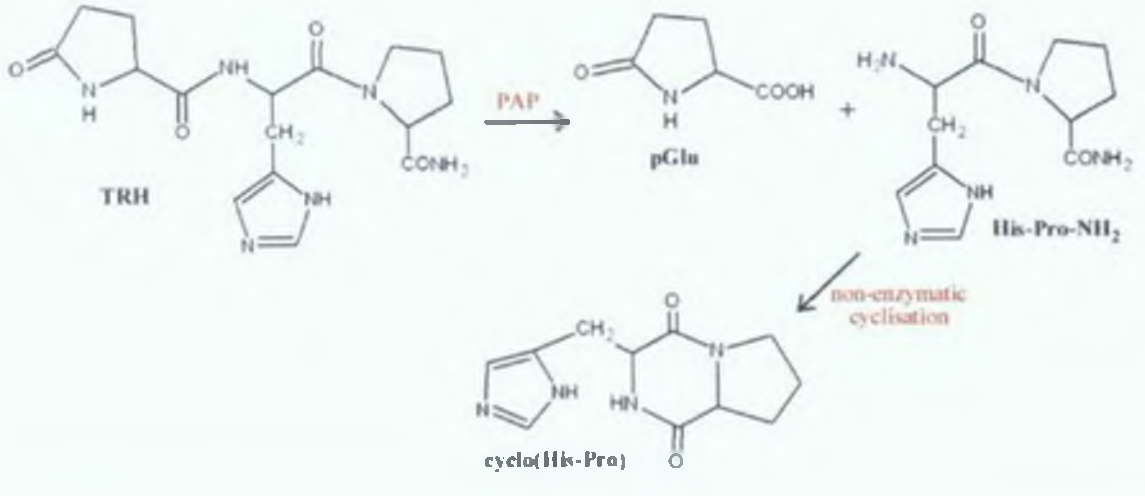

Figure 1.1 PAP Cleavage of TRH
The cleavage of TRH by PAP liberates pGlu. The remaining His-Pro-NH_2 undergoes non-enzymatic cyclisation to cyclo(His-Pro). Illustrated using ChemSketch (see Section 2.11).

The cleavage of TRH by PAP yields free pGlu and His-Pro-NH_2 (see Figure 1.1). The subsequent non-enzymatic cyclisation of His-Pro-NH_2 generates cyclo(His-Pro) which has been shown to posses pharmacological, endocrine, electrophysiological and cardiovascular activity of its own (Prasad, 1995). Functions of pGlu as a free acid are less clear. It has been observed in the tissues of patients with Hawkinsinuria disease, whilst elevated levels of free pGlu have been demonstrated in the plasma of patients suffering from Huntington's disease (Cummins and O'Connor, 1998). Russo *et al.*, 2002 reported that amyloid-β-peptides commencing with pGlu residues have a higher tendancy to form insoluble aggregates than other amyloid-β-peptides and as a result are likely to worsen the progression of Alzheimers Disease

1.3 PAP1

1.3.1 Discovery and Occurrence of PAP1

PAP1 activity was initially discovered in prokaryotic cells by Doolittle and Armentrout in 1968. The original aim of their work was to isolate an enzyme which would open pyrrolidone rings to aid amino acid sequencing work. A mircoorganism which was capable of utilizing free pGlu as a sole carbon and nitrogen source was isolated and identified as a strain of *Pseudomonas fluorescens*. A crude extract of *P. fluorescens* was tested and resulted in free pGlu and alanine being liberated from pGlu-alanine. This hydrolysis was due to novel enzyme PAP1 (*Pfu*PAP1).

PAP1 was subsequently documented in a wide range of prokaryotes including *Bacillus subtilis* (*Bsu*PAP1, Szewczuk and Mulczyk, 1969), *Klebsiella cloacae* (*Kcl*PAP1, Kwiatkowska *et al.*, 1974), *Streptococcus cremoris* (*Scr*PAP1, Exterkate, 1977), *Streptococcus faecium* (*Sfa*PAP1, Sullivan *et al.*, 1977), *Bacillus amyloliquefaciens* (*Bam*PAP1, Tsuru *et al.*, 1978), *Streptococcus pyogenes* (*Spy*PAP1, Cleuziat *et al.*, 1992), *Staphylococcus aureus* (*Sau*PAP1, Patti *et al.*, 1995), *Enterococcus faecalis* (*Efa*PAP1, Mineyama and Saito 1998), *Pyrococcus horikoshii* (*Pho*PAP1, Kawarabayasi *et al.*, 1998), *Pyrococcus furiosus* (*Pfu*PAP1, Tsunasawa *et al.*, 1998), *Thermococcus litoralis* (*Tli*PAP1, Singleton *et al.*, 1999a) and *Mycobacterium bovis* (*Mbo*PAP1, Kim *et al.*, 2001).

In 1970 Szewczuk and Kwiatkowska reported the presence of PAP1 activity in various vertebrates and plants. Vertebrate sources included human (*Homo sapiens*: *Hsa*PAP1), bovine (*Bos taurus*: *Bta*PAP1), porcine (*Sus scrofa*: *Ssc*PAP1), rabbit (*Oryctolagus*

cuniculus *Ocu*PAP1), mouse (*Mus musculus* *Mmu*PAP1), Rat (*Rattus norvegicus* *Rno*PAP1), guinea-pig (*Cavia porcellus* *Cpo*PAP1), pigeon (*Columba* *Col*PAP1), chicken (*Gallus gallus* *Gga*PAP1) and fish (*Cyprinus carpio* *Cca*PAP1) PAP1 activity was detected in all tissues examined including pancreas, spleen, lung, intestines, brain, heart muscle, skeletal muscle and uterus with highest activity found in both liver and kidney Various plants which were tested included bean, oats, wheat, parsley, carrot, cabbage, potato and cauliflower Non-mammalian animal sources such as avian, fish and amphibian tissues have also been reported to display PAP1 activity (Albert and Szewczuk, 1972, Tsuru *et al*, 1982, Prasad *et al*, 1982, Szewczuk and Kwiatkowska, 1970) Morty *et al*, (2006) report a protozoan form of PAP1 activity from African trypanosome which has been detected in the plasma of infected rats

1 3 2 Classification of PAP1

PAP1 is classified as a cysteine omega peptidase (EC 3 4 19 3) which hydrolytically removes the amino terminal L-pyroglutamic acid (pGlu) residue from pGlu-peptides and pGlu-proteins PAP1 was initially classified as EC 3 4 11 8 and has also been referred to as pyrrolidonyl peptidase, pyrrolidone carboxyl peptidase, 5-oxoprolyl-peptidase, pyrase and pyroglutamyl aminopeptidase (Awade *et al*, 1994)

Omega peptidases (EC 3 4 19) are exopeptidases that remove terminal residues which are substituted, cyclized or linked by isopeptide bonds

In cysteine peptidases the catalytic mechanism (see Figure 1 2) requires a nucleophile and a proton donor The nucleophile is the thiol group of a Cys residue The proton donor is usually the imidazolium ring of a Histidine residue In some cases a third residue is required to orientate the imidazolium ring of the His, there are a number of families in which only a catalytic dyad is necessary (Barret *et al*, 1998)

In the Merops database PAP1 has been assigned as family C15, clan CF To date, no other peptidases have been assigned to this family or clan (Barret and Rawings, 2001)

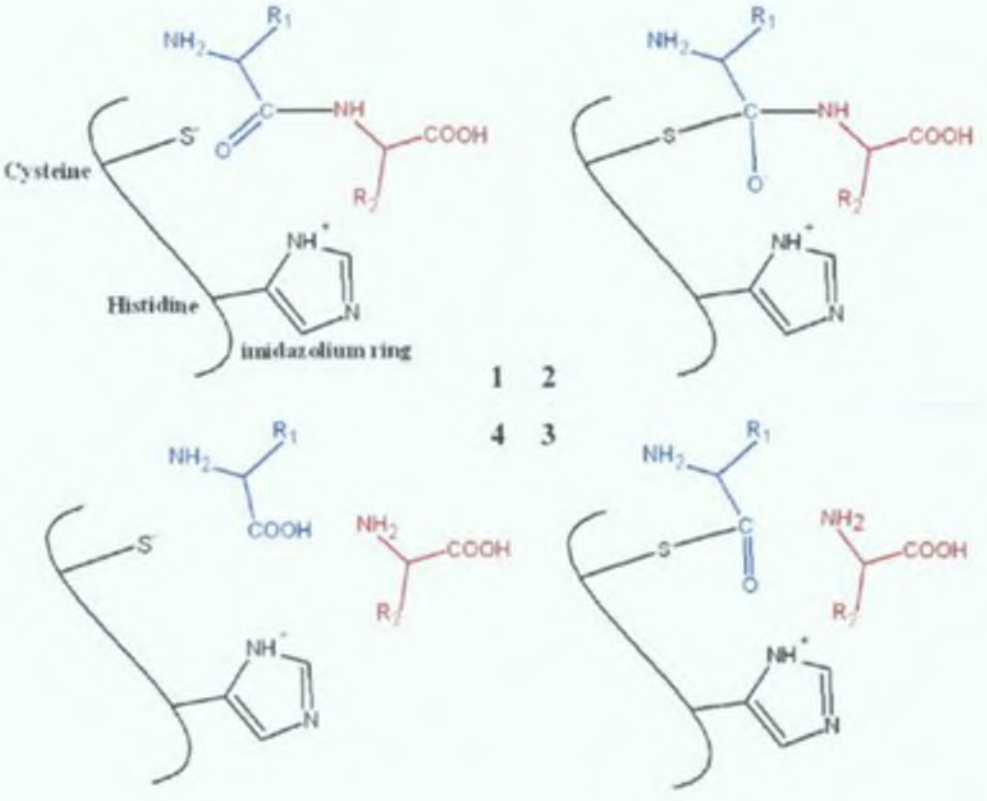

Figure 1.2 Catalytic Mechanism of Cysteine Peptidases
The catalytic mechanism of cysteine proteases is represented via a generic dipeptide (blue-red). The thiolate ion of the Cys residue is the catalytic nucleophile and is stabilized through the formation of an ion pair with neighbouring imidazolium ring of a His residue (1). Catalysis proceeds through the formation of a covalent intermediate (2). The dipeptide is cleaved (3) and both fragments are liberated (4). For amino acid information see Appendix D. Illustrated using ChemSketch (see Section 2.11).

1.3.3 Purification of PAP1

PAP1 has been purified from various prokaryotic cell cultures including *P. fluorescens* (Armentrout and Doolittle, 1969), *B. subtilis* (Swewczuk and Kwiatkowska, 1970), *Kiebsiella cloacae* (Kwiatkowska *et al.*, 1974), *S. faecium* (Sullivan *et al.*, 1977) and *B. amyloliquefaciens* (Tsuru *et al.*, 1978) to name but a few. This enzyme has also been purified from a wide range of eukaryotic tissues including rat (Armentrout, 1969), chicken (Tsuru *et al.*, 1982), bovine (Cummins and O'Connor, 1996) and human (Mantle *et al.*, 1989, 1990, 1991). Recently, trypanosome PAP1 (*Tbr*PAP1) was purified from the plasma of rats infected with *Trypanosoma brucei brucei* (Morty *et al.*, 2006). Conventional chromatography methods were employed to purify PAP1 including ammonium sulphate fractionation, gel filtration, anion exchange chromatography, hydrophobic interaction chromatography and thiol affinity chromatography.

The substrate analogue/inhibitor 2-pyrrolidone was often used as a PAP1 stabilizing agent during purification (Armentrout and Doolittle, 1969).

The cloning of various PAP1 genes (see Section 1 3 9) facilitated the over-expression of several recombinant prokaryotic and eukaryotic active PAP1 enzymes in *E coli* (Cleuziat *et al*, 1992, Gonzalès and Awade, 1992, Awadé *et al*, 1992, Yoshimoto *et al*, 1993, Gonzales and Robert-Baudouy, 1994, Tsunasawa *et al*, 1998, Singleton *et al*, 2000, Sokabe *et al*, 2002) Dando *et al*, (2003) overexpressed both the human and mouse PAP1 enzymes utilizing *Spodoptera frugiperda* insect cells In some cases a fusion with six histidine codons allowed expression of PAP1 enzymes having a 6xHis tag on their N-terminal (Patti *et al*, 1995, Kim *et al*, 2001), facilitating a one-step purification by nickel chelate affinity chromatography

1 3 4 Detection of PAP1 Activity

In 1970, Mulczyk and Szewczuk developed a simple colorimetric assay using synthetic PAP1 substrate L-pyrrolidonal-β-naphthylamide (pGlu-β-NA) The release of β-NA by PAP1 was determined colorimetrically using coupling with azotised-*o*-dianisidine

Various commercial kits using pGlu-β-NA to detect PAP1 activity were developed using paper strips which contained dried chromogenic substrates for PAP1 They proved very useful for the rapid differentiation of entrococci and streptococci in clinical material (Mitchell *et al*, 1987, Dealler *et al*, 1989, Kaufhold *et al*, 1989)

Assays using both synthetic chromogenic substrate pGlu-*p*-nitroaniline and fluorogenic substrate pGlu-7-amino-4-methylcourmarin (pGlu-AMC) were developed for detection of PAP1 activity by Fujiwara and Tsuru (1978) Hydrolysis by PAP1 could be followed by conventional colorimetric and fluorimetric procedures Liberation of *p*-nitroaniline by PAP1 caused an increase in the absorbance at 410 nm while cleavage of pGlu yielded free AMC which can be detected fluorometrically at emission and excitation wavelengths of 440 and 370 nm, respectively (see Figure 1 3) The fluorogenic assay which was used throughout this work was reported to be one thousand fold more sensitive than the chromogemc assay

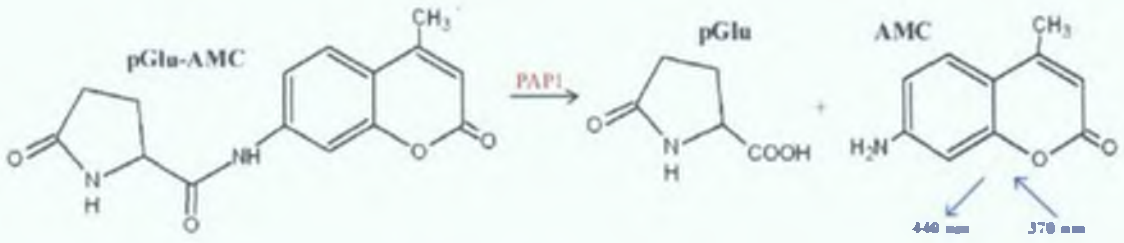

Figure 1.3 PAP1 Cleavage of pGlu-AMC
pGlu-AMC is cleaved by PAP1 to yield free AMC, which fluoresces at 440 nm when exited at 370 nm. Illustrated using ChemSketch (see Section 2.11).

1.3.5 Physiological Significance of PAP1

Identification of the exact physiological role of PAP1 currently remains unaccomplished although numerous suggestions have been put forward. Albert and Szewczuk (1972) suggested that PAP1 may participate in the absorption of peptides and proteins from the mammalian alimentary tract due to the presence of this enzyme in the small intestine, intestinal mucous membrane and duodenum.

An extensive distribution in differing tissues including skeletal muscle, brain, kidney, heart, liver, spleen and intestine has led some researchers to believe that PAP1 may be involved in the intracellular catabolism of peptides to free amino acids and consequently play a role in regulating the cellular pool of free pGlu (Szewcuk and Kwiatkowska 1970; Lauffart *et al.*, 1989; Mantle *et al.*, 1990;1991).

The physiological implications of this were demonstrated by Falkous *et al.*, (1995) who reported a significant increase in levels of PAP1 activity in spinal cords of patients suffering from motor neuron disease.

The inability of PAP1 to obtain an extracellular location has raised doubt with regards to a physiologically significant role for this enzyme in neuropeptide metabolism (Charli *et al.*, 1987). As a result, researchers have hypothesized that PAP1, together with other cytosolic enzymes may be involved in a mechanism of returning pGlu terminating neuropeptides released from damaged or aging vesicles back to the cellular amino acid pool (O'Cuinn *et al.*, 1990).

An interesting series of studies carried out by De Gandarias *et al.*, (1992; 1994; 1998; 2000) has indicated that there is a correlation between PAP1 activity and TRH levels in the developing mammalian brain. Their results have indicated that a decrease in PAP1 activity coincides with an increase in TRH levels as the brain develops and as a result has suggested that PAP1 could play a role in normal development of mammalian brain. During early stages of brain development, increased PAP1 activity was found to reflect

an increase in cyclo (His-Pro) levels This research group also suggest that during the ontogency of the brain, PAP1 has different functions in brain development depending on the subcellular structure

Sanchez *et al*, (1996) have demonstrated that environmental light conditions influences PAP1 activity resulting in increased levels in the hypothalamus and retina of rat

Analysis carried out on various human semen fractions has indicated presence of PAP1 activity (Valdivia *et al*, 2004) PAP1 activity was predominantly found in membrane-associated (particulate sperm and prostasome) fractions Activity was higher in semen fractions which were obtained from necrozoospermic fractions This research has indicated that PAP1 may participate in regulating the levels of seminal TRH analogues and in mediating sperm death associated with necrozoospermia

Abe *et al*, (2004) found that PAP1 was distributed intracellularly in the pituitary, the target tissue of TRH, indicating that PAP1 might not be dominantly involved in the degradation of TRH in rats, although further depth into this study is required

It has been demonstrated by Morty *et al*, (2006) that PAP1 released from African trypanosomes could modulate plasma neuropeptide levels of infected hosts both in *vitro* and in *vivo* The abnormal degradation of TRH and gonadotropin-releasing hormone (GnRH) by trypanosome PAP1, may contribute to some of the endocrine lesions observed in African trypanosomiasis

Recently, a comprehensive study was conducted by Monsuur *et al*, (2006) on the involvement of PAP1 in coeliac disease They found that the PAP1 gene is located in a coeliac disease susceptibility locus and also determined PAP1 activity in duodenal biopsies However, following DNA sequencing, genetic association testing and quantifying RNA expression they reported that PAP1 is not involved in the aetiology and pathology of coeliac disease

Prokaryotic PAP1s are generally thought to be involved in protein maturation, protein degradation and in the utilization of peptides nutrients (Awade *et al*, 1994, Gonzales and Robert-Baudouy, 1996) Since accumulation of peptides with an N-terminal pGlu may abnormally acidify prokaryotic cell cytoplasm, PAP1 may be involved in the detoxification of pGlu-peptides (Awade *et al*, 1994)

1.3.6 Inhibitors of PAP1

A series of active site-directed inhibitors were synthesised by Fujiwara *et al.*, (1981a, 1981b, 1982) for *B. amyloliquefaciens* PAP1 (see Figure 1.4). These inhibitors pGlu-chloromethyl ketone (pGluCK), Z-pGlu-chloromethyl ketone (Z-pGluCK) and Z-pGlu-diazomethyl ketone (Z-pGluDK) were found to be highly specific, potent and irreversible inhibitors of PAP. Later in 1985, Wilk *et al.*, synthesised another inhibitor pGlu-diazomethyl ketone (pGluDK) which proved to be significantly more inhibitory than its Z-derivative mentioned above. Activity could be completely restored by dialysis with a dithiothreitol (DTT) or 2-β-mercaptoethanol (2-ME) based buffer.

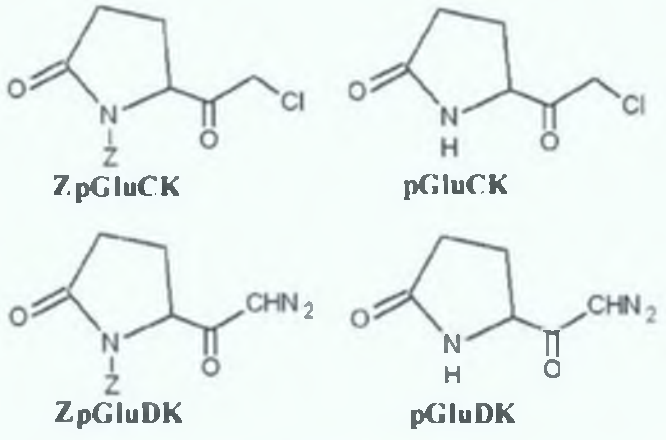

Figure 1.4 Active Site-Directed Inhibitors of PAP1
Synthetic active site-directed inhibitors of PAP1: L-pGlu chloromethyl ketone (pGluCK), N^{α}-carbobenzoxy-L-pGlu chloromethyl ketone (ZpGluCK), L-pGlu diazomethyl ketone (pGluDK) and N^{α}-carbobenzoxy-L-pGlu diazomethyl ketone (ZpGluDK). Illustrated using ChemSketch (see Section 2.11).

The substrate analogue 2-pyrrolidone (see Figure 1.5) was initially used by Armentrout and Doolittle (1969) as a stabilizing agent for PAP1 activity following instability problems which were encountered by this enzyme in solution. 2-pyrrolidone acts as a reversible non-competitive inhibitor of PAP1 (Armentrout, 1969; Mudge and Fellows, 1973; Sullivan *et al.*, 1977; Cummins and O'Connor, 1996). Up to 50 % inhibition was observed with 0.1 M 2-pyrrolidone and complete inhibition was not achieved by increased concentrations. 100% activity was recovered following the removal of 2-pyrrolidone by dialysis.

Benarthin, a competitive inhibitor of PAP1 was found in the fermentation broth of *Streptomyces xathophaeus* MJ244-SF1. It was isolated as a colourless powder. An IC_{50} value of 2.0 $\mu g.ml^{-1}$ was determined for this inhibitor against PAP1. Benarthin has a low toxicity as no deaths occurred following its intravenous injection of 100 mg/kg to mice

(Aoyagi *et al.*, 1992a). The same group discovered another PAP1 inhibitor, pyrizinostatin, from culture filtrate of the microbial strain SA2289 which had been isolated from a marine soil and was confirmed to belong to the genes *Strepomyces*. Pyrizinostatin was found to act as a non-competitive inhibitor towards PAP1 with an IC_{50} value of 1.8 $\mu g.ml^{-1}$ (Aoyagi *et al.*, 1992b).

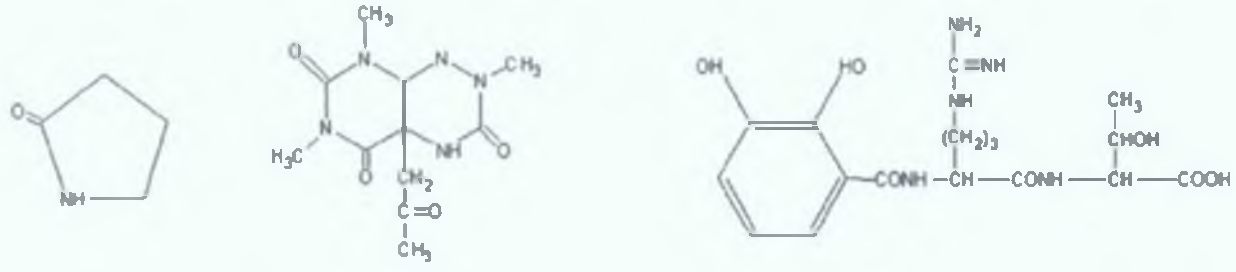

Figure 1.5 Inhibititors 2-Pyrrolidone, Pyrizinostatin and Benarthin
Chemical structures of reversible non-competitive inhibitor 2-Pyrrolidone, non-competitive inhibitor Pyrizinostatin and competitive inhibitor Benarthin. Illustrated using ChemSketch (see Section 2.11).

Many cations such as Hg^{2+}, Zn^{2+}, Cu^{2+}, Co^{2+}, Ca^{2+}, Mn^{2+}, Mg^{2+}, Ni^{2+}, Ba^{2+}, Sr^{2+} and Cd^{2+} have been reported to have an inhibitory effect on PAP1 activity. Activity could be partially restored by addition of EDTA to enzyme assay or by subjecting the enzyme to dialysis to remove the metal ion (Szewczuk and Mulczyk, 1969, Dando *et al.*, 2003).

1.3.7 Substrate Specificity

Following the initial discovery of PAP1 in *P. fluorescens* (Doolittle and Armentrout, 1969), numerous researchers have undertaken various studies to investigate the substrate specificity of PAP1 (Uliana and Doolittle,1969; Szewczuk and Mulczyk, 1969; Armentrout, 1969; Mudge and Fellows, 1973; Kwiatkowska *et al.*, 1974; Sullivan *et al.*, 1977; Podell and Abraham, 1978; Fujiwara *et al.*, 1979; Tsuru *et al.*, 1982; Browne and O'Cuinn, 1983; Lauffart *et al.*, 1989; Mantle *et al.*, 1990; Mantle *et al.*, 1991; Cummins and O'Connor, 1996; Mineyama and Saito, 1998; Tsunasawa *et al.*, 1998; Dando *et al.*, 2003; Morty *et al.*, 2006). A distinctive feature of PAP1 is its broad substrate specificity. It hydrolytically removes the pyroglutamic acid residue (pGlu) from the amino terminus of pGlu-peptides and proteins with an apparent specificity for

L-pGlu-L-amino acid optical isomers Results highlighted that the size of the peptide does not affect specificity and that the amino acid directly adjacent to pGlu affects the rate of hydrolysis The order of preference is Thr > Glu > Met > Ala > Lys > Gly > Ser > Tyr > Arg > Phe > His > Trp > Asp > Leu > Ile >> Val as determined for *Bam*PAP1, which is generally in agreement with the other PAP1s tested pGlu-Pro was not hydrolysed by PAP1, with one notable exception being *Kcl*PAP1 However, the hydrolysis of pGlu-Pro by *Kcl*PAP1 was significantly slower than pGlu-Ala or even pGlu-Val (Fujiwara *et al*, 1979)

Cleavage of pGlu from several bioactive peptides including TRH, LHRH, GnRH, Liliberin, Neurotensin, Bombesin, Eledoisin and Leukopyrokinin has been widely demonstrated Synthetic substrates such as pGlu-AMC and pGlu-βNA are readily hydrolysed by PAP1 Substrate specificity of PAP1 towards several organic nitrates and L-pGlu-L-Ala analogues was recently investigated by Abe *et al*, 2004b They demonstrated that PAP1 allowed the replacements of the carbon atom at the 4-position of the L-pGlu moiety with a sulphur atom (L-OTCA), an oxygen atom (L-OOCA) or an NH group (L-OICA) (see Figure 1 6) The carbon atom at the 4-position of the L-pGlu moiety was located in the hydrophobic pocket of PAP1, suggesting that these compounds could insert into the hydrophobic pocket of PAP1 The affinities of these substrates were much lower than substrates having the L-pGlu moiety indicating that the relatively large molecular size of the sulphur atom or the hydrophilic nature of the oxygen and nitrogen atoms compared to the carbon atom at the 4-position of the L-pGlu moiety may interfere with the insertion of the moieties into the hydrophobic pocket of PAP1

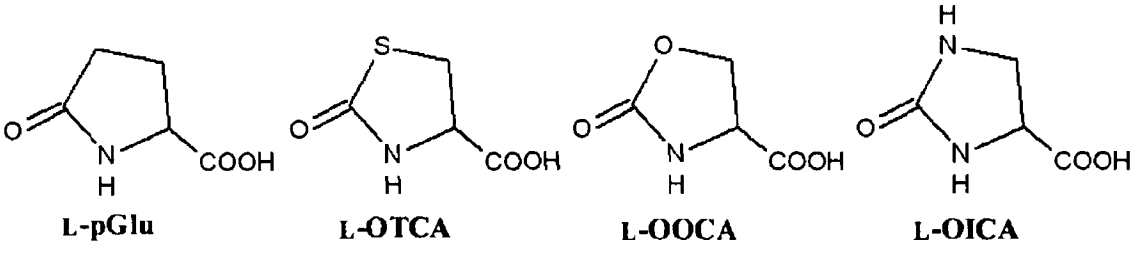

Figure 1 6 Substitution Analogues of L-pGlu
Synthetic analogues of L-pGlu (L-5-oxopyrrolidine-2-carboxylic acid) having the carbon atom at position 4 replaced by sulphur (L-5-oxothiazolidine-2-carboxylic acid, L-OTCA), oxygen (L-5-oxooxazolidine-2-carboxylic acid, L-OOCA) and nitrogen (L-5-oxoimidazolidine-2-carboxylic acid, L-OICA) Illustrated using ChemSketch (see Section 2 11)

1 3 8 Biochemical Characterisation of PAP1

Over the last few decades extensive research has been carried out on the biochemical characterisation of both eukaryotic and prokaryotic PAP1 (Szewczuk and Kwiatkowska, 1970, Kwiatkowska *et al*, 1974, Sullivan *et al*, 1977, Tsuru *et al*, 1978, Busby *et al*, 1982, Tsuru *et al*, 1982, Browne and O'Cuinn, 1983, Tsuru *et al*, 1984, Lauffart and Mantle, 1988, Lauffart *et al*, 1989, Mantle *et al*, 1991, Gonzales and Awadé, 1992, Awadé *et al*, 1992, Yoshimoto *et al*, 1993, Gonzales and Robert-Baudouy, 1994, Patti *et al*, 1995, Cummins and O'Connor, 1996, Mineyama and Saito, 1998, Tsunasawa *et al*, 1998, Singleton *et al*, 2000, Kim *et al*, 2001, Dando *et al* 2003, Morty *et al*, 2006) Studies have shown that mammalian PAP1 exists as a soluble cytosolic monomeric enzyme with a low molecular mass of approximately 24 kDa under denaturing and non-denaturing conditions Molecular mass determinations for the prokaryotic enzyme under denaturing conditions indicate an average subunit mass of 25 kDa, while an increase in molecular mass is obtained under native conditions The quaternary 3-D structure of *Bam*PAP1, *Tli*PAP1, *Pfu*PAP1 and *Pho*PAP1 have been reported to be tetrameric (see Section 1 3 11 3)

Physiological temperature of 37°C has been used as the standard temperature for experimental analysis of eukaryotic PAP1 An optimum temperature of 50°C was determined for human PAP1 by Dando *et al*, 2003 A range of temperatures have been reported for prokaryotic PAP1 Mesophilic prokaryotic PAP1 have been reported to be optimally active in the temperature range of 30 to 45°C while thermophilic enzymes *Tli*PAP1 and *Pfu*PAP1 displayed optimum activity at 70 and 90°C, respectively

An optimum pH in the range of 6 0 and 9 5 has been determined for PAP1 in general, with a mean pH of 7 5

Classified as a cysteine peptidase (see Section 1 3 2) PAP1 displayed a strict requirement for a thiol-reducing agent, such as DTT or β-ME In support of this, several studies have reported the inhibitory nature of sulfhydryl-blocking reagents such as N-ethylmaleimide, PCMB, iodoacetamide and iodacetic acid

Table 1 2 Characteristics of Various PAP1 Enzymes

	PAP1	Denatured size (Da)	Native size (Da)	Optimum pH	PI	Optimum Temp (°C)	K_m (mM)
eukaryotic	*Hsa*PAP1 [r9 r10 r11 r22]	n d	24,000	7 0 – 9 5	n d	50	0 05 [b]
	*Bta*PAP1 [r17]	24,000	23,700	8 5	n d	n d	0 015 [b], 0 021 [a]
	*Cpo*PAP1 [r7]	n d	24,000	n d	n d	n d	0 15 [b]
	*Ocu*PAP1 [r1]	n d	33,000	7 5	n d	n d	n d
	*Col*PAP1 [r1]	n d	33,000	7 5	n d	n d	0 13 [a]
	*Rno*PAP1 [r5]	n d	60,000	8 0 – 8 4	n d	n d	n d
	*Gga*PAP1 [r6]	n d	86,000	7 0 – 8 0	5 5	n d	0 73 [a], 0 04 [b]
	*Tbr*PAP1 [r23]	25,000	n d	7 5 - 8 5	n d	n d	0 28 [b]
prokaryotic	*Pfl*PAP1 [r15]	23,500	41,000	6 5 – 8 5	4 9	30	0 21 [a]
	*Bsu*PAP1 [r12]	25,200	91,000	6 8 – 7 5	n d	n d	1 04 [a]
	*Spy*PAP1 [r13]	23,500	85,000	7 0	n d	n d	1 79 [a]
	*Kcl*PAP1 [r2]	n d	74,000	6 0 – 7 5	n d	n d	n d
	*Efa*PAP1 [r18]	40,500	82,000	7 2 – 7 5	4 2	35 – 45	0 55 [a]
	*Sfa*PAP1 [r3]	42,000	n d	7 6	n d	n d	0 86 [a]
	*Bam*PAP1 [r4 r8 r14]	24,000	72,000 or 51,000	7 0 – 8 0	5 4	45	0 13 [a]
	*Tli*PAP1 [r20]	24,000	96,000	7 0 – 8 0	n d	70	n d
	*Pfu*PAP1 [r19]	22,937	96,300 or 45,643	6 0 – 9 0	n d	90	n d
	*Sau*PAP1$_{6H}$ [r16]	30,000	46,000	7 8	n d	n d	n d
	*Mbo*PAP1$_{6H}$ [r21]	29,000	46,000	n d	n d	n d	n d

[n d - not determined, a - determined for pGlu-β-NA, b - determined for pGlu-AMC, r1, Szewczuk and Kwiatkowska, 1970, r2, Kwiatkowska *et al* 1974, r3, Sullivan *et al* 1977, r4, Tsuru *et al*, 1978, r5, Busby *et al* 1982, r6, Tsuru *et al*, 1982, r7, Browne and O'Cuinn, 1983, r8, Tsuru *et al* 1984, r9, Lauffart and Mantle, 1988, r10 Lauffart *et al* 1989, r11, Mantle *et al*, 1991, r12, Gonzales and Awade, 1992, r13, Awade *et al* 1992, r14, Yoshimoto *et al*, 1993, r15, Gonzales and Robert-Baudouy, 1994, r16, Patti *et al* 1995, r17, Cummins and O'Connor, 1996, r18, Mineyama and Saito, 1998, r19, Tsunasawa *et al*, 1998, r20, Singleton *et al*, 2000, r21, Kim *et al*, 2001, r22, Dando *et al* 2003, r23, Morty *et al* 2006]

1.3.9 Sequence Data and Analysis of PAP1

The first PAP1 genes to be cloned and sequenced were *Bsu*PAP1 (Awadé *et al.*, 1992a) and *Spy*PAP1 (Cleuziat *et al.*, 1992) respectively. These genes were isolated from *B. subtilis* and *S. pyogenes* by the construction of genomic libraries which were followed by the subsequent transformation into *E. coli*. A plate colony assay using pGlu-β-NA as described by Mulczyk and Szewczuk (1970) was utilised to screen the prokaryotic gene libraries for PAP1 activity in *E. coli*. Potential clones were subjected to restriction analysis followed by DNA sequencing and as a result the open reading frames (ORFs) of *Bsu*PAP1 and *Spy*PAP1 were identified. At that time, these sequences did not display homology with any other data available on Genbank (Benson *et al.*, 1996), suggesting that these prokaryotic PAPs belonged to a new and unique class of peptidases. Several other prokaryotic PAP1 genes were later sequenced and ORFs for all prokaryotic PAP1's were approximately 600-700 base pairs in length (see Table 1.3).

Table 1.3 Prokaryotic PAP1 Sequences

Organism	PAP1 Gene	GenBank Accession	ORF (bp)	PAP1 Enzyme	Amino Acids	Reference
B. subtilis	*Bsu-pap1*	X66034	645	*Bsu*PAP1	215	Awadé *et al.*, 1992
S. pyogenes	*Spy-pap1*	X65717	645	*Spy*PAP1	215	Cleuziat *et al.*, 1992
B. amyloliquefaciens	*Bam-pap1*	D11035	645	*Bam*PAP1	215	Yoshimoto *et al.*, 1993
P. fluorescens	*Pfl-pap1*	X75919	639	*Pfl*PAP1	213	Gonzalès and Robert-Baudouy, 1994
S. aureus	*Sau-pap1*	U19770	636	*Sau*PAP1	212	Patti *et al.*, 1995
P. furiosus	*Pfu-pap1*	AB015291	624	*Pfu*PAP1	208	Tsunasawa *et al.*, 1998
T. litoralis	*Tli-pap1*	Y13966	660	*Tli*PAP1	220	Singleton *et al.*, 2000
M. bovis	*Mbo-pap1*	U91845	666	*Mbo*PAP1	222	Kim *et al.*, 2001
P. horikoshii	*Pho-pap1*	AP000002	618	*Pho*PAP1	206	Sokabe *et al.*, 2002

An alignment of all confirmed prokaryotic PAP1 amino acid sequences is shown in Figure 1.7. Sequence homology is represented in grey scale shading, with black being the highest homology. The highly conserved areas have been labelled domains 1 to 4. Homology scores corresponding to this alignment are shown in Table 1.4. *Bsu*PAP1 and *Bam*PAP1 display the highest degree of sequence homology showing 72% identity and 85% similarity, while least homology exists between *Mbo*PAP1 and *Sau*PAP1 (27% identity, 48% similarity).

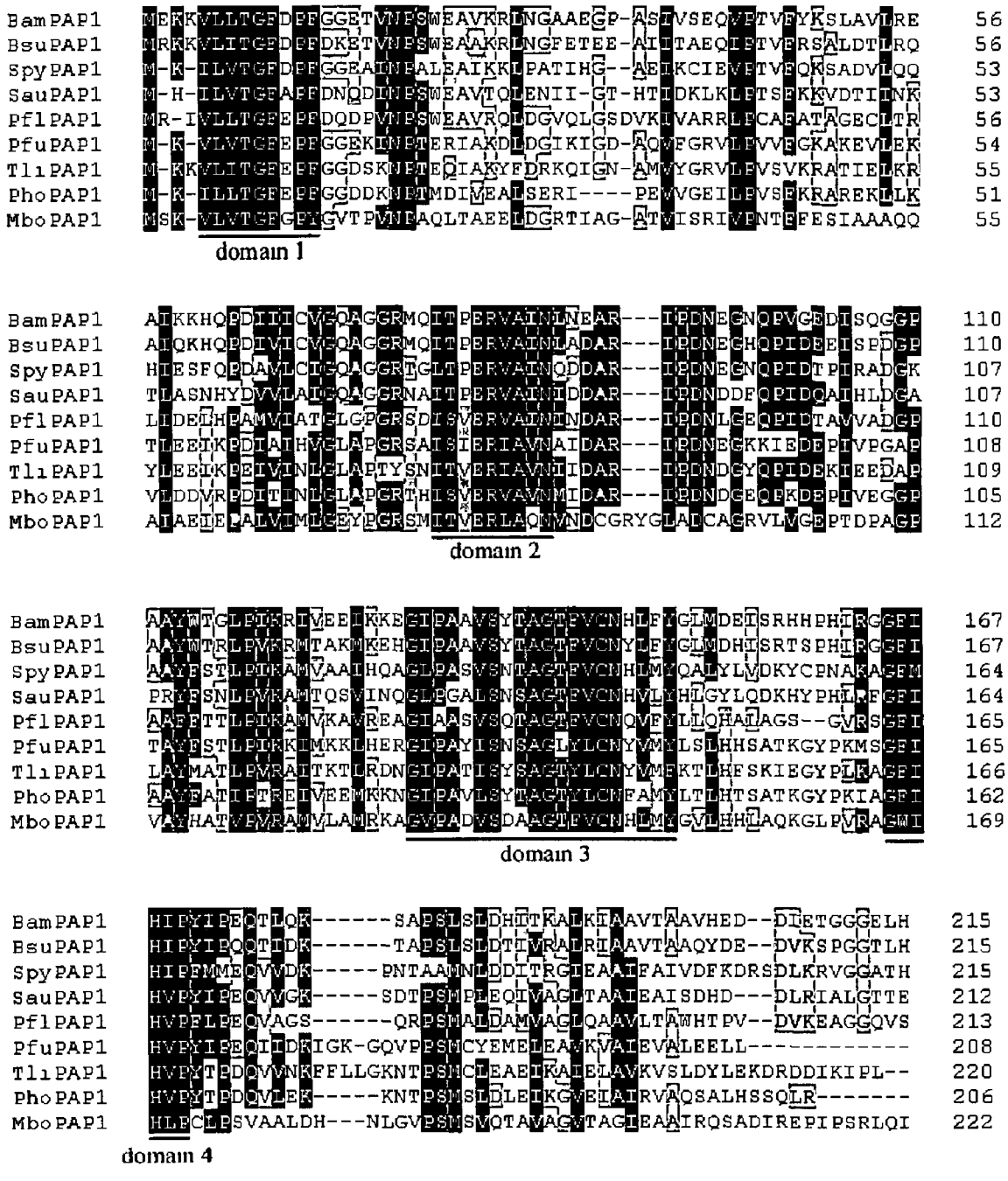

Figure 1 7 Amino Acid Sequence Alignment of Prokaryotic PAP1

Alignment was created using MultAlin with Blosum62-12-2 parameters and edited using GenDoc (Section 2 11) Sequence homology is represented by grey scale shading, with black being the highest homology The most highly conserved domains have been labelled 1 to 4 For amino acid information see Appendix D

Table 1 4 Homology Scores for Prokaryotic PAP1 Sequences

	***Bsu*PAP1**	***Spy*PAP1**	***Sau*PAP1**	***Pfl*PAP1**	***Pfu*PAP1**	***Tli*PAP1**	***Pho*PAP1**	***Mbo*PAP1**
***Bam*PAP1**	72 (85)	48 (68)	41 (62)	43 (63)	38 (57)	32 (57)	41 (59)	32 (52)
	***Bsu*PAP1**	47 (65)	43 (62)	46 (65)	39 (57)	36 (59)	37 (56)	33 (50)
		***Spy*PAP1**	49 (66)	41 (61)	36 (57)	34 (59)	39 (60)	31 (49)
			***Sau*PAP1**	43 (60)	35 (50)	34 (54)	36 (51)	27 (48)
				***Pfl*PAP1**	38 (56)	37 (55)	40 (57)	36 (51)
					***Pfu*PAP1**	53 (71)	51 (73)	33 (54)
						***Tli*PAP1**	53 (69)	32 (53)
[Identity scores are given, with similarity in parenthesis]							***Pho*PAP1**	34 (47)

Dando *et al*, (2003) were the first group to clone and sequence two eukaryotic forms of PAP1 from vertebrates Both human PAP1 (*Hsa*PAP1) and mouse PAP1 (*Mmu*PAP1) genes were expressed in insect cells The deduced amino acid sequences each consisted of 209 amino acid residues that display 95% identity with each other Following this other eukaryotes including rat PAP1 (*Rno*PAP1) and trypanosome PAP1 (*Tbr*PAP1) were later cloned and sequenced using similar approached (Abe *et al*, 2003, Morty *et al*, 2006)

A BLAST search (see Section 2 11) of known PAP1 sequences against the current GenBank data reveals a number of confirmed and putative eukaryotic PAP1 gene sequences (see Table 1 5) many of which have not yet been documented in publications

Table 1 5 Eukaryotic PAP1 Sequences

Organism	Common Name	PAP1 Gene	GenBank Accession	ORF (bp)	PAP1 gene product	Amino Acids
H sapiens	Human	*Hsa-pap1*	AJ278828[a]	627	*Hsa*PAP1	209
M musculus	Mouse	*Mmu-pap1*	AJ278829[a]	627	*Mmu*PAP1	209
R norvegicus	Rat	*Rno-pap1*	AB098134[b]	624	*Rno*PAP1	208
Trypanosoma Bruci	African Trypanosome	*Tbr-pap1*	AJ278829[c]	669	*Tbr*PAP1	222
Strongylocentrotus purpurtus	Purple Urchin	*Spu-pap1**	XM_781811	594	*Spu*PAP1*	197
Takifugu rubripes	Japanese Pufferfish	*Tru-pap1**	AJ301641	633	*Tru*PAP1*	211
Xenopus tropicalis	Frog	*Xtr-pap1**	BC075524	624	*Xtr*PAP1*	208
Brachydanio rerio	Zebra	*Bre-pap1**	XM_681991	624	*Bre*PAP1*	208
Anopheles gambiae	Mosquito	*Aga-pap1**	XM_308793	627	*Aga*PAP1*	209
Drosophila melanogaster	Fruit Fly	*Dme-pap1**	NM_168616	672	*Dme*PAP1*	224
Arabidopsis thaliana	Cress	*Ath-pap1**	NM_104547	657	*Ath*PAP1*	219
Caenorhabditis elegans	Nematode	*Cel-pap1**	NM_060090	822	*Cel*PAP1*	274

[[a] Dando *et al*, 2003, [b] Abe *et al*, 2003, [c] Morty *et al*, 2006, * Putative sequences]

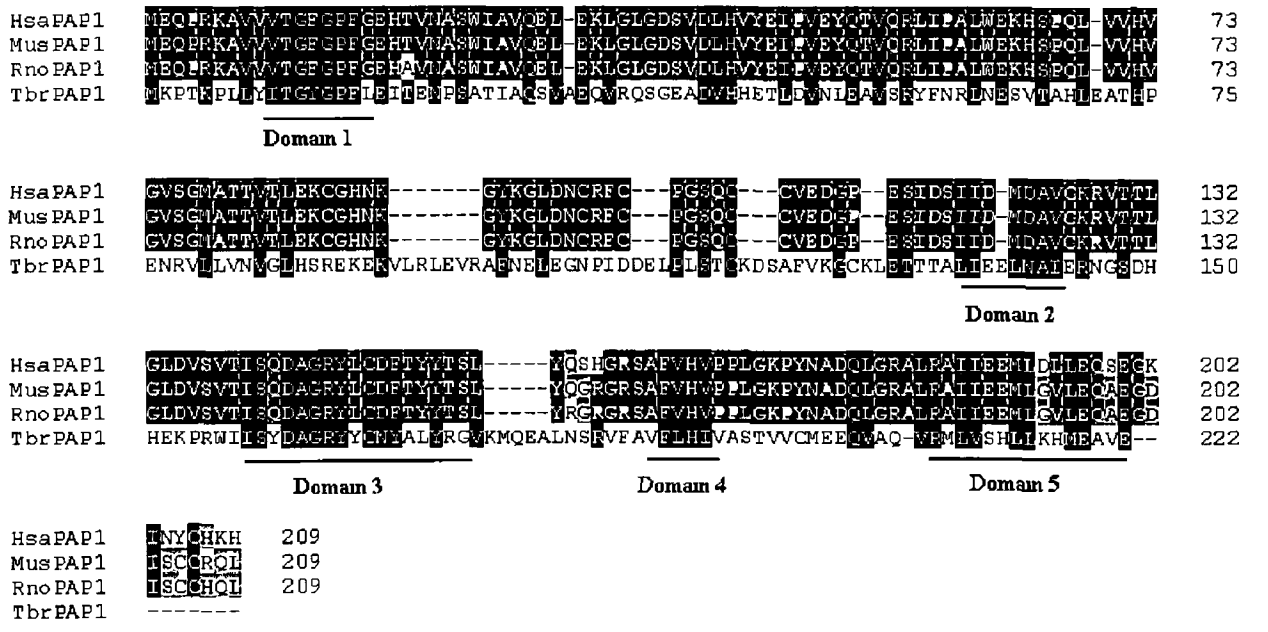

Figure 1 8 Alignment of Confirmed Ammo Acid Sequences of Eukaryotic PAP1

Alignment was created using MultAlin with Dayhoff-8-0 parameters and edited using GenDoc (Section 2 11) Sequence homology is represented by grey scale shading, with black being the highest homology The most highly conserved domains have been labelled A to E For amino acid information see Appendix D

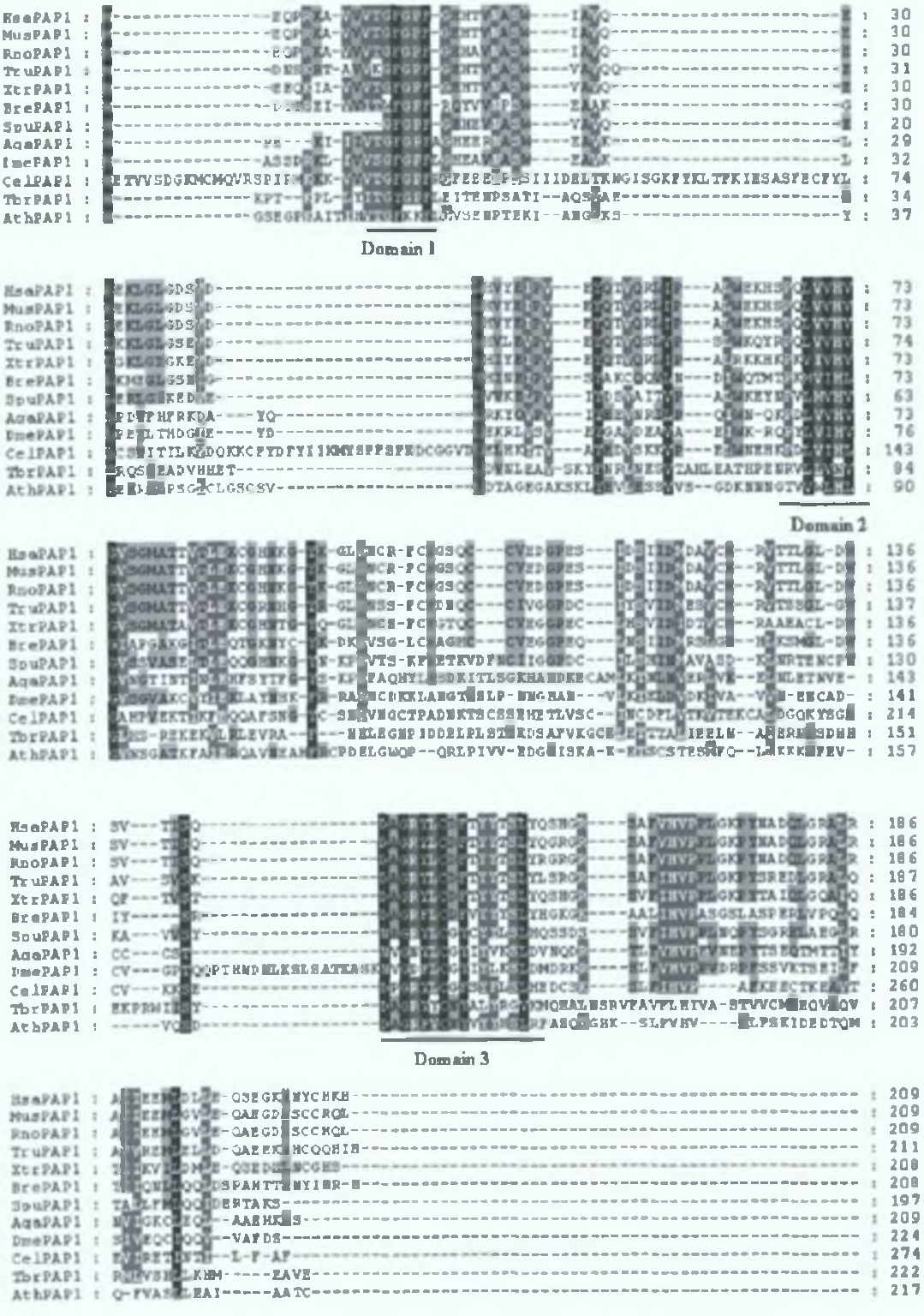

Figure 1.9 Amino Acid Sequence Alignment of All Eukaryotic PAP1

Alignment was created using MultAlin with Dayhoff-8-0 parameters and edited using GenDoc (Section 2.11). Sequence homology is represented by grey scale shading, with black being the highest homology. The most highly conserved domains have been labelled A to E. For amino acid information see Appendix D.

Figure 1 8 shows an alignment of four eukaryotic PAP1 amino acid sequences, namely *Hsa*PAP1, *Mmu*PAP1, *Rno*PAP1 and *Tbr*PAP1, which have been confirmed (Dando *et al*, 2003, Abe *et al* 2003, Morty *et al*, 2006) On this alignment the regions of highest homology have been designated domains 1 to 5 Catalytic residues cysteine and histidine are conserved in domains 3 and 4, respectively

An alignment of all eukaryotic PAP1 sequences, both confirmed and putative is shown in Figure 1 9, highlighting conserved domains 1, 2 and 3 The *Cel*PAP1 sequence has approximately 50-60 additional amino acid residues when compared to other eurkaryotic PAP1 sequences This as a result has led to a decrease in homologous domains within this alignment Table 1 6 gives a summary of the homology scores for this alignment The greatest degree of homology exists between the rodent sequences *Mmu*PAP1 and *Rno*PAP1 (98% identity, 99% similarity) These also show closest homology to *Hsa*PAP1 (94% identity, 96% similarity) The trypanosome sequence *Tbr*PAP1, plant sequence *Ath*PAP1 and nematode sequence *Cel*PAP1 exhibit the greatest divergence from all other eukaryotic sequences

Table 1 6 Homology Scores for Eukaryotic PAP1 Sequences

	***Mmu*PAP1**	***Rno*PAP1**	***Spu*PAP1**	***Tru*PAP1**	***Xtr*PAP1**	***Bre*PAP1**	***Aga*PAP1**	***Dme*PAP1**	***Tbr*PAP1**	***Ath*PAP1**	***Cel*PAP1**
***Hsa*PAP1**	94 (96)	94 (96)	42 (58)	68 (84)	73 (84)	41 (65)	29 (49)	28 (44)	12 (27)	15 (31)	20 (34)
	***Mmu*PAP1**	98 (99)	41 (57)	68 (84)	71 (82)	41 (65)	29 (47)	29 (45)	12 (27)	15 (31)	20 (33)
		***Rno*PAP1**	41 (57)	67 (83)	70 (82)	41 (65)	29 (47)	29 (45)	12 (27)	15 (31)	20 (33)
			***Spu*PAP1**	44 (59)	41 (60)	29 (46)	29 (46)	25 (43)	14 (29)	15 (31)	19 (31)
				***Tru*PAP1**	63 (80)	41 (62)	28 (46)	28 (44)	12 (26)	17 (30)	21 (33)
					***Xtr*PAP1**	39 (60)	28 (48)	25 (44)	11 (25)	15 (30)	18 (32)
						***Bre*PAP1**	22 (41)	21 (40)	10 (29)	15 (29)	18 (29)
							***Aga*PAP1**	35 (56)	10 (30)	14 (29)	23 (39)
								***Dme*PAP1**	10 (20)	14 (29)	28 (35)
									***Tbr*PAP1**	23 (44)	10 (24)
[Identity scores are given, with similarity in parenthesis]										***Ath*PAP1**	12 (24)

The prokaryotic sequence that *Hsa*PAP1 exhibits most homology with is *Bam*PAP1. Figure 1.10 shows an alignment of these two sequences. They exhibit an identity of 25% and a similarity of 45%, which is a higher score than seen among some of the eukaryotic sequences (see Table 1.6).

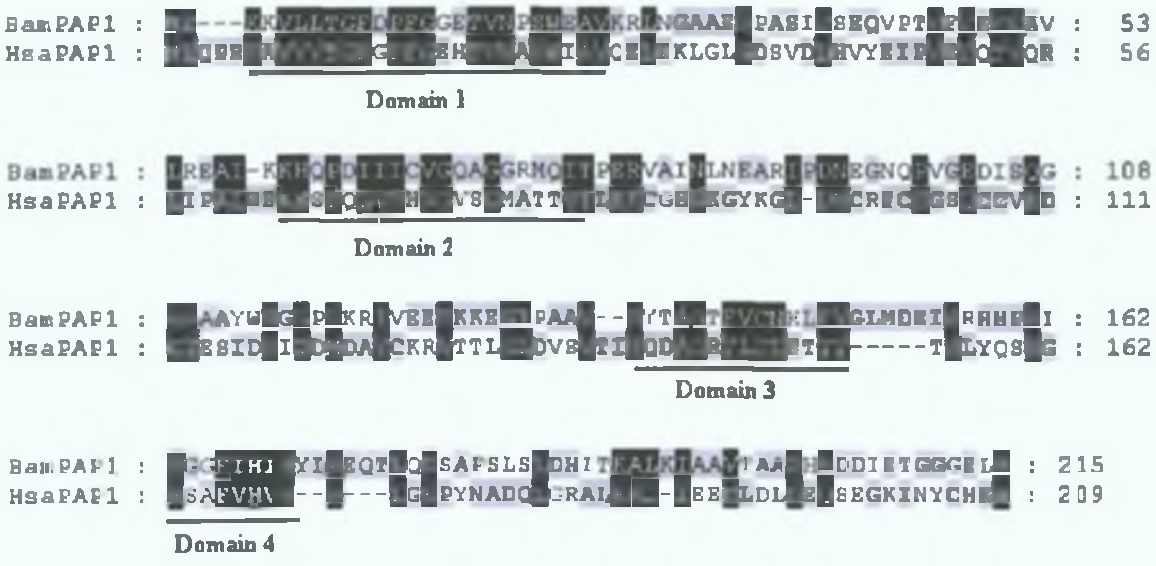

Figure 1.10 Amino Acid Sequence Alignment of *Hsa*PAP1 and *Bam*PAP1
Alignment was created using MultAlin with Blosum62-12-2 parameters and edited using GenDoc (Section 2.11). Sequence homology is represented by grey scale shading, with black being the highest homology. For amino acid information see Appendix D.

1.3.10 Catalytic Residues of PAP1

The catalytic importance of a cysteine thiol group in PAP1 activity has been well demonstrated by its absolute requirement for a thiol-reducing agent such as DTT or 2-ME (Armentrout, 1969; Szewczuk and Mulczyk, 1969; Szewczuk and Kwiatkowska, 1970; Kwiatkowska *et al.*, 1974; Tsuru *et al.*, 1978; Tsuru *et al.*, 1982; Tsuru *et al.*, 1984; Prasad, 1987; Mantle *et al.*, 1991; Cummins and O'Connor, 1996; Tsunasawa *et al.*, 1998; Singleton and Littlechild, 2001; Dando *et al.*, 2003; Morty *et al.*,2006).

Further demonstrating this are the findings that PAP1 activity is highly sensitive to µM concentrations of thiol-blocking compounds such as iodoacetate, iodoacetamide, *p*-chloromercuribenzoate (*p*-CMB), *p*-mercuriphenylsulphonate, *N*-ethylmaleimide and sodium tetrathionate (Doolittle and Armentrout, 1968; Szewczuk and Mulczyk, 1969; Szewczuk and Kwiatkowska, 1970; Mudge and Fellows, 1973; Kwiatkowska *et al.*,

1974; Prasad and Peterkofsky, 1976; Tsuru *et al.*, 1978; Bauer and Kleinkhauf, 1980; Tsuru *et al.*, 1982; Browne and O'Cuinn, 1983; Awadé *et al.*, 1992; Gonzalès and Robert-Baudouy, 1994; Patti *et al.*, 1995; Cummins and O'Connor, 1996; Tsunasawa *et al.*, 1998; Mineyama and Saito, 1998; Singleton *et al.*, 2000; Singleton and Littlechild, 2001; Dando *et al.*, 2003).

The selective serine peptidase inhibitor phenylmethylsulphonyl fluoride (PMSF) was found to exert no effect on the activity of PAP1 (Tsuru *et al.*, 1982; Lauffart *et al.*, 1989; Mantle *et* al., 1990; Gonzalès and Robert-Baudouy, 1994; Singleton *et al.*, 2000).

Site-specific mutagenesis studies were conducted by various research groups to identify the catalytic residues of PAP1. The two cysteine residues of *Bam*PAP1, Cys68 and Cys144, were mutated to Ser by Yoshimoto *et al.* (1993). The mutant *Bam*PAP1_C68mS had wild type activity while *Bam*PAP1_C144mS was completely inactive, implicating Cys144 as providing the essential active site thiol group. Le Saux *et al.* (1996) investigated several residues as possible contributors to the active site of *Pfl*PAP1, based on homology alignments with known PAP1 sequences. Substitutions of Cys144 and His166 by Ala and Ser, respectively, were found to completely abolish activity of *Pfl*PAP1 without affecting protein conformation as shown by gel electrophoresis. Similarly, one of Glu81, Asp89 or Asp94 were shown to be a likely third member of an active triad of *Pfl*PAP1 (Le Saux *et al.*, 1996). Tsunasawa *et al.* (1998) substituted the Cys142 residue of *Pfu*PAP1 with Ser, resulting in loss of activity. In light of published data and by sequence analysis, these authors proposed the catalytic triad of *Pfu*PAP1 to consist of Cys142, His166 and Glu79, which correspond to Cys144, His168 and Glu81 of *Bam*PAP1 respectively. This catalytic triad was later confirmed by studies of the tertiary structure of *Bam*PAP1 and *Pfu*PAP1 as outlined in Section 1.3.11.3.

Recently, Morty *et al.*, (2006) substituted Cys167 of trypanosome PAP1 with Ala, which resulted in complete loss of PAP1 enzyme activity. Residues Glu104, Cys167 and His191 were fully conserved within the *Tbr*PAP1 amino acid sequence when compared to a number of PAP1 sequences including *Hsa*PAP1 and *Bam*PAP1.

1.3.11 Stucture of PAP1

Recently the three-dimensional structures of four prokaryotic PAP1 enzymes were solved using X-ray crystallography. These four structures; the mesophilic *Bam*PAP1 (Odagaki *et al.*, 1999), the thermophillic *Tli*PAP1 (Singleton *et al.*, 1999a; 1999b),

*Pfu*PAP1 (Tanaka *et al.*, 2001) and *Pho*PAP1 (Sokabe *et al.*, 2002) have been deposited in the Protein Data Bank (see Section 2.11) as structural coordinate files [1AUG], [1A2Z], [1IOF] and [1IU8] respectively.

1.3.11.1 Crystallisation of PAP1

Crystallisation studies were carried out using the hanging drop vapour-diffusion method as described in Section 2.19. Initial screening was carried out with the sparse matrix conditions using a crystal screen kit.

Initial crystals for *Bam*PAP1 were obtained using an ammonium sulphate solution. Needle-shaped crystals were produced and proved to cause problems at the diffraction stage. These crystals did not diffract to high resolution and as a result crystallisation conditions were screened again. Protein crystals obtained from the following attempt were pentagonal in shape with average dimensions of 0.3 x 0.3 x 0.4 mm^3 and were suitable for diffraction studies. A *Bam*PAP1 protein concentration of 7 mg was used for this study. Crystallisation was performed using 0.05 M sodium cacodylate/KH_2PO^4 buffer with 0.1 M magnesium acetate, pH 6.5. 10% w/v PEG 4000 was used as precipitant. All of the aforementioned prokaryotic PAP1 enzymes were crystallised using methods similar to the above and crystals diffracted to a resolution of 2.0, 1.73, 2.2 and 1.6 Å for *Bam*PAP1, *Tli*PAP1, *Pfu*PAP1 and *Pho*PAP1 respectively.

1.3.11.2 Monomeric Structure of PAP1

The subunit monomers of *Bam*PAP1, *Tli*PAP1, *Pfu*PAP1 and *Pho*PAP1 (see Figures 1.11 - 1.14) are folded into single α/β globular domains with approximate dimensions of 75 Å x 55 Å x 45 Å. The central core is an α/β twisted open-sheet with α helices on both sides of the β sheet. The active site is located within each monomer and faces toward the central channel of the tetrameric structure (see Figure 1.15).

A hydrophobic pocket comprising of Phe10, Phe13, Thr45, Gln71, Ile92, Phe142 and Val143 is found near the catalytic triad of *Bam*PAP1. The feasibility of this substrate-binding pocket in *Bam*PAP1 was investigated by manually placing a pGlu-His model into the pocket through the use of molecular dynamics simulation software. Two methylene carbon atoms from the pGlu pyrrolidone ring point to the bottom of the hydrophobic pocket. The pyrrolidone ring is held between the aromatic ring of Phe13 and the methylene chain of Gln71. The pGlu main chain carbonyl forms a hydrogen bond with the guanidino group of Arg91, while the imidazole nitrogen of the histidine

side-chain hydrogen bonds with the main-chain of amide proton of Thr141, indicating that PAP1 is not selective for residues in the second position. The mechanism of substrate recognition was observed (Ito *et al.*, 2001) by X-ray crystallography of the substrate-inhibitor complex of *Bam*PAP1 and aldehyde pGlu analog 5-oxoprolinal. Results have indicated that the enzymatic recognition of the pyrrolidone ring of pyroglutamic acid is achieved by two hydrogen bonds between the inhibitor and the main chain located at the side of the cavity. These hydrogen bonds help to orientate the pGlu residue for nucleophilic attack by Cys144. Van der Waals interactions between the pyrrolidone ring and the hydrophobic pocket are also essential. The benzene rings of the 3 phenylalanine residues of the hydrophobic pocket of PAP1 and the pyrrolidone ring of the inhibitor are almost parallel. These three residues also fix the substrate pyrrolidone ring into the pocket. Phe13 along with Gln71 serve as an induced fit mechanism, while Phe142 provides hydrophobic properties. Phe10 was conserved in most enzymes, however, Phe13 and Phe147 have been replaced with Tyr in some cases.

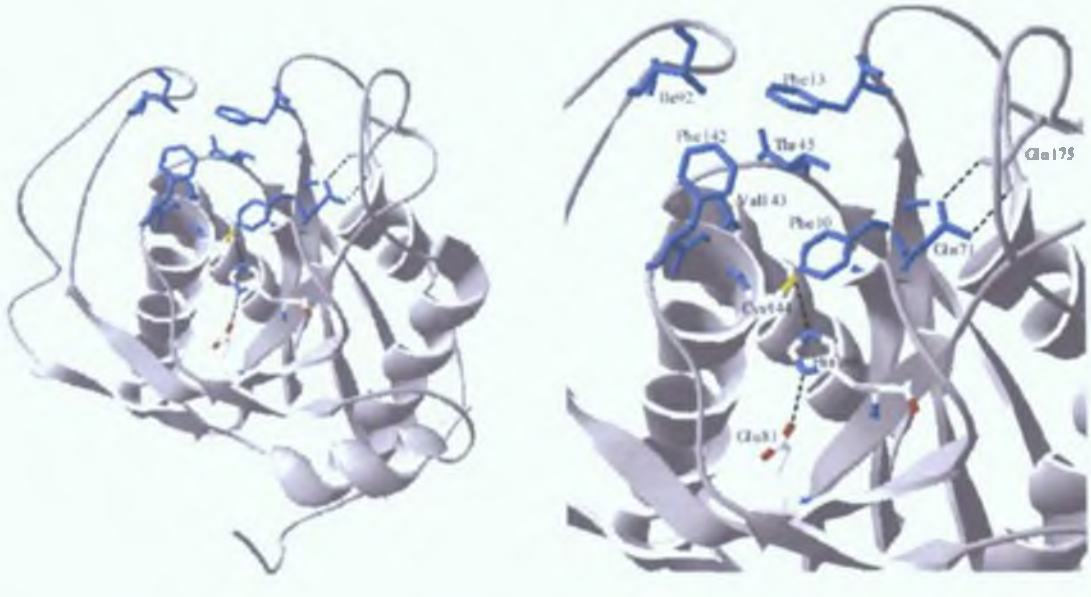

Figure 1.11 Subunit Monomer of *Bam*PAP1 With Detail of Active Site Region
Ribbon diagram of the subunit monomer of *Bam*PAP1. The entire monomer is shown on the left. On the right is a detail of the active site region. Residues Phe10, Phe 13, Thr45, Gln71, Ile92, Phe142 and Val143 contributing to the hydrophobic pocket are coloured blue. The side-chain of Gln71 is oriented by hydrogen bonding to Gln175. The catalytic triad is coloured by CPK colour scheme (C = white, O = red, N = blue and S = yellow). For amino acid information see Appendix D. Generated using DeepView (see Section 2.11).

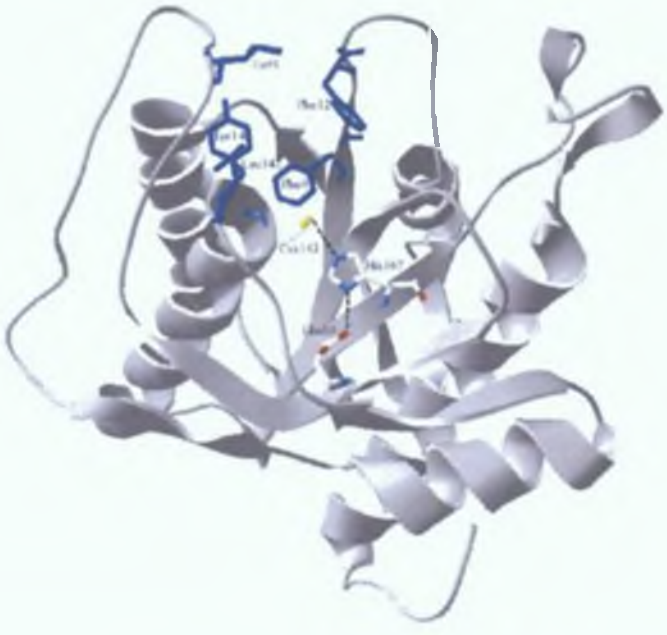

Figure 1.12 Subunit Monomer of *Tli*PAP1 Highlighting Active Site
Ribbon diagram of the subunit monomer of *Tli*PAP1. Residues contributing to the hydrophobic pocket are coloured blue while the catalytic triad is coloured by CPK colour scheme (C = white, O = red, N = blue and S = yellow). For amino acid information see Appendix D. Generated using DeepView (see Section 2.11).

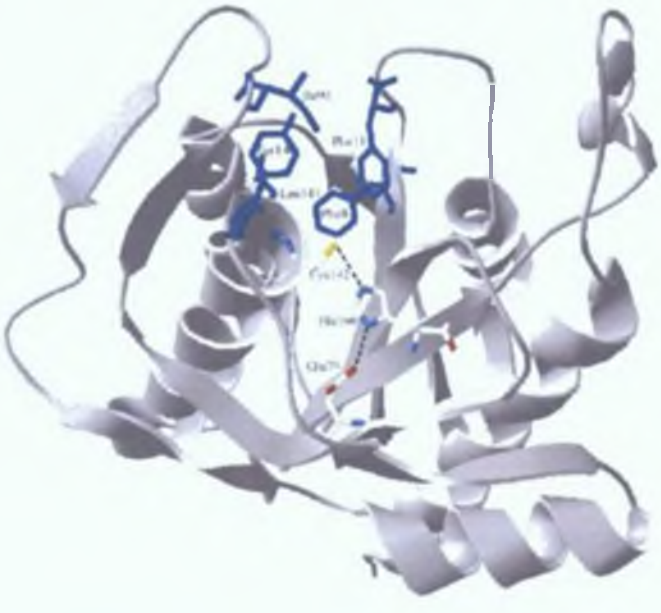

Figure 1.13 Subunit Monomer of *Pfu*PAP1 Highlighting Active Site
Ribbon diagram of the subunit monomer of *Pfu*PAP1. Residues contributing to the hydrophobic pocket are coloured blue while the catalytic triad is coloured by CPK colour scheme (C = white, O = red, N = blue and S = yellow). For amino acid information see Appendix D. Generated using DeepView (see Section 2.11).

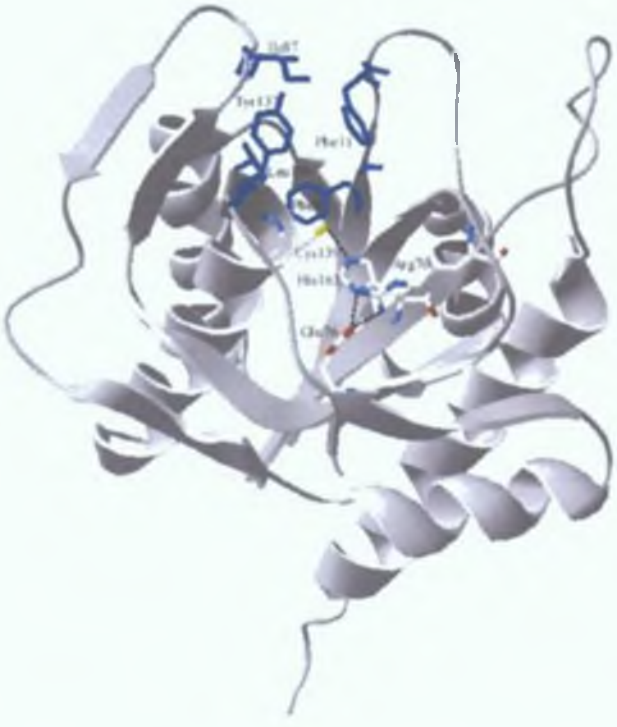

Figure 1.14 Subunit Monomer of *Pho*PAP1 Highlighting Active Site
Ribbon diagram of the subunit monomer of *Pho*PAP1. Residues contributing to the hydrophobic pocket are coloured blue while residues involved in catalysis are coloured by CPK colour scheme (C = white, O = red, N = blue and S = yellow). For amino acid information see Appendix D. Generated using DeepView (see Section 2.11).

1.3.11.3 Quaternary Structure of PAP1

The quaternary structure for *Bam*PAP1, *Tli*PAP1, *Pfu*PAP1 and *Pho*PAP1 is tetrameric and is composed of four identical monomeric subunits designated A to D (see Figure 1.15). Each monomer forms extensive contacts with two other monomers in the tetramer, one running along the longest axis of the tetramer and the other across the short axis.

The A-D interaction of *Bam*PAP1 (see Figure 1.16) buries 1427 $Å^2$ of primarily hydrophobic surface, although apparent salt bridges are also found (Odagaki *et al.*, 1999). Hydrophobic contacts dominate the A-D interaction. Ile85, Asn86, Leu87, Ala111, Ala112, Trp114, Tyr137, Thr138 and Thr141 are all involved in hydrophobic interactions and have close contacts with the nearest atoms of the adjacent monomer.

The A-C interaction (see Figure 1.17) buries less hydrophobic surface (1355 $Å^2$) than A-D interaction and forms no salt bridges. The following residues are involved in hydrophobic interactions; Met76, Ile131, Pro132, Pro173, Thr176, Leu177, Ala181, Pro182 and His 188. The A-C interaction also features a thin well-ordered water layer between the monomers. This layer covers almost one third of the A-C interface, and some of the hydrogen bonding between A and C is mediated by water molecules.

The tetrameric core of *Tli*PAP1 is approximately 6000 $Å^3$ comprised of loops of each monomer of the enzyme (Singleton *et al*, 1999) The core structure is maintained by hydrophobic interactions involving Phe179, Phe180, Leu181 and Leu182 of each subunit The A-B interface has hydrophobic interactions and salt bridges involving Arg81, Asp88, Asp101 and Arg119 also exist (see Figure 1 18) The A-C interface is formed by an external loop which folds towards the core structure Disulfide bridges exist between Cys190 of each monomer (see Figure 1 19)

The A-C and A-D interfaces of *Pfu*PAP1 consist mostly of hydrophobic interactions (Tanaka *et al*, 2001) There are no ionic interactions present at the A-C interface while, ten ionic bonds are present at the A-D interface (see Figure 1 20)

The A-B surface of *Pho*PAP1 is rich in hydrophobic residues Val78, Val80, Asn81, Met82, Ala106, Ala107, Phe109, Val129 and Leu130 which create an intersubunit hydrophobic core between A and B (Sokabe *at al*, 2002) Residues Asp84, Asp97, Arg77, Arg115 and Tyr132 are also involved in ionic interactions at the A-B interface (see Figure 1 21) Two salt bridges (Glu173-Lys122) and four hydrogen bonds (His72-Val171, His72-Lys174) exist between subunits A and C Most of the interactions between A and C are hydrogen bonds mediated by water, due to presence of a thin layer of water

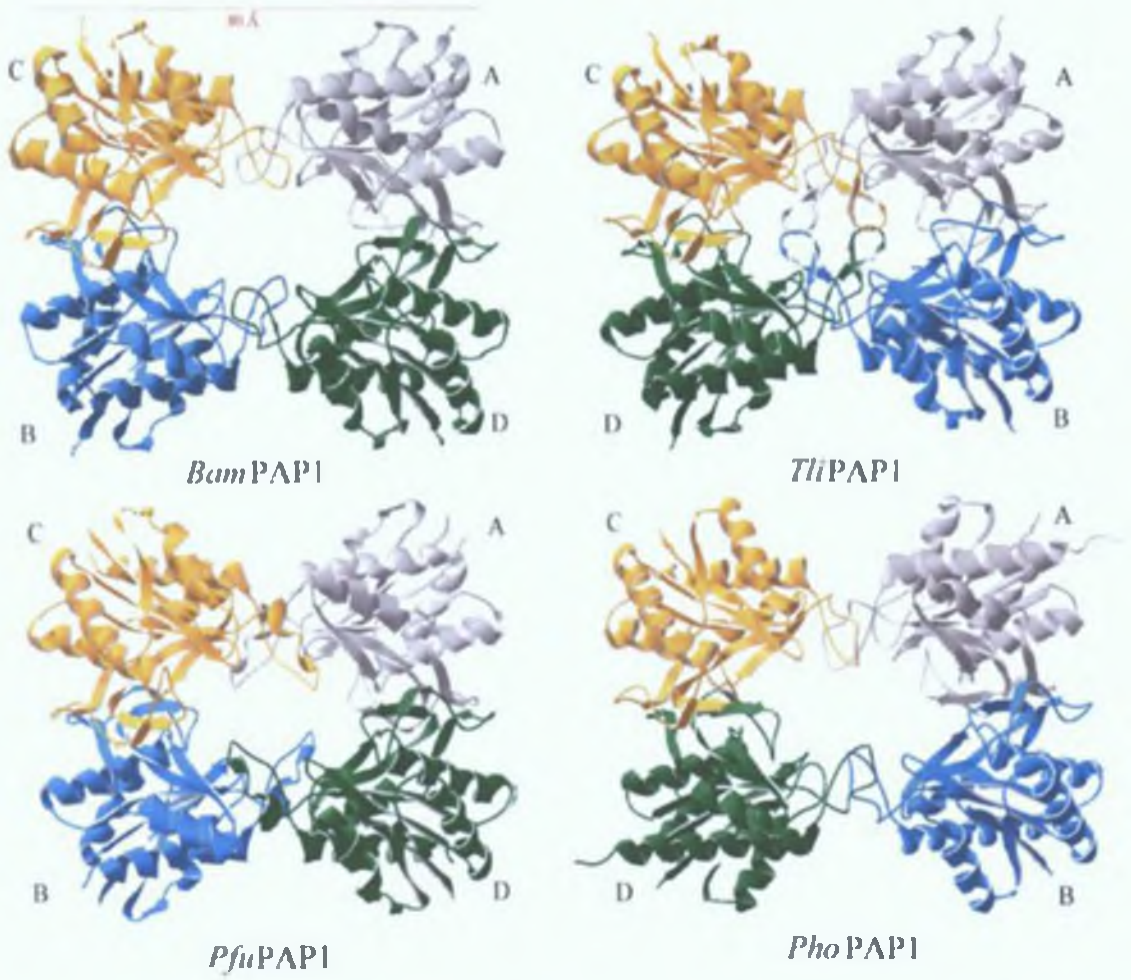

Figure 1.15 Tetrameric Arrangement of PAP1.
Ribbon diagrams of the tetrameric crystal structures of *Bam*PAP1, *Tli*PAP1, *Pfu*PAP1 and *Pho*PAP1. The monomeric subunits are labelled A to D and individually coloured. To give an idea of size, the distance of 80 Å has been indicated for *Bam*PAP1. Generated using DeepView (see Section 2.11).

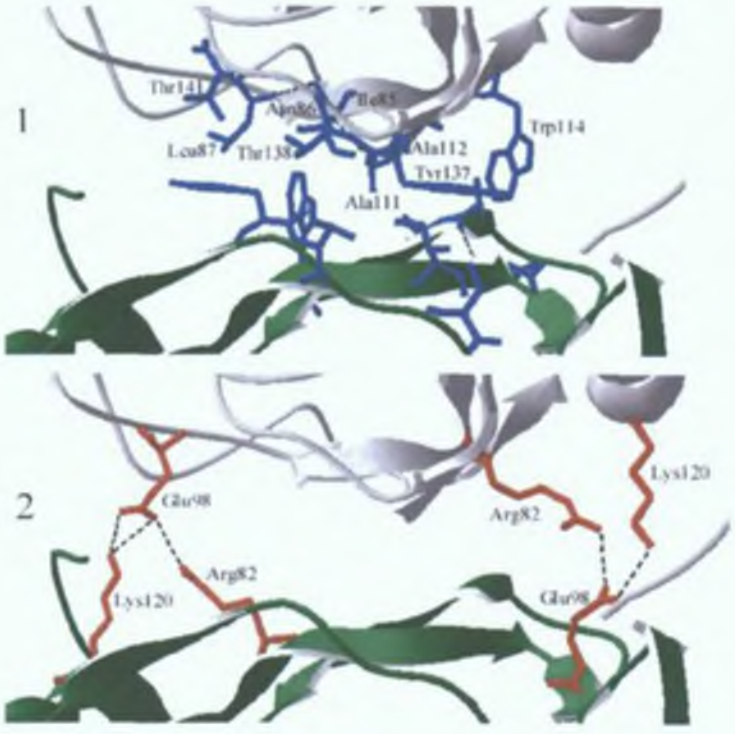

Figure 1.16 The A-D Interface of *Bam*PAP1.
Ribbon diagram of the A-D interface of *Bam*PAP1. The same subunit colour coding as in Figure 1.11 applies. (**1**): Residues Ile85, Asn86, Leu87, Ala111, Ala112, Trp114, Tyr137, Thr138 and Thr141 of each monomer contributing to hydrophobic interactions are shown. Only the residues from subunit A have been labelled. (**2**): Residues Arg82, Glu89 and Lys120 of each monomer involved in ionic interactions are shown. For amino acid information see Appendix D. Generated using DeepView (see Section 2.11).

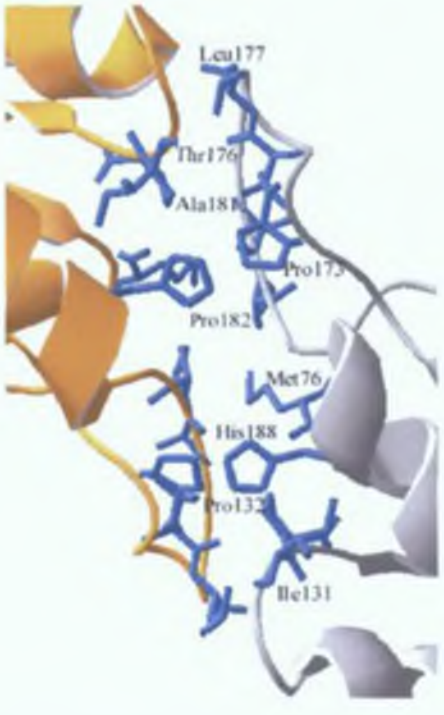

Figure 1.17 The A-C Interface of *Bam*PAP1
Ribbon diagram of the A-C interface of *Bam*PAP1. The same subunit colour coding as in Figure 1.11 applies. Residues Met76, Ile131, Pro132, Pro173, Thr176, Leu177, Ala181, Pro182 and His188 contributing to hydrophobic interactions are shown. Only the residues from subunit A have been labelled. For amino acid information see Appendix D. Generated using DeepView (see Section 2.11).

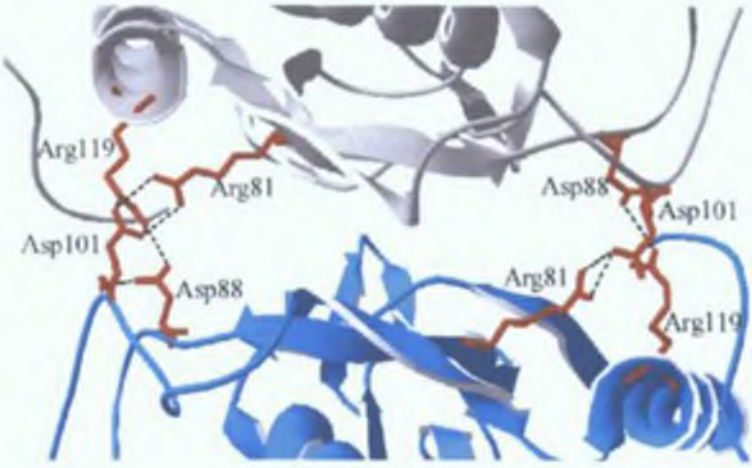

Figure 1.18 The A-B Interface of *Tli*PAP1

Ribbon diagram of the A-B interface of *Tli*PAP1. The same subunit colour coding as in Figure 1.11 applies. Residues involved in ionic interactions are shown. For amino acid information see Appendix D. Generated using DeepView (see Section 2.11).

Figure 1.19 The A-C Interface of *Tli*PAP1

Ribbon diagram of the A-C interface of *Tli*PAP1. The same subunit colour coding as in Figure 1.11 applies. The disulphide bridge is shown and coloured by CPK colour scheme (C = white, O = red, N = blue and S = yellow). For amino acid information see Appendix D. Generated using DeepView (see Section 2.11).

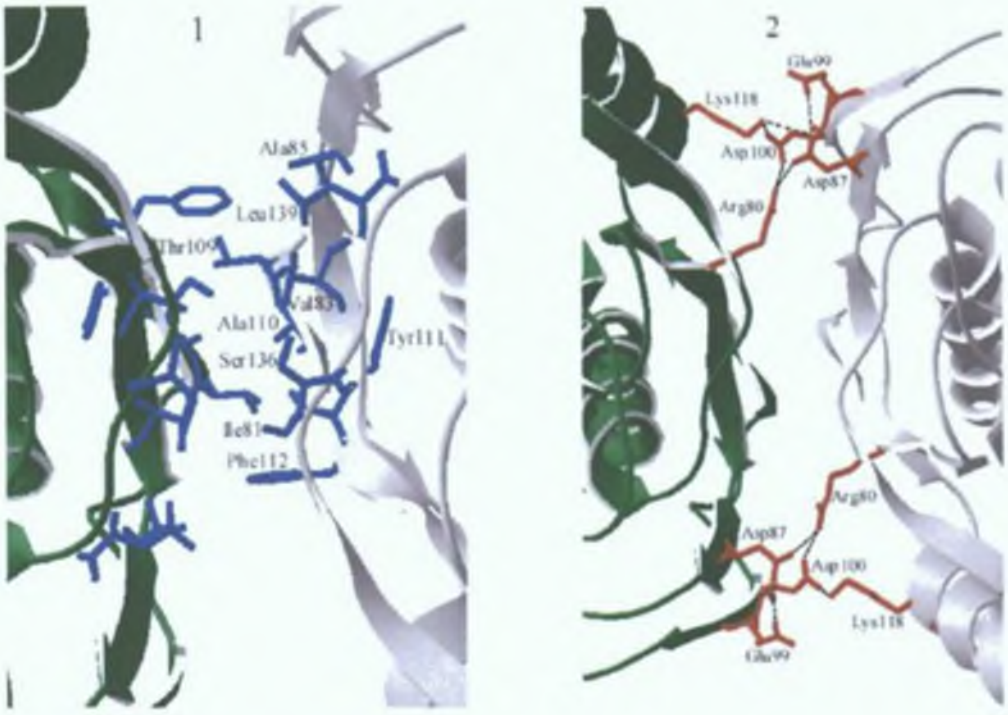

Figure 1.20 The A-D Interface of *Pfu*PAP1

Ribbon diagram of the A-D interface of *Pfu*PAP1. The same subunit colour coding as in Figure 1.11 applies. (1): Residues contributing to hydrophobic interactions are shown. Only the residues from subunit A have been labelled. (2): Residues Arg80, Asp87, Glu99, Asp100 and Lys118 involved in ionic interactions are shown. For amino acid information see Appendix D. Generated using DeepView (see Section 2.11).

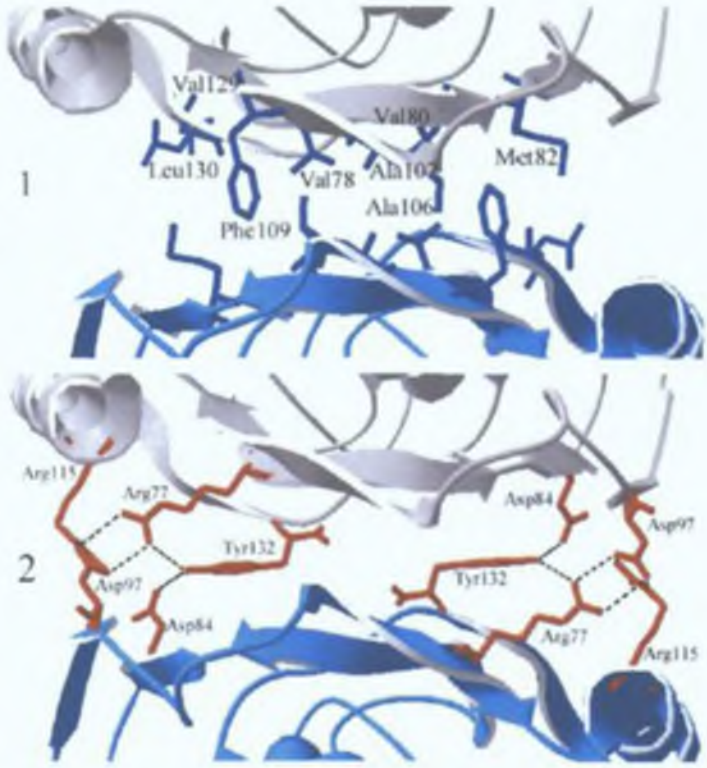

Figure 1.21 The A-B Interface of *Pho*PAP1

Ribbon diagram of the A-B interface of *Pho*PAP1. The same subunit colour coding as in Figure 1.11 applies. (**1**): Residues Val78, Val80, Met82, Ala106, Ala107, Phe109, Val129 and Leu130 contributing to hydrophobic interactions are shown. Only the residues from subunit A have been labelled. (**2**): Residues Arg77, Asp84, Asp97, Arg115 and Tyr132 involved in ionic interactions are shown. For amino acid information see Appendix D. Generated using DeepView (see Section 2.11).

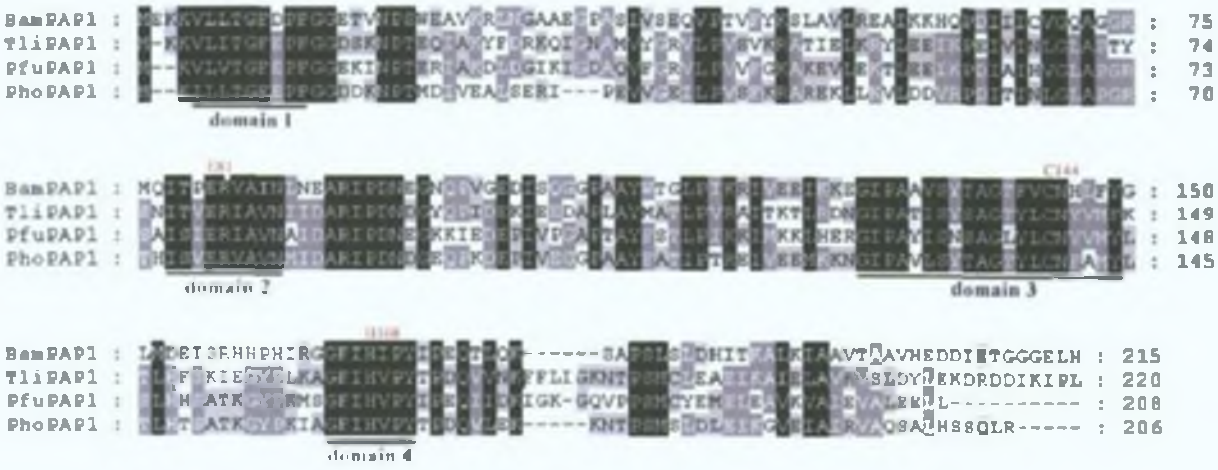

Figure 1.22 Amino Acid Alignment of *Bam*PAP1, *Tli*PAP1, *Pfu*PAP1 and *Pho*PAP1

Alignment was created using MultAlin with Blosum62-12-2 parameters and edited using GenDoc (see Section 2.11). Sequence homology is represented by grey scale shading, with black being the highest homology. Catalytic residues have been marked in red (numbering applies to *Bam*PAP1). For amino acid information see Appendix D.

1.3.12 Mutational Analysis of PAP1

A series of studies have been carried out using site-directed mutagenesis to probe a relationship between structure and function of PAP1. This approach has also been used to determine the essential residues of the catalytic triad (see Section 1.3.10).

The three *Bam*PAP1 residues of the hydrophobic pocket Phe10, Phe13 and Phe142 (see Section 1.3.11.2) were mutated to Tyr and Ala by Ito *et al.*, 2001. The catalytic efficiency of both *Bam*PAP1_F13mA and *Bam*PAP1_F142mA decreased more than 1000-fold while *Bam*PAP1_F10mA which was severely destabilised and suffered a major structural change could not be purified. The K_m value and K_{cat} obtained for *Bam*PAP1_F10mY were 3.6-fold higher and 5.8-fold lower, respectively than wild type values.

The increased thermostability of *Tli*PAP1 (see Section 1.3.8) has been attributed to the inter subunit disulphide bond formed by Cys190 (see Figure 1.19). This residue corresponds to Ser185 in *Bam*PAP1, Cys188 in *Pfu*PAP1 and Ser181 in *Pho*PAP1 by sequence alignment (see Figure 1.22). Although Cys188 of *Pfu*PAP1 is located in a similar position to Cys190 in *Tli*PAP1, *Pfu*PAP1 does not exhibit a disulphide bridge in the crystal structure (see Section 1.3.11.3).

To investigate the possibility of intersubunit disulfide bonds effecting thermal stability in oligomeric enzymes Kabashima *et al.*, (2001) substituted Ser185 with a cysteine residue to yield *Bam*PAP1_S185mC. The enzyme was analysed by SDS-PAGE both with and without 2-ME. A molecular mass of 30 kDa and 60 kDa were obtained for the mutant, with and without 2-ME, respectively. These results suggest that the disulphide bridge between the mutated Cys185 bonded two subunits. Introduction of the disulphide bond did not affect the catalytic efficiency of the enzyme, while thermal stability was increased by 30°C. However, under reducing conditions using 1 mM DTT, no difference in thermal stability was observed, indicating that the enhanced thermostability was due to the introduction of the intersubunit disulphide bond.

1.4 PAP2

In 1981, Browne *et al.*, were the first to report the presence of two distinct pyroglutamyl peptidase activities in guinea pig brain. They reported the presence of a membrane-associated enzyme (classified PAP2) that possessed a high molecular weight and was rendered inactive in the presence of DTT and EDTA, while the soluble form of PAP (see Section 1.3) required these substances to remain active.

The Enzyme Commission List classifies PAP2 as an omega peptidase (E C 3 4 19 6) In the alternative Merops database PAP2 has been assigned under metallopeptidase clan MA, family M1 Zinc has been identified as the catalytically active metal ion for the majority of metalloproteases Researchers observed that after the enzyme was inactivated by EDTA treatment that it could be restored by the addition of Zn^{2+} (Czekay and Bauer, 1993, Gallagher and O'Connor, 1998)

PAP2 is primarily located in the mammalian central nervous system with significantly smaller levels observed in other tissues It appears to be associated exclusively with neurons, primarily on the synaptosomal membrane, and has been identified in a number of sources which include rat (Taylor and Dixon, 1979, Bauer, 1994), porcine (Bauer, 1994, Schmeitmeier, *et al*, 2002, bovine (O'Leary and O'Connor, 1995, Gallagher and O'Connor, 1998, guinea pig (O'Connor and O'Cuinn, 1985), rabbit (Wilk and Wilk, 1989), mouse (Cruz *et al*, 1991), human (Schomburg *et al*, 1999)

PAP2 is of relatively large molecular size with estimates of 230,000-240,000 Da (O Connor and O'Cuinn, 1984, Wilk and Wilk, 1989, Bauer, 1994, O'Leary and O'Connor, 1995) The enzyme was found to be inhibited by the metal chelators EDTA, EGTA, 8-hydroxyquinoline, 1-10-phenanthroline and showed no sensitivity towards sulphydryl reagents (O'Connor and O'Cuinn, 1984, Wilk and Wilk, 1989, Bauer, 1994, O'Leary and O'Connor, 1995, Gallagher and O'Connor, 1998) Inhibitors of cysteine, serine and aspartyl proteases did not affect PAP2 activity Active site directed inhibitors of PAP1 were also ineffective towards PAP2

In recent times a specific inhibitor of PAP2 has been identified It was identified by screening extracts from marine species of the Cuban coastline and was isolated from the marine annelida *Hermodice carunculata,* (HcPL) HcPL inhibited PAP2 with an apparent K_i of 51 nM It was found to reduce both mouse pituitary and brain PAP2 activities It was the first M1 family zinc metallopeptidase inhibitor to be isolated from marine invertebrates (Pascual *et al*, 2004)

The predominant feature of PAP2 is its unique substrate specificity PAP2 has been reported to remove the N-terminal pGlu residue from only TRH or closely related tripeptides or tripeptide amides (O'Connor and O'Cuinn, 1984, , Elmore *et al*, 1990)

Enzyme activity was abolished when the pGlu residue of the TRH sequence was replaced with a Glu residue or when the His was replaced with either a Phe or Nval residue While PAP2 was capable of limited hydrolysis of pGlu-His-Pro-Gly, the lengthened substrates pGlu-His-Pro-Gly-NH_2 and pGlu-His-Pro-Gly-Lys were not hydrolysed Only tripeptides

containing histidine in the central position were hydrolysed Pyroglutamate-containing dipeptides including pyroglutamyl histidine were not hydrolysed nor were pyroglutamyl-containing peptides with more than three amino acids (O'Connor and O'Cuinn, 1984)

The genes for rat and human PAP2 were cloned (Schauder *et al* 1994, Schomburg *et al* , 1999) The deduced highly homologous amino acid sequences are consistent with a glycosylated, membrane anchored peptidase The extracellular domain of PAP2 contains the HEXXH + E motif which is consistent with zinc-dependent metallopeptidases where the three zinc ligands are the two His residues and the Glu residue C-terminal to the HEXXH motif

Human and rat PAP2 sequences were found to exhibit a high degree of conservation with 96% of residues being identical Northern blot analysis demonstrated a restricted tissue distribution with highest transcript levels in the brain Southern analysis suggested that the gene is present as a single copy in human, monkey, rat, mouse, dog, bovine, rabbit and chicken DNA

A serum form of PAP2 of liver origin has been reported, which has the same degree of specificity for TRH and identical biochemical characteristics as the membrane-bound form (Cummins and O'Connor, 1998) A recent study (Schmitmeier *et al* , 2002) has supported the hypothesis that both forms of PAP2 are derived from the same gene, whereby the serum enzyme is generated by proteolytic cleavage of the membrane-bound form in the liver

1 5 Project Aims and Objectives

The main objective of this research project was to clone the gene for bovine PAP1 followed by expression of this protein utilizing a method which had been previously developed for the expression of human PAP1 Following expression bovine PAP1 could be then purified using one-step affinity-tag chromatography This would allow for the molecular, biochemical and kinetic characterisation of bovine PAP1 Due to the availability of recombinant human PAP1 (Vaas, 2005), a comparative study of these two enzymes could be employed This study will allow us to further characterise this family of cysteine peptidases There are multiple homologues of this family and it is important to compare them to determine functionality and identify essential amino acid residues

A series of site-directed and random mutants would be generated for human PAP1, giving valuable insight into the catalytic and structural properties of human PAP1

An attempt to crystallise human PAP1 would be made using a sparse matrix screening approach A visit to a laboratory specialising in protein crystallography in Toronto, Canada would also be made during this work Using X-ray crystallography and site-directed mutagenesis a structure/function relationship could be investigated Such studies would present an improved understanding of molecular structures and interactions of proteins could open way to inhibitor design

CHAPTER TWO

Materials & Methods

2.1 Bacterial Strains, Primers and Plasmids

The bacterial strains, primers and plasmids used in this work are listed in Tables 2.1, 2.2 and 2.3 respectively.

Table 2.1 Bacterial Strains

Strain	Genotype	Features/Uses	Source
Escherichia coli			
XL-10 Gold	Δ(*mcr*A)183 Δ(*mcr*CB-*hsd*SMR-mrr)173 *end*A1 *rec*A1 *rel*A1 *gyr*A96 *sup*E44 *thi*-1 *lac* Hte [F' *pro*AB *lacI*^{q}ZΔM15 ::Tn10(*tet*^{R}) Amy (*cam*^{R})]	High transformation efficiency Antibiotic resistance Expression host	Stratagene

Table 2.2 Primers (obtained from MWG-Biotech AG)

Name	Sequence (5' – 3')	T_m (°C)
Human PAP1 Analysis/Mutagenesis		
PAPHsA	AACAGAAGCAGGTCCGAGG	58.8
PAPHsB	CAGGATGAGGTCTTAGGAGA	57.3
PAPHsEmK-F	ACAGTCACACTGAAGAAATGTGGACACAAC	65.4
PAPHsEmK-R	GTTGTGTCCACATTTCTTCAGTGTGACTGT	65.4
PAPHsEmQ-F	ACAGTCACACTGCAGAAATGTGGACACAAC	66.8
PAPHsEmQ-R	GTTGTGTCCACATTTCTGCAGTGTGACTGT	66.8
PAPHsEmD-F	ACAGTCACACTGGATAAATGTGGACACAAC	66.3
PAPHsEmD-R	GTTGTGTCCACATTTATCCAGTGTGACTGT	66.3
Bovine PAP1 Cloning/Mutagenesis		
PAPBtA	GAACCCGCCATGGAGCAGCCCAGGAAGGCGG	75.0
PAPBtB	CAGCAAGGATCCGTGTTCATGGCAACAGTTG	69.5
PAPBtEmQ-F	AACCGCAGTCACACTGGACAAGTGTGGACA	69.5
PAPBtEmQ-R	TGTCCACACTTGTCCAGTGTGACTGCGGTT	69.5
PAPBtCmF-F	GCAGGCAGGTACCTCTTCGACTTCACCTAC	70.9
PAPBtCmF-R	GTAGGTGAAGTCGAAGAGGTACCTGCCTGC	70.9
PAPBtHmD-F	CGCTCAGCCTTTGTTGACGTGCCCCCTCTG	73.6
PAPBtHmD-R	CAGAGGGGGCACGTCAACAAAGGCTGAGCG	73.6
PAPBtAmT-F	TCAGGCATGGCAACCACAGTCACACTGGAG	70.9
PAPBtAmT-R	CTCCAGTGTGACTGTGGTTGCCATGCCTGA	70.9

PAPBtCmY-F	CAGTCAGAAGGCAAAATCAACTATTGCCAT	64.0
PAPBtCmY-R	ATGGCAATAGTTGATTTTGCCTTCTGACTG	64.0
PAPBtEmK-F	GGCAAAATCAACTGTTGCCATAAACACGGA	65.4
PAPBtEmK-R	TCCGTGTTTATGGCAACAGTTGATTTTCCG	65.4
Amp-for	GAGTATTCAACATTTCCGTGTCGC	61.0
Amp-rev	CCAATGCTTAATCAGTGAGGCAC	60.7

T_m takes into account only those bases that bind.

$T_m = [69.3 + 0.41(\%GC)] - 650/length$

Sequencing		
M13rev(-29)	CAGGAAACAGCTATGACC	(pCR2.1 forward primer, MWG-Biotech)
M13uni(-21)	TGTAAAACGACGGCCAGT	(pCR2.1 reverse primer, MWG-Biotech)
PQEfor	GTATCACGAGGCCCTTTCGTCT	(pQE-60 forward primer, MWG-Biotech)
PQErev	CATTACTGGATCTATCAACAGGAG	(pQE-60 reverse primer, MWG-Biotech)
PTrcHisrev	CTTCTGCGTTCTGATTTAATCTG	(pPC225 forward primer, MWG-Biotech)
M13rev(-49)	GAGCGGATAACAATTTCACACAGG	(pPC225 reverse primer, MWG-Biotech)

Table 2.3 Plasmids

Plasmid	Description	Source
Vectors		
pCR2.1	TA cloning vector: P*lac*, *amp*^{R}, *kan*^{R}, *lacZ*α, ColE1 origin. Figure 2.1	Invitrogen
pQE-60	Expression vector: T5 promoter/*lac* operon, *amp*^{R}, 6xHis sequence at 3' end of MCS, ColE1 origin. Figure 2.2	Qiagen
pPC223	Modified derivative of pKK223-3 expression vector from Amersham Pharmacia: P*tac*, *amp*^{R}. ColE1 origin. Elimination of *Bam*HI site external to MCS	Clarke (2000)
pPC225	Modified derivative of pPC223. Insertion of 1800 bp fragment in *Bam*HI of MCS for ease of cloning. Figure 2.3	Clarke (2000)
pBR322	Cloning vector: P*lac*, *amp*^{R}, *lacZ*α, *tet*^{R}.	Amersham Pharmacia
Constructs		
pZK1	pCR2.1 containing bovine PAP1 ORF	This Work
pZK2	pQE-60 containing bovine PAP1 ORF with 3' 6xHis sequence fusion.	This Work
pZK3	pPC225 containing bovine PAP1 ORF with 3' 6xHis sequence fusion, sub-cloned from pZK2, for expression and subsequently	This Work

	purification	
pRV5	pPC225 containing human PAP1 ORF with 3' 6xHis sequence fusion for expression and subsequently purification	Vaas, 2005
pZK3 mutant derivatives		
pZK3_E85mQ	Mutation: E85 to Q (GAA to CAA)	This Work
pZK3_C149mF	Mutation: C149 to F (TGC to TTC)	This Work
pZK3_H168mD	Mutation: H168 to D (CAC to GAC)	This Work
pZK3_A81mT	Mutation: A81 to T (GCA to ACA)	This Work
pZK3_C205mY	Mutation: C205 to Y (TGT to TAT)	This Work
pZK3_E208mK	Mutation: E208 to K (GAA to AAA)	This Work
pRV5 mutant derivatives		
Site-Directed Mutagenesis		
pZK_E85mD	Mutation: E85 to D (GAG to GAT)	This Work
pZK_E85mK	Mutation: E85 to K (GAG to AAG)	This Work
pZK_E85mQ	Mutation: E85 to Q (GAG to CAG)	This Work
Random Mutagenesis		
pZK_G35mD	Mutation: G33 to T (GGC to GAC)	This Work
pZK_N90mD	Mutation: N90 to D (AAC to GAC)	This Work
pZK_M192mT	Mutation: M192 to T (ATG to ACG)	This Work
pZK_K94mR	Mutation: K94 to R (AAG to AGG)	This Work
pZK_A165mV	Mutation: A165 to V (GCC to GTC)	This Work
pZK_P48mR	Mutation: P48 to R (CCG to CGG)	This Work
pZK_A184mP	Mutation: A184 to P (GCC to CCC)	This Work
pZK_P48mQ,D143mH	Mutation: P48 to Q (CCG to CAG), D143 to H (GAT to CAT)	This Work
pZK_P67mR	Mutation: P67 to R (CAC to CGC)	This Work
pZK_M122mV	Mutation: M122 to V (ATG to GTG)	This Work
pZK_G77mD	Mutation: G77 to D (GGC to GAC)	This Work
pZK_N22mH	Mutation: N22 to H (AAC to CAC)	This Work
pZK_A27mT	Mutation: A27 to T (GCA to ACA)	This Work
pZK_P4mS,S164mP	Mutation: P4 to C (CCG to TCG), S164 to P (TCA to CCA)	This Work

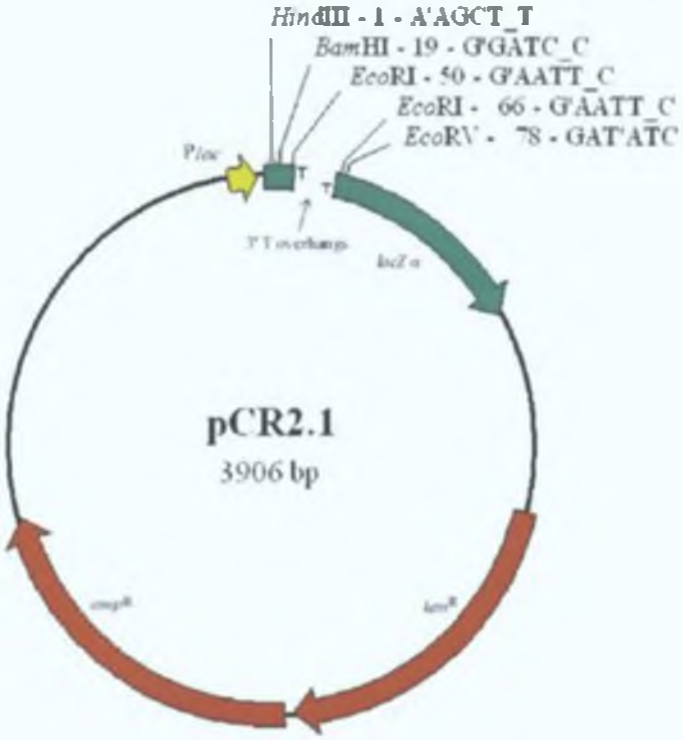

Figure 2.1 pCR2.1 Vector

The 3906 bp TA cloning vector pCR2.1 (see Table 2.3). The multiple cloning site (MCS) enzymes are indicated. The TA cloning site is situated within the *LacZα* ORF (green), which is under the control of the P_{lac} promoter (yellow). Ampicillin and Kanamycin resistance genes (*amp*^{R} & *kan*^{R}) are shown in red. Generated using pDRAW32 (see Section 2.11).

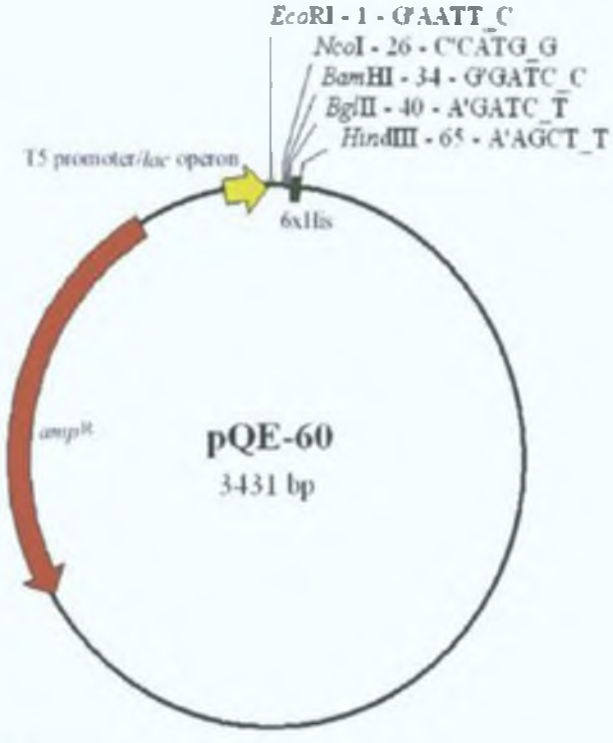

Figure 2.2 pQE-60 Vector

The 3431 bp cloning/expression vector pQE-60 (see Table 2.3). The multiple cloning site (MCS) enzymes are indicated. The 6xHis coding sequence (green) is situated at the 3' end of the MCS, which in turn is situated downstream of the T5 promoter/*lac* operon (yellow). Ampicillin resistance gene (*amp*^{R}) is shown in red. Generated using pDRAW32 (see Section 2.11).

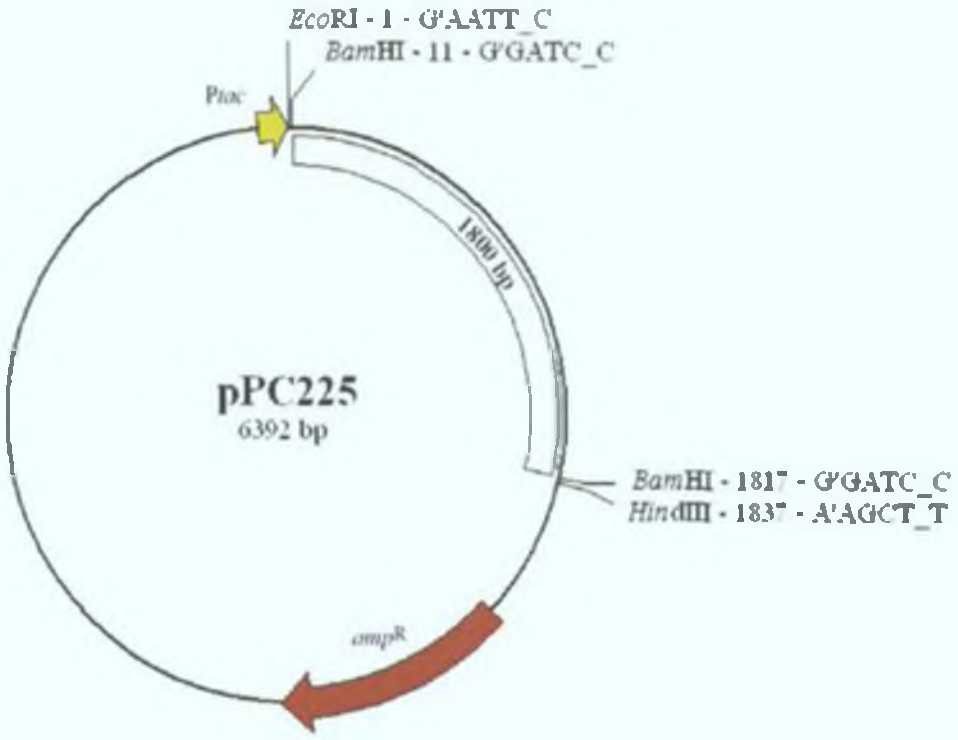

Figure 2.3 pPC225 Vector

The 6392 bp cloning/expression vector pPC225 (see Table 2.3). The multiple cloning site (MCS) enzymes are indicated. A 1800 bp sequence (white box) is situated within the MCS, which in turn is situated downstream of the P_{tac} promoter (yellow). Ampicillin resistance gene (*amp*^{R}) is shown in red. Generated using pDRAW32 (see Section 2.11).

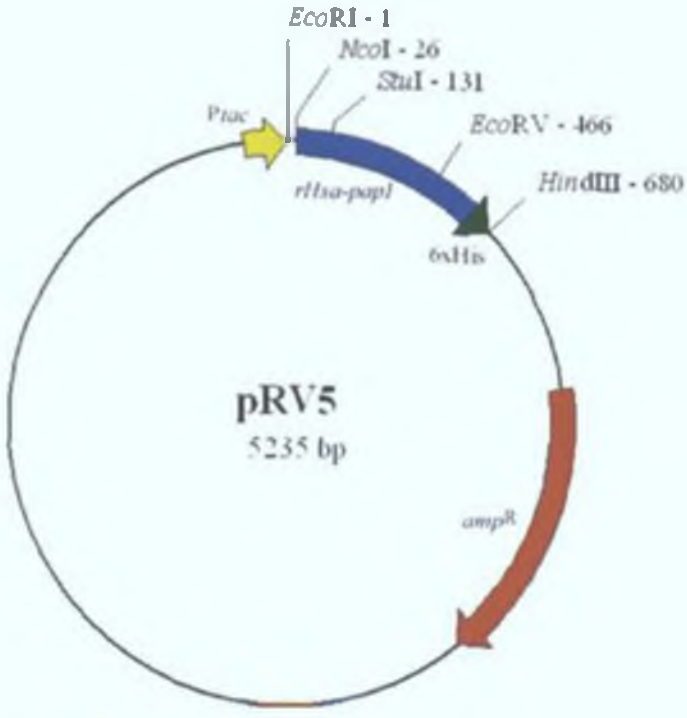

Figure 2.4 pRV5 Vector

The 5,235 bp construct pPRV5 (see Table 2.3). pPC225 containing PAP1 ORF with 3' 6xHis sequence fusion, sub-cloned from pQE60, for expression and subsequently purification. The Ampicillin resistance gene (*amp*^{R}) is shown in pink. Generated using pDRAW32 (see Section 2.11).

2 2 Media, Solutions and Buffers

All chemicals and reagents were obtained from Sigma-Aldrich unless otherwise stated All chemicals were Analar grade Microbiological media were obtained from Oxoid Sterilisation was achieved by autoclaving at 121°C and 15 lb/in^2 for 20 min, unless otherwise stated

Luria Bertani Broth (LB)

Tryptone	10 g/L
NaCl	10 g/L
Yeast Extract	5 g/L

Adjusted to pH 7 0 with NaOH Sterilised by autoclaving For solid broth LB, 15 g/L Technical Agar No 3 (Oxoid) was included

SOB Broth

Tryptone	20 g/L
NaCl	500 mg/L
Yeast Extract	5 g/L
KCl	2 5 mM
pH	7 0

After autoclaving, $MgCl_2$ and $MgSO_4$ were added to 10 mM of sterile 1 M stock solutions

TE Buffer

Tris-HCl	10 mM
Na_2-EDTA	1 mM
pH	8 0

TAE Buffer (50X)

Tris	242 g/L
Glacial Acetic Acid	57 1 ml/L
EDTA	100 ml/L (of 0 5 M stock)
pH	8 0

STET Buffer

Sucrose	8% (w/v)
Triton X-100	5% (v/v)
Tris-HCl	50 mM
Na_2-EDTA	50 mM
pH	8 0

Solution 1 of 1-2-3 Method (see Section 2 4 1 2)

Glucose	50 mM
Na_2-EDTA	10 mM (from 0 5 M stock)
Tris-HCl	25 mM (from 1 M stock)

Solution 2 of 1-2-3 Method (see Section 2 4 1 2)

NaOH	200 mM
SDS	1% (w/v)

Solution 3 of 1-2-3 Method (see Section 2 4 1 2)

Potassium acetate	3 M
pH	4 8

To 60 ml of 5M potassium acetate, 11 5 ml of glacial acetic acid and 28 5 ml of dH_2O were added The resulting solution was 3 M with respect to potassium and 5 M with respect to acetate

TB Buffer

Pipes	10 mM
$CaCl_2$	15 mM
KCl	250 mM
pH	6 7

The pH was adjusted with KOH and then $MnCl_2$ was added to 55 mM The solution was filter sterilised through a 0 22 μM membrane (Millipore) and stored at 4°C

RF1 Buffer

RbCl	100 mM
$CaCl_2$	10 mM
Potassium acetate	30 mM
Glycerol	15% (v/v)
pH (with HCl)	5 8

After the pH had been adjusted $MnCl_2$ was added to 50 mM The solution was filter sterilised through a 0 22 μM membrane (Millipore) and stored at 4°C

RF2 Buffer

RbCl	10 mM
MOPS	10 mM
$CaCl_2$	75 mM
Glycerol	15% (v/v)
pH	6 8

The solution was filter sterilised through a 0 22 μM membrane (Millipore) and stored at 4°C

Gel Loading Dye (6X)

Bromophenol Blue	0 25%
Xylene Cyanol	0 25%
Ficoll (Type 400)	15%

Bromophenol Blue and/or Xylene Cyanol were used as appropriate On a 1% agarose gel, bromophenol blue and xylene cyanol migrate approximately with the 300 base pairs and 4000 base pairs DNA fragments respectively

Ethidium Bromide Stain

A 10 mg/ml stock solution in dH_2O was stored at 4°C in the dark For the staining of agarose gels, 100 μl of the stock solution was mixed into 1 L of dH_2O The staining solution was kept in a plastic tray and covered to protect against light After use ethidium bromide stain was collected and filtered through a deactivating filter according to the method of Schleicher & Schuell

2.3 Antibiotics

- Ampicillin was prepared in dH_2O at a concentration of 100 mg/ml and stored at –20°C. The working concentration for *E. coli* was 100 μg/ml.
- Chloramphenicol was prepared in ethanol at a concentration of 100 mg/ml and stored at –20°C. The working concentration for *E. coli* was 25 μg/ml.
- Tetracycline was prepared in 50 % ethanol at a concentration of 10 mg/ml and stored at –20°C. The working concentration for *E. coli* was 10 μg/ml.
- Kanamycin was prepared in dH_2O at a concentration of 100 mg/ml and stored at –20°C. The working concentration for *E. coli* was 30 μg/ml.

2.4 Isolation and Purification of DNA and RNA

2.4.1 Isolation of Plasmid DNA

Two procedures for the isolation of plasmid DNA were variably employed. The 1-2-3 Method (see Section 2.4.1.1) was used routinely. The Genelute Plasmid Miniprep Kit (Sigma, see Section 2.4.1.2) was used to prepare consistently pure and supercoiled plasmid DNA, mostly for the purpose of DNA sequencing.

2.4.1.1 1-2-3 Method

This method is adapted from the procedure described by Birnboim and Doly (1979). 1.5 ml of a bacterial culture was centrifuged in a microfuge tube at 13,000 rpm for 5 min to collect the cells. The supernatant was discarded and the cell pellet re-suspended in 200 μl of Solution 1. Alternatively, bacterial growth was taken off an LB agar culture plate with a sterile loop and re-suspended in 200 μl of Solution 1. The re-suspension was left for 5 min at room temperature. 200 μl of Solution 2 was added, the tube was mixed by inversion and placed on ice for 5 min. 200 μl of Solution 3 was added and the tube mixed by inversion and placed on ice for 10 min. A clot of chromosomal DNA was collected by centrifugation at 13,000 rpm for 10 min (Hermle Bench Centrifuge, Z160M). The supernatant was removed and placed in a new microfuge tube with 400 μl of phenol chloroform isoamylalcohol (25:24:1) and mixed by brief vortexing. Upon centrifugation at 13,000 rpm for 5 min the mixture is divided into an upper aqueous and lower organic layer. The aqueous layer was removed to a new microfuge tube with an equal volume of isopropanol and mixed by inversion. The tube was left at room temperature for 5 min and then centrifuged at 13,000 rpm for 20 min to pellet the plasmid DNA. The pellet was washed with 70% ethanol and then dried briefly in a

SpeedVac (Savant) vacuum centrifuge. The plasmid DNA was resuspended in 50 μl of TE buffer and 1 μl of Ribonuclease A (see Section 2.8) was added to digest co-purified RNA. Plasmid DNA was stored at –20°C.

2.4.1.2 GenElute Plasmid Miniprep Kit

This miniprep kit was used according to the manufacturer's instructions: 1.5 ml of a bacterial culture in a microfuge tube was centrifuged at 13,000 rpm for 5 min (Hermle Bench Centrifuge, Z160M) to collect the cells. The supernatant was discarded and the cell pellet was completely re-suspended in 200 μl of re-suspension solution. 200 μl of lysis solution was mixed in by inversion to lyse the cells. 350 μl neutralisation/binding buffer was added and mixed by inversion to precipitate cell debris, lipids, proteins and chromosomal DNA. The precipitate was collected by centrifugation at 13,000 rpm for 10 min. The supernatant was transferred to a spin column in a microfuge tube and centrifuged at 13,000 rpm for 1 min to bind the plasmid DNA. The flow through was discarded and 750 μl of washing solution was added followed by further centrifugation at 13,000 rpm for 1 min. The flow through was discarded and the column was centrifuged at 13,000 rpm for 1 min to dry the spin column. The spin column was transferred to a new microfuge tube and 100 μl TE buffer was added. The DNA was collected by centrifugation at 13,000 rpm for 1 min.

2.4.2 Isolation of DNA From Agarose Gels

The PerfectPrep Kit (Eppendorf, see Section 2.4.2.1) was used to purify DNA from agarose gels.

2.4.2.1 PerfectPrep Kit

The kit was used according to the manufacturer's instructions: The desired DNA band was excised from the agarose gel using a scalpel. The gel slice was weighed and placed in a microfuge tube. The tube was incubated at 65°C for 10 min to completely dissolve the agarose in the chaotropic (binding buffer) solution. One gel slice volume of isopropanol was added and mixed by inversion. The solution was transferred to a filter column in a microfuge tube and centrifuged at 13,000 for 1 min to bind the plasmid DNA. The flow through was discarded and 750 μl of washing solution was added followed by further centrifugation at 13,000 rpm for 1 min. The flow through was discarded and the column was centrifuged at 13,000 rpm for 1 min to dry the spin

column The spin column was transferred to a fresh microfuge tube and 30 µl TE buffer was added The DNA was eluted by centrifugation at 13,000 rpm for 1 min

2 4 3 Purification and Concentration of DNA Samples

The sample containing the DNA to be precipitated was brought to 400 µl with dH_2O 400 µl of phenol chloroform isoamylalcohol (25 24 1) was added and mixed by brief vortexing (5 seconds) Upon centrifugation at 13,000 rpm for 5 min the mixture is divided into an upper aqueous and lower organic layer The aqueous layer was removed to a new microfuge tube with an equal volume of chloroform and mixed by brief vortexing The tube was centrifuged at 13,000 rpm for 5 min and the aqueous layer was transferred to a new microfuge tube A 1/10 volume of 3 M sodium acetate was added followed by an equal volume of isopropanol and mixed by inversion The tube was left at room temperature for 60 min and then centrifuged at 13,000 rpm for 20 min to pellet the DNA The pellet was washed with 70% ethanol and then dried briefly in a SpeedVac (Savant) vacuum centrifuge The DNA was resuspended in 20-50 µl of TE buffer

2 4.4 Isolation of RNA

RNA was isolated using Trizol Reagent (Invitrogen), a mono-phasic solution of phenol and guanidine isothiocyanate This was based on the method developed by Chomczynski and Sacchi (1987) 100 mg of tissue was homogenised in 1 ml of Trizol reagent using a glass-Teflon homogeniser (treated with RNase AWAY, Molecular *Bio*-Products, *inc*) and transferred to a microfuge tube Alternatively, a pellet of cultured cells was lysed in 1 ml of Trizol reagent by repeated pipetting The sample was incubated at room temperature for 5 min to allow complete dissociation of nucleoprotein complexes 200 µl of chloroform was added, mixed by brief vortexing and incubated at room temperature for 3 mm The phases were separated by centrifugation at 13,000 rpm for 15 min The upper aqueous layer was transferred to a fresh microfuge tube 500 µl of isopropanol was added and mixed by inversion The sample was incubated at room temperature for 10 min to precipitate the RNA and then centrifuged at 13,000 rpm for 10 min The supernatant was discarded and the RNA pellet was washed with 1 ml of 70% ethanol The RNA pellet was air-dried and dissolved in 30 µl RNase-free water Any possible DNA contamination was eliminated by treatment with Deoxyribonuclease I (see Section 2 8)

2 4 5 Quantification of DNA and RNA

Nucleic Acid concentration was quantified by UV spectrometry A dilution of the sample (typically 1/50) in dH_2O was measured for absorbance at 260 nm A reading of 1 0 corresponds to 50 μg/ml of DNA or 40 μg/ml of RNA

2 5 Agarose Gel Electrophoresis

DNA was analysed by migrating electrophoretically through (typically 0 7-2 %) agarose gels in a BioRad horizontal gel apparatus Agarose was added to TAE buffer to the required concentration and dissolved by boiling The agarose solution was poured into plastic trays and allowed to set with a plastic comb fitted to create sample wells TAE buffer was used as the running buffer Loading dye was mixed with the DNA samples to facilitate loading and to give indication of migration distance during electrophoresis When RNA samples were being analysed 0 1% (v/v) DEPC was included in the TAE buffer Gels were run at 140 volts for 20-40 min depending on size of gel Gels were stained for 15 min by immersion in an ethidium bromide staining solution Gels were visualised using a UV transilluminator coupled with an image analyser to capture the image to a PC On every gel 0 5 μg of 1 Kb Plus DNA Ladder (Invitrogen, see Figure 2 5) was run as a molecular size marker

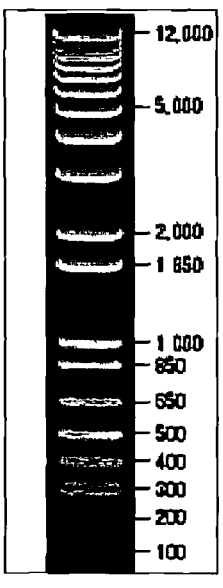

Figure 2 5 DNA Ladder 1 Kb Plus (Invitrogen)
1 0% Agarose Gel

2.6 Competent Cells

The two methods used to prepare competent cells were the rubidium chloride method (see Section 2.6.1) and the TB method (see Section 2.6.2). The former method was favoured for its reliability.

2.6.1 Rubidium Chloride Method

This is an adaptation of the method outlined by Hanahan (1985). Sterile conditions were used throughout. 10 ml of LB broth containing the relevant antibiotics was inoculated with a single colony of the desired bacterial strain from a plate stock and cultured overnight at 37°C. A 1 L flask with 200 ml of LB broth was inoculated with 2 ml of the overnight culture and incubated at 37°C shaking at 225 rpm (Oribsafe Heated Orbital Shaker, Sanyo). When the culture had reached an OD_{600} of ~0.5 (early-mid exponential phase) the flask was cooled in ice water. All subsequent transactions took place at 4°C. The culture was transferred to a sterile centrifuge bottle. The cells were collected by centrifugation at 3,000 rpm for 5 min (using a Beckman JA-14 rotor). The supernatant was decanted and the cells gently re-suspended in 60 ml of chilled RF1 buffer. The suspension was left on ice for 90 min. The cells were again collected by centrifugation at 3,000 rpm for 5 min. The supernatant was decanted and the cells gently re-suspended in 8 ml of chilled RF2 buffer. Aliquots of 800 µl were prepared in sterile 1.5 ml microfuge tubes and flash frozen using –70°C ethanol. The competent cells were stored at –70°C. Cells were routinely used within a few weeks.

2.6.2 TB Method

This method was developed by Inoue *et al.* (1990). Sterile conditions were used throughout. 10 ml of LB broth containing the relevant antibiotics was inoculated with a single colony of the desired bacterial strain from a plate stock and cultured overnight at 37°C. A 1 L flask with 200 ml of SOB broth was inoculated with 2 ml of the overnight culture and incubated at 37°C shaking at 225 rpm. When the culture had reached an OD_{600} of 0.4, as optimised by Inoue *et al.* (1990), the flask was cooled in ice water. All subsequent transactions took place at 4°C. The culture was transferred to a sterile centrifuge bottle. The cells were collected by centrifugation at 3,000 rpm for 5 min (using a Beckman JA-14 rotor). The supernatant was decanted and the cells gently re-suspended in 80 ml of chilled TB buffer. The suspension was left on ice for 10 min. The cells were again collected by centrifugation at 3,000 rpm for 5 min. The supernatant was

decanted and the cells gently re-suspended in 15 ml of chilled TB buffer DMSO was added drop-wise to 7% (v/v) The suspension was left on ice for 10 min Aliquots of 800 μl were prepared in sterile 1 5 ml microfuge tubes and flash frozen using –70°C ethanol The competent cells were stored at –70°C Cells were routinely used within a few weeks

2 6 3 Transformation of Competent Cells

An aliquot of competent cells was thawed on ice 200 μl of the cell suspension was mixed gently with 1-50 μl of plasmid DNA in a sterile 1 5 ml microfuge tube The mixture was left on ice for 30 min The cells were heat-shocked at 42°C for 30 seconds and placed back on ice for 2 min 800 μl of LB broth was added to the cells followed by incubation at 37°C for 60 min 100 μl of the transformation suspension was spread on an LB agar plate containing the relevant antibiotics and incubated at 37°C overnight

2 6 4 Determining Cell Efficiency

Competent cell efficiency is defined in terms of the number of colony forming units obtained per μg of transformed plasmid DNA A 10 ng/μl stock of pBR322 plasmid DNA was diluted to 1 ng/μl, 100 pg/μl and 10 pg/μl 1 μl of each dilution was transformed as described above The cell efficiency was calculated from the number of colonies obtained, taking into account the dilution factor and the fraction of culture transferred to the spread plate

2 7 Bacterial Storage

Bacterial strains were stored as 40% glycerol stocks 750 μl of an overnight culture was mixed with 750 μl sterile 80% glycerol in a microfuge tube If the bacterial strains contained plasmids, the selective antibiotic was included in the culture Duplicate stocks were stored at –20°C and –70°C Working stocks streaked on LB agar plates, containing antibiotics where appropriate, were stored at 4°C Bacterial samples containing plasmids to be sent for commercial DNA sequencing were prepared as stab cultures 1 ml of LB agar containing the selective antibiotic was added to a microfuge tube and allowed to set The tube was inoculated by stabbing using a sterile pin with bacterial growth taken from an LB broth culture

2 8 Enzymes

All restriction endonucleases, Antarctic Phosphatase, T4 DNA ligase were obtained from Invitrogen Life Technologies or New England Biolabs Deoxyribonuclease I (Ribonuclease free), Ribonuclease A (Deoxyribonuclease free), RED*Taq* polymerase were obtained from Sigma-Aldrich *PfuTurbo* DNA polymerase was obtained from Stratagene AMV reverse Transcriptase was obtained from Promega Enzymes were used with their relevant buffers according to the manufacturers instructions

2 8 1 Reverse Transcription

1 μg of RNA was combined with 0 5 μg oligo$(dT)_{15}$ primer (alternatively 1 μl of 25 μM specific reverse primer) and the volume made to 5 μl with dH_2O The mixture was incubated at 70°C for 10 min and then placed on ice for 5 min To the mixture were added dNTP's to a final concentration of 500 μM each, 1 unit AMV reverse transcriptase and 2 μl specific 10x enzyme buffer The volume was brought to 20 μl with dH_2O The first strand was synthesised at 42°C for 60 min followed by inactivation of the transcriptase at 95°C for 2 min 1 μl of the reaction was used as template for PCR

2 8 2 Polymerase Chain Reaction

PCR reactions (Mullis and Faloona, 1987) were carried out using a Peltier Thermal Cycler The standard PCR reaction volume was 50 μl containing 1 μl template (10-100 ng), 1-2 5 mM $MgCl_2$, 0 5 μM of each primer, 200 μM of each dNTP, 1 unit RED*Taq* DNA polymerase and 5 μl specific 10x enzyme buffer The standard PCR program was

Stage 1	Step 1 95°C for 10 min
Stage 2 (30 cycles)	Step 1 95°C for 1 min
	Step 2 T_{ann} for 30 sec
	(T_{ann} was routinely 5°C below the T_m of the primers)
	Step 3 72°C for 1 min per Kb to be synthesised
Stage 3	Step 1 72°C for 10 min

2 8 3 Alkaline Phosphatase, Calf Intestinal (CIP) Treatment

The standard CIP reaction volume was 20 μl containing 16 μl plasmid preparation (10-100 ng), 1 unit Alkaline Phosphatase enzyme and 2 μl specific 10x enzyme buffer The reaction mixture was incubated at 37°C overnight

2 9 Gene Manipulation

A variety of plasmid-based gene cloning approaches such as described by Maniatis *et al*, (1982) were used, employing PCR techniques (see Section 2 8 2), restriction endonucleases, antartic phosphatase and DNA ligase (see Section 2 8)

2 9 1 TA Cloning of PCR Products

PCR products were cloned using the TA cloning vector pCR2 1 (Invitrogen, Table 2 3, Figure 2 1) The cloning method using this vector exploits the fact that thermostable polymerases such as *Taq* DNA polymerase leave 3' A-overhangs due to their lack of 3'-5' exonuclease activity The pCR2 1 vector is provided with a location in the *lacZα* gene open with 3' T overhangs (see Figure 2 1) PCR products with 3' A-overhangs can be directly ligated into this cloning site The ligation was transformed into *E coli* XL10-Gold (see Table 2 1) cells as described in Section 2 6 3 100 μl of the transformation reaction was plated on an LB agar plate containing ampicillin and kanamycin (see Section 2 3 for required antibiotic concentrations) The agar plate was previously overlaid with 60 μl of 40 mg/ml X-gal to test for α-complementation of β-galactosidase X-gal stock was prepared in DMF and stored in the dark at -20°C The *lacZα* gene encodes the α-peptide of β-galactosidase, which cleaves the X-gal substrate yielding a blue product This allows for positive selection of transformants harbouring plasmids with PCR product inserts Routinely a small proportion of colonies are blue It is assumed that these arise as a result of re-circularisation of the pCR2 1 vector

2 9 2 Site-Directed Mutagenesis

Point mutations were introduced into open reading frames on plasmid constructs by PCR amplification using the Quick Change Site-Directed Mutagenesis Kit (Stratagene) and complementary primers carrying the desired mutation 50 μl reactions were set up, containing 10-100 ng of plasmid template isolated from *dam*$^{+}$ *E coli* (e g XL-10 Gold strains, see Table 2 1), 0 5 μM of each primer, 200 μM of each dNTP, 3 μl Quick Change Solution, 2 5 units of *PfuTurbo* DNA polymerase and 5 μl specific 10x enzyme buffer The particular PCR program used was

Stage 1	Step 1	95°C for 1 min
Stage 2 (18 cycles)	Step 1	95°C for 50 sec
	Step 2	60°C for 50 sec
	Step 3	68°C for 2 min per Kb of template plasmid

Stage 3	Step 1: 68°C for 7 min

The template DNA was eliminated by digestion with 20 units of *Dpn* I restriction endonuclease. *Dpn* I is biased toward a methylated recognition sequence. It selectively digests the template DNA from *dam*$^+$ *E. coli* strains mentioned above and not the newly synthesised DNA. Subsequently the samples were transformed into *E. coli* XL10-Gold. Potential mutants were verified by DNA sequencing.

2.9.3 Random Mutagenesis

Random mutations were introduced into open reading frames on plasmid constructs by adding manganese chloride ions to the standard PCR (see Section 2.8.2). 50 µl reactions were set up, containing 1 µl template (10-100 ng), 1-2.5 mM $MgCl_2$, 0.5 µM of each primer, 200 µM of each dNTP, 0.05mM $MnCl_2$,1 unit RED*Taq* DNA polymerase and 5 µl specific 10x enzyme buffer. The random mutagenesis PCR program was:

Stage 1	Step 1: 95°C for 10 min
Stage 2 (30 cycles)	Step 1: 95°C for 1 min
	Step 2: T_{ann} for 30 sec
	(T_{ann} was routinely 5°C below the T_m of the primers)
	Step 3: 72°C for 1 min per Kb to be synthesised
Stage 3	Step 1: 72°C for 10 min

2.10 DNA Sequencing

Recombinant clones and potential mutants were verified by DNA sequencing. Commercial sequencing services were provided by MWG Biotech AG. Suitable sequencing primers (see Table 2.2) for standard vectors were provided as part of the service. Samples were sent as dried plasmid DNA preparations.

2.11 Bio-Informatics

Nucleotide and Amino Acid sequences were analysed using a variety of web-based tools. The BLAST programs (Altschul *et al.*, 1997) at the National Centre for Biotechnology Information (http://www.ncbi.nlm.nih.gov) were used to identify homologous sequences deposited in GenBank (Benson *et al.*, 1996). Protein sequences and structure files were obtained from the Swiss-Prot database (Bairoch and Apweiler, 1996) at (http://us.expasy.org) and the Protein Data Bank (PDB, Berman *et al.*, 2000) at

(http://www.rcsb.org/pdb). Alignments of DNA and Protein sequences were performed using the MultAlin program (Corpet, 1988) available at (http://prodes.toulouse.inra.fr/multalin/multalin.html) and edited using the GeneDoc program (Nicholas *et al.*, 1997) available for download at (www.psc.edu/biomed/genedoc). Plasmid maps were constructed using the pDRAW32 program available for download at (http://www.acaclone.com). Chemical structures were drawn using the ACD/Labs ChemSketch program available for download at (http://www.acdlabs.com). DNA sequences were analysed for restriction enzyme sites using the Webcutter 2.0 tool at (http://rna.lundberg.gu.se/cutter2). Tertiary protein structure was predicted by the automated SWISS-MODEL server (Schwede *et al.*, 2003, http://swissmodel.expasy.org), subsequently analysed and visualised using the DeepView software (Guex and Peitsch, 1997) available for download at (http://ca.expasy.org/spdbv). Rare codons were analysed using rare codon calculator available at http://nihserver.mbi.ucla.edu/RACC/.

2.12 Protein Expression

2.12.1 Standard Expression Culture

100 mL of LB broth was inoculated with 1 ml of a stationary phase culture of *E. coli* that had been transformed with an expression plasmid. Where 1 L cultures were used, 1 L of LB broth was inoculated with 10 ml of a stationary phase culture of *E. coli*. Selective antibiotics were included in the LB broth. The culture was incubated at 37°C, shaking at 220 rpm, until an optical absorbance (A_{600}) of 0.3-0.5 was reached. IPTG was added (from 10 mM stock) to a final concentration of 50 μM to induce expression. The culture was allowed to incubate for 4 hr and was centrifuged at 5,000 rpm for 5 min (using a Beckman JA-14 rotor) to pellet the cells. The supernatant was discarded and the pellets were stored at -20°C.

2.12.2 Preparation of Cleared Lysate

Expression culture cell pellets were washed in potassium phosphate buffer, pH 8.0 followed by centrifugation at 4,000 rpm for 10 min (using a Beckman JA-20 rotor). The supernatant was discarded and the cells were re-suspended in 40 ml potassium phosphate buffer, pH 8.0. The cells were disrupted on ice with a 3 mm micro-tip sonicator (Sonics & Materials Inc.) using 2.5 sec, 40 kHz pulses for 40 sec. The cell debris was removed by centrifugation at 4,000 rpm for 20 min at 4°C (using a Beckman

JA-20 rotor). The cleared lysate was transferred to a fresh universal container and stored at 4°C.

2.13 Protein Purification

Immobilised Metal Affinity Chromatography (IMAC) was used to purify recombinant bovine and human PAP1 having a C-terminal 6xHis tag (see Table 2.3).

2.13.1 Standard IMAC Procedure

1 ml of nickel-nitrilotriacetic acid resin (Ni-NTA, Qiagen) was gently mixed with 10 ml of cleared lysate for 60 min at 4°C. For 1 L cultures 2 ml of resin was mixed with 30 ml of cleared lysate. The mixture was poured into a 0.7 x 15 cm column, allowing the resin to settle. The column was washed four times with 10 ml potassium phosphate buffer, pH 8.0 containing 20 mM imidazole and then eluted with 5 ml potassium phosphate buffer, pH 8.0 containing 200 mM imidazole. The elute was dialysed overnight against 1 L potassium phosphate buffer, pH 8.0. Samples taken throughout the procedure were analysed by SDS-PAGE (see Section 2.16). Protein concentration was determined by the standard BCA assay (see Section 2.14) and PAP1 activity was determined by the fluorimetric assay (see Section 2.15).The purified PAP1 sample was aliquoted and stored at 4°C or –20°C with 40% glycerol.

2.13.2 Optimised Protein Purification for Protein Crystallisation

100ml crude lysate was mixed with 2 ml nickel-nitrilotriacetic acid resin (Ni-NTA, Qiagen) for 60 min at 4°C and subsequently poured into 0.7 x 15 cm column and allowed to settle. The flow-through was collected and the column was then washed with six different 20mls washes in the following sequence: 50 mM Potassium Phosphate with 300 mM NaCl, 20 mM imidazole pH 8.0, 50 mM Potassium Phosphate with 2 M NaCl pH 8.0, 50 mM Potassium Phosphate with 20 mM β-ME pH 8.0, 50 mM Potassium Phosphate with 2% Tween-20 pH 8.0, 50 mM Potassium Phosphate with 20% ethanol pH 8.0 and finally 50mM Potassium Phosphate with 40% glycerol pH 8.0. Bound protein was then eluted with 3 x 5 ml washes of 50mM Potassium Phosphate containing 200 mM imidazole buffer pH 8.0. The elute was dialysed against 3L ultra pure water overnight at 4°C. Samples were assayed for PAP1 activity according to Section 2.15. Protein content in each fraction was determined using the coomassie assay according to Section 2.14.

2 13 3 Recharging of Ni-NTA Resin

This procedure was routinely used before re-using the Ni-NTA Resin The resin was poured into a column and washed with 2 column volumes (2cv) of distilled water followed by 2cv 50% ethanol The resin was stripped with 3cv 100 mM EDTA, pH 8 0 The resin was washed with 2cv 500 mM NaCl followed by 2cv distilled water The resin was re-charged with 2cv 100 mM $NiSO_4$ The resin was washed with 2cv distilled water, transferred to a plastic container and stored at 4°C in 20% ethanol

2 13 4 Preparation of Dialysis Tubing

The required amount of tubing was placed in a 1 L glass beaker and rinsed thoroughly with distilled water The beaker was filled with distilled water and ~1 g of EDTA was added The beaker was brought to boil and boiled for 2 min The water was allowed to cool and then poured off The beaker was re-filled with fresh distilled water and boiled again for 2 min The water was allowed to cool and poured off The tubing was thoroughly rinsed with distilled water The tubing was stored at 4°C in distilled water

2 14 Protein Concentration

2 14 1 Quantitative Determination By BCA Assay

The Bicinchoninic acid (BCA) assay described by Smith *et al* (1985) was used for the colorimetric detection and quantification of total protein in the range of 20-2,000 μg/ml All samples were dialysed against dH_2O and diluted appropriately to achieve a concentration within range of the assay 50 μl of sample was added in triplicate to 200 μl of BCA reagent (Sigma) and incubated at 37°C for 30 min Absorbances were read at 570 nm on a Tecan Plate Reader Bovine serum albumin (BSA) was used as the reference protein BSA standards (0-2 mg/ml) were prepared in dH_2O and assayed in triplicate to yield a standard curve (see Appendix A) Protein concentration of samples was determined from this standard curve

2 14 2 Quantitative Determination By Coomassie Assay

The Coomassie Plus assay (Bradford, 1976) was used for the colorimetric detection and quantification of total protein in the range of 100-1,500 μg/ml All samples were dialysed against dH_2O and diluted appropriately to achieve a concentration within range of the assay 50 μl of sample was added in triplicate to 1 ml of Coomassie Plus reagent (Pierce) and mixed gently Absorbances were read at 595 nm on a spectrometer blanked

with dH_2O Bovine serum albumin (BSA) was used as the reference protein BSA standards (0-2 mg/ml) were prepared in dH_2O and assayed in triplicate to yield a standard curve (see Appendix A) Protein concentration of samples was determined from this standard curve

2 15 Fluorescence Spectrometry

2 15 1 AMC Standard Curve

A 100 μM stock of 7-Amino-4-Methyl-Coumarin (AMC) was prepared in 50 mM potassium phosphate buffer, pH 8 0 containing 4% (v/v) methanol This stock solution was stored in the dark at 4°C for up to one month AMC standards were prepared by dilution of the stock solution with potassium phosphate buffer, pH 8 0 to the range of 0-20 μM 500 μl of each standard was incubated in triplicate at 37°C for 15 min followed by the addition of 1 ml of 1 5 M acetic acid The fluorescence intensities of the standards were read using a Perkin Elmer LS50 Fluoresence Spectrophotometer at excitation and emission wavelengths of 370 nm and 440 nm respectively Excitation slit width was 10 nm while emission slit width was 2 5 nm This AMC standard curve is shown in Appendix A

2 15 2 Quantitative Fluorimetric PAP1 Assay

Quantitative pGlu-AMC degrading PAP1 activity was determined according to the method by Fujiwara and Tsuru (1978), as modified by Browne and O'Cuinn (1983) PAP1 sample was suitably diluted in 50 mM potassium phosphate buffer, pH 8 0 100 μl was incubated in triplicate at 37°C for 15 min with 400 μl of pGlu-AMC substrate (final concentration 250 μM) in 50 mM potassium phosphate, pH 8 0 containing at final concentration 10 mM DTT, 2 mM EDTA and 5% (v/v) DMSO Blanks were set up by substituting 100 μl 50 mM potassium phosphate buffer, pH 8 0 for PAP1 sample The reaction was terminated by the addition of 1 ml 1 5 M acetic acid Liberated AMC was detected using a Perkin-Elmer LS-50 fluorescence spectrophotometer with excitation and emission wavelengths of 370 and 440 nm, respectively The fluorescence readings were converted to nanomoles of AMC released per minute by calculations shown in Appendix C, using a standard curve of free AMC (Appendix A), prepared as described in Section 2 15 1 under identical assay conditions Units of PAP1 activity were defined as nanomoles of AMC released per minute at 37°C (unit = nmoles min^{-1})

2 15.3 Quantitative 96-Well Plate Fluorimetric PAP1 Assay

A quantitative version of the above assay was carried out on a 96-well plate 25 μl of sample was incubated in triplicate with 100 μl of the substrate solution used in Section 2 15 2 at 37°C for 15 min The reaction was terminated by the addition of 100 μl 1 5 M acetic acid Liberated AMC was detected fluorometrically using a Perkin Elmer LS-50B plate reader attachment with excitation and emission wavelengths of 370 and 440 nm, respectively

2.15 4 Fluorimetric Colony Assay

Screening for transformants with PAP1 activity was carried out by a fluorimetric plate assay similar to that described by Mulczyk and Szewczuk (1970) Selective agar plates with colonies from an overnight transformation were flooded with 250 μM pGlu-AMC substrate in 50 mM potassium phosphate, pH 8 0 with 10 mM DTT, 2 mM EDTA and 5% (v/v) DMSO After 30 min incubation at 37°C the plates were viewed under UV light A digital camera was used to capture the images to a PC

2 16 SDS-PAGE

Protein samples were analysed by sodium dodecyl sulphate polyacrylamide gel electrophoresis (SDS-PAGE), based on the method outlined by Laemmli (1970)

2 16 1 Preparation of SDS Gels

10% and 15% resolving and 4% stacking polyacrylamide gels were prepared as per Table 2 4 Gels were cast using an ATTO vertical mini electrophoresis system Upon the addition of the TEMED to the resolving gel it was poured immediately and overlaid with 50% ethanol After polymerisation, the overlay was removed Upon the addition of the TEMED to the stacking gel it was poured immediately and allowed to polymerise around a comb placed into the top of the gel liquid to form loading wells

Table 2 4 Preparation of SDS-PAGE Gels

Solution	10% Resolving Gel	15% Resolving Gel	4% Stacking Gel
1 5 M Tris-HCl, pH 8 8 Resolving Gel buffer	1 625 ml	1 625 ml	-
0 5 M Tris-HCl, pH 6 8 Stacking Gel buffer	-	-	0 625 ml
dH_2O	2 64 ml	1 56 ml	1 538 ml
Acrylamide/Bis-acrylamide 30%/0 8% (w/v)	2 17 ml	3 25 ml	0 335 ml
10% (w/v) Ammonium Persulphate	32 5 µl	32 5 µl	12 5 µl
20% (w/v) SDS	32 5 µl	32 5 µl	12 5 µl
TEMED	3 25 µl	3 25 µl	2 5 µl

2 16 2 Sample Preparation

20 µl of sample was added to 5 µl solubilisation buffer (5X) consisting of 50% (v/v) glycerol, 2% (w/v) SDS, 5% (v/v) 2-mercaptoethanol, 0 1% (w/v) bromophenol blue and 62 5 mM Tris-HCl, pH 6 8 Samples were boiled for 3 minutes and stored on ice until application

2 16 3 Sample Application

Routinely 25 µl of each prepared sample was applied to the SDS PAGE gel 10 µl relative molecular weight protein marker (M_r) solution (SigmaMarker, Sigma, see Figure 2 6) was also applied to the gel consisting of Rabbit Muscle Myosin (205 kDa), *E coli* β-Galactosidase (116 kDa), Rabbit Muscle Phosphorylase b (97 kDa), Rabbit Muscle Fructose-6-phosphate Kinase (84 kDa), Bovine Serum Albumin (66 kDa), Bovine Liver Glutamic Dehydrogenase (55 kDa), Chicken Egg Ovalbumin (45 kDa), Rabbit Muscle Glyceraldehyde-3-phosphate Dehydrogenase (36 kDa), Bovine Erythrocyte Carbonic Anhydrase (29 kDa), Bovine Pancreas Trypsinogen (24 kDa), Soybean Trypsin Inhibitor (20 kDa), Bovine Milk α-Lactalbumin (14 2 kDa) and Bovine Lung Aprotinin (6 5 kDa) Gels were run at 125 V for 1-2 hrs at room temperature using Running Buffer containing 25 mM Tris-HCl, 192 mM glycine and 0 1% (w/v) SDS

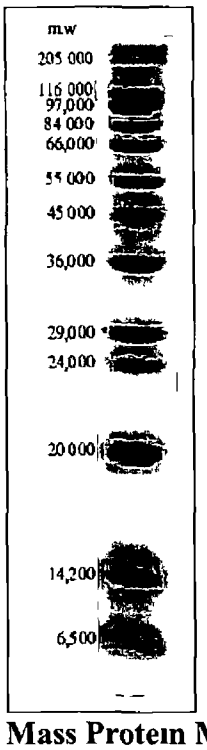

Figure 2 6 Relative Molecular Mass Protein Marker (M_r)
15% polyacrylamide gel

2 16 4 Gel Staining

Polyacrylamide gels removed from the electrophoresis chamber and washed with dH_2O for 5 min Routinely, gels were stained for 60 min in a 0 25% (w/v) Coomassie blue solution containing 10% (v/v) Acetic Acid/45% (v/v) methanol and then de-stained overnight using 10% (v/v) Acetic Acid/45% (v/v) methanol Subsequent soaking in dH_2O enhanced the protein bands further If this did not sufficiently stain the gel, the more intense silver staining method (Blum *et al*, 1987) was used as outlined in table 2 5

Table 2 5 Silver Staining of SDS-PAGE Gels

Step	Duration	Reagent
Fix	60 min	50% ethanol, 12% acetic acid, 0 05% formaldehyde (37% stock)
Wash	3 x 20 min	50% ethanol
Pre-Treat	1 min	200 µl of a 5% $Na_2S_2O_3$ x H_2O stock solution in 100 ml dH_2O
Rinse	2 x 20 sec	dH_2O
Impregnate	20 min	0 1g $AgNO_3$, 70 µl formaldehyde in 100 ml dH_2O
Rinse	2 x 20 sec	dH_2O
Development	10 min (max)	3g Na_2CO_3, 50 µl formaldehyde, 4 µl $Na_2S_2O_3$ x H2O stock solution in 100 ml dH_2O
Stop	5 min	0 1 M EDTA

2 16 5 Gel Analysis

Gels were placed between two transparent sheets and scanned using a flatbed scanner (Dell Photo 924, All in One) allowing the image to be saved to a PC

2 17 UV Zymography

2 17 1 Native PAGE

A 15% native polyacrylamide gel was prepared as in Section 2 16 1 with the omission of SDS and set up at 4°C with running buffer as in Section 2 16 3 with the omission of SDS 20 μl of sample was added to 5 μl non-denaturing solubilisation buffer consisting of 50% (v/v) glycerol, 0 0125% (w/v) bromophenol blue and 62 5 mM Tris-HCl, pH 6 8 The samples were applied directly to the gel The gel was run at constant 100 V at 4°C for up to 2 5 hrs

2 17 2 UV Zymogram Development

After native PAGE the gel was gently rinsed with ice cold dH_2O and then incubated at 37°C in 20 ml of 5 μM pGlu-AMC in 50 mM potassium phosphate, pH 8 0 containing at final concentration 10 mM DTT, 2 mM EDTA and 5% (v/v) DMSO After 10-15 min the gel was visualised using a UV transilluminator (Image Master VDS) coupled with an image analyser to capture the image to a PC

2 18 PAP1 Characterisation

A range of biochemical and kinetic properties of recombinant PAP1 were determined (see Sections 2 18 1 to 2 18 7) including native size, pH optimum, optimum temperature, Michaelis constant, turnover number, maximal velocity, inhibition constants and effect of inhibitors

2 18 1 Size Exclusion Chromatography

The native molecular mass of recombinant PAP1 under native conditions was determined by size exclusion chromatography A 2 5 x 48 cm Sephadex G-100 gel-filtration column (Sigma-Aldrich) was equilibrated with potassium phosphate buffer, pH 8 0 containing 100 mM NaCl at 4°C The void volume of the column was determined by eluting 250 μl blue dextran (8 mg/ml) at a flowrate of 0 3 ml/min 1 ml fractions were collected and optical density read at 620 nm To calibrate the column, standard molecular mass markers were applied separately to the column and eluted at a

flowrate of 0 3 ml/min The markers applied were 100 µl BSA (66 kDa, 2 mg/ml), 300 µl Carbonic Anhydrase (29 kDa, 1 mg/ml), and 300 µl cytochrome c (12 kDa, 2 mg/ml) 1 ml fractions were assayed for protein concentration using the BCA method described in Section 2 14 1 100 µl of purified PAP1 (250 µg/ml) was applied to the column 1 ml fractions were assayed for activity using the 96-well plate method described in Section 2 15 3 A linear plot of log molecular mass versus V_e/V_o was constructed The relative molecular mass of PAP1 was estimated using this plot

2 18 2 Determination of pH Optimum

The pH activity profile of PAP1 was determined by carrying out the standard activity assay as described in Section 2 15 3 at pH range 6 0-10 5 This range was established using the following buffers 50 mM potassium phosphate for pH range 6 0-8 0, 50 mM Tris-HCl for pH range 7 5-9 5 and 50 mM NaOH/glycine for pH range 9 5-10 5 PAP1 samples were pre-incubated in the above buffers for 10 min at 37°C prior to addition of the substrate solution, also prepared in the respective buffers

2 18 3 Determination of Temperature Optimum

Purified enzyme was assayed in triplicate for 15 minutes at temperatures ranging from 4-60°C, after ten minute pre-incubation at the appropriate temperature prior to assay as per section 2 15 3 with temperature alteration A plot of residual PAP1 activity (%) verus temperature (°C) was constructed

2 18 4 Thermal Stability at 37°C

Purified enzyme was incubated at 37°C for up to three hours Aliquots of enzyme were removed at various time points and stored on ice All samples were brought to thermal equilibrium for 15 mins at 37°C and assayed under standard conditions according to the method described in Section 2 15 3

2 18 5 Inhibition

A selection of compounds (see Table 2 6) were investigated for their effect on the pGlu-AMC degrading activity of PAP1 If the effect was inhibitory, the IC_{50} value was determined i e the inhibitor concentration resulting in the PAP1 activity being reduced to 50% pGlu-AMC (250 µM) substrate solutions were prepared in 50 mM potassium phosphate, pH 8 0 containing (at final concentration) 10 mM DTT 2 mM EDTA and

5% (v/v) DMSO and the compounds summarised in Table 2 6 PAP1 samples were pre-incubated with the same relevant compound concentration for 10 min at 37°C PAP1 activity was assayed in triplicate using these substrate solutions as outlined in Section 2 15 3

Table 2 6 Compounds Tested For Inhibition

Inhibitor	Assay conc range (mM)
L-pGlu	0-5
2-pyrrolidone	0-5
Iodoacetic Acid	0-5
Iodacetamide	0-5

2 18 6 Kinetic Studies

2 18 6 1 K_m Determination For pGlu-AMC

The Michaelis constant (K_m) was determined using a range of concentrations of pGlu-AMC (10-500 μM), prepared in 50mM potassium phosphate, pH 8 0 containing at final concentration 10 mM DTT, 2 mM EDTA and 5% (v/v) DMSO Purified PAP1 activity was assayed in triplicate with each substrate concentration as described in Section 2 15 3 K_m, V_{max} (maximal velocity) and K_{cat} (turnover number) values of PAP1 for the substrate pGlu-AMC were obtained by fitting the data to Lineweaver-Burk, Eadie-Hofstee and Hanes-Woolf kinetic models (see Appendix C)

2 18 6 2 K_i Determination Using Selected Synthetic Peptides

The effect of selected synthetic peptides on the kinetic interaction between PAP1 and the substrate pGlu-AMC were determined pGlu-AMC substrate concentrations were prepared (10-500 μM) in 50 mM potassium phosphate, pH 8 0 containing at final concentration 10 mM DTT, 2 mM EDTA, 5% (v/v) DMSO along with 250 μM of the desired peptide PAP1 activity was assayed in triplicate as outlined in Section 2 15 3 The data obtained was applied to the Lineweaver-Burk model, whereby the dissociation, or inhibition constant (K_i), and the type of inhibition observed were determined as outlined in Appendix C

Table 2 7 Peptide Preparation for K_i Determinations

Peptide	Stock Conc (mM)	Solubility	Assay Conc (μM)
pGlu-Ala	10	5% v/v DMSO	250
pGlu-Pro	10	5% v/v DMSO	250
pGlu-Thr	10	5% v/v DMSO	250
pGlu-Val	10	5% v/v DMSO	250
pGlu-Ala-Ala	10	5% v/v DMSO	250
pGlu-Glu-Ala	10	5% v/v DMSO	250
pGlu-His-Pro-NH_2 (TRH)	10	5% v/v DMSO	250
pGlu-Met-Ala	10	5% v/v DMSO	250
pGlu-Thr-Ala	10	5% v/v DMSO	250

2 19 Crystallisation

2 19 1 Determination of Crystallisation Conditions

Preliminary screening was carried out to determine conditions under which recombinant PAP1 could form crystals The sparse matrix screening strategy (Jancarik and Kim, 1991, Cudney *et al*, 1994) was employed using Crystal Screen 1 and 2 reagent kits (Hampton Research) The kits consist of a panel of reagents combining various salts, buffers, precipitants and solvents The composition of the Screen 1 and Screen 2 reagents are shown in Tables 2 8 and 2 9 respectively

Purified PAP1 was dialysed extensively into dH_2O and then concentrated to 1 5-12 mg/ml using a SpeedVac (Savant) vacuum centrifuge The screening was carried out by the hanging drop vapour diffusion method, section 2 19 2 The drops were monitored daily using a microscope (10x magnification) Observations were recorded and images transferred to a PC using a digital camera attached to the microscope

2 19 2 Hanging Drop Method

1 ml of each Screen reagent was aliquoted into a separate reservoir of a 24-well sample plate Vaseline was applied around the upper edge of each reservoir 2 μl of reagent was taken from each reservoir and placed onto a glass cover slide 2 μl of purified PAP1 sample was mixed with the drop of reagent The slide was inverted and pressed gently over the reservoir, creating a seal with the Vaseline and resulting in the drop hanging over the reservoir

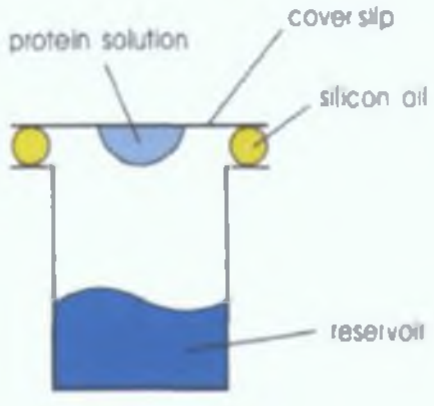

Figure 2.7 Schematic of Hanging Drop Crystallisation Technique

2.19.3 Crystal Mounting For X-Ray Diffraction

CryoLoops were used to mount, freeze, and secure the crystal during cryocrystallographic procedures and X-ray data collection. The nylon loop was first dipped into 0.5% Formvar solution (Sigma Aldrich) to form a thin film. The film provides extra support for fragile crystals, and can result in much sharper reflections with just slightly higher background. After use the loop is cleaned by dipping it in alcohol to dissolve the support.

Table 2.8 Crystal Screen 1

Reagent	Salt	Buffer	Precipitant
1	0.02 M Calcium chloride dehydrate	0.1 M Sodium acetate trihydrate pH 4.6	30 % v/v 2-methyl-2,4-pentanediol
2	None	None	0.4 M Potassium sodium tartrate tetrahydr
3	None	None	0.4 M Ammonium dihydrogen phosphate
4	None	0.1 M Tris hydrochloride pH 8.5	2 M Ammonium sulphate
5	0.2 M tri-Sodium citrate dehydrate	0.1 M Sodium HEPES pH 7.5	30% v/v 2-methyl-2,4-pentanediol
6	0.2 M magnesium chloride hexahydrate	0.1 M Tris hydrochloride pH 8.5	30% w/v polyethylene glycol 4000
7	None	0.1 M sodium cacodylate pH 6.5	1.4 M sodium acetate trihydrate
8	0.2 M tri-sodium citrate dehydrate	0.1 M sodium cacodylate pH 6.5	30% v/v iso-propanol
9	0.2 M ammonium acetate	0.1 M tri-sodium citrate dihydrate pH 5.6	30% w/v polyethylene glycol 4000
10	0.2 M ammonium acetate	0.1 M Sodium acetate trihydrate pH 4.6	30% w/v polyethylene glycol 4000
11	None	0.1 M tri-sodium citrate dihydrate pH 5.6	1 M Ammonium dihydrogen phosphate
12	0.2 M magnesium chloride hexahydrate	0.1 M Sodium HEPES pH 7.5	30% v/v iso-propanol
13	0.2 M tri-Sodium citrate dehydrate	0.1 M Tris hydrochloride pH 8.5	30% v/v polyethylene glycol 400
14	0.2 M Calcium chloride dehydrate	0.1 M Sodium HEPES pH 7.5	30% v/v polyethylene glycol 400
15	0.2 M ammonium sulphate	0.1 M sodium cacodylate pH 6.5	30% w/v polyethylene glycol 8000
16	None	0.1 M Sodium HEPES pH 7.5	1.5 M lithium sulfate monohydrate
17	0.2 M lithium sulfate monohydrate	0.1 M Tris hydrochloride pH 8.5	30% w/v polyethylene glycol 4000
18	0.2 M magnesium acetate tetrahydrate	0.1 M sodium cacodylate pH 6.5	20% w/v polyethylene glycol 8000
19	0.2 M ammonium acetate	0.1 M Tris hydrochloride pH 8.5	30% v/v iso-propanol
20	0.2 M ammonium sulphate	0.1 M Sodium acetate trihydrate pH 4.6	25% w/v polyethylene glycol 4000
21	0.2 M magnesium acetate tetrahydrate	0.1 M sodium cacodylate pH 6.5	30% v/v 2-methyl-2,4-pentanediol
22	0.2 M sodium acetate trihydrate	0.1 M Tris hydrochloride pH 8.5	30% w/v polyethylene glycol 4000
23	0.2 M magnesium chloride hexahydrate	0.1 M Sodium HEPES pH 7.5	30% v/v polyethylene glycol 400
24	0.2 M Calcium chloride dehydrate	0.1 M Sodium acetate trihydrate pH 4.6	20% v/v iso-propanol
25	None	0.1 M imidazole pH 6.5	1 M Sodium acetate trihydrate
26	0.2 M ammonium acetate	0.1 M tri-sodium citrate dihydrate pH 5.6	30% v/v 2-methyl-2,4-pentanediol
27	0.2 M tri-Sodium citrate dehydrate	0.1 M Sodium HEPES pH 7.5	20% v/v iso-propanol
28	0.2 M sodium acetate trihydrate	0.1 M sodium cacodylate pH 6.5	30% w/v polyethylene glycol 8000
29	None	0.1 M Sodium HEPES pH7.5	0.8 M Potassium sodium tartrate tetrahydr
30	0.2 M ammonium sulphate	None	30% w/v polyethylene glycol 8000
31	0.2 M ammonium sulphate	None	30% w/v polyethylene glycol 4000
32	None	None	2 M Ammonium sulfate
33	None	None	4 M Sodium formate
34	None	0.1 M sodium acetate trihydrate pH 4.6	2 M Sodium formate
35	None	0.1 M Sodium HEPES pH 7.5	0.8 M Sodium dihydrogen phosphate 0.8 M potassium dihydrogen phosphate
36	None	0.1 M Tris hydrochloride pH 8.5	8% w/v polyethylene glycol 8000
37	None	0.1 M Sodium acetate trihydrate pH 4.6	8% w/v polyethylene glycol 4000
38	None	0.1 M Sodium HEPES pH 7.5	1.4 M tri-sodium citrate dihydrate
39	None	0.1 M Sodium HEPES pH 7.5	2% v/v polyethylene glycol 400 2 M ammonium sulfate
40	None	0.1 M tri-sodium citrate dihydrate pH 5.6	20% v/v iso-propanol 20% w/v polyethylene glycol 4000
41	None	0.1 M Sodium HEPES pH 7.5	10% v/v iso-propanol 20% w/v polyethylene glycol 4000
42	0.05 M mono-Potassium dihydrogen Phosphate	None	20% w/v polyethylene Glycol 8000
43	None	None	30% w/v polyethylene glycol 1500
44	None	None	0.2 M magnesium formate
45	0.2 M Zinc acetate dehydrate	0.1 M sodium cacodylate pH 6.5	18% w/v polyethylene glycol 8000
46	0.2 M calcium acetate hydrate	0.1 M sodium cacodylate pH 6.5	18% w/v polyethylene glycol 8000
47	None	0.1 M Sodium acetate trihydrate pH 4.6	2 M Ammonium sulfate
48	None	0.1 M Tris hydrochloride pH 8.5	2 M Ammonium dihydrogen phosphate
49	1 M Lithium sulfate monohydrate	None	2% w/v polyethylene glycol 8000
50	0.5 M lithium sulfate monohydrate	None	15% w/v polyethylene glycol 8000

Table 2 9 Crystal Screen 2

R	Salt	Buffer	Precipitant
1	2 0 M sodium chloride	None	10% w/v PEG 6000
2	0 01 M Hexadecyltrimethylammonium Bromide	None	0 5 M sodium chloride 0 01 M magnesium chloride hexahydrate
3	None	None	25% v/v ethylene glycol
4	None	None	35% v/v dioxane
5	2 0 M ammonium sulfate	None	5% v/v iso propanol
6	None	None	1 0 M imidazole pH 7 0
7	None	None	10% w/v polyethylene glycol 1000 10% w/v polyethylene glycol 8000
8	1 5 M sodium chloride	None	10% v/v ethanol
9	None	0 1 M sodium acetate trihydrate pH 4 6	2 0 M sodium chloride
10	0 2 M sodium chloride	0 1 M sodium acetate trihydrate pH 4 6	30 % v/v MPD
11	0 01 M cobaltous chloride hexahydrate	0 1 M sodium acetate trihydrate pH 4 6	1 0 M 1 6 hexanediol
12	0 1 M cadmium chloride dehydrate	0 1 M sodium acetate trihydrate pH 4 6	30% v/v polyethylene glycol 400
13	0 2 M ammonium sulfate	0 1 M sodium acetate trihydrate pH 4 6	30% w/v polyethylene glycol monomethyl ether 20
14	0 2 M potassium sodium tartrate tetrahydrate	0 1 M tri sodium citrate dihydrate pH 5 6	2 0 M ammonium sulfate
15	0 5 M ammonium sulfate	0 1 M tri sodium citrate dihydrate pH 5 6	1 0 M lithium sulfate monohydrate
16	0 5 M sodium chloride	0 1 M tri-sodium citrate dihydrate pH 5 6	2% w/v ethylene imine polymer
17	None	0 1 M tri-sodium citrate dihydrate pH 5 6	35% v/v tert butanol
18	0 01 M ferric chloride hexahydrate	0 1 M tri sodium citrate dihydrate pH 5 6	10% v/v jeffamine M-600
19	None	0 1 M tri sodium citrate dihydrate pH 5 6	2 5 M 1 6 hexanediol
20	None	0 1 M MES pH 6 5	1 6 M magnesium sulfate heptahydrate
21	0 1 M sodium dihydrogen phosphate 0 1 M potassium dihydrogen phosphate	0 1 M MES pH 6 5	2 0 M sodium chloride
22	None	0 1 M MES pH 6 5	12% w/v polyethylene glycol 20 000
23	1 6 M ammonium sulfate	0 1 M MES pH 6 5	10% v/v dioxane
24	0 05 M cesium chloride	0 1 M MES pH 6 5	30% v/v jeffamine M-600
25	0 01 M cobaltous chloride hexahydrate	0 1 M MES pH 6 5	1 8 M ammonium sulfate
26	0 2 M ammonium sulfate	0 1 M MES pH 6 5	30% w/v polyethylene glycol monomethyl ether 50
27	0 01 M zinc sulfate heptahydrate	0 1 M MES pH 6 5	25% v/v/ polyethylene glycol monomethyl ether 55
28	None	None	1 6 M tri-sodium citrate dehydrate
29	0 5 M ammonium sulfate	0 1 M HEPES pH 7 5	30% v/v MPD
30	None	0 1 M HEPES pH 7 5	10% w/v polyethylene glycol 6000 5% v/v MPD
31	None	0 1 M HEPES pH 7 5	20% v/v jeffamine M-600
32	0 1 M sodium chloride	0 1 M HEPES pH 7 5	1 6 M ammonium sulfate
33	None	0 1 M HEPES pH 7 5	2 0 M ammonium formate
34	0 05 M cadmium sulfate hydrate	0 1 M HEPES pH 7 5	1 0 M sodium acetate
35	None	0 1 M HEPES pH 7 5	70% v/v MPD
36	None	0 1 M HEPES pH 7 5	4 3 M sodium chloride
37	None	0 1 M HEPES pH 7 5	10% w/v polyethylene glycol 8000 8% v/v ethylene glycol
38	None	0 1 M HEPES pH 7 5	20% w/v polyethylene glycol 10000
39	0 2 M magnesium chloride hexahydrate	0 1 M tris pH 8 5	3 4 M 1 6 hexanediol
40	None	0 1 M tris pH 8 5	25% v/v tert-butanol
41	0 01 M nickel (II) chloride hexahydrate	0 1 M tris pH 8 5	1 0 M lithium sulfate monohydrate
42	1 5 M ammonium sulfate	0 1 M tris pH 8 5	12% v/v glycerol anhydrous
43	0 2 M ammonium dihydrogen phosphate	0 1 M tris pH 8 5	50% v/v MPD
44	None	0 1 M tris pH 8 5	20% v/v ethanol
45	0 01 M nickel (II) chloride hexahydrate	0 1 M tris pH 8 5	20% w/v polyethylene glycol monomethyl ether 20
46	0 1 M sodium chloride	0 1 M bicine pH 9 0	20% w/v polyethylene glycol monomethyl ether 55

Table 2 10 CryoScreen 1

Reagent	Crystallant	Buffer (0 1 M)	Additive(s)
1	40% (v/v) 2 methyl 2 4-pentanediol	phosphate citrate pH 4 2	None
2	40% (v/v) ethylene glycol	acetate pH 4 5	None
3	50% (v/v) PEG-200	citrate pH 5 5	None
4	40% (v/v) PEG 300	HEPES pH 7 5	0 2 M NaCl
5	40% (v/v) PEG-400	citrate pH 5 5	0 2 M $MgCl_2$
6	40% (v/v) PEG 600	cacodylate pH 6 5	0 2 M $Ca(OAc)_2$
7	40% (v/v) ethanol	Tris pH 8 5	0 05 M $MgCl_2$
8	35% (v/v) 2 ethoxyethanol	cacodylate pH 6 5	None
9	35% (v/v) 2 propanol	phosphate citrate pH 4 2	None
10	45% (v/v) glycerol	imidazole pH 8 0	None
11	35% (v/v) 2-methyl 2 4 pentanediol	Tris pH 8 5	0 2 M $(NH_4)_2SO_4$
12	50% (v/v) ethylene glycol	acetate pH 4 5	5% (w/v) PEG 1000
13	30% (v/v) PEG 200	MES pH 6 0	5% (w/v) PEG 3000
14	20% (v/v) PEG 300	phosphate citrate pH 4 2	0 2 M $(NH_4)_2SO_4$ 10% (v/v) glycerol
15	50% (v/v) PEG-400	CHES pH 9 5	0 2 M NaCl
16	30% (v/v) PEG-600	MES pH 6 0	5% (w/v) PEG-1000 10% (v/v) glycerol
17	40% (v/v) 1 2 propanediol	HEPES pH 7 5	None
18	35% (v/v) 2 ethoxyethanol	imidazole pH 8 0	0 05 M $Ca(OAc)_2$
19	35% (v/v) 2-propanol	Tris Ph 8 5	None
20	30% (v/v) 1,2 propanediol	citrate pH 5 5	20% (v/v) 2 methyl-2 4-pentanediol
21	40% (v/v) 1,2 propanediol	Acetate pH 4 5	0 05 M $Ca(OAc)_2$
22	40% (v/v) ethylene glycol	Na/K phosphate pH 6 2	None
23	40% (v/v) 2 methyl 2 4 pentanediol	Tris pH 7 0	0 2 M $(NH_4)_2SO_4$
24	40% (v/v) PEG-400	Na/K phosphate pH 6 2	0 2 M NaCl
25	30% (v/v) PEG-200	Tris pH 8 5	0 2 M $(NH_4)_2HPO_4$
26	40% (v/v) PEG-300	CHES pH 9 5	0 2 M NaCl
27	30% (v/v) PEG-400	CAPS pH 10 5	0 5 M $(NH_4)_2SO_4$ 10% (v/v) glycerol
28	30% (v/v) PEG 600	HEPES pH 7 5	0 05 M Li_2SO_4 10% (v/v) glycerol
29	40% (v/v) PEG 300	CHES pH 9 5	0 2 M sodium citrate
30	35% (v/v) 2 ethoxyethanol	citrate pH 5 5	None
31	35% (v/v) 2 propanol	citrate pH 5 5	5% (w/v) PEG 1000
32	40% (v/v) 1,2 propanediol	CHES pH 9 5	0 2 M sodium citrate
33	25% (v/v) 1 2 propanediol	imidazole pH 8 0	0 2 M $Zn(OAc)_2$ 10% (v/v) glycerol
34	40% (v/v) 2 methyl 2 4-pentanediol	imidazole pH 8 0	0 2 M $MgCl_2$
35	40% (v/v) ethylene glycol	HEPES pH 7 5	5% (w/v) PEG 3000
36	50% (v/v) PEG 200	Tris pH 7 0	0 05 M Li_2SO_4
37	40% (v/v) PEG 300	cacodylate pH 6 5	0 2 M $Ca(OAc)_2$
38	40% (v/v) PEG-400	Tris pH 8 5	0 2 M Li_2SO_4
39	40% (v/v) PEG-600	phosphate citrate pH 4 2	None
40	40% (v/v) ethanol	phosphate-citrate pH 4 2	5% (w/v) PEG-1000
41	25% (v/v) 1 2 propanediol	phosphate-citrate pH 4 2	5% (w/v) PEG-3000 10% (v/v) glycerol
42	40% (v/v) ethylene glycol	Tris pH 7 0	None
43	50% (v/v) ethylene glycol	Tris pH 8 5	0 2 M $MgCl_2$
44	50% (v/v) PEG 200	cacodylate pH 6 5	0 2 M $Zn(OAc)_2$
45	20% (v/v) PEG-300	Tris pH 8 5	5% (w/v) PEG 8000 10% (v/v) glycerol
46	40% (v/v) PEG-400	MES pH 6 0	5% (w/v) PEG-3000
47	50% (v/v) PEG-400	Acetate pH 4 5	0 2 M Li_2SO_4
48	40% (v/v) PEG 600	imidazole pH 8 0	0 2 M $Zn(OAc)_2$

Table 2.11 CryoScreen 2

Reagent	Crystallant	Buffer (0.1 M)	Additive(s)
1	40% (v/v) 2-methyl-2,4-pentanediol	cacodylate pH 6.5	5% (w/v) PEG-8000
2	50% (v/v) PEG-200	CHES pH 9.5	None
3	40% (v/v) ethylene glycol	phosphate-citrate pH 4.2	0.2 M $(NH_4)_2SO_4$
4	40% (v/v) PEG-400	HEPES pH 7.5	0.2 M $Ca(OAc)_2$
5	40% (v/v) PEG-300	Tris pH 7.0	5% (w/v) PEG-1000
6	30% (v/v) PEG-600	cacodylate pH 6.5	1 M NaCl, 10% (v/v) glycerol
7	40% (v/v) ethanol	Tris pH 7.0	None
8	35% (v/v) 2-ethoxyethanol	Na/K phosphate pH 6.2	0.2 M NaCl
9	35% (v/v) 2-propanol	imidazole pH 8.0	0.05 M $Zn(OAc)_2$
10	40% (v/v) 1,2-propanediol	acetate pH 4.5	None
11	25% (v/v) 1, 2-propanediol	Na/K phosphate pH 6.2	10% (v/v) glycerol
12	40% (v/v) 1,2-propanediol	citrate pH 5.5	0.2 M NaCl
13	35% (v/v) 2-methyl-2,4-pentanediol	cacodylate pH 6.5	0.05 M $Zn(OAc)_2$
14	40% (v/v) ethylene glycol	imidazole pH 8.0	0.2 M $Ca(OAc)_2$
15	50% (v/v) PEG-200	Na/K phosphate pH 6.2	0.2 M NaCl
16	20% (v/v) PEG-300	imidazole pH 8.0	1 M $(NH_4)_2SO_4$, 10% (v/v) glycerol
17	50% (v/v) PEG-400	MES pH 6.0	None
18	40% (v/v) PEG-300	phosphate-citrate pH 4.2	None
19	40% (v/v) PEG-600	acetate pH 4.5	0.2 M $MgCl_2$
20	50% (v/v) ethylene glycol	CHES pH 9.5	0.5 M K/Na tartrate
21	35% (v/v) 2-ethoxyethanol	Tris pH 8.5	0.2 M Li_2SO_4
22	35% (v/v) 2-propanol	cacodylate pH 6.5	0.2 M $MgCl_2$
23	30% (v/v) 1,2-propanediol	HEPES pH 7.5	20% (v/v) PEG-400
24	25% (v/v) 1, 2-propanediol	Tris pH 8.5	0.2 M $MgCl_2$, 10% (v/v) glycerol
25	40% (v/v) 2-methyl-2,4-pentanediol	CAPS pH 10.5	None
26	40% (v/v) ethylene glycol	MES pH 6.0	0.2 M $Zn(OAc)_2$
27	50% (v/v) PEG-200	Tris pH 7.0	None
28	40% (v/v) PEG-300	imidazole pH 8.0	0.2 M $Zn(OAc)_2$
29	30% (v/v) PEG-400	HEPES pH 7.5	5% (w/v) PEG-3000, 10% (v/v) glycerol
30	40% (v/v) PEG-600	citrate pH 5.5	None
31	40% (v/v) PEG-600	CHES pH 9.5	None
32	35% (v/v) 2-propanol	acetate pH 4.5	None
33	45% (v/v) glycerol	cacodylate pH 6.5	0.2 M $Ca(OAc)_2$
34	25% (v/v) 1, 2-propanediol	Tris pH 7.0	0.2 M $(NH_4)_2SO_4$, 10% (v/v) glycerol
35	40% (v/v) 2-methyl-2,4-pentanediol	citrate pH 5.5	None
36	50% (v/v) PEG-200	cacodylate pH 6.5	0.2 M $MgCl_2$
37	50% (v/v) ethylene glycol	imidazole pH 8.0	none
38	40% (v/v) PEG-400	acetate pH 4.5	none
39	30% (v/v) PEG-600	Tris pH 7.0	0.5 M $(NH_4)_2SO_4$, 10% (v/v) glycerol
40	40% (v/v) 2-methyl-2,4-pentanediol	CHES pH 9.5	none
41	50% (v/v) ethylene glycol	HEPES pH 7.5	0.2 M Li_2SO_4
42	30% (v/v) PEG-200	acetate pH 4.5	0.1 M NaCl
43	40% (v/v) PEG-400	imidazole pH 8.0	none
44	35% (v/v) 2-methyl-2,4-pentanediol	acetate pH 4.5	10% (v/v) glycerol
45	40% (v/v) PEG-300	acetate pH 4.5	0.2 M NaCl
46	30% (v/v) PEG-200	CAPS pH 10.5	0.2 M $(NH_4)_2SO_4$
47	50% (v/v) PEG-200	HEPES pH 7.5	none
48	50% (v/v) PEG-200	phosphate-citrate pH 4.2	0.2 M NaCl

CHAPTER THREE

Cloning, Expression and Characterisation of Purified Recombinant Bovine PAP1

3 1 Overview

This chapter describes cloning of the bovine PAP1 gene from cDNA and the subsequent expression of recombinant protein utilizing an expression system which was developed by Vaas (2005) during the expression of recombinant human PAP1 Various biochemical, kinetic and functional studies were then carried out on the purified bovine PAP1 enzyme and a comparative study with the recombinant human PAP1 investigated This study will allow us to further characterise this family of cysteine peptidases There are multiple homologues of this family and it is important to compare them to determine functionality and identify essential amino acid residues

3 2 Cloning of Bovine PAP1 Gene

Bovine brain tissue samples were obtained from Kepak, (Co Meath, Ireland) Total RNA was isolated from bovine brain tissue as described in Section 2 4 4 Figure 3 1A shows analysis of this RNA by agarose gel electrophoresis (see Section 2 5)

The sequence for putative bovine PAP1 mRNA (**XM866409**, see Figure 3 2) was obtained from GenBank (Benson *et al*, 1996) The 700 bp sequence contains a 630 bp open reading frame (ORF) for bovine PAP1 (*Bta-pap1*) Primers PAPBtA and PAPBtB (see Table 2 2) were designed external to this ORF to amplify the putative PAP1 gene (see Figure 3 2) as a 648 bp fragment cDNA was generated from the bovine brain RNA using the specific reverse primer PAPBtB as described in Section 2 8 1 The cDNA was used as template for PCR (see Section 2 8 2) using primers PAPBtA and PAPBtB The resulting RT-PCR product, analysed by agarose gel electrophoresis (see Section 2 5), is shown in Figure 3 1B A band corresponding to the expected size of 648 bp was obtained

The PCR product shown in Figure 3 1C was cloned into the TA cloning vector pCR2 1 (see Table 2 3, Figure 2 1) as described in Section 2 9 1 Several white colonies were purified and plasmid DNA was isolated (see Section 2 4 1) Screening for a TA clone, having the desired ~700 bp recombinant *Bta-pap1* insert (*rBta-pap1*), was carried out by enzymatic restriction analysis with *Eco*RI (see Figure 3 3, Section 2 8) *Eco*RI specifically cuts the TA insert out of the pCR2 1 vector Restriction with *Eco*RI produces a band corresponding to the expected ~700 bp fragment containing the *rBta-pap1* sequence

This clone (pZK1) was analysed by agarose gel electrophoresis (see Figure 3 4) The *EagI* restriction resulted in bands corresponding to 510 and 180 bp, suggesting that the

rBta-pap1 sequence had inserted in the opposite orientation to the *lacZα* ORF of pCR2 1 The *Nco*I restriction similarly supported this opposite orientation The successful cloning of *rBta-pap1* was confirmed by DNA sequencing (see Section 2 10) The sequence was clearly confirmed to be that of Bovine PAP1 shown in Genbank The sequencing data is given in Appendix B A map of pZK1 is shown in Figure 3 5

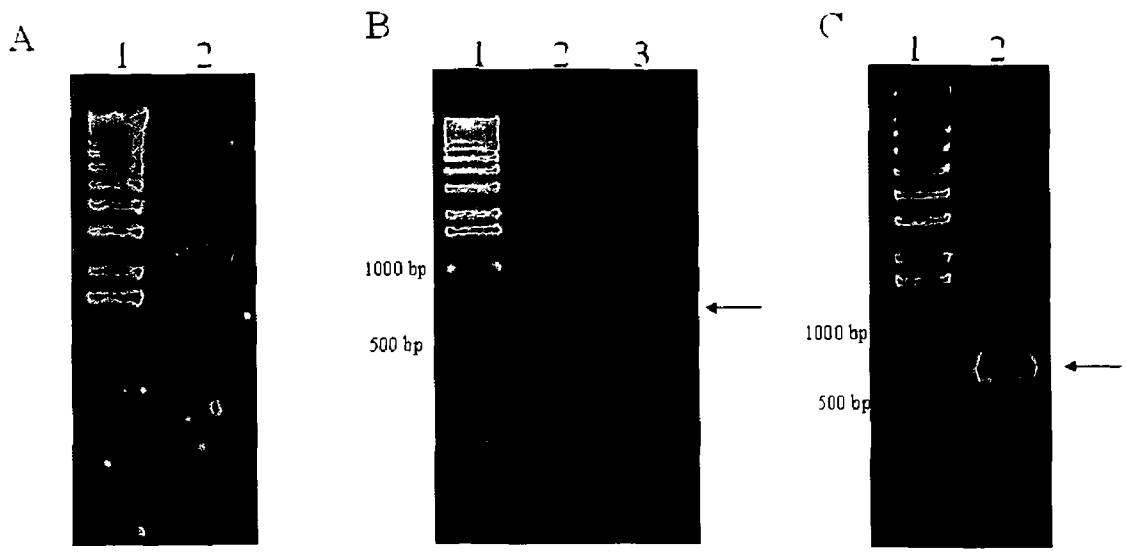

Figure 3 1 Amplification of Bovine PAP1 cDNA
1% agarose gels (**A**) Lane 1, DNA Ladder, Lane 2, RNA isolated from bovine brain tissue (**B**) Lane 1, DNA Ladder (sizes as in Figure 2 6), Lane 2, negative control, Lane 3, product of RT-PCR (see Section 2 8 1 & 2 8 2) on bovine brain tissue RNA using primers PAPBtA and PAPBtB (see Table 2 2, Figure 3 2) The band corresponding to the expected PAP1 product is indicated by blue arrow (**C**) Lane 1, DNA Ladder, Lane 2, product of PCR (see Section 2 8 2) on pZK1 using primers PAPBtA and PAPHtB (see Table 2 2) The band corresponding to the expected PAP1 product is indicated by blue arrow

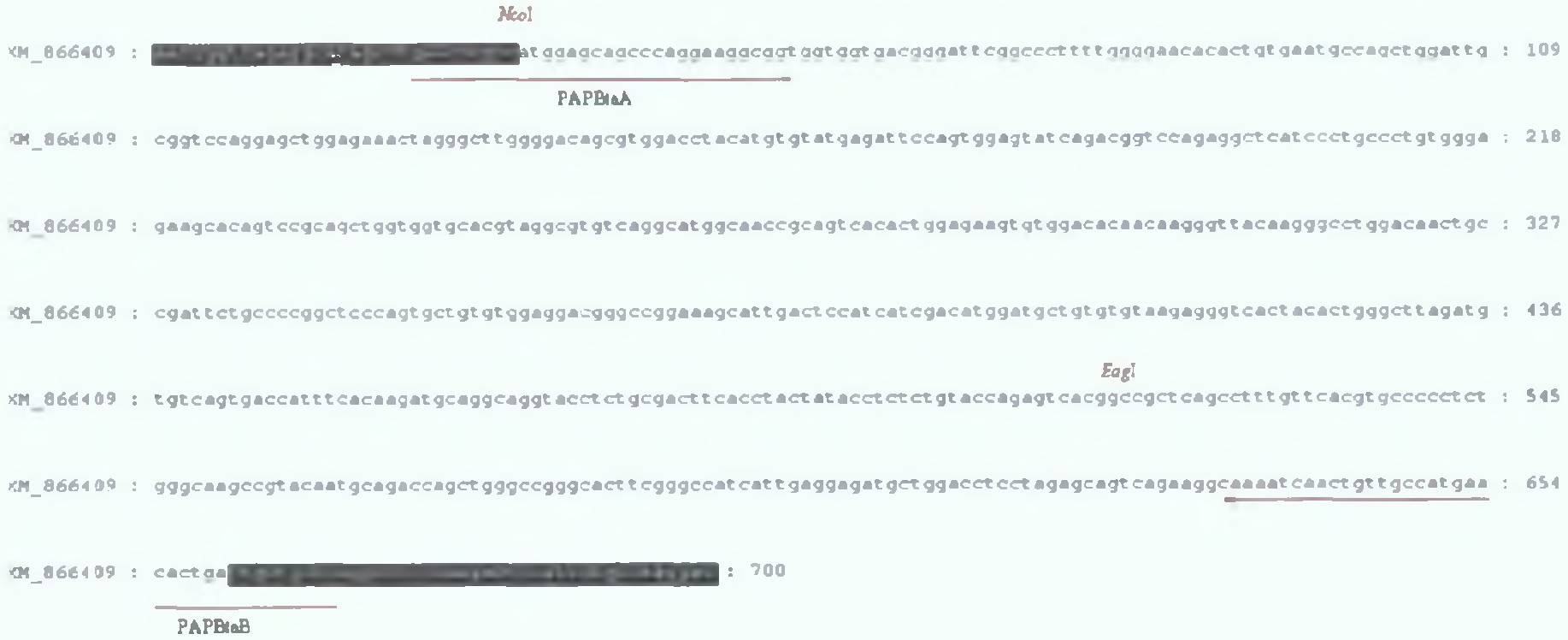

Figure 3.2 Bovine PAP1 Putative mRNA Sequence (U→T)
Nucleotide sequence XM866409: bovine putative PAP1 mRNA. ORF is highlighted. Location of primers PAPHsA and PAPHsB (see Table 2.2) are indicated. Restriction sites on corresponding DNA are marked in red. Illustrated using GenDoc (see Section 2.11).

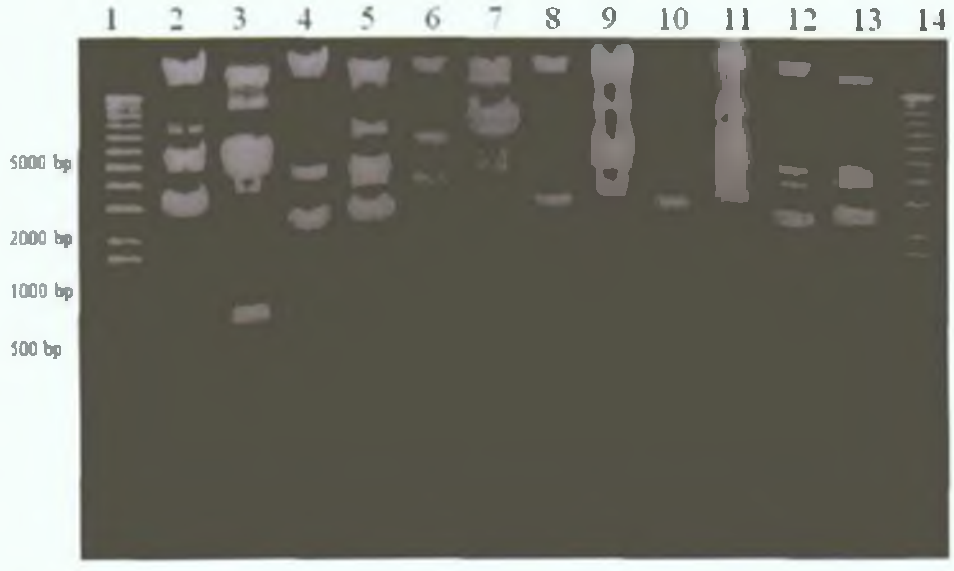

Figure 3.3 Screening for Potential pZK1 Clone Using *Eco*RI Restriction Analysis
*Eco*RI restriction digest of potential pZK1 clones analysed on 1% agarose gel (see Section 2.5). Lane 1, DNA Ladder (sizes as in Figure 2.6); Lane 2, Clone 1 uncut; Lane 3, Clone 1 *Eco*RI cut (possessing bovine PAP1 insert); Lane 4, Clone 2 uncut; Lane 5, Clone 2 *Eco*RI cut; Lane 6, Clone 3 uncut; Lane 7, Clone 3 *Eco*RI cut; Lane 8, Clone 4 uncut; Lane 9, Clone 4 *Eco*RI cut; Lane 10, Clone 5 uncut; Lane 11, Clone 5 *Eco*RI cut, Lane 12, Clone 6 uncut; Lane 13, Clone 6 *Eco*RI cut; Lane 14, DNA Ladder.

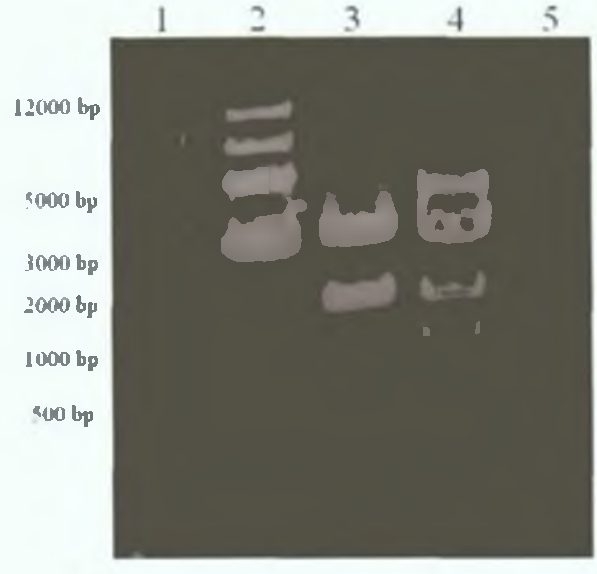

Figure 3.4 Verification Digest of pZK1
Restriction digest of pZK1 clone analysed on 1% agarose gel (see Section 2.5): Lane 1, DNA Ladder (sizes as in Figure 2.5); Lane 2, uncut (prominent covalently closed, open circular and linear bands are visible); Lane 3, *Nco*I; Lane 4, *Eag*I; Lane 5, DNA Ladder.

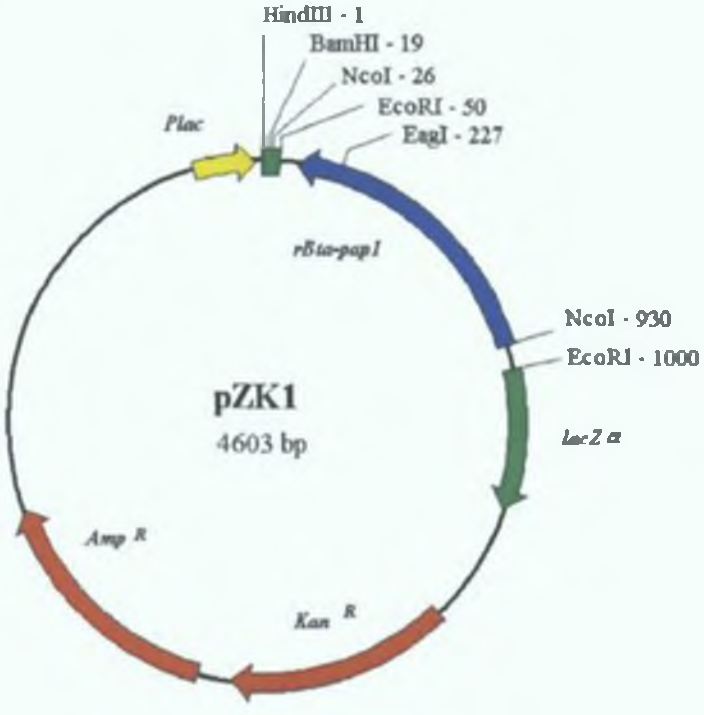

Figure 3.5 pZK1 Plasmid Map
The *rBta-pap1* gene fragment (blue) is inserted in opposite orientation relative to the *LacZα* ORF (green), which is under the control of the *Plac* promoter (yellow). Ampicillin and kanamycin resistance genes (*amp*^{R} & *kan*^{R}) are shown in red. See Figure 2.1 for map of parent vector pCR2.1. Illustrated using pDRAW32 (see Section 2.11).

3.3 Expression System for Recombinant Bovine PAP1 in *E. coli*

The expression system adopted for expression of r*Bta*PAP1$_{6H}$ was developed by Vaas (2005) whereby r*Hsa*PAP1$_{6H}$ was expressed in *E. coli*. The plasmids pQE-60 and pPC225 were used in this system. The resulting constructs had introduced 6 consecutive His codons (His$_6$) as a 3' extension to the *rHsa-pap1* ORF. This His-tag did not interfere with catalytic activity and was exploited during protein purification.

3.3.1 Sub-Cloning of Bovine PAP1 Gene into *E. coli* Expression Vector pQE-60

The vector pQE-60 (see Table 2.3, Figure 2.2) features an optimised hybrid promoter-operator element (Bujard *et al.*, 1987) consisting of the phage T5 transcriptional promoter and a *lac* operator sequence, which increases *lac* protein (LacI) binding, thus enabling repression of this strong promoter. Associated with this operator region is a synthetic ribosome binding site (RBS) designed for high translation rates. The β-lactamase gene conferring resistance to ampicillin (*amp*^{R}) is present on the vector. Most significantly, the vector has six consecutive His codons (His$_6$) followed by a stop codon,

at the 3' end of the multiple cloning site (MCS) This enables translation of a fusion protein having a C-terminal His-tag, which can be exploited during protein purification (see Section 3 5)

The *rBta-pap1* sequence was sub-cloned from pZK1 into pQE-60 by the strategy outlined in Figure 3 6 The pQE-60 MCS conveniently has an *Nco*I site as the 5' insertion point As can be seen in Figure 3 2 the *rBta-pap1* sequence already features this site within the mRNA *rBta-pap1* was amplified by PCR with primers PAPBtA and PAPBtB (see Table 2 2) and ligated into vector pCR2 1 as described in Section 2 9 1 PAPBtA was designed to include the *Nco*I site at the 5' end of *rBta-pap1* (see Figure 3 2) and PAPBtB to add a *Bam*HI site at the 3' end, replacing the stop codon *rBta-pap1* was excised from this intermediate clone by an *Nco*I/*Bam*HI restriction and ligated into pQE-60, which had been opened by an *Nco*I/*Bgl*II restriction *Bam*HI and *Bgl*II sites have compatible ends which, when fused, eliminate the restriction site Cloning into pQE-60 thus results in *rBta-pap1* in fusion with a His_6 ORF (r*Bta*$PAP1_{H6}$)

The *Nco*I/*Hin*dIII restriction resulted in a band corresponding to the expected 654 bp fragment containing the *rBta-pap1*-His_6 fusion (see Figure 3 7) *Eco*RI and *Nco*I single restrictions produced bands corresponding to the expected 4046 bp linearised plasmid

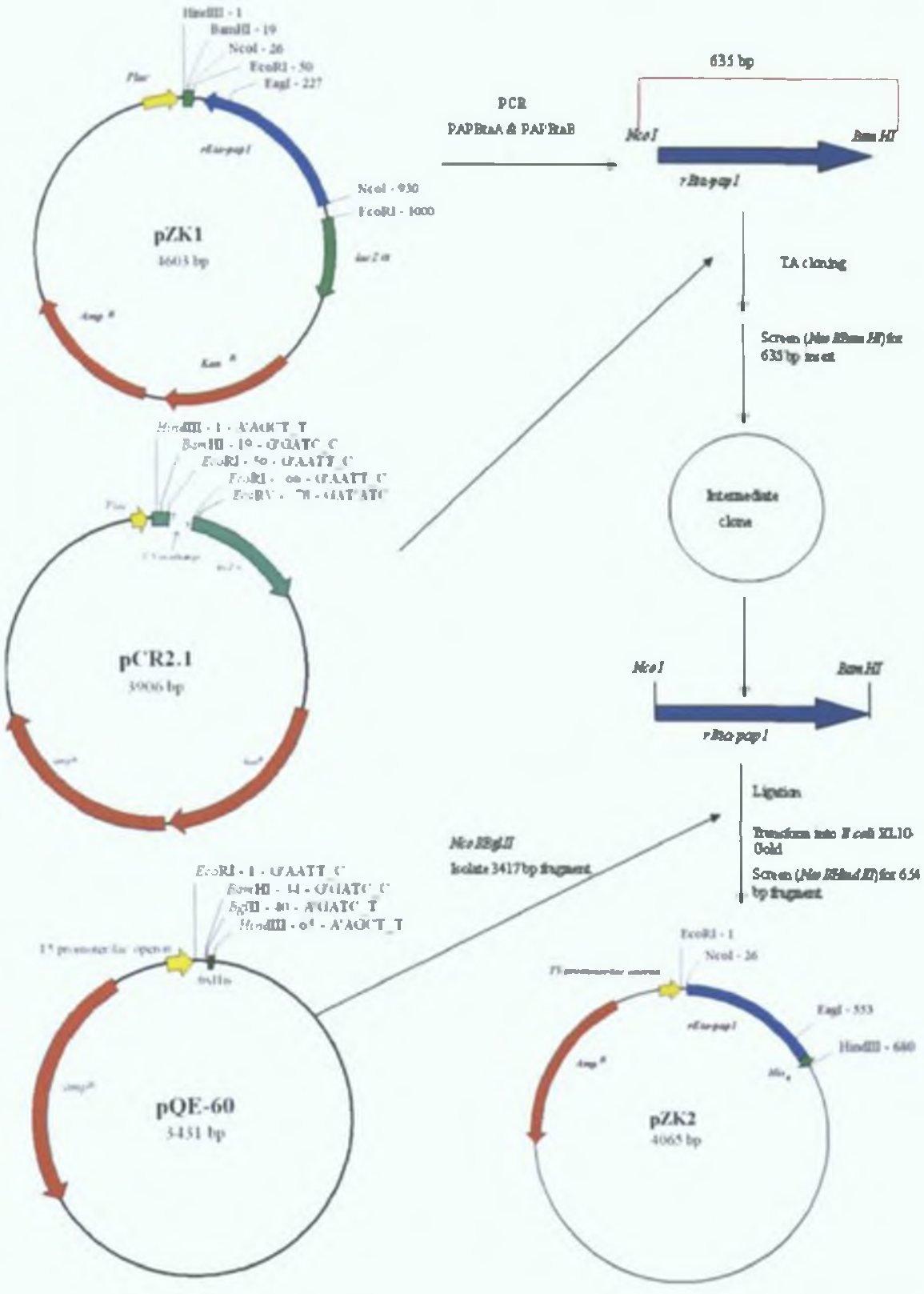

Figure 3.6 Cloning Strategy for pZK2

Outline of sub-cloning strategy from pZK1 to generate pZK2. PCR (see Section 2.8.2) on pZK1 using primers PAPBtA and PAPBtB (see Table 2.2) generates product containing *rBta-pap1* without stop codon and having *Nco*I and *Bam*HI site tags, which is ligated into pCR2.1. *rBta-pap1* is excised from intermediate clone by *Nco*I/*Bam*HI restriction and ligated into pQE-60 (see Table 2.3, Figure 2.2), which has been opened with *Nco*I/*Bgl*II restriction. Resulting construct, pZK2, has 6x1lis sequence cloned to 3' end of *rBta-pap1* followed by stop codon. Illustrated using pDRAW32 (see Section 2.11).

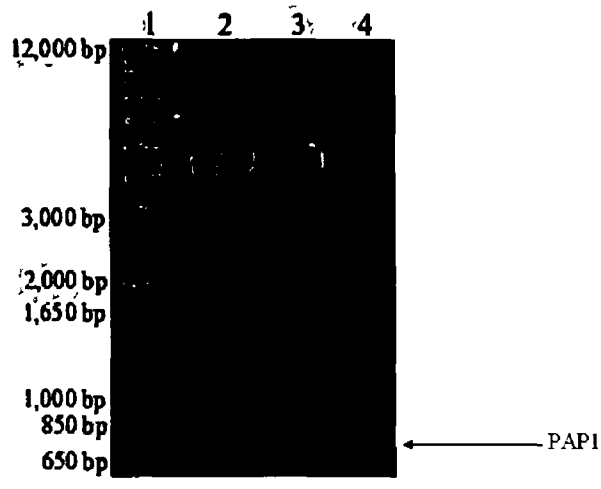

Figure 3.7 Verification Digest of pZK2
Restriction digest of pZK2 construct analysed on 1% agarose gel (see Section 2 5) Lane 1, DNA Ladder (sizes as in Figure 2 5), Lane 2, *Eco*R1, Lane 3, *Nco*1, Lane 4, *Nco*1/*Hin*dIII

3 3 2 Sub-Cloning of Bovine PAP1 Gene into *E coli* Expression Vector pPC225

rBta-pap1 was sub-cloned from pZK2 into the vector pPC225 (see Table 2 3, Figure 2 3) as outlined in Figure 3 8 pPC225 features the *tac* transcriptional promoter (P*tac*) P*tac* is a hybrid promoter consisting of the –35 region from the *trp* promoter fused to the –10 region (Pribnow box), operator and RBS (Shine-Dalgarno sequence) from P*lac* DeBoer *et* al (1983) reported on the high efficiency of P*tac* in expressing foreign genes in *E coli* as opposed to the parental promoters P*tac* can be repressed by the LacI protein pPC225 contains amp^R and another useful feature, noted during cloning, was that the 1800 bp fragment within the MCS (see Figure 2 3) allowed for easy differentiation of linear from uncut vector

An *Eco*RI/*Hin*dIII restriction enabled the entire *rBta-pap1*-His_6 fusion to be transferred from pZK2 to pPC225, which had been opened with *Eco*RI/*Hin*dIII Figure 3 9 shows a restriction digest of this construct, pZK3 *Nco*I, *Eco*RI and *Hin*dIII single restrictions produced bands corresponding to the expected 5235 bp linearised plasmid (see Figure 3 10A) The *Eco*RI/*Hin*dIII restriction produced a band corresponding to the expected 680 bp fragment containing the *rBta-pap1*-His_6 fusion (see Figure 3 10B)

pZK3 was subsequently verified by DNA sequencing (see Appendix B) Figure 3 11 details the *rBta-pap1* region of pZK3 showing the promoter elements, translated sequence, restriction sites and the His_6 tag

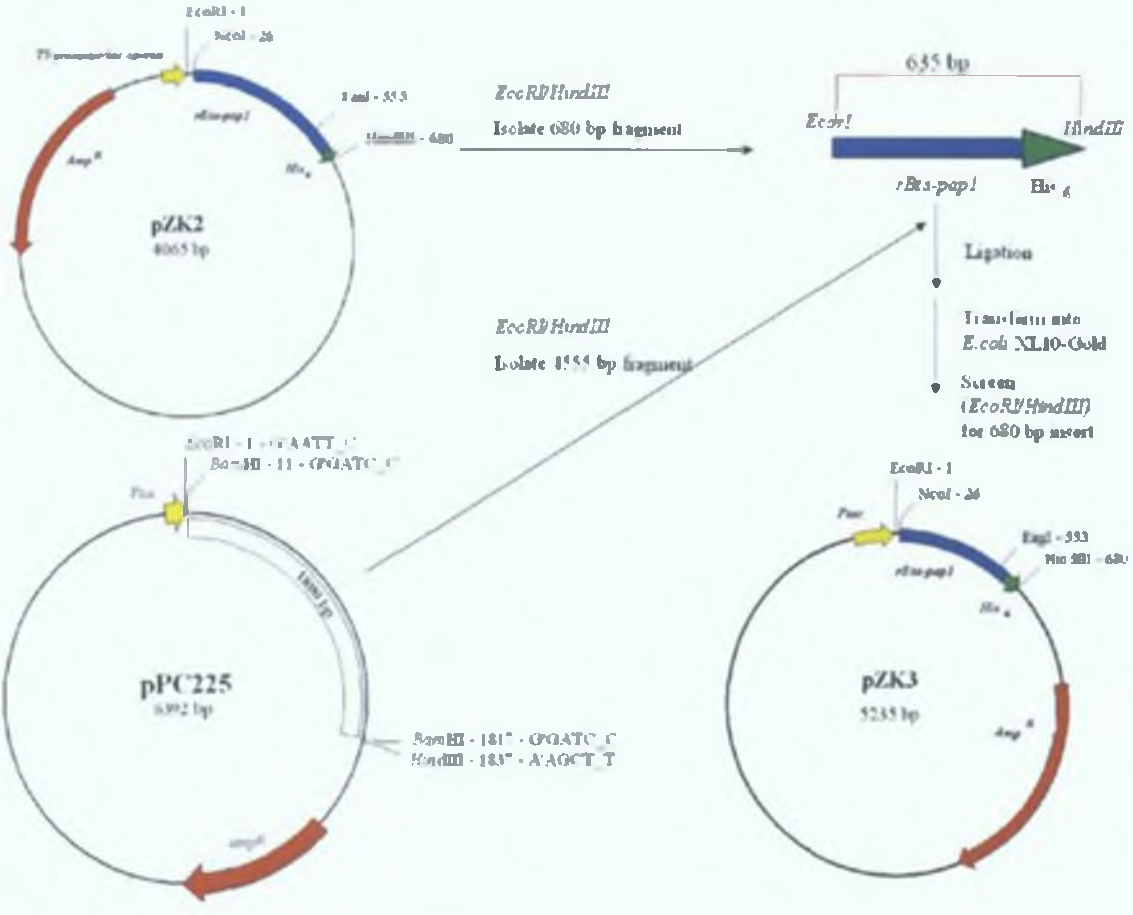

Figure 3.8 Cloning Strategy for pZK3

Outline of sub-cloning strategy from pZK2 to generate pZK3. The *rBta-pap1*-His_6 fusion is excised from pZK2 by restriction with *Eco*RI and *Hin*dIII. This 680 bp fragment is ligated into pPC225, which has been opened with *Eco*RI and *Hin*dIII. Resulting construct, pZK3, has *rBta-pap1*-His_6 fusion under control of P*tac* promoter. Illustrated using pDRAW32 (see Section 2.11).

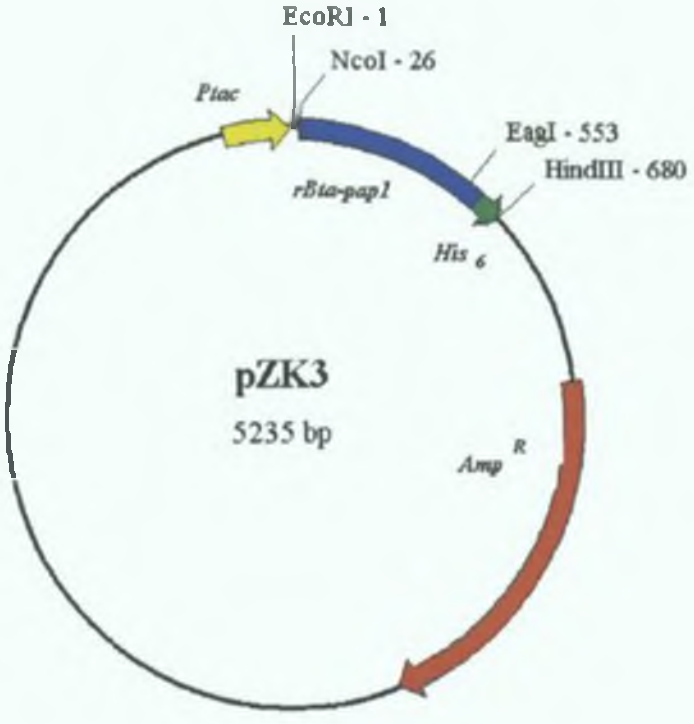

Figure 3.9 pZK3 Plasmid Map
The *rBta-pap1* gene fragment is shown in blue which is under the control of the P*tac* promoter (yellow). His tag fusion is shown in green and Ampicillin resistance gene (amp^R) in red. See Figure 2.3 for map of parent vector pPC225. Illustrated using pDRAW32 (see Section 2.11).

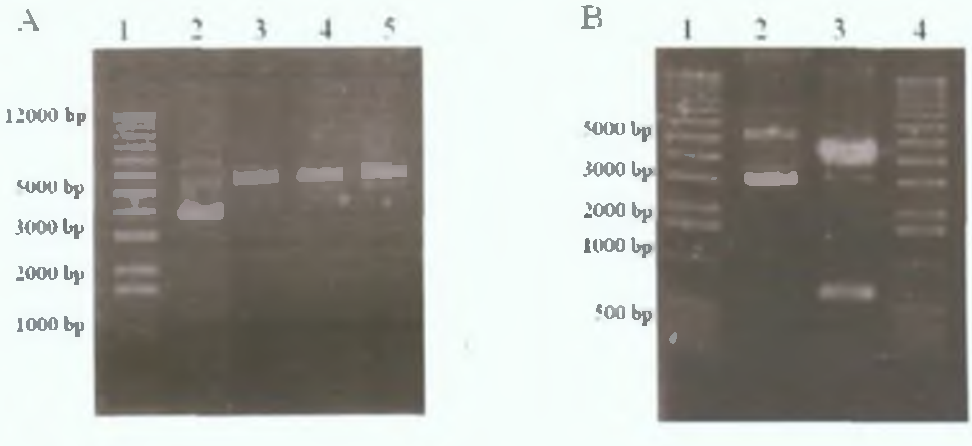

Figure 3.10 Verification Digest of pZK3
Restriction digest of pZK3 construct analysed on 1% agarose gel (see Section 2.5): **(A)** Lane 1, DNA Ladder (sizes as in Figure 2.5); Lane 2, uncut; Lane 3, *Nco*I; Lane 4, *Eco*RI; Lane 5, *Hind*III. **(B)** Lane 1, DNA Ladder; Lane 2, uncut; Lane 3, *Eco*RI/*Hind*III; Lane 4, DNA Ladder.

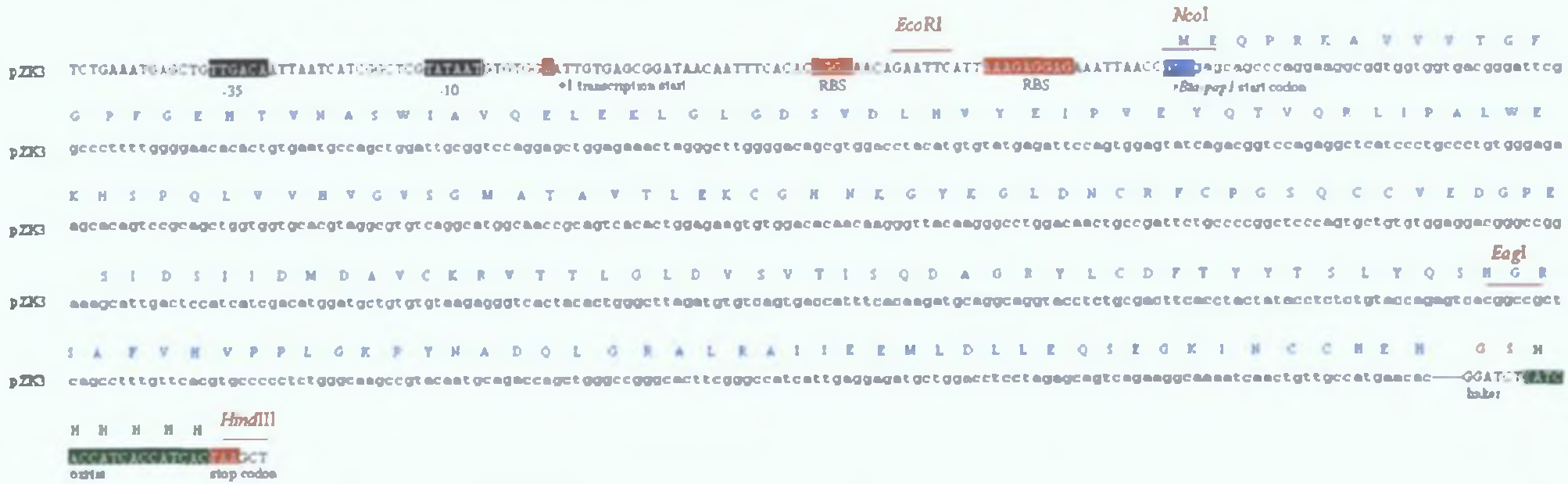

Figure 3.11 pZK3 Sequence Detail
The *rBta-pap1* and P*tac* promoter (black) regions of pZK3 are shown in detail. The translation of *rBta-pap1* is shown in blue above the ORF. The 6xHis tag sequence is shown in green, joined to *rBta-pap1* by a Gly-Ser linker. Two ribosome binding sites (RBS, red) are shown. The first RBS upstream from the *rBta-pap1* start codon was subcloned from pZK2 (see Figure 3.6) while the second RBS was present on pPC225 associated with the P*tac* promoter. Restriction enzymes are marked in red. For amino acid information see Appendix D. Illustrated using GenDoc (see Section 2.11).

3 4 Expression of Recombinant Bovine PAP1 in *E coli* XL10-Gold

The expression plasmid pZK3 (see Figure 3 9) was transformed into *E coli* strains XL10-Gold (see Table 2 1), by the method described in Section 2 6 3

XL10-Gold strains contain F factors, which carry the *lacI*^{q} allele The *lacI*^{q} allele is a promoter mutation that expresses the LacI repressor protein at high levels, resulting in strong repression of the P*tac* promoter unless the inducer IPTG is added, which binds and inactivates LacI and thus induces transcription from P*tac*

A number of parameters were investigated during the optimisation of the expression system for recombinant human PAP1 (Vaas, 2005) These parameters namely *E coli* strain, effect of induction time, effect of IPTG and effect of sonication time were optimised Various *E coli* strains including DH5α, INVαF', BL21, Nova Blue, Rosetta, RosettaBlue and XL10-Gold were analysed for expression Optimal protein expression was found when *E coli* strain XL10-Gold was utilised

The optimal concentration of IPTG for induction was found to be 50 μM Relatively low levels of recombinant protein were obtained when using 0 5 or 1 mM IPTG Sonication was found to have a major negative effect on the r*Hsa*PAP1$_{6H}$ enzyme Sonication time of greater than 30 sec was found to result in a sharp reduction of r*Hsa*PAP1$_{6H}$ activity Therefore a standard sonication time of 30 seconds was utilised

The *E coli* XL10-Gold culture (1 litre culture), expressing r*Bta*PAP1$_{6H}$ (see Section 2 12) was induced with 50 μM IPTG until the A_{600} had reached 0 35 and allowed to grow for a further 4 hrs as described in Section 2 12 1

3 5 Purification of Recombinant Bovine PAP1

Nitrilotriacetic acid (NTA) is a tetradentate chelator, allowing it to occupy four of the six ligand binding sites in the coordination sphere of Ni^{2+}, therefore binding the metal ion far more stably, retaining it even under stringent wash conditions In the Ni-NTA resin, two ligand binding sites of each Ni^{2+} are free to interact with the six consecutive imidazole groups of a His_6 tag Ni-NTA was used in this work to purify r*Bta*PAP1$_{6H}$ as reported in the following Section 3 5 1

3.5.1 IMAC Purification of Recombinant Bovine PAP1

The standard procedure to purify r*Bta*PAP1$_{6H}$ from cleared lysate, obtained from *E. coli* cultures expressing r*Bta*PAP1$_{6H}$, using Ni-NTA is described in Section 2.13.1. Both washing and elution was carried out using free imidazole as a counter-ligand.

Figure 3.12 shows the SDS-PAGE analysis (see Section 2.16) of a routine IMAC purification of r*Bta*PAP1$_{6H}$, using four 20 mM imidazole washes and three 200 mM imidazole elutions. The protein concentration and specific activity values for the cleared lysate and first elutions are given in Table 3.1. Zymogram analysis (see Section 2.17) was carried out on purified r*Bta*PAP1$_{6H}$, shown in Figure 3.13.

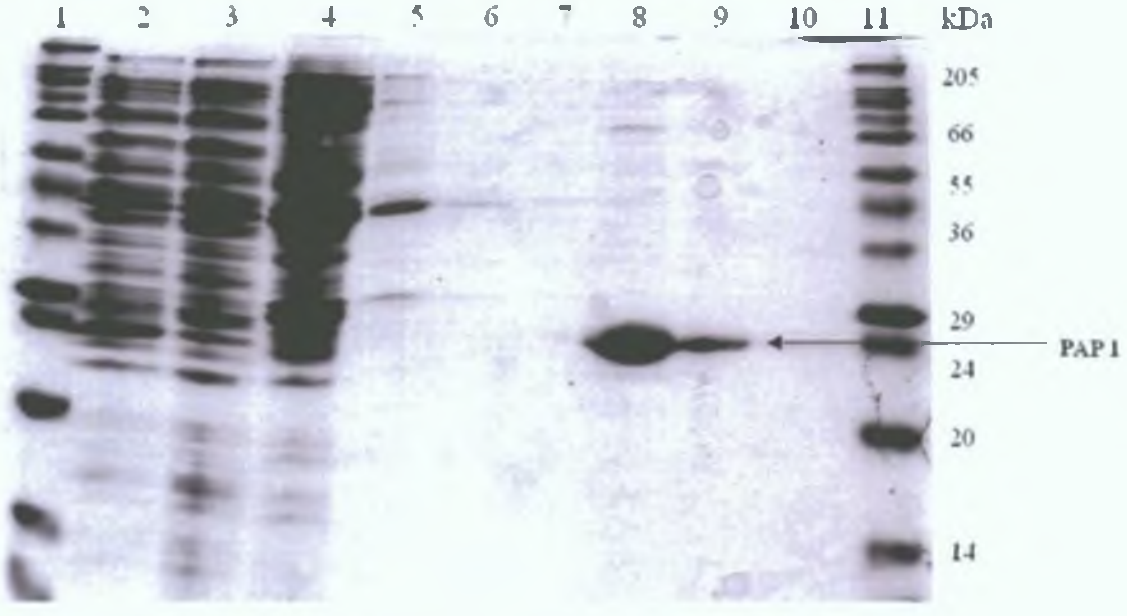

Figure 3.12 SDS-PAGE of Bovine PAP1 at Each Stage of Purification

Lane 1 and 11, protein molecular marker; lane 2, crude supernatant; lane 3, flow-through; lane 4-7, sequential column washings; lane 8-10, elution of recombinant bovine PAP1 protein from the column. The relevant sizes (kDa) of the protein marker are indicated.

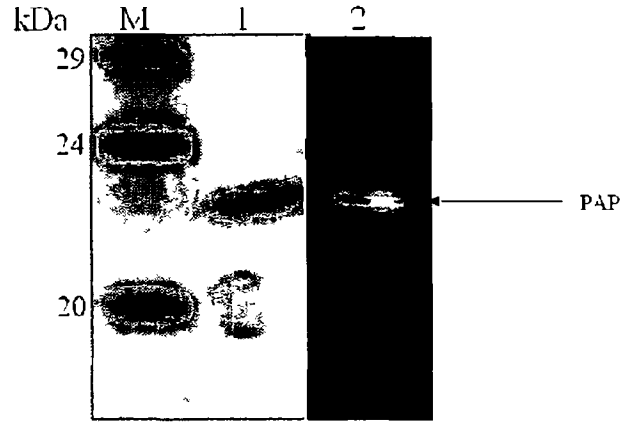

Figure 3 13 Zymogram Analysis of Purified Bovine
Bovine PAP1 activity band is highlighted which correlates with protein band on SDS-PAGE Lane 1, protein molecular marker, lane 2, purified bovine PAP1 on SDS-PAGE, lane 3, zymogram of purified bovine PAP1 on Native-PAGE

Table 3 1 Summary of Recombinant Bovine PAP1 Purification.

	Volume (ml)	Total Activity[a] (Units)	Total Protein (mg)	Specific Activity (Units mg ^{1})	Purification Factor	Yield (%)
Crude PAP1	30	35,197	103 25	340	1	100
Purified PAP1 (Elution 1)	5	9,388	2 6	3,633	106 8	27

[a] Units = nmoles min ^{1} i e Units are expressed as nanomoles of AMC released per minute at 37°C

3.6 Biochemical Properties of Recombinant Bovine PAP1

3.6.1 Relative Molecular Mass

As outlined in Section 2.18.1, 100 μl of purified r*Bta*PAP1$_{6H}$, at a concentration of 200 μg/ml, was analysed by size exclusion chromatography. Figure 3.14 shows the protein concentration profile corresponding to the elution of r*Bta*PAP1$_{6H}$ and the protein standards BSA, Carbonic Anhydrase and Cytochrome c. Also shown is the profile of PAP1 activity corresponding to the elution of r*Bta*PAP1$_{6H}$. Figure 3.15 shows a plot of elution volume over void volume (V_e/V_o) versus the log of molecular weight. From this plot the relative molecular weight of r*Bta*PAP1$_{6H}$ was determined as 24.7 kDa.

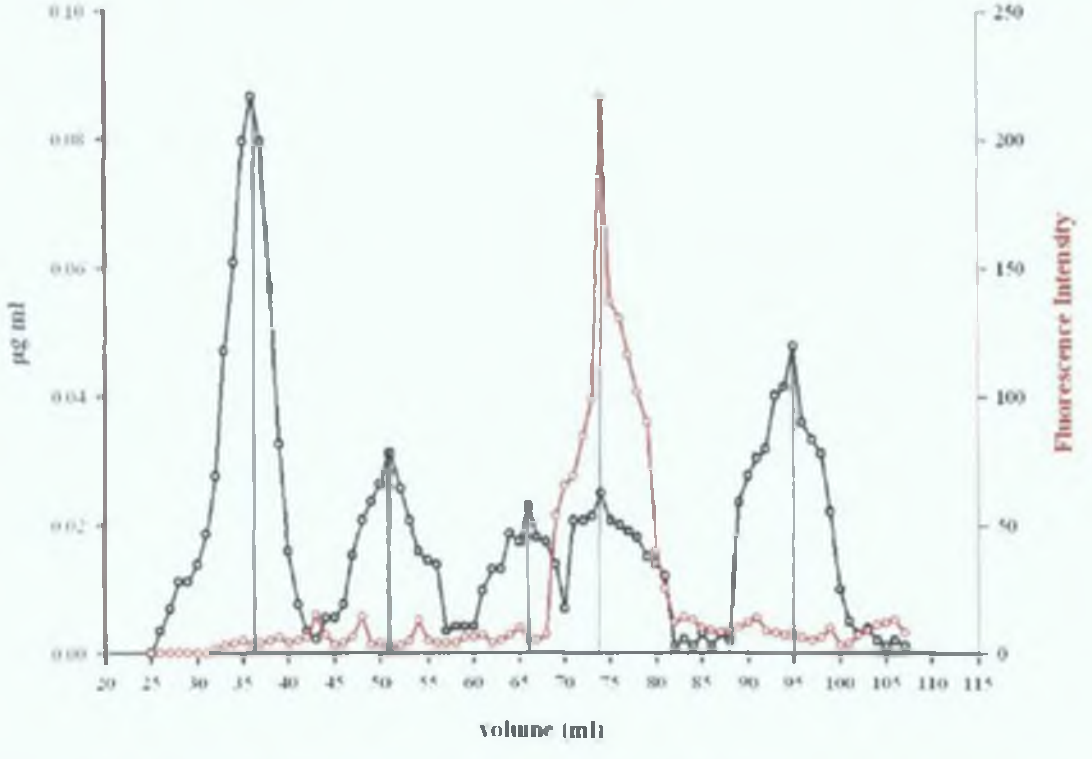

Figure 3.14 Size Exclusion Chromatography of r*Bta*PAP1$_{6H}$
Size exclusion chromatography (see Section 2.18.1) of r*Bta*PAP1$_{6H}$. Void volume of 36 ml was ascertained using blue dextran. Elution of r*Bta*PAP1$_{6H}$ at 74 ml was determined using PAP1 activity assay (see Section 2.15.3) and is represented by fluorescent intensity, shown in red. Elution volumes of molecular weight standards BSA (51 ml), Carbonic Anhydrase (67 ml) and Cytochrome c (94 ml), were determined by protein assay (see Section 2.14.1) and used to construct a plot of V_e/V_o versus log MW (see below).

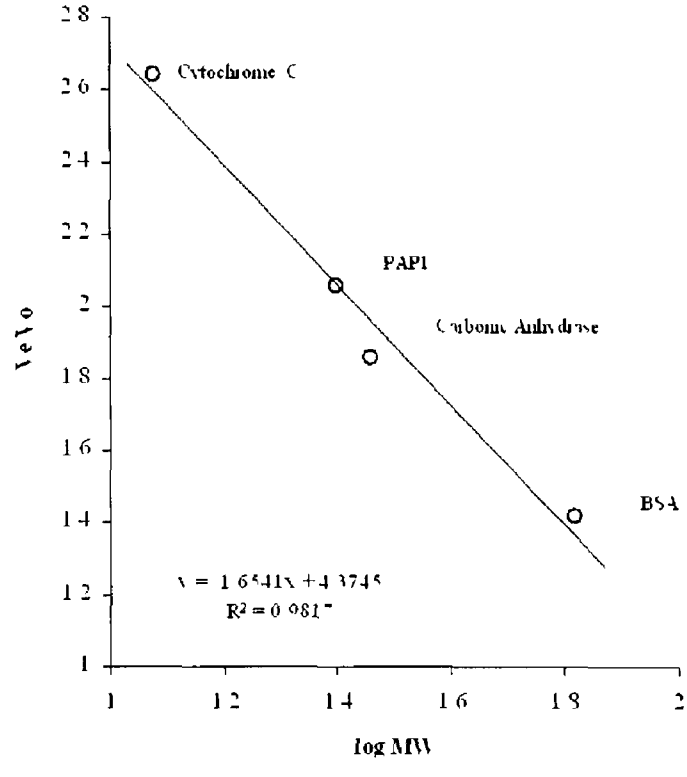

Figure 3 15 Determination of r*Bta*PAP1$_{6H}$ Native Size
Plot of elution volume over void volume (V_e/V_o) versus the log of molecular weight This plot was used to establish the relative molecular weight of r*Bta*PAP1$_{6H}$ to be 24 7 kDa

3 6 2 pH Profile

The effect of pH on the activity of r*Bta*PAP1$_{6H}$ was investigated as outlined in Section 2 18 2 Figure 3 16 shows the pH profile for purified r*Bta*PAP1$_{6H}$ Prominent PAP1 activity was detected between pH 7 5-10 0, with activity rapidly dropping off outside this pH range Bovine PAP1 exhibited its optimum activity within the peak range of 9 0-9 5

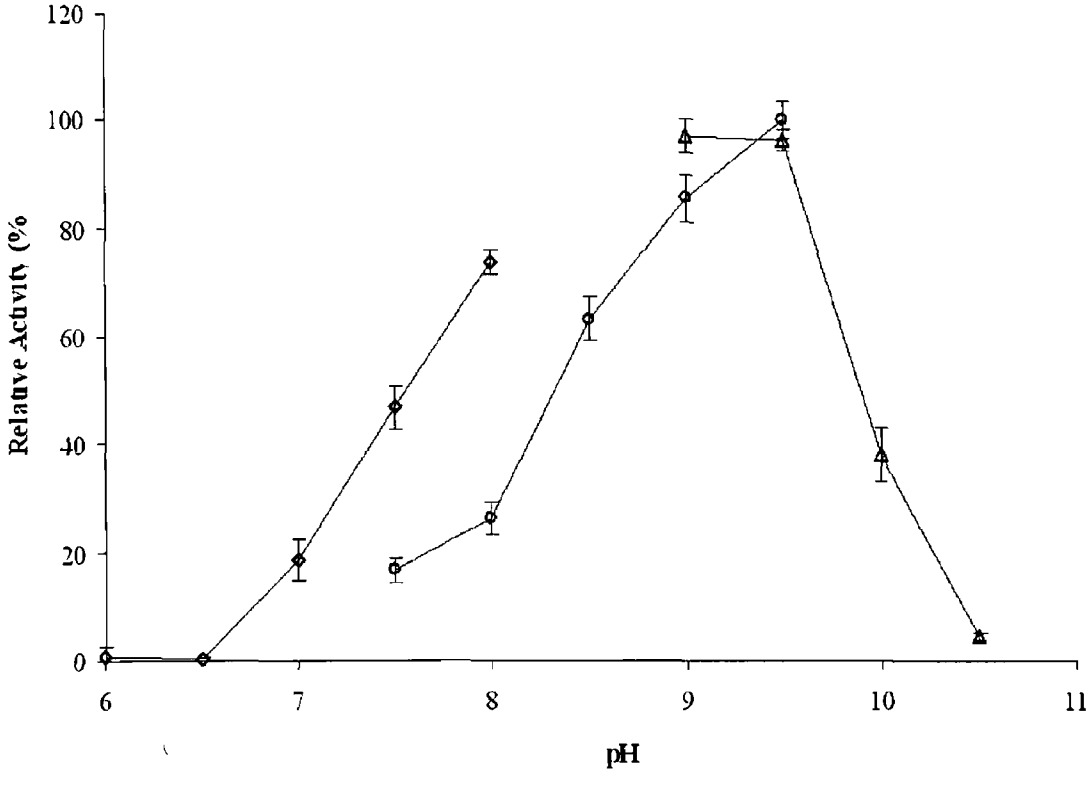

Figure 3 16 Effect of pH on r*Bta*PAP1$_{6H}$ Activity

Effect of pH on recombinant bovine PAP1 activity Enzyme activity was measured under standard assay conditions over the range pH 6 0-10 5 with buffers as described in materials and methods The buffers used were ◊, potassium phosphate, ○, Tris/HCL and Δ, glycine/NaOH Error bars represent the SD of triplicate readings

3.6.3 Temperature Studies

The effect of temperature on the activity of r*Bta*PAP1$_{6H}$ was investigated. As outlined in Section 2.15.3, the standard activity assay was carried out at a range of temperatures. The resulting 15 min temperature profile is shown in Figure 3.17. Maximal activity was observed at 37°C.

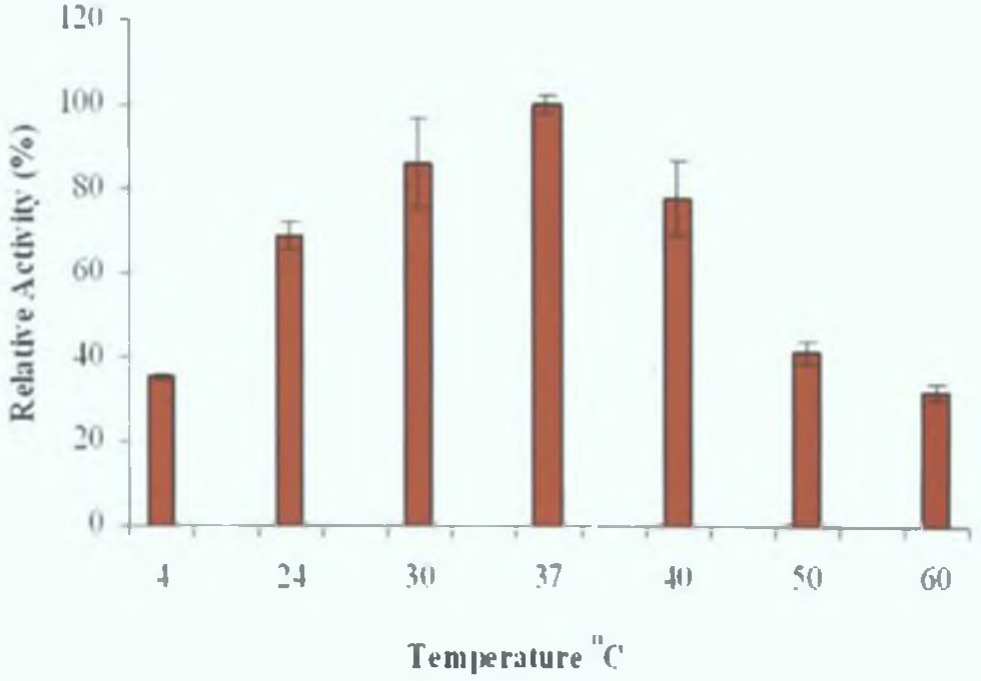

Figure 3.17 Effect of Temperature on r*Bta*PAP1$_{6H}$ Activity
The effect of temperature on the activity of r*Bta*PAP1$_{6H}$ activity was determined by carrying out the standard assay (see Section 2.15.3) at 4 to 60°C for 15 min. Error bars represent the SD of triplicate readings.

3 6 4 Effect of DTT and EDTA

DTT and EDTA are essential components of the standard PAP1 activity assay (see Section 2 15 3) In order to optimise the assay concentrations, their effect on r*Bta*PAP1$_{6H}$ activity was determined Figures 3 18 and 3 19 show the influence of DTT and EDTA, respectively, on r*Bta*PAP1$_{6H}$ activity Bovine PAP1 activity was heavily dependent on thiol reducing agent DTT A rapid increase in activity was observed from 2 mM to 10 mM and above this concentration a plateau effect was observed EDTA had an insignificant effect on activity and as a result 2 mM EDTA was used throughout

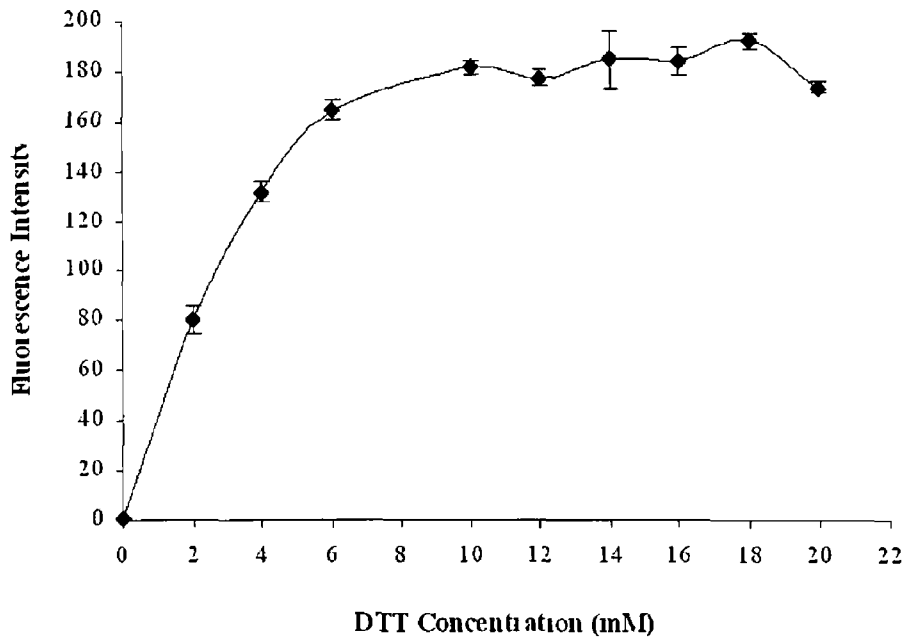

Figure 3 18 Effect of DTT on r*Bta*PAP1$_{6H}$ Activity
The effect of DTT concentration on the activity of r*Bta*PAP1$_{6H}$ activity was determined by carrying out the standard assay (see Section 2 15 3) using a range of DTT concentrations up to 20 mM Error bars represent the SD of triplicate readings

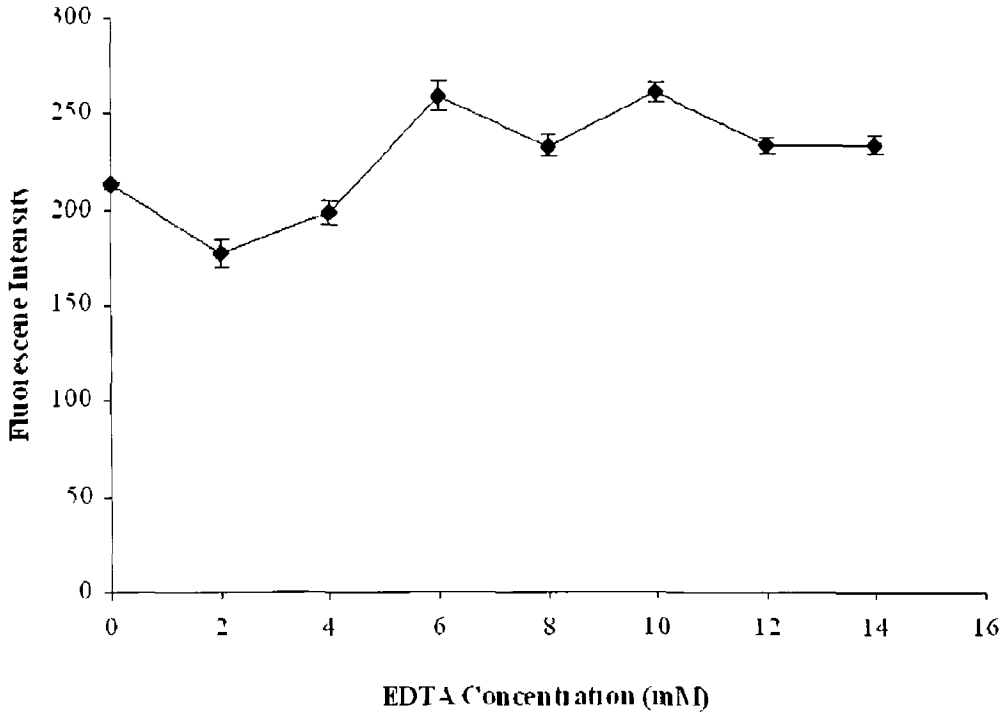

Figure 3 19 Effect of EDTA on r*Bta*PAP1$_{6H}$ Activity
The effect of EDTA concentration on the activity of r*Bta*PAP1$_{6H}$ activity was determined by carrying out the standard assay (see Section 2 15 3) using a range of EDTA concentrations up to 15 mM Error bars represent the SD of triplicate readings

3 6 5 Inhibition Studies

A number of compounds were analysed for their possible inhibitory effect on r*Bta*PAP1$_{6H}$ activity (see Section 2 18 5) IC_{50} values were determined, whereby this value represents the inhibitor concentration at which 50% of enzymatic activity is lost

A value of 0 8mM was determined for the thiol-blocking compound iodoacetic acid (see Figure 3 20)

Inhibition by free $_{L}$- pGlu and the substrate analogue 2-pyrrolidone is shown in Figures 3 21 and 3 22 IC_{50} values determined were 1 6 and 0 75 mM, respectively

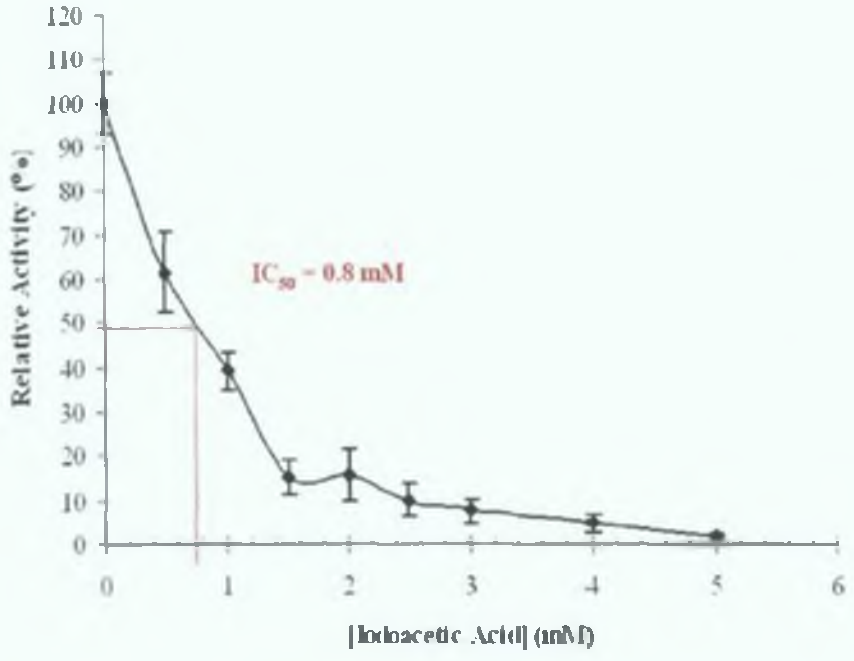

Figure 3.20 Effect of Iodoacetic Acid on r*Bta*PAP1$_{6H}$ Activity
The effect of iodoacetic acid on the activity of r*Bta*PAP1$_{6H}$ was determined by the procedure outlined in Section 2.18.5, using iodoacetic acid at concentrations up to 5 mM. Error bars represent the SD of triplicate readings.

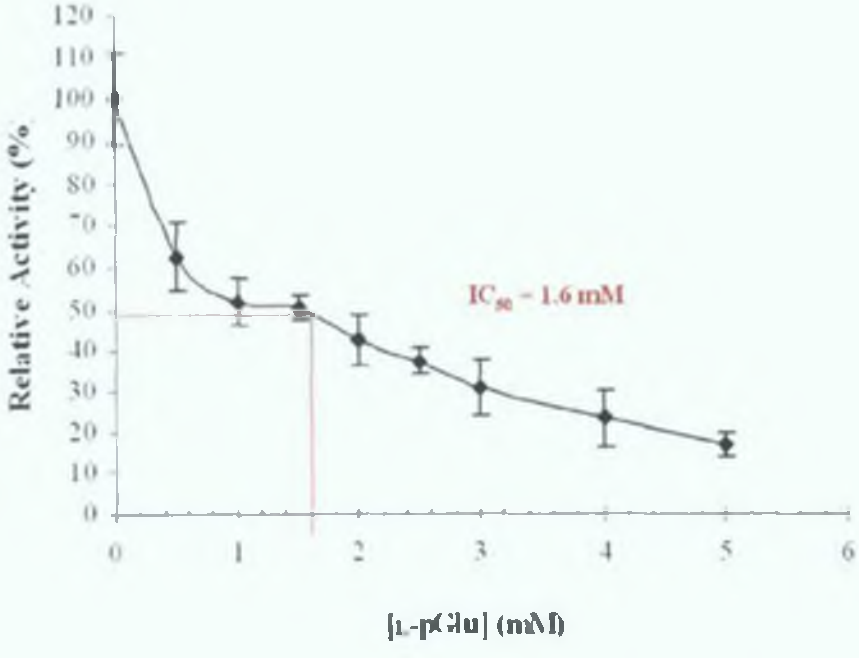

Figure 3.21 Effect of $_{L}$-pGlu on r*Bta*PAP1$_{6H}$ Activity
The effect of $_{L}$-pGlu on the activity of r*Bta*PAP1$_{6H}$ was determined by the procedure outlined in Section 2.18.5, using $_{L}$-pGlu at concentrations up to 5 mM. Error bars represent the SD of triplicate readings.

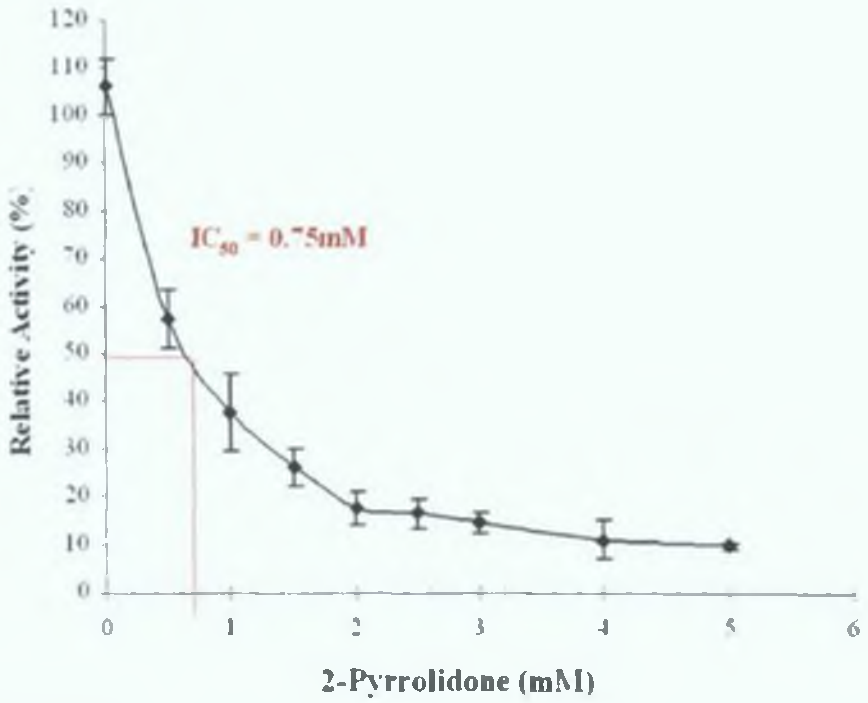

Figure 3.22 Effect of 2-Pyrrolidone on r*Bta*PAP1$_{6H}$ Activity
The effect of 2-Pyrrolidinone on the activity of r*Bta*PAP1$_{6H}$ was determined by the procedure outlined in Section 2.18.5, using 2-Pyrrolidone at concentrations up to 5 mM. Error bars represent the SD of triplicate readings.

3.7 Kinetic Studies

Kinetic analysis on purified bovine PAP1 were performed as outlined in Section 2.18.6.

3.7.1 Determination of Kinetic Parameters K_m, V_{max} and K_{cat} for Recombinant Bovine PAP1

It was necessary to dilute purified r*Bta*PAP1$_{6H}$ to a concentration of 1-5 $\mu g.ml^{-1}$ in order to ensure the fluorescent intensity values fell within the measurable range of the Perkin-Elmer LS-50B plate reader spectrophotometer used in this work (see Section 2.15.3).

This procedure, which required PAP1 activity to be assayed at various pGlu-AMC concentrations, as outlined in Section 2.18.6.1, was carried out with purified r*Bta*PAP1$_{6H}$. The resulting Michaelis-Menten curve for purified r*Bta*PAP1$_{6H}$ is shown in Figure 3.23.

This data was applied to the three kinetic models described in Appendix C, namely: Lineweaver-Burk (see Figure 3.24), Eadie-Hofstee (see Figure 3.25) and Hanes-Woolf (see Figure 3.26). From these plots the maximal enzyme velocity (V_{max}) and the Michaelis constant (K_m) were determined, which are given in Table 3.2. Also shown in

this table is the turnover number (K_{cat}) for purified r*Bta*PAP1$_{6H}$, which was determined as described in Appendix C. These parameters were also determined using Enzfitter software from Biosoft, Cambridge, UK.

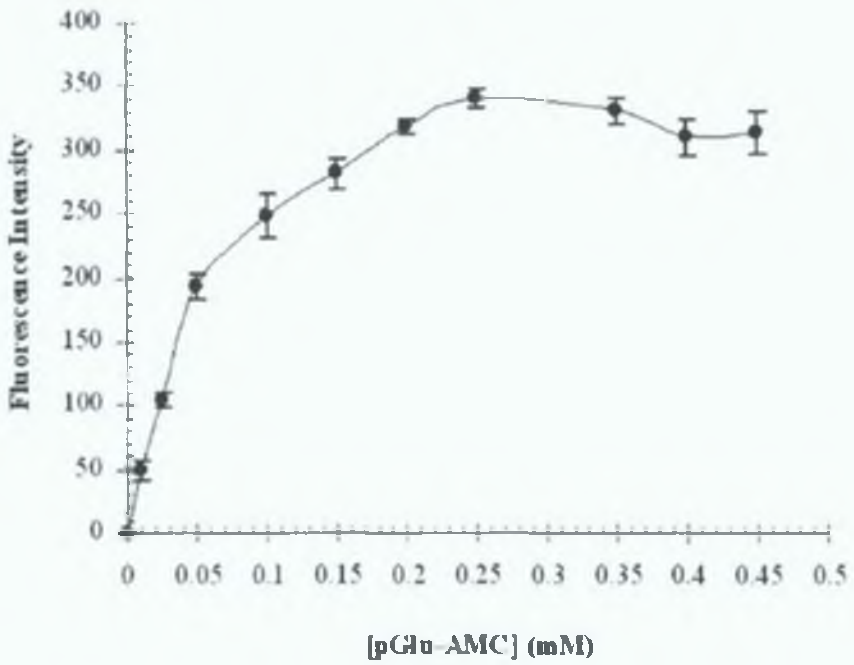

Figure 3.23 Michaelis-Menten Curve for Purified r*Bta*PAP1$_{6H}$
Plot of substrate concentration ([pGlu-AMC]) versus reaction rate, represented by fluorescence intensity (Fi), for purified r*Bta*PAP1$_{6H}$ diluted to 2.5 µg/ml. Data obtained by the procedure described in Section 2.18.6.1. Error bars represent the SD of triplicate readings.

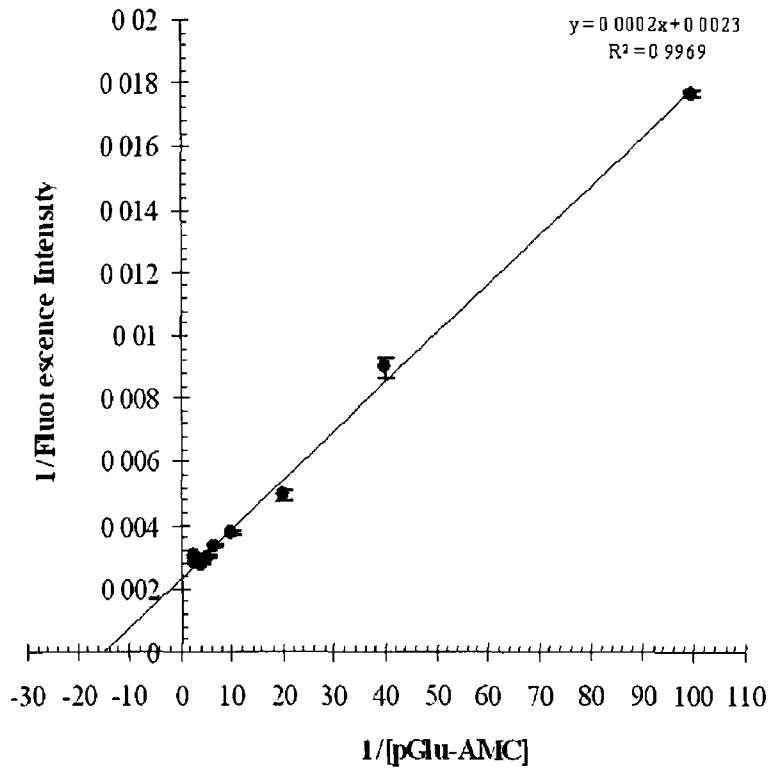

Figure 3 24 Lineweaver-Burk Plot for Purified r*Bta*PAP1$_{6H}$

Data from Figure 3 23 fitted to the Lineweaver-Burk model for the determination of kinetic parameters, as outlined in Appendix C Equation and regression are shown K_m and V_{max} values given in Table 3 2 Error bars represent the SD of triplicate readings

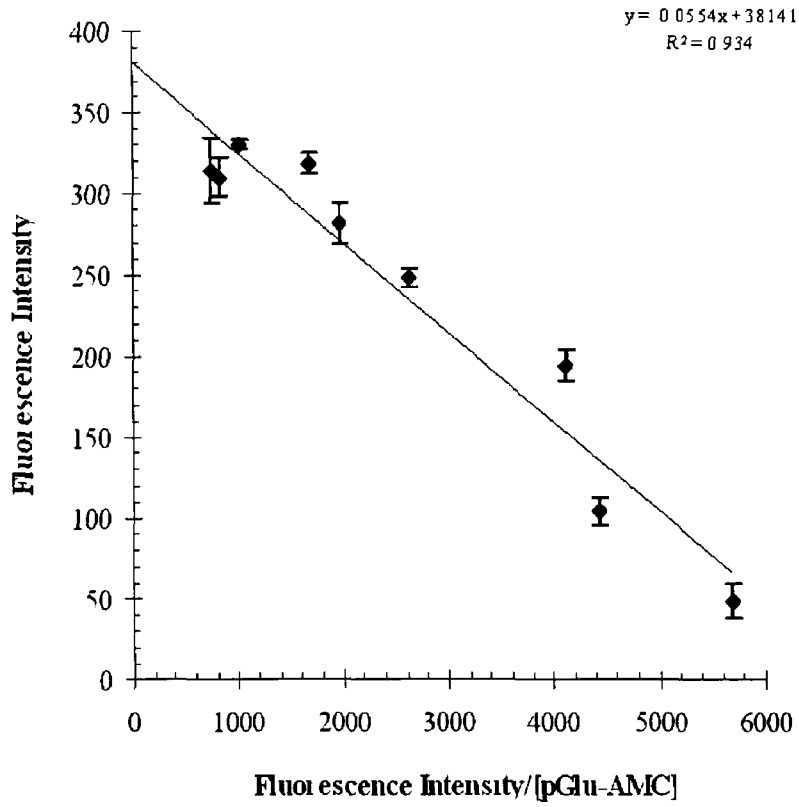

Figure 3 25 Eadie-Hofstee Plot for Purified r*Bta*PAP1$_{6H}$

Data from Figure 3 23 fitted to the Eadie-Hofstee model for the determination of kinetic parameters, as outlined in Appendix C Equation and regression are shown K_m and V_{max} values given in Table 3 2 Error bars represent the SD of triplicate readings

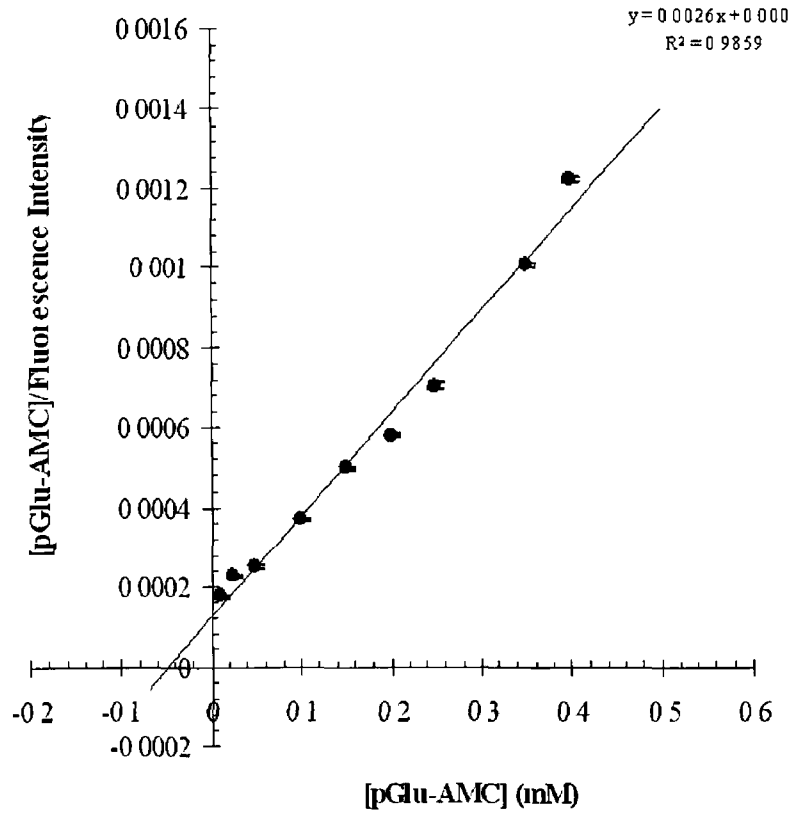

Figure 3 26 Hanes-Woolf Plot for Purified r*Bta*PAP1$_{6H}$

Data from Figure 3 23 fitted to the Hanes-Woolf model for the determination of kinetic parameters, as outlined in Appendix C Equation and regression are shown K_m and V_{max} values given in Table 3 2 Error bars represent the SD of triplicate readings

Table 3 2 Kinetic Parameters Obtained for r*Bta*PAP1$_{6H}$

Method	K_m μM	V_{max} Units ml^{-1}	K_{cat} s^{-1}
Lineweaver-Burk	66	3 3	3 6
Eadie-Hofstee	55	2 93	3 25
Hanes-Woolf	50	3 04	3 37
Enzfitter Software	63	3 22	3 57
Average	*59*	*3 12*	*3 5*

[K_m and V_{max} values obtained from Figures 3 24 to 3 26 K_{cat} calculated as outlined in Appendix C]

3 7 2 Determination of K_i Values for Pyroglutamyl-Peptides

Determination of K_i values in the PAP1-catalysed hydrolysis of pGlu-AMC using pyroglutamyl-containing peptides was performed according to Section 2 18 6 2 $K_{m\,(app)}$ and V_{max} values were determined graphically for each of the peptides using the Lineweaver-Burk kinetic plot K_i values and the nature of inhibition were estimated for each peptide Figures 3 27 to 3 33 represent Lineweaver-Burk plots for each peptide studied A K_i value of 44 μM was determined for tripeptide TRH showing the relative highest affinity for bovine PAP1 Table 3 3 lists the $K_{m\,(app)}$ K_i values and the type of inhibition obtained for peptides tested The significance of these results is discussed in Section 3 8

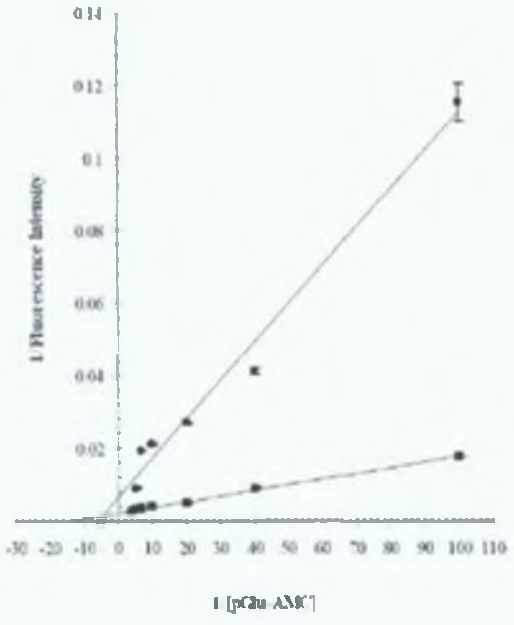

Figure 3.27 Kinetic Analysis of the Effect of pGlu-Ala (●) on Bovine PAP1 Catalysed Hydrolysis of pGlu-AMC (■). Lineweaver-Burk reciprocal plot of fluorescent intensity versus [pGlu-AMC]. Plot illustrates mixed inhibition of PAP1 by pGlu-Ala. Error bars represent the SD of triplicate readings.

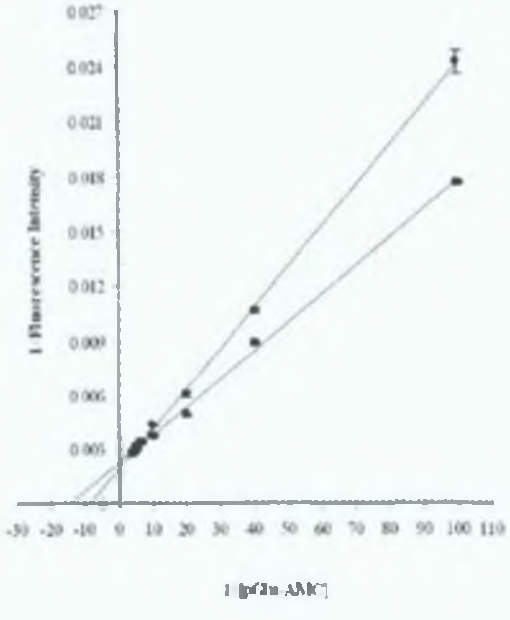

Figure 3.28 Kinetic Analysis of the Effect of pGlu-Thr (●) on Bovine PAP1 Catalysed Hydrolysis of pGlu-AMC (■). Lineweaver-Burk reciprocal plot of fluorescent intensity versus [pGlu-AMC]. Plot illustrates competitive inhibition of PAP1 by pGlu-Thr. Error bars represent the SD of triplicate readings.

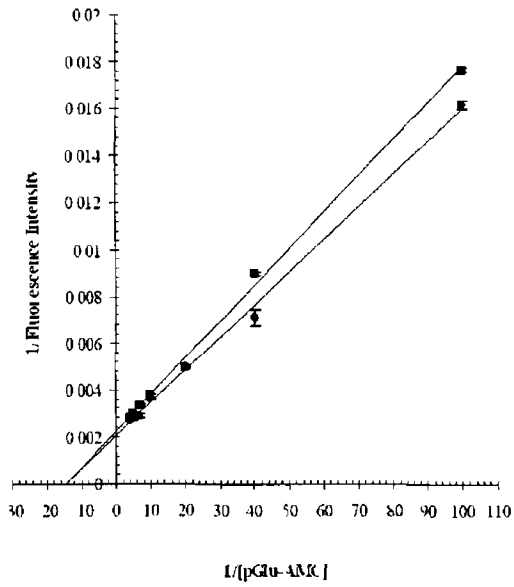

Figure 3 29 Kinetic Analysis of the Effect of pGlu-Pro (•) on Bovine PAP1 Catalysed Hydrolysis of pGlu-AMC (■) Lineweaver-Burk reciprocal plot of fluorescent intensity versus [pGlu-AMC] Plot illustrates non-competitive inhibition of PAP1 by pGlu-Pro Error bars represent the SD of triplicate readings

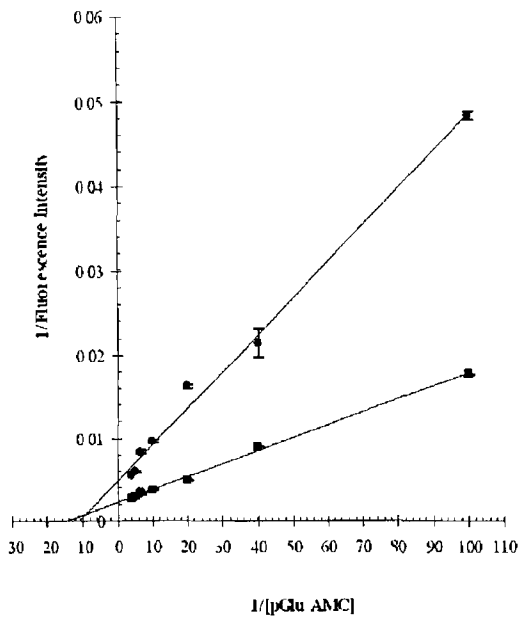

Figure 3 30 Kinetic Analysis of the Effect of pGlu-Val (•) on Bovine PAP1 Catalysed Hydrolysis of pGlu-AMC (■) Lineweaver-Burk reciprocal plot of fluorescent intensity versus [pGlu-AMC] Plot illustrates mixed inhibition of PAP1 by pGlu-Val Error bars represent the SD of triplicate readings

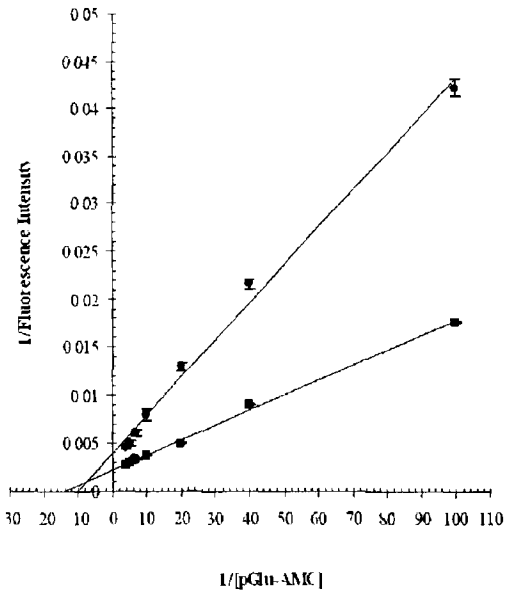

Figure 3.31 Kinetic Analysis of the Effect of pGlu-Ala-Ala (•) on Bovine PAP1 Catalysed Hydrolysis of pGlu-AMC (■) Lineweaver-Burk reciprocal plot of fluorescent intensity versus [pGlu-AMC] Plot illustrates mixed inhibition of PAP1 by pGlu-Ala-Ala Error bars represent the SD of triplicate readings

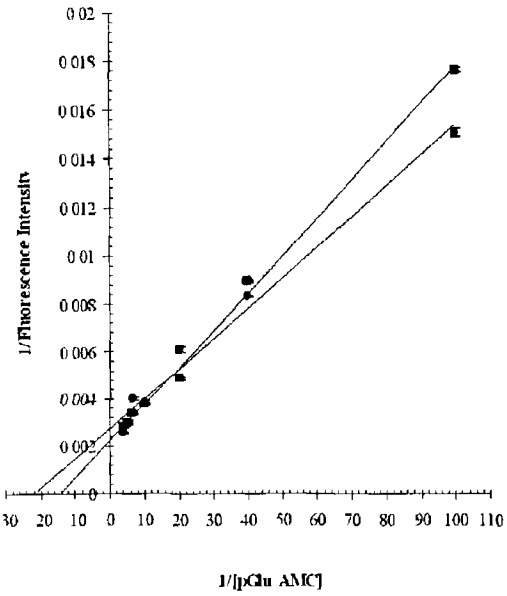

Figure 3 32 Kinetic Analysis of the Effect of pGlu-Glu-Ala (•) on Bovine PAP1 Catalysed Hydrolysis of pGlu-AMC (■). Lineweaver-Burk reciprocal plot of fluorescent intensity versus [pGlu-AMC] Plot illustrates competitive inhibition of PAP1 by pGlu-Glu-Ala Error bars represent the SD of triplicate readings

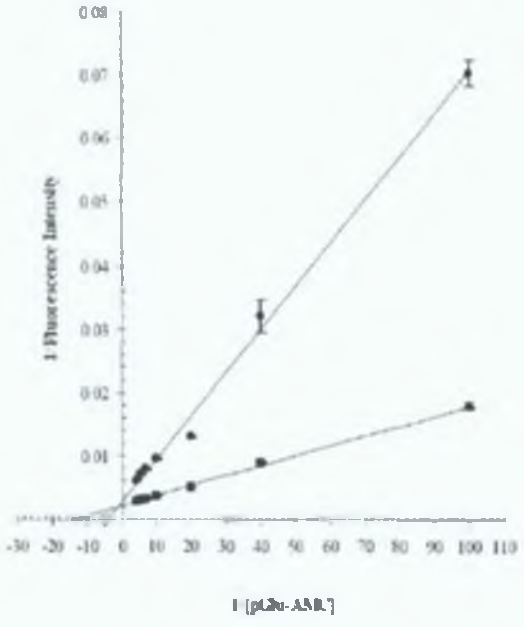

Figure 3.33 Kinetic Analysis of the Effect of pGlu-His-Pro-NH_2 (●) on Bovine PAP1 Catalysed Hydrolysis of pGlu-AMC (■). Lineweaver-Burk reciprocal plot of fluorescent intensity versus [pGlu-AMC]. Plot illustrates competitive inhibition of PAP1 by pGlu-His-Pro-NH_2. Error bars represent the SD of triplicate readings.

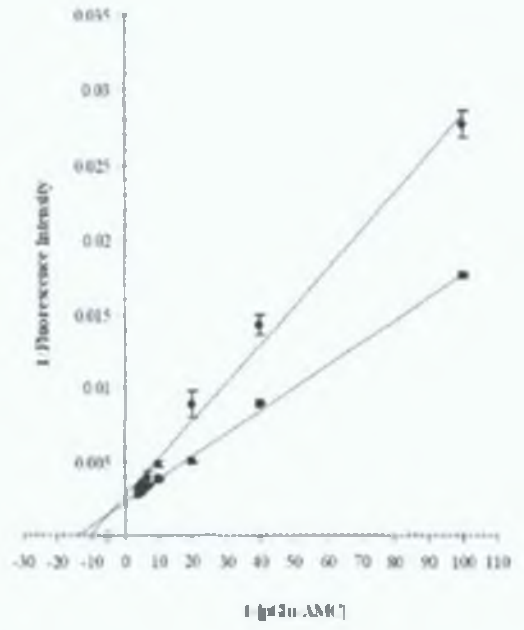

Figure 3.34 Kinetic Analysis of the Effect of pGlu-Met-Ala (●) on Bovine PAP1 Catalysed Hydrolysis of pGlu-AMC (■). Lineweaver-Burk reciprocal plot of fluorescent intensity versus [pGlu-AMC]. Plot illustrates mixed inhibition of PAP1 by pGlu-Met-Ala. Error bars represent the SD of triplicate readings.

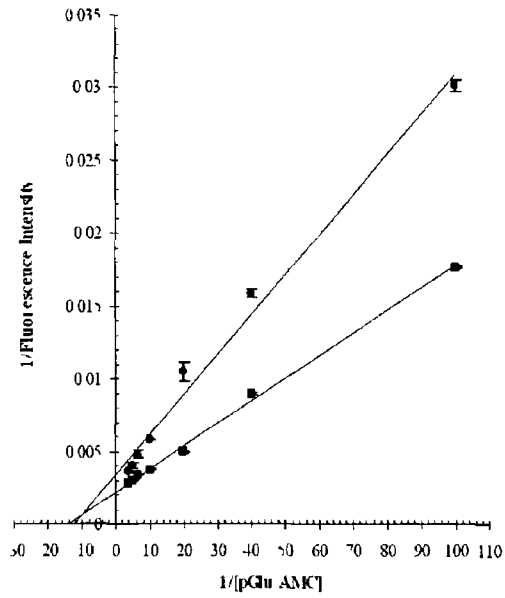

Figure 3.35 Kinetic Analysis of the Effect of pGlu-Thr-Ala (•) on Bovine PAP1 Catalysed Hydrolysis of pGlu-AMC (■) Lineweaver-Burk reciprocal plot of fluorescent intensity versus [pGlu-AMC] Plot illustrates mixed inhibition of PAP1 by pGlu-Thr-Ala Error bars represent the SD of triplicate readings

Table 3 3 K_i Values Obtained for Pyroglutamyl Peptides

Peptide	$K_{m\ (app)}$ (μM)	K_i (μM)	Inhibition Type
pGlu-Ala	166	141	Mixed
pGlu-Thr	125	279	Competitive
pGlu-Pro	71	3,300	Non-Competitive
pGlu-Val	83	625	Mixed
pGlu-Ala-Ala	111	366	Mixed
pGlu-Glu-Ala	47	n d	Competitive
pGlu-His-Pro-NH_2 (TRH)	400	44 1	Competitive
pGlu-Met-Ala	111	366	Mixed
pGlu-Thr-Ala	83	625	Mixed

Activity of bovine PAP1 towards pyroglutamyl peptides Enzyme assays were carried out as described in Materials and methods [K_m^{app} values obtained from Figure 3 27 - 3 35 K_i calculated as outlined in Appendix C]

3 8 Comparative Study of Recombinant Bovine PAP1 with Recombinant Human PAP1

Given that a member of our research group (Vaas, 2005) had previously cloned, expressed and purified the recombinant human PAP1 enzyme it was possible to carry out a comparative study with recombinant bovine PAP1

Nucleotide and amino acid sequences of both genes were aligned (see Figure 3 36 and 3 37, respectively)

3 8 1 Expression and Purification

Both r*Bta*PAP1$_{6H}$ and r*Hsa*PAP1$_{6H}$ were then expressed in *E coli* XL10-Gold (1 Litre Culture, see Section 2 12) and purified using IMAC (see Section 2 13)

SDS-PAGE resolved a band of ~23-24 kDa for both bovine and human PAP1 (see Figure 3 38) Following purification, bovine PAP1 produced a yield of 2 6 mg of PAP1 protein per litre culture Interestingly, the human PAP1 enzyme produced a higher yield of 6 5 mg PAP1 per litre culture (see Table 3 4) Total activity for r*Hsa*PAP1$_{6H}$ is almost three times greater than r*Bta*PAP1$_{6H}$ activity Overall, specific activity for r*Bta*PAP1$_{6H}$ and r*Hsa*PAP1 were 3,633 units mg^{-1} and 4,623 units mg^{-1}, respectively

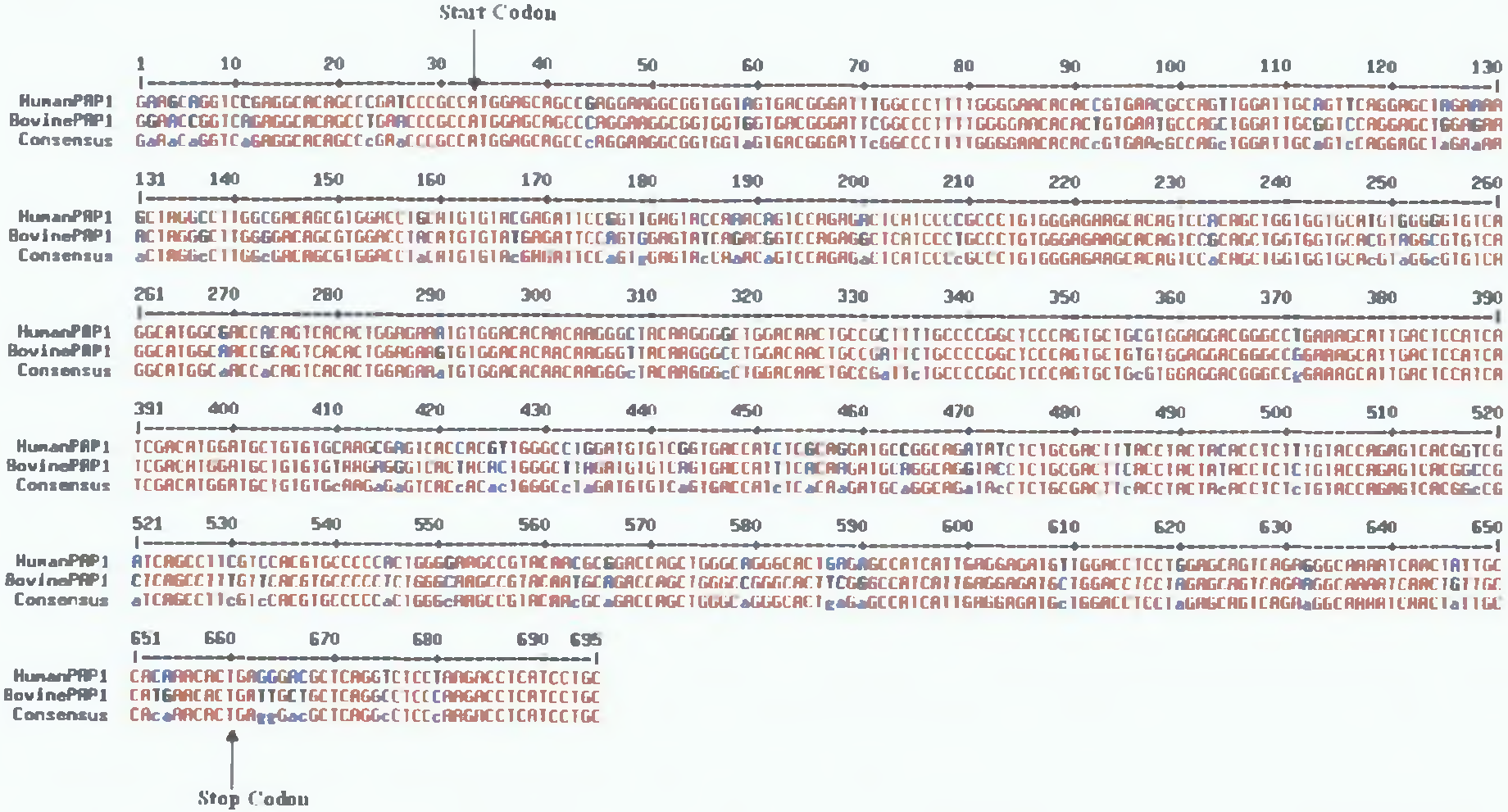

Figure 3.36 PAP1 Nucleotide Alignments

Alignment of the recombinant bovine PAP 1 XM866409 (Bovine PAP1) nucleotide sequence with human PAP1 AJ278828 (Human PAP1) highlighting the 71 nucleotide variations throughout. The sequences were annotated using the Multialign program. (see Section 2.11).

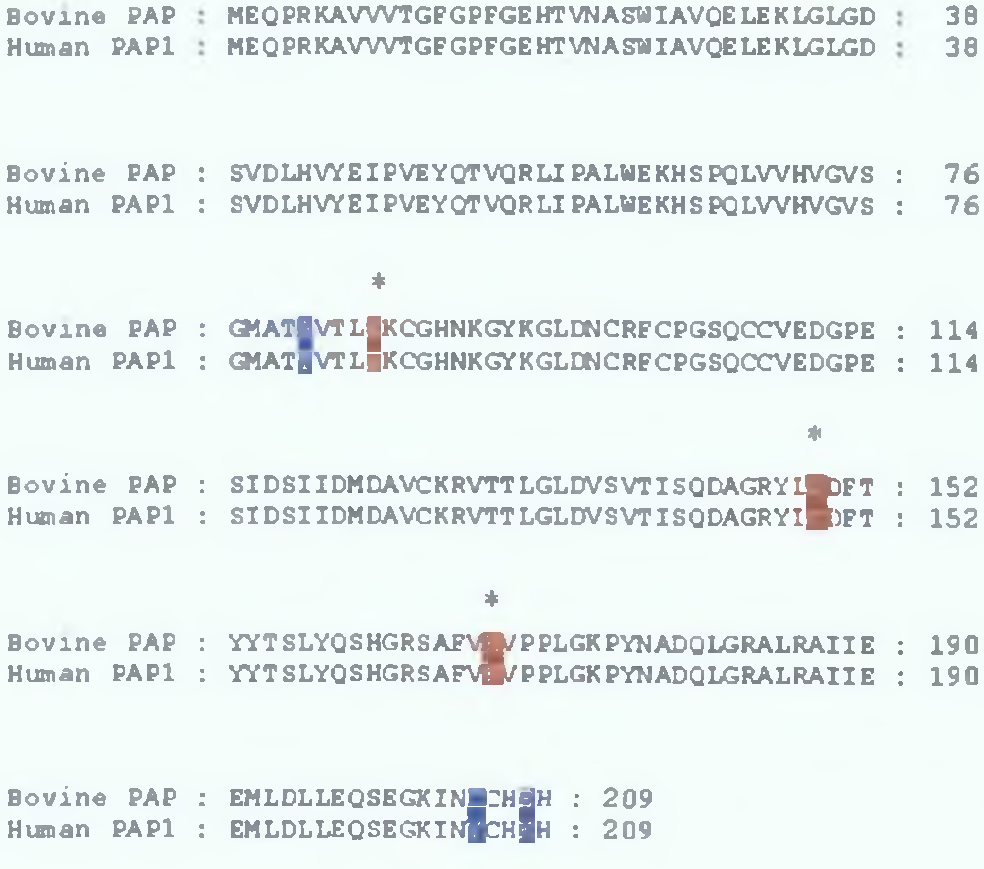

Figure 3.37 PAP1 Amino Acid Alignments

Alignment of the recombinant bovine PAP1 XM866409 (bovine pap1) amino acid sequence with human PAP1 AJ278828 (human pap1) highlighting the three amino acid variations at positions 81, 205 and 208 in blue. Active site residues (*) are highlighted in red. The sequences were annotated using the Genedoc program (see Section 2.11).

Table 3 4 Recombinant Bovine and Human PAP1 Purification

	Total Activity[a] (Units)	Total Protein (mg)	Specific Activity (Units mg $^{-1}$)
Purified Bovine PAP1	9,388	2 6	3,633 8
Purified Human PAP1	30,192	6 5	4,623 1

Summary of recombinant bovine and human PAP1 purification from 1 L expression runs [a] Units = nmoles mm $^{-1}$ 1 e Units are expressed as nanomoles of AMC released per minute at 37°C

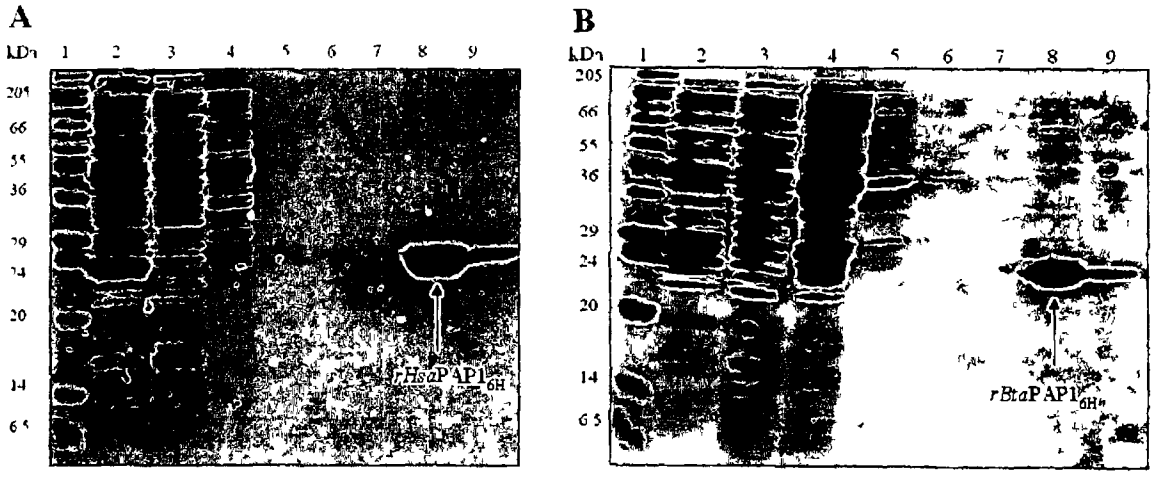

Figure 3 38 SDS-PAGE of Human and Bovine PAP1 Purification
A SDS-PAGE of purification of human PAP1 **B** SDS-PAGE of purification of bovine PAP1 Lane 1, protein molecular marker, lane 2, crude supernatant, lane 3, flow-through, lane 4-7, sequential column washings, lane 8-10, elution of recombinant PAP1 protein from the column The relevant sizes (kDa) of the protein marker are indicated

3 8 2 Investigation into Reduced Yields of Bovine PAP1 Protein

Due to the fact that there is 98% identity between the two amino acid sequences (see Figure 3 29), it was decided to investigate the reduced yields of r*Bta*PAP1$_{6H}$ (2 6 mg) compared to the high yields of r*Hsa*PAP1$_{6H}$ (6 5 mg) Factors such as media (batch to batch variation), IPTG, sonication and purification were eliminated from contributing to this decrease in both specific activity and total protein concentration as both proteins were expressed simultaneously with each other and media from the same batch was utilised in the expression process

There are two major elements which could possibly contribute to these reductions including rare codon usage (see Section 3 8 2 1) and amino acid residue differences (see Section 3 8 2 2)

3 8 2 1 Rare Codon Usage

Codon usage can have adverse effects on synthesis and yield of recombinant proteins Genes in both prokaryotes and eukaryotes show a non-random usage of synonymous codons meaning that there is a bias for one or two codons for most degenerate codon families Certain codons are most frequently used by different genes, for example CCG is the preferred triplet encoding proline

It has been observed that highly expressed genes exhibit a greater degree of codon bias than do poorly expressed genes This implies that recombinant heterologous genes that are enriched with codons which are rarely used by *E coli* may not be expressed efficiently in *E coli* (Makrides, 1996) Low usage codons in *E coli* include arginine, proline, leucine and isoleucine

It was decided to compare rare codon content of the human PAP1 nucleotide sequence with the bovine PAP1 nucleotide sequence in the hope of resolving the reduced expression level yields in bovine PAP1 Analysis shows that human PAP1 has a greater number of rare codons than bovine PAP1 Human PAP1 possesses 13 rare codons while bovine PAP1 has 11 rare codons (see Figure 3 39)

atg gag cag CCC agg aag gcg gtg gtg gtg acg gga ttc ggc cct ttt ggg
gaa cac act gtg aat gcc agc tgg att gcg gtc cag gag ctg gag aaa CTA
ggg ctt ggg gac agc gtg gac CTA cat gtg tat gag att cca gtg gag tat
cag acg gtc cag agg ctc atc cct gcc ctg tgg gag aag cac agt ccg cag
ctg gtg gtg cac gta ggc gtg tca ggc atg gca acc gca gtc aca ctg gag
aag tgt gga cac aac aag ggt tac aag ggc ctg gac aac tgc cga ttc tgc
CCC ggc tcc cag tgc tgt gtg gag gac ggg ccg gaa agc att gac tcc atc
atc gac atg gat gct gtg tgt aag agg gtc act aca ctg ggc tta gat gtg
tca gtg acc att tca caa gat gca ggc agg tac ctc tgc gac ttc acc tac
tat acc tct ctg tac cag agt cac ggc cgc tca gcc ttt gtt cac gtg CCC
cct ctg ggc aag ccg tac aat gca gac cag ctg ggc cgg gca ctt cgg gcc
atc att gag gag atg ctg gac ctc CTA gag cag tca gaa ggc aaa atc aac
tgt tgc cat gaa cac tga

Red = rare Arg codons AGG, AGA, CGA
Green = rare Leu codon CTA
Blue = rare Ile codon ATA
Orange = rare Pro codon CCC

Figure 3.39 Rare Codon Analysis of Bovine PAP1
Nucleotide sequence coding for r*Bta*PAP1, as found on pZK3 (see Figure 3.9).Rare codons are highlighted in red, green and orange (see Section 2.11). http://nihserver.mbi.ucla.edu/RACC.

3.8.2.2 Site-Directed Mutagenesis of r*Bta*PAP1$_{6H}$

Using site-directed mutagenesis (see Section 2.9.2) it was possible to modify each of these three amino acid residues Ala81, Cys205 and Glu208 (see Figure 3.40) individually, thus reverting back to amino acid residues which are present in human PAP1 amino acid sequence. This may perhaps reveal whether or not individual amino acid residues at positions 81, 205 and 208 are responsible for reduced activity and protein expression.

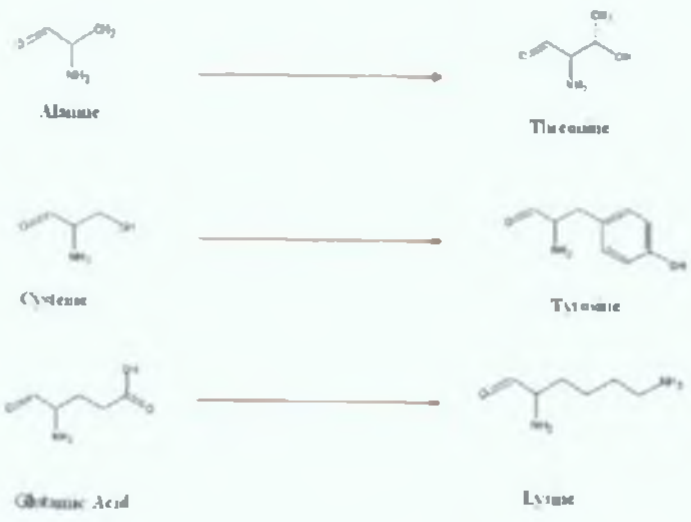

Figure 3.40 Substitution of r*Bta*PAP1$_{6H}$ Residues Ala81, Cys205 and Glu208
Amino acid side-chains of the three varied residues Ala81, Cys205 and Glu208, which were substituted with threonine, tyrosine and lysine respectively. For amino acid information see Appendix D. Illustrated using ChemSketch (see Section 2.11).

3 8 2 2 1 Analysis of Recombinant Bovine PAP1 Mutants

The mutant plasmid derivatives of pZK3 (see Table 3 5) were transformed into *E coli* XL10-Gold as described in Section 2 6 3 Expression cultures (100 ml) were prepared as outlined in Section 2 12 Purified samples were assayed for PAP1 activity (see Section 2 15 3) and total PAP1 protein (see Section 2 14) An increased yield of bovine PAP1 protein was obtained for r*Bta*PAP1_C205mY$_{6H}$ and increases were also observed with specific activity Specific activity dramatically increased for both C-terminus mutations r*Bta*PAP1_C205mY$_{6H}$ and r*Bta*PAP1_E208mK$_{6H}$ (see Table 3 5)

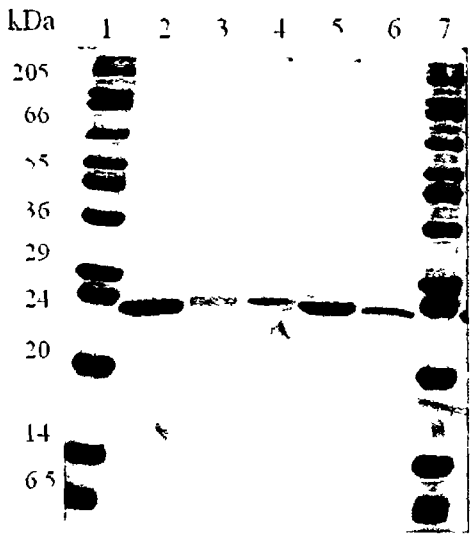

Figure 3 41 Purification of Bovine PAP1 Mutants
Lane 1 and 7, protein molecular marker, lane 2, r*Hsa*PAP1$_{6H}$, lane 3, r*Bta*PAP1$_{6H}$, lane 4, r*Bta*PAP1_A81mT$_{6H}$, lane 5, r*Bta*PAP1_C205mY$_{6H}$, lane 6, r*Bta*PAP1_E208mK$_{6H}$ The relevant sizes (kDa) of the protein marker are indicated

Table 3 5 Properties of r*Hsa*PAP1$_{6H}$, r*Bta*PAP1$_{6H}$ and Mutant Derivatives

Enzyme	Specific Activity (Units mg ^{1})	Total Protein (mg)	Temperature (°C)	K_m (μM)
r*Bta*PAP1$_{6H}$	5,321	0 13	37	59
r*Hsa*PAP1$_{6H}$	13,951	0 5	50	53
r*Bta*PAP1_A81mT$_{6H}$	7,376	0 14	37	83
r*Bta*PAP1_C205mY$_{6H}$	10,019	0 4	50	50
r*Bta*PAP1_E208mK$_{6H}$	8,220	0 12	37	45

3.8.3 Active Site Mutagenesis of Bovine PAP1

Previous work carried out on human PAP1 enzyme indicated that its catalytic triad consisted of Glu-Cys-His. By sequence alignment (see Figure 3.37) these residues correspond to Glu85, Cys149 and His168 in *rBta-pap1*. These three residues occupy the identical position in the *rHsa-pap1* sequence.

The catalytic mechanism of cysteine peptidases require a nucleophile and a proton donor. The nucleophile is the thiol group of a Cys residue and the proton donor is usually the imidizolium ring of a His residue. In some cases a third residue is required to orientate the imidazolium ring of His (Barrett and Rawlings, 2001).

If these residues constitute the catalytic site of *rBta-pap1*, one would expect the enzyme activity to be affected dramatically. Using a site-specific mutagenic approach Glu85, Cys149 and His168 were substituted with glutamine, phenylalanine and aspartic acid, respectively (see Figure 3.42). This was carried out as described in Section 2.9.2, using primers listed in Table 2.2. The choice of these amino acid replacements was based on altering properties of the amino acids. For example, glutamic acid which is an acidic amino acid was replaced with the basic amino acid glutamine. The resulting mutant constructs are listed in Table 3.6. All mutations caused a complete loss of activity, supporting the catalytic significance of these residues. SDS-PAGE shows expression of mutant bovine PAP1 proteins at levels comparable to r*Bta*PAP1$_{6H}$ (see Figure 3.43).

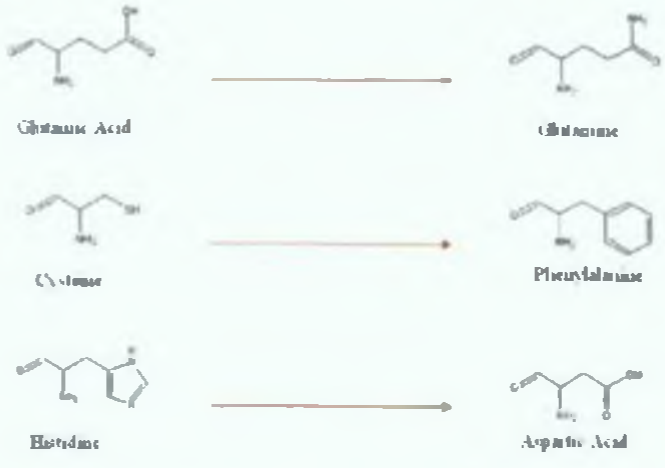

Figure 3.42 Substitution of r*Bta*PAP1$_{6H}$ residues Glu85, Cys149 and His168
Amino acid side-chains of the active site residues Glu85, Cys149 and His168, which were substituted with glutamine, phenylalanine and aspartic acid respectively. For amino acid information see Appendix D. Illustrated using ChemSketch (see Section 2.11).

Table 3.6 r*Bta*PAP1$_{6H}$ Active Site Mutant Derivatives

Mutation	Plasmid	Enzyme
E85 to Q	pZK3_E85mQ	r*Bta*PAP1_E85mQ$_{6H}$
C149 to F	pZK3_C149mF	r*Bta*PAP1_C149mF$_{6H}$
H168 to D	pZK3_H168mD	r*Bta*PAP1_H168mD$_{6H}$

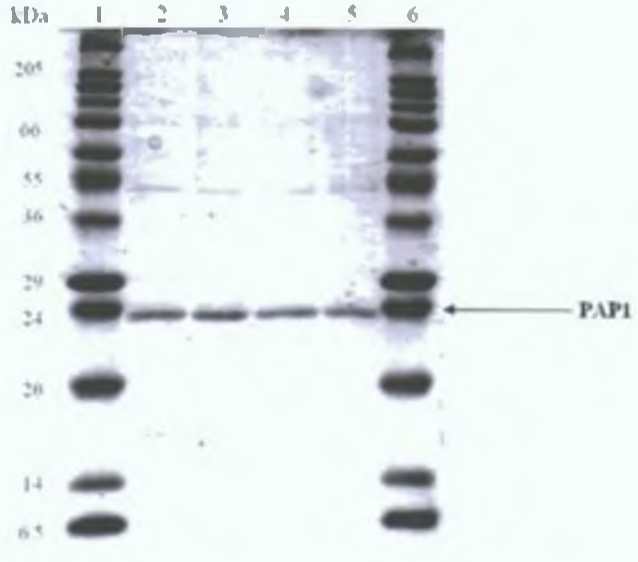

Figure 3.43 Purification of Active Site r*Bta*PAP1$_{6H}$ Mutants
Lane 1 and 6, protein molecular marker; lane 2, r*Bta*PAP1$_{6H}$; lane 3, r*Bta*PAP1_E85mQ$_{6H}$; lane 4, r*Bta*PAP1_C149mF$_{6H}$, lane 5, r*Bta*PAP1_H168mD$_{6H}$.The relevant sizes (kDa) of the protein marker are indicated.

3.9 Discussion

3.9.1 Cloning, Expression and Purification of Bovine PAP1

The 680 bp bovine PAP1 gene was successfully cloned from bovine mRNA (plasmid pZK1, see Figure 3.5). Bovine PAP1 was then expressed in an *E.coli* based system which was developed by Vaas (2005) which was used to express recombinant human PAP1. At that time it was hoped that human PAP1 could be expressed in *E.coli* since it shared many biochemical characteristics and sequence homology with its prokaryotic counterparts.

The bovine PAP1 gene was cloned into the TA cloning vector pCR2.1 and subsequently cloned using the *Nco*I and *Bam*HI sites into the pQE60 vector. This construct (pZK2) was sub-cloned, utilizing the pQE-60 encoded *Eco*R1 and *Hin*dIII sites, into the expression vector pPC225. This generated a pZK3 expression plasmid having the gene for recombinant *Bos taurus* in fusion with a His$_6$ ORF (r*Bta*PAP1$_{6H}$) (see Figure 3.9). r*Bta*PAP1$_{6H}$ was purified by metal affinity chromatography as reported in Section 3.5.

SDS-PAGE of recombinant bovine PAP1 resolved a band with an estimated size of 24 kDa (Figure 3.12). This agrees well with previously reported data (Cummins and O'Connor, 1996). This expression run yielded 2.6 mg of bovine PAP1 protein and a specific activity of 3,633 units.mg^{-1} (see Table 3.1). Zymogram analysis which was carried out on purified preparation displayed a clear band which correlates with SDS-PAGE analysis (see Figure 3.13).

3.9.2 Biochemical and Kinetic Analysis of Bovine PAP1

Size exclusion chromatography (see Section 2.18.1) has indicated that r*Bta*PAP1$_{6H}$ has a relative molecular mass of 24.7 kDa (see Section 3.6.1). This value correlates very well with results obtained from SDS-PAGE (see Figure 3.12) and zymographic analysis (see Figure 3.13). This agrees well with findings reported by Dando *et al.*, (2003) who found human PAP1 to have a relative molecular mass of 24 kDa. From this it can be concluded that recombinant bovine PAP1 is active as a monomeric enzyme.

Bovine PAP1 displayed an optimum pH of 9.0-9.5 (see Figure 3.16). This compares well with data obtained from other researchers which examine the effect of pH on PAP1 activity. Cummins and O'Connor (1996) found optimal pH of bovine brain to be 8.5 and Dando *et al.*, (2003) obtained maximal activity in the range of pH 7.0-9.0 for human PAP1. Awadé *et al.*, (1992) found bacterial PAP1 to display an optimum pH between 7.0-9.0.

Optimum temperature for maximal bovine PAP1 activity was found to be 37°C (see Figure 3.17). The optimal temperature for human PAP1 activity was found at 50°C (Dando *et al.*, 2003), however bovine PAP1 displayed 50 % reduced activity at 50°C and 60°C. Cummins and O'Connor (1996) found that incubating purified bovine enzyme at 37°C for 45 min had no apparent effect on PAP1 stability. However, when incubated at 40°C and 50°C for the same incubation period PAP1 activity decreased by 17 % and 65 % respectively.

As with all cysteine peptidases (Cummins and O'Connor, 1998), bovine PAP1 displayed an absolute requirement for a thiol-reducing agent for recombinant bovine PAP1 enzyme activity. The thiol group is a very reactive functional group. In *vivo*, this group can form complexes with various metal ions and is readily oxidised, forming cysteine disulphide bonds. Thiol-reducing agents such as DTT are required to prevent oxidation from occurring. Optimum activity was obtained using 10 mM DTT (see Figure 3.18). The thiol-dependent nature of r*Bta*PAP1$_{6H}$ was demonstrated by complete

PAP1 activity inhibition by 5 mM iodoacetic acid, an IC_{50} value of 0.8 mM was obtained (see Figure 3.20).

The chelating agent EDTA, although not a requirement for PAP1 activity (see Figure 3.19), was routinely including in the standard PAP1 activity assay (see Section 2.15.3), as a stabilising agent for DTT, according to the modified method described by Browne and O'Cuinn (1983).

Inhibitors L-pGlu (IC_{50} = 1.6 mM, Figure 3.21) and 2-pyrrolidone (IC_{50} = 0.75 mM, see Figure 3.22) proved to have an inhibitory effect on bovine PAP1 activity due the competitive binding into the catalytic site. (Tsuru *et al.*, 1978, Mudge and Fellows, 1973).

The kinetic parameters of purified recombinant bovine PAP1 were determined (see Table 3.2). A K_m value of 59 μM was determined for the recombinant bovine PAP1 using various pGlu-AMC substrate concentrations ranging between 10 and 500 μM. This compares well with Dando *et al.*, (2003) whom obtained a K_m value of 50 μM for human PAP1. It is interesting to note that Cummins and O'Connor (1996) obtained a K_m value of 16 μM for bovine PAP1 which was purified from bovine brain tissue.

V_{max} and K_{cat} values obtained for bovine PAP1 were 3.15 units.mg^{-1} and 3.5 s^{-1} respectively.

Kinetic studies were carried out with a number of pyroglutamyl peptides which were tested with the recombinant bovine enzyme (see Table 3.3). When initial kinetic analysis was carried out, K_i values were determined for only three pyroglutamyl peptides, namely pGlu-His-Pro-NH_2 (TRH), pGlu-Ala and pGlu-Val. From this data, it was assumed that PAP1 activity possesses a higher affinity for the hydrolysis of tripeptide substrates over dipeptide substrates. However, this does not appear to be the case with the pyroglutamyl peptides listed in Table 3.3.

Bovine PAP1 has a higher affinity for dipeptides pGlu-Ala (see Figure 3.27) and pGlu-Thr (see Figure 3.28) than for tripeptides pGlu-Ala-Ala (see Figure 3.31) and pGlu-Thr-Ala (see Figure 3.35). The addition of the alanine residue to each of the dipeptides appears to affect enzyme/substrate binding causing an increase in the K_i values determined and overall decreasing the affinity of bovine PAP1 for these tripeptides.

Dipeptides pGlu-Glu and pGlu-Met would have been interesting candidates for this work. A K_i value for pGlu-Glu-Ala (see Figure 3.32) could not be determined, while a K_i of 366 μM was determined for pGlu-Met Ala (see Figure 3.34).

Poor affinity of PAP1 has been observed for pyroglutamyl peptides which possess a valine residue positioned directly adjacent to the pyroglutamyl residue, while lowest affinity has been reported for dipeptide pGlu-Pro which is not hydrolysed by PAP1, with one notable exception being *Klebsiella cloacae* PAP1 (Fujiwara *et al*, 1978)

A K_i of 625 μM was obtained for pGlu-Val showing mixed inhibition (see Figure 3 30)

The dipeptide pGlu-Pro produced a K_i value of 3,300 μM and uncompetitive inhibition can be seen in Figure 3 29

TRH produced the lowest K_i of 44 1 μM (indicating the relative highest affinity) and behaved as a competitive inhibitor (see Figure 3 33) We can conclude from this that the high affinity observed is not due to the fact that TRH is a tripeptide but most probably due to the identity and sequence of the amino acid residues in the second (P_2) and third (P_3) positions of the peptide

A comparison with published data from Cummins and O'Connor (1996) of the kinetic constants (K_i) which were evaluated for bovine PAP1 (purified from bovine brain tissue) with different substrates unveil a number of interesting observations

K_i values for a number of bioactive peptides were determined for purified bovine PAP1 which include LHRH (**pGlu-His-Trp**-Ser-Tyr-Gly-Leu-Arg-Pro-Gly-NH_2), Acid TRH (**pGlu-His-Pro**-OH), TRH (**pGlu-His-Pro**-NH_2) and Anorexigenic Peptide (**pGlu-His-Gly**-OH) All of the aforementioned peptides produced K_i values ranging between 20 and 50 μM It is interesting to note that that all of the above peptides commence with pGlu-His followed by a tryptophan residue (LHRH), a proline residue (Acid TRH and TRH) and a glycine residue (Anorexigenic Peptide)

Bombesin (**pGlu-Gln-Arg**-Leu-Gly-Asn-Gln-Trp-Ala-Val-Gly-His-Leu-Met-NH_2) was also analysed and produced a K_i of 64 μM

From reported findings and the data obtained from this research, kinetic analysis would seem to show that bovine PAP1 has greatest affinity for a hydrophilic amino acid residue in the P_2 position (e g pGlu-His, pGlu-Gln) with less affinity for hydrophobic amino acid residues in this position (e g pGlu-Ala, pGlu-Val, pGlu-Met)

Ultimately, the His_6 tag did not prevent the exhibition of characteristic mammalian PAP1 enzymatic activity, as shown by specific cleavage of pGlu from pGlu-AMC and sensitivity to the thiol reducing agent DTT We cannot eliminate completely the possibility that the His_6 tag exerts some degree of an effect on the catalytic properties of the enzyme However, if such an effect exists it may be quite minimal As described, the primary sequence of bovine PAP1 differs from that of human PAP1 by only three

residues, leading one to expect no substantial differences in kinetic properties. Kinetic and biochemical parameters reported for recombinant human PAP1 having no His_6 tag (Dando *et al.*, 2003) correlate very closely to those presented here for recombinant His_6-tagged bovine PAP1. Furthermore, the value for K_m obtained here (59 μM) fits well into the range of K_m values (15-150 μM) and various biochemical parameters reported for diverse mammalian native PAP1 enzymes (Cummins and O'Connor, 1996).

3.9.3 Comparative Study of Bovine PAP1 with Human PAP1

The comparative study which was carried out as described in Section 3.8 has shown that there is little variation at the amino acid level between *rBta-pap1* and *rHsa-pap1* (see Figure 3.37). In fact there are only three amino acid variations at positions 81, 205 and 208. There are 71 nucleotide variations (see Figure 3.36), however, the majority of these proved to be silent mutations when the amino acid residues were aligned. In view of the fact that there is little variation between the two amino acid alignments and that the bovine PAP1 sequence possessed 98% identity with the human PAP1 sequence, one would have expected to find properties of both to be similar given that both were expressed, purified and assayed under the same conditions. However, this was not the case with results which were obtained for PAP1 activity and protein concentration (see Table 3.4).

Total activity and total protein for r*Hsa*$PAP1_{6H}$ are almost three times greater than *rBta*$PAP1_{6H}$ total activity and total protein. Overall, specific activity for r*Bta*$PAP1_{6H}$ and r*Hsa*$PAP1_{6H}$ were 3,633.8 units.mg^{-1} and 4,623.1 units.mg^{-1}, respectively.

SDS-PAGE produced a band of ~23-24kDa for both bovine and human PAP1 (see Figure 3.38).

As a result of reduced bovine PAP1 protein yields when compared to human PAP1 yields, both rare codon usage and different amino acid residues were investigated. Reduced protein yields could also be due to the differing nucleotide bases upstream from the ATG start codon which may be affecting protein translation efficiency (see Figure 3.36). Analysis revealed that rare codon usage does not contribute to the reduced yield of protein seen in bovine PAP1 (see Figure 3.39). If findings highlighted that bovine PAP1 possessed a greater number of rare codons than human PAP1, one could assume that the rare codon usage could be a contributing factor to reduced expression levels of bovine PAP1 as described in Section 3.8.2.1.

Utilising site-directed mutagenesis (see Section 2 9 2) amino acids Ala81, Cys205 and Glu208 were substituted with Thr, Tyr and Lys respectively (see Figure 3 40) After examining the position of these residues in the bovine PAP1 amino acid sequence it is clear that both Cys205 and Glu208 are positioned at the C-terminal end, while Ala81 is closely located to active site residue Glu85 (see Figure 3 37) From this, one could speculate that the residue change at position 81 could be responsible for the reduced r*Bta*PAP1 yields Alanine could be causing a change in the structure of the hydrophobic pocket to occur, thus decreasing the amount of substrate being hydrolysed and as a result reducing r*Bta*PAP1 total activity and protein

The pZK3 derivates (see Table 3 5) were expressed in *E coli* XL10-Gold (see Section 2 12) and subsequently purified (see Figure 3 41, Section 2 13)

It is evident that the potential susceptibility of the cysteine residue at position 205 is having an adverse affect on bovine PAP1 protein yields and activity (see Figure 3 41, Table 3 5) Substitution with a tyrosine residue has resulted in a dramatic increase in total protein and activity Optimal temperature has increased from 37°C to 50°C Presence of a cysteine residue at position 208 may have resulted in the bovine PAP1 structure to change conformation This in turn may have resulted in bovine PAP1 becoming prone to proteolytic degradation and protein instability Disulphide bonds between cysteine residues may also have been introduced, supporting the above theory of a change occurring in the bovine PAP1 structure These findings suggest that the C-terminal region of PAP1 plays a role in PAP1 protein expression and PAP1 enzymatic activity

The orientation of the catalytic triad (Glu-Cys-His) of bovine PAP1 is identical to human PAP1 Amino acid residues Glu85, Cys149 and His168 are fully conserved in both sequences (see Figure 3 37) Mutation of the residues Glu85, Cys149 and His168 individually (see Section 3 8 3) in r*Bta*PAP1$_{6H}$ resulted in complete loss of catalytic activity, strongly implicating them in the catalytic triad of r*Bta*PAP1$_{6H}$

CHAPTER FOUR

Biochemical, Kmetic and Functional Analysis of Recombinant Human PAP1Using Site-Directed and Random Mutagenesis

4 1 Overview

This chapter describes further characterisation of human PAP1 To date, there has been no publication of the three-dimensional (3D) structure for human or other eukaryotic PAP1 enzymes However, the 3D structures of four prokaryotic PAP1 enzymes have recently been solved using X-ray crystallography These PAP1 structures, namely for *B amyloliquefaciens* (*Bam*PAP1) (Odagaki *et al*, 1999), *T litoralis* (*Tli*PAP1) (Singleton *et al*, 1999a, 1999b), *P furiosus* (*Pfu*PAP1) (Tanaka *et al*, 2001) and *P horikoshii* (*Pho*PAP1) (Sokabe *et al*, 2002) *Hsa*PAP1 has considerable homology to prokaryotic PAP1 enzymes, displaying greatest homology with *Bam*PAP1 Based on this homology a 3D structure model of *Hsa*PAP1 (see Figure 4 1) was created by SWISS-MODEL (see Section 2 11), using the prokaryotic structures as templates

This series of mutants are biochemically characterised in this work The active site residue glutamic acid at position 85 of human PAP1 is investigated A second series of mutants are generated using random mutagenesis which are also characterised both biochemically and kinetically Kinetic analysis was also carried out on human PAP1 using a number of pyroglutamyl peptides

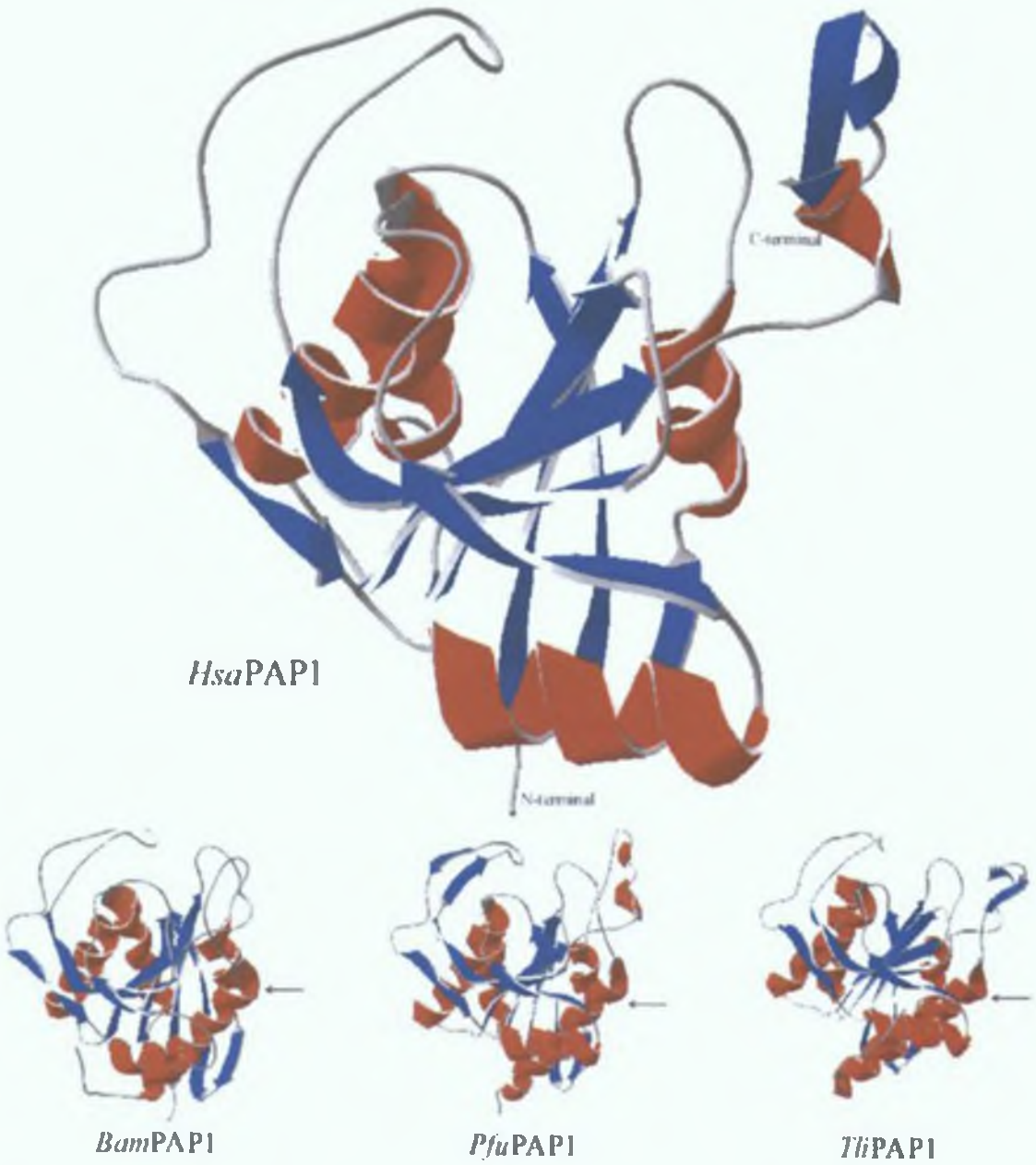

Figure 4.1 *Hsa*PAP1 3D model compared with structural templates (Vaas, 2005)
Ribbon diagram of the 3D *Hsa*PAP1 model, which was predicted using the SWISS-MODEL server (see Section 2.11), taking the structures of *Bam*PAP1, *Pfu*PAP1 and *Tli*PAP1 as templates. α -helices are coloured red and β-strands are coloured blue. 3 N-terminal and 24 C-terminal *Hsa*PAP1 residues were excluded from the model. The residues of *Bam*PAP1, *Pfu*PAP1 and *Tli*PAP1 correlating to the excluded C-terminal residues form α-helices, indicated by arrows. Generated using DeepView (see Section 2.11).

4.2 Human PAP1 Kinetic Analysis

Kinetic analysis was performed (see Section 2.18.6.2) using a number of pyroglutamyl peptides (see Table 2.7). The significance of these results is discussed in Section 4.6.

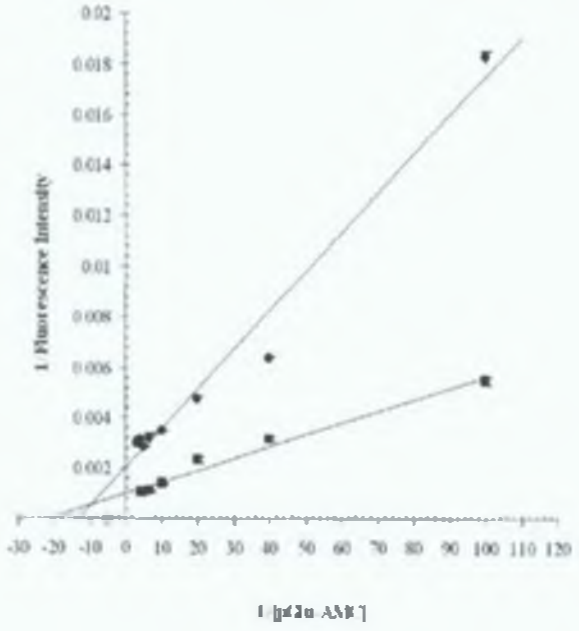

Figure 4.2 Kinetic Analysis of the Effect of pGlu-Ala (●) on Human PAP1 Catalysed Hydrolysis of pGlu-AMC (■). Lineweaver-Burk reciprocal plot of fluorescent intensity versus [pGlu-AMC]. Plot illustrates competitive inhibition of PAP1 by pGlu-Ala. Error bars represent the SD of triplicate readings.

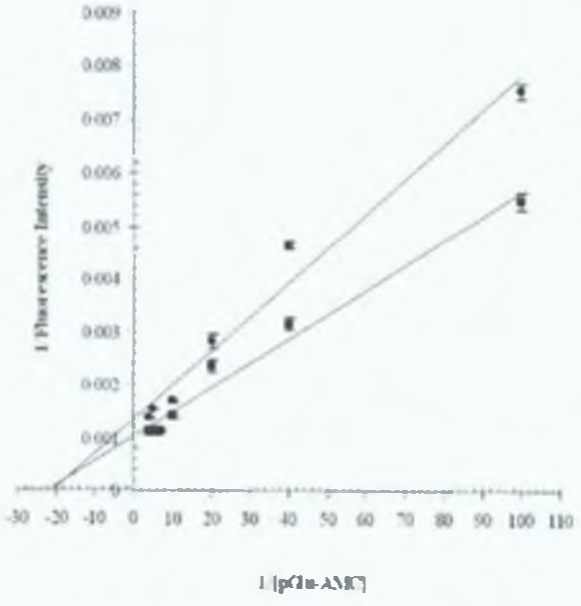

Figure 4.3 Kinetic Analysis of the Effect of pGlu-Thr (●) on Human PAP1 Catalysed Hydrolysis of pGlu-AMC (■). Lineweaver-Burk reciprocal plot of fluorescent intensity versus [pGlu-AMC]. Plot illustrates competitive inhibition of PAP1 by pGlu-Thr. Error bars represent the SD of triplicate readings.

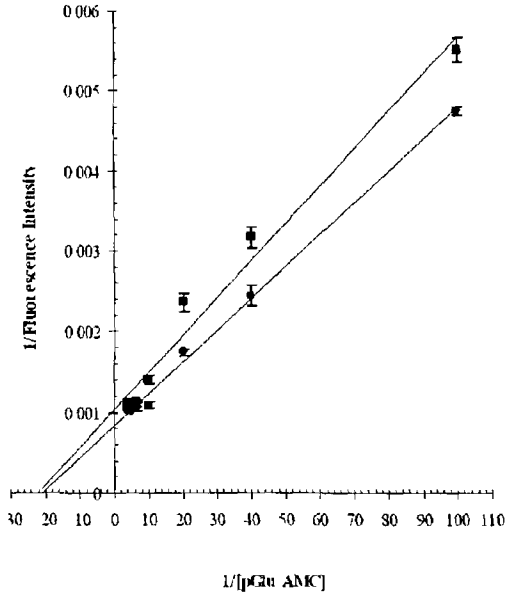

Figure 4 4 Kinetic Analysis of the Effect of pGlu-Pro (•) on Human PAP1 Catalysed Hydrolysis of pGlu-AMC (■) Lineweaver-Burk reciprocal plot of fluorescent intensity versus [pGlu-AMC] Plot illustrates uncompetitive inhibition of PAP1 by pGlu-Pro Error bars represent the SD of triplicate readings

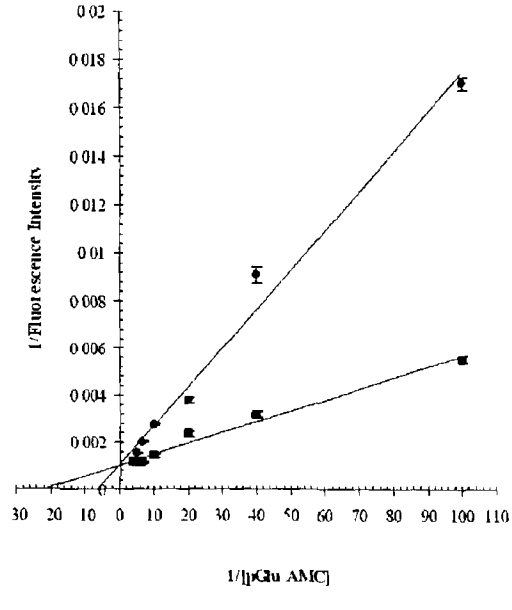

Figure 4 5 Kinetic Analysis of the Effect of pGlu-Ala-Ala (•) on Human PAP1 Catalysed Hydrolysis of pGlu-AMC (■) Lineweaver-Burk reciprocal plot of fluorescent intensity versus [pGlu-AMC] Plot illustrates competitive inhibition of PAP1 by pGlu-Ala-Ala Error bars represent the SD of triplicate readings

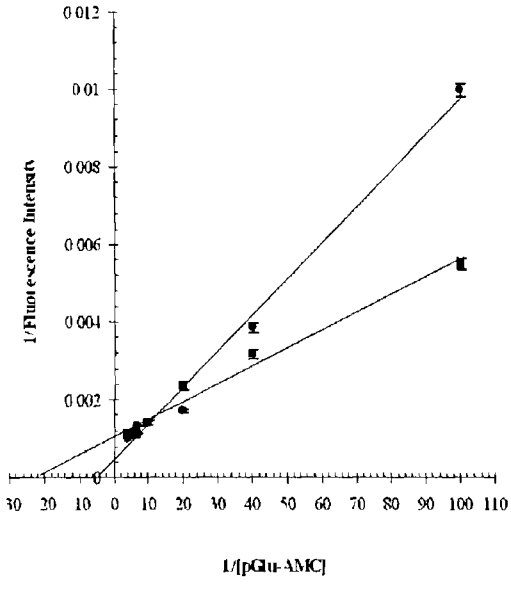

Figure 4 6 Kinetic Analysis of the Effect of pGlu-Glu-Ala (•) on Human PAP1 Catalysed Hydrolysis of pGlu-AMC (■) Lineweaver-Burk reciprocal plot of fluorescent intensity versus [pGlu-AMC] Plot illustrates mixed inhibition of PAP1 by pGlu-Glu-Ala Error bars represent the SD of triplicate readings

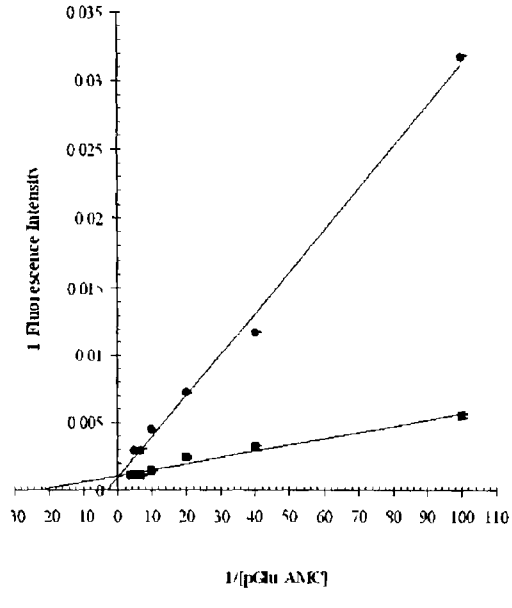

Figure 4 7 Kinetic Analysis of the Effect of pGlu-His-Pro-NH_2 (•) on Human PAP1 Catalysed Hydrolysis of pGlu-AMC (■) Lineweaver-Burk reciprocal plot of fluorescent intensity versus [pGlu-AMC] Plot illustrates competitive inhibition of PAP1 by pGlu-His-Pro-NH_2 Error bars represent the SD of triplicate readings

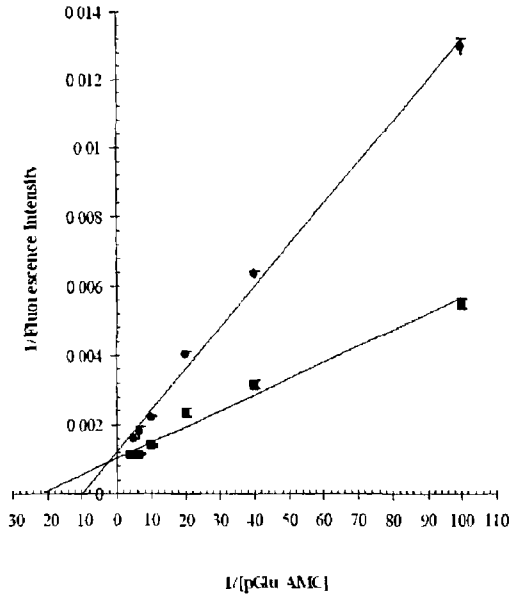

Figure 4 8 Kinetic Analysis of the Effect of pGlu-Met-Ala (•) on Human PAP1 Catalysed Hydrolysis of pGlu-AMC (■) Lineweaver-Burk reciprocal plot of fluorescent intensity versus [pGlu-AMC] Plot illustrates competitive inhibition of PAP1 by pGlu-Met-Ala Error bars represent the SD of triplicate readings

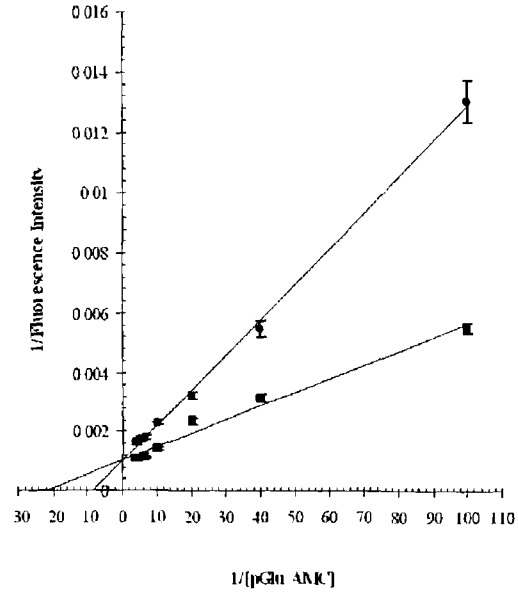

Figure 4 9 Kinetic Analysis of the Effect of pGlu-Thr-Ala (•) on Human PAP1 Catalysed Hydrolysis of pGlu-AMC (■) Lineweaver-Burk reciprocal plot of fluorescent intensity versus [pGlu-AMC] Plot illustrates competitive inhibition of PAP1 by pGlu-Thr-Ala Error bars represent the SD of triplicate readings

Table 4 1 K_i Values Obtained for Pyroglutamyl Peptides

Peptide	$K_{m\ (app)}$ (μM)	K_i (μM)	Inhibition Type
pGlu-Ala	111	204	Competitive
pGlu-Thr	66	781	Competitive
pGlu-Pro	50	n d	Uncompetitive
pGlu-Ala-Ala	166	107	Competitive
pGlu-Glu-Ala	200	83	Mixed
pGlu-His-Pro-NH_2 (TRH)	333	44	Competitive
pGlu-Met-Ala	111	204	Competitive
pGlu-Thr-Ala	125	166	Competitive

Activity of human PAP1 towards pyroglutamyl peptides Enzyme assays were carried out as described in Materials and methods [K_m^{app} values obtained from Figure 4 2 – 4 9 K_i calculated as outlined in Appendix C]

4 3 Human PAP1 Site-Directed Mutagenesis

A series of site-directed mutants were generated by a previous member of this research group to carry out a functional analysis study on human PAP1 (Vaas, 2005) The nine active mutants are listed in Table 4 2 and are also highlighted on *Hsa*PAP1 3D model (see Figure 4 10) Majority of mutations were made to the substrate binding pocket of human PAP1, with mutations also been made to the extended outer loop and the C-terminal end The mutations were based on a study which was previously carried out on *Bam*PAP1 (Ito *et al*, 2001) This study highlighted that Phe10, Phe13 and Phe142 play an essential role in the substrate binding pocket of *Bam*PAP1 These residues correspond to Phe13, Phe16 and Tyr147 in *Hsa*PAP1 Asp97 and Asn98 which are located on the outer edge of the binding pocket were also mutated On an extended loop of *Hsa*PAP1 the motif Ser115-Ile116-Asp117 was changed to Ala-Tyr-Phe, the latter three amino acids being commonly found in prokaryotic PAP1 enzymes The 3D model structure for *Hsa*PAP1 which is based on three of the prokaryotic sequences failed to include the C-terminal 24 amino acid residues from the model As a result, a deletion mutation was produced, where the 9 terminal amino acids were deleted from the *Hsa*PAP1 sequence

Table 4.2 Mutant derivatives of r*Hsa*PAP1$_{6H}$

Mutation	Plasmid	Enzyme
F13 to Y	pRV5_F13My	r*Hsa*PAP1_F13mY$_{6H}$
F16 to Y	pRV5_F16mY	r*Hsa*PAP1_F16mY$_{6H}$
Y147 to F	pRV5_Y147mF	r*Hsa*PAP1_Y147mF$_{6H}$
N98 to Q	pRV5_N98mQ	r*Hsa*PAP1_N98mQ$_{6H}$
N98 to V	pRV5_N98mV	r*Hsa*PAP1_N98mV$_{6H}$
S115 to A, I116 to Y, D117 to F	pRV5_SID115mAYF	r*Hsa*PAP1_SID115mAYF$_{6H}$
Q180 to E	pRV5_Q180mE	r*Hsa*PAP1_Q180mE$_{6H}$
Q180 to E, N177 to Y	pRV5_Q180mE.N177mY	r*Hsa*PAP1_Q180mE.N177mY$_{6H}$
C-terminal deletion: G201 to H209	pRV5_Δ3'	r*Hsa*PAP1_ΔC$_{6H}$

[For amino acid information see Appendix D.]

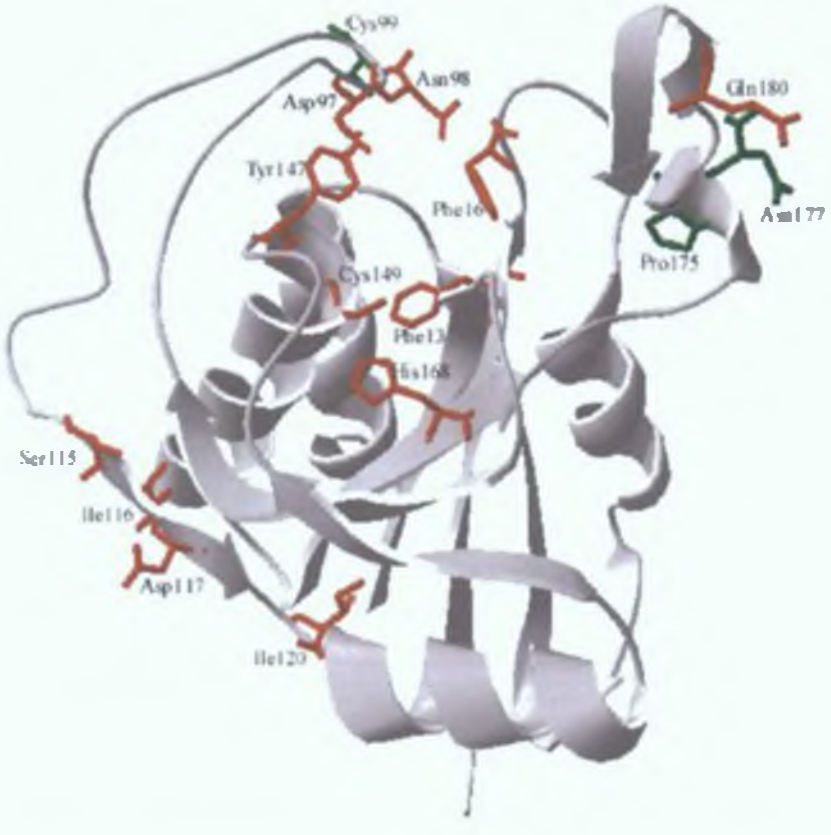

Figure 4.10 *Hsa*PAP1 3D Model Showing Residues Targeted For Mutagenesis (Vaas, 2005)

Ribbon diagram of the 3D *Hsa*PAP1 model. Residues targeted for site-specific mutagenesis are visualised in red. Residues affected by unintentional mutagenesis are marked in green. For amino acid information see Appendix D. Generated using DeepView (see Section 2.11).

4.3.1 Biochemical Analysis of Human PAP1 Mutations

4.3.1.1 Effect of Temperature

The effect of temperature on human PAP1 and the mutants listed in Table 4.1 was investigated as outlined in Section 2.18.3. Figures 4.11 - 4.13 illustrate the effect of temperature on each of the mutants compared to the human PAP1 wild-type form. The significance of these results is discussed in Section 4.6.

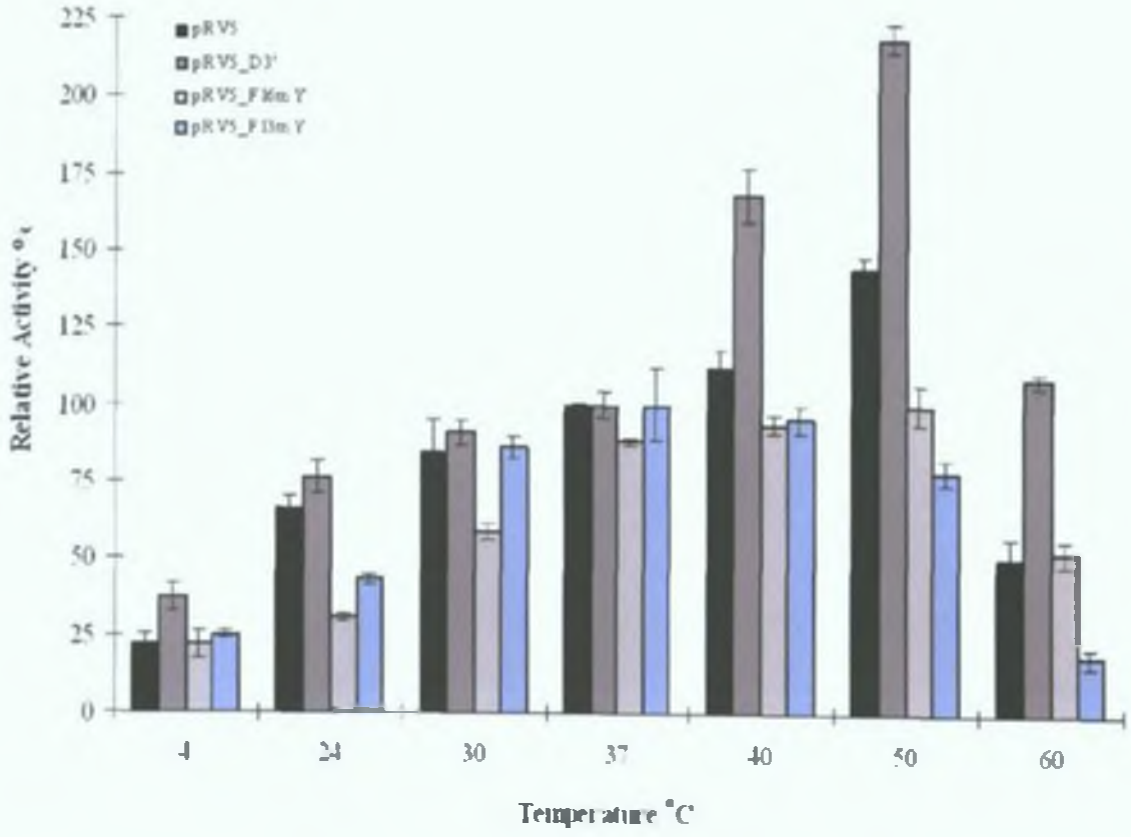

Figure 4.11 Plots of Mutant Relative Enzyme Activities Versus Temperature
Figure 4.11 shows the effect of temperature on mutants *rHsa*PAP1_Δ3'$_{6H}$, *rHsa*PAP1_F13mY$_{6H}$ and *rHsa*PAP1_F16mY$_{6H}$. Black bars represent *rHsa*PAP1$_{6H}$ activity. Enzyme activities are expressed as a percentage of the fluorescence observed at 37°C. Error bars represent the SD of triplicate readings.

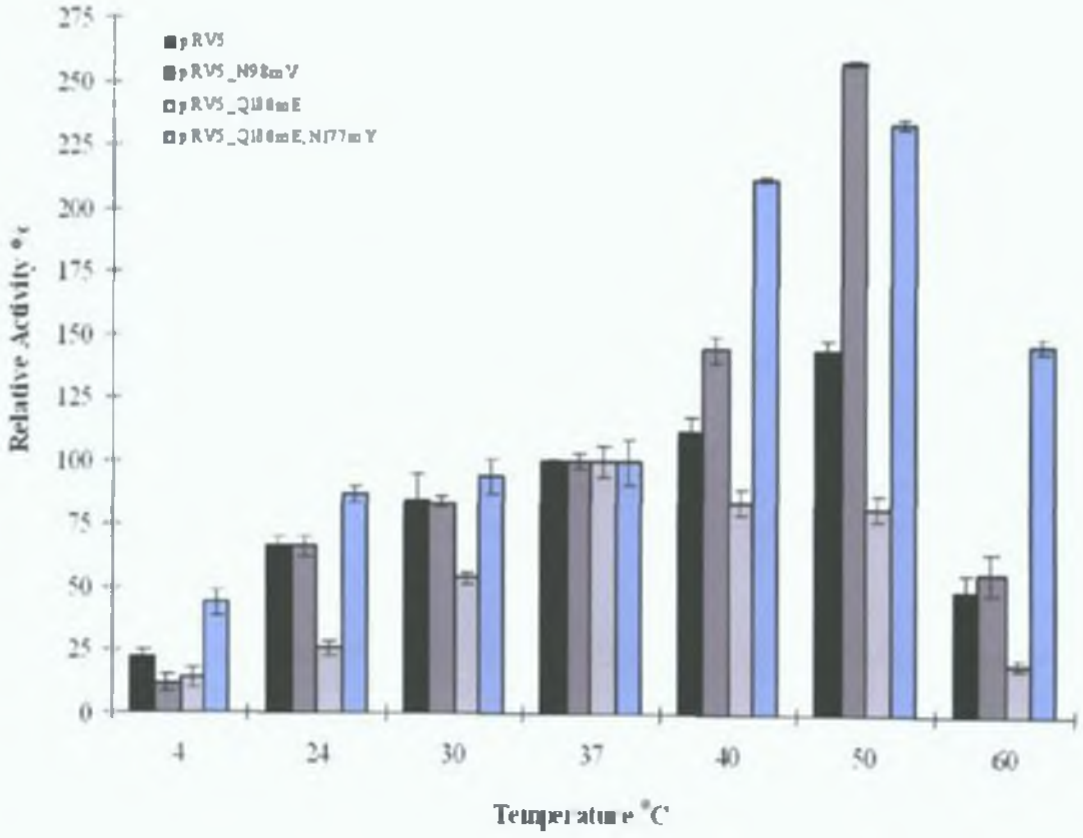

Figure 4.12 Plots of Mutant Relative Enzyme Activities Versus Temperature
Figure 4.12 shows the effect of temperature on mutants r*Hsa*PAP1_N98mV$_{6H}$, r*Hsa*PAP1_Q180mE$_{6H}$ and r*Hsa*PAP1_Q180mE,N177mY$_{6H}$. Black bars represent r*Hsa*PAP1$_{6H}$ activity. Enzyme activities are expressed as a percentage of the fluorescence observed at 37°C. Error bars represent the SD of triplicate readings.

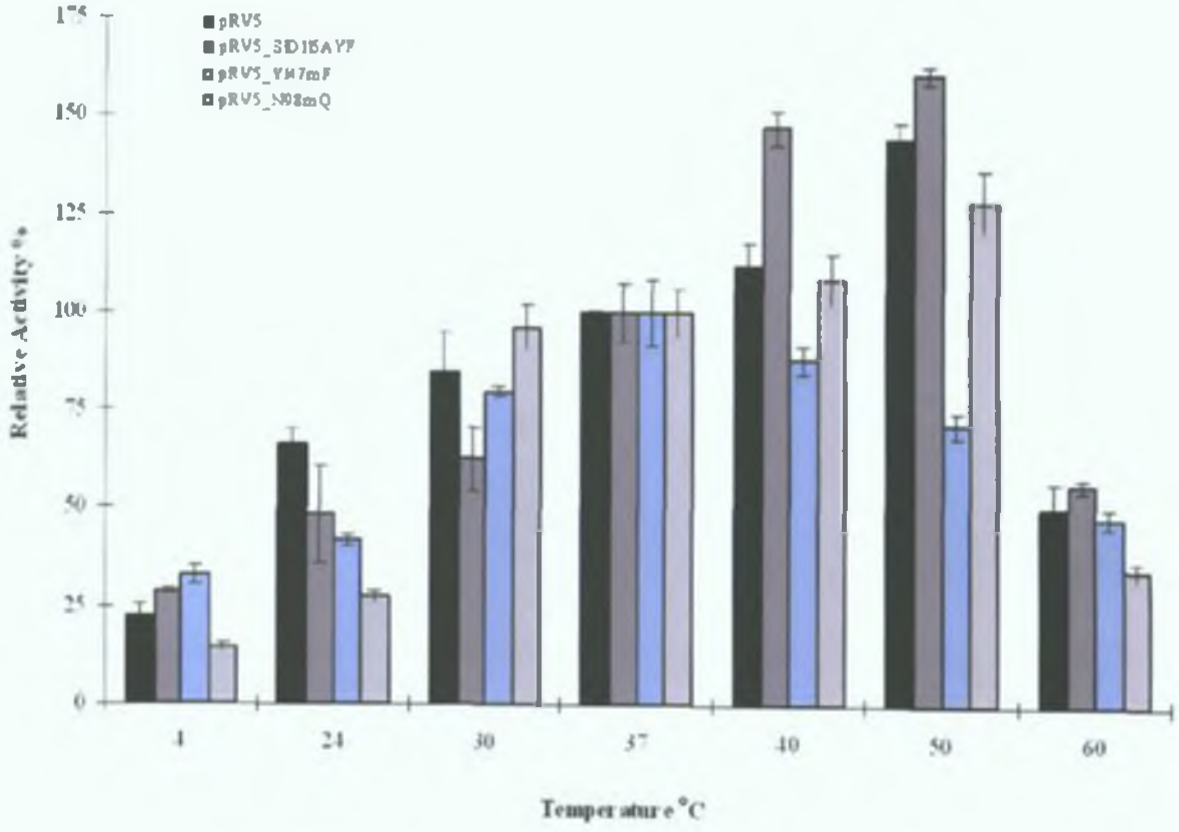

Figure 4.13 Plots of Mutant Relative Enzyme Activities Versus Temperature

Figure 4.13 shows the effect of temperature on mutants r*Hsa*PAP1_SID15AYF$_{6H}$, r*Hsa*PAP1_Y147mF$_{6H}$ and r*Hsa*PAP1_N98mQ$_{6H}$ Black bars represent r*Hsa*PAP1$_{6H}$ activity. Enzyme activities are expressed as a percentage of the fluorescence observed at 37°C. Error bars represent the SD of triplicate readings.

4.3.1.2 Thermal Stability at 37°C

Thermal stability studies were carried as described in Section 2.17.3 and the significance of these results is discussed in Section 4.6.

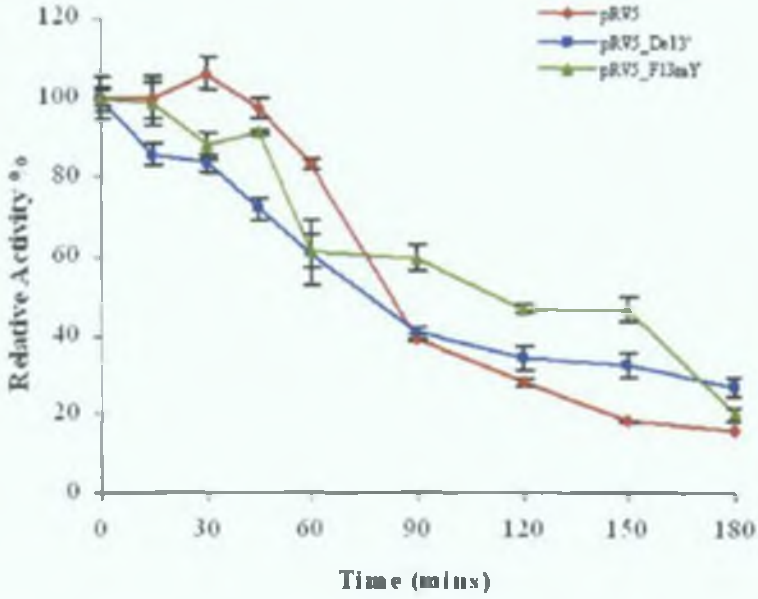

Figure 4.14 Relative Human PAP1 Enzymatic Activity Versus Time
Figure 4.14 shows the effect of temperature on wild type r*Hsa*PAP1$_{6H}$, r*Hsa*PAP1_F13mY$_{6H}$ and r*Hsa*PAP1_Δ3'$_{6H}$ activity. Enzyme activities are expressed as a percentage of the fluorescence observed at 0 minutes. Error bars represent the SD of triplicate readings.

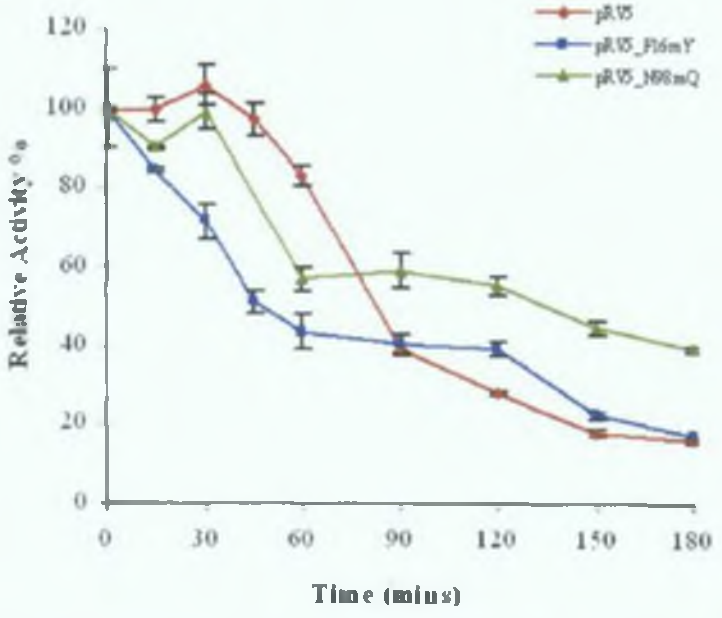

Figure 4.15 Relative Human PAP1 Enzymatic Activity Versus Time
Figure 4.15 shows the effect of temperature on wild type r*Hsa*PAP1$_{6H}$, r*Hsa*PAP1_F16mY$_{6H}$ and r*Hsa*PAP1_N98mQ$_{6H}$ activity. Enzyme activities are expressed as a percentage of the fluorescence observed at 0 minutes. Error bars represent the SD of triplicate readings.

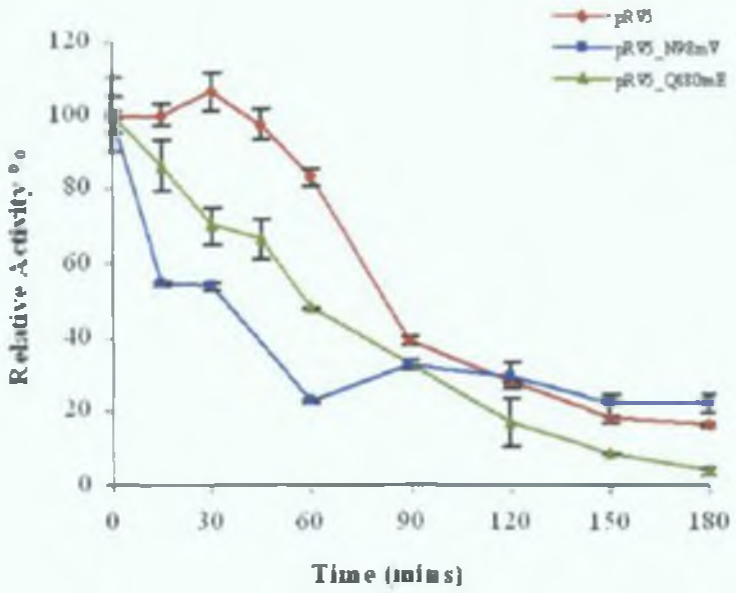

Figure 4.16 Relative Human PAP1 Enzymatic Activity Versus Time
Figure 4.16 shows the effect of temperature on wild type r*Hsa*PAP1$_{6H}$, r*Hsa*PAP1_N98mV$_{6H}$ and r*Hsa*PAP1_Q180mE$_{6H}$ activity. Enzyme activities are expressed as a percentage of the fluorescence observed at 0 minutes. Error bars represent the SD of triplicate readings.

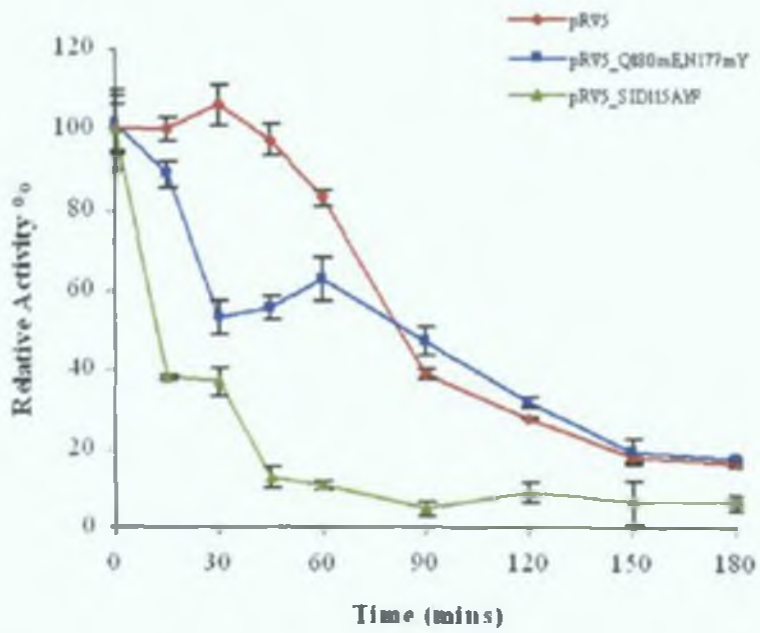

Figure 4.17 Relative Human PAP1 Enzymatic Activity Versus Time
Figure 4.17 shows the effect of temperature on wild type r*Hsa*PAP1$_{6H}$, r*Hsa*PAP1_Q180mE,N177mY$_{6H}$ and r*Hsa*PAP1_SID115AYF$_{6H}$ activity. Enzyme activities are expressed as a percentage of the fluorescence observed at 0 minutes. Error bars represent the SD of triplicate readings.

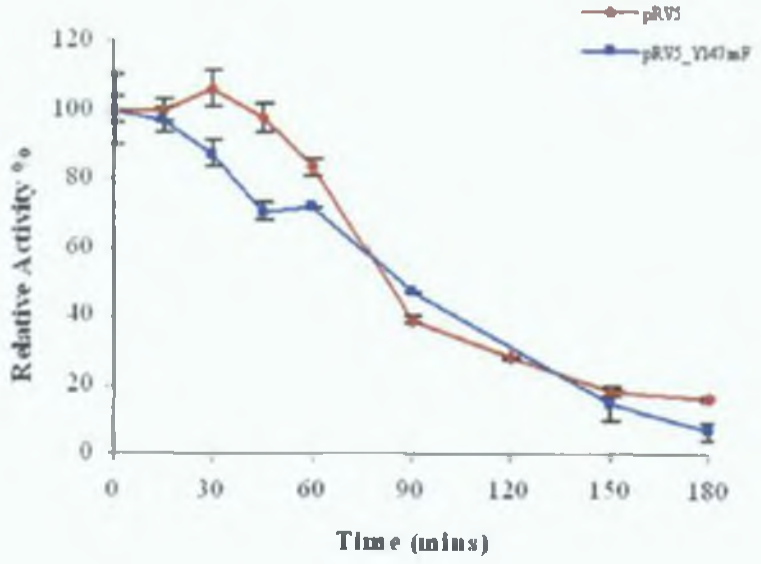

Figure 4.18 Relative Human PAP1 Enzymatic Activity Versus Time
Figure 4.18 shows the effect of temperature on wild type r*Hsa*PAP1$_{6H}$ and r*Hsa*PAP1_Y147mE$_{6H}$ activity. Enzyme activities are expressed as a percentage of the fluorescence observed at 0 minutes. Error bars represent the SD of triplicate readings.

4.3.1.3 Inhibitors

4.3.1.3.1 Determination of IC_{50} Values

The effect of thiol-directed inhibitors iodoacetamide and substrate analogue 2-pyrrolidone on wild-type and its mutant forms listed in Table 4.2 were investigated as outlined in Section 2.18.5. Figures 4.19 – 4.28 illustrate the effect of these inhibitors on each of the mutant activities. The significance of these results is discussed in Section 4.6.

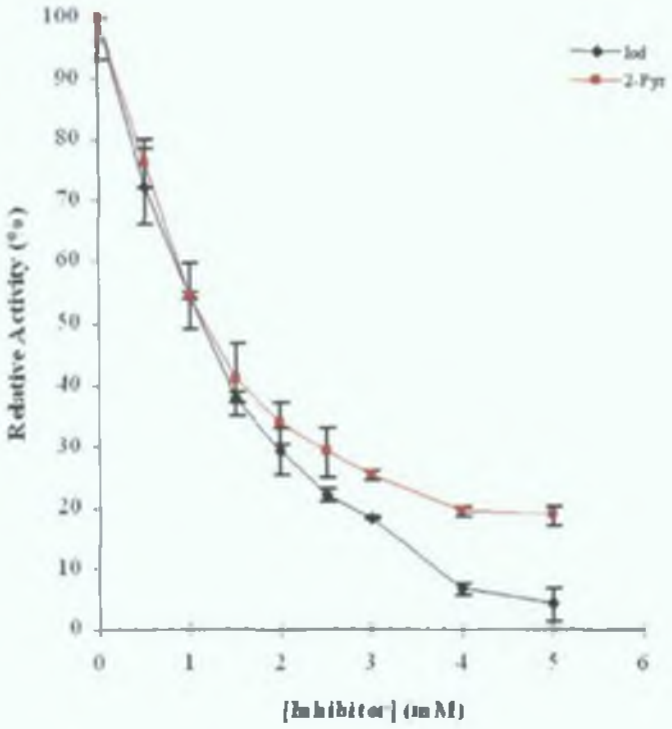

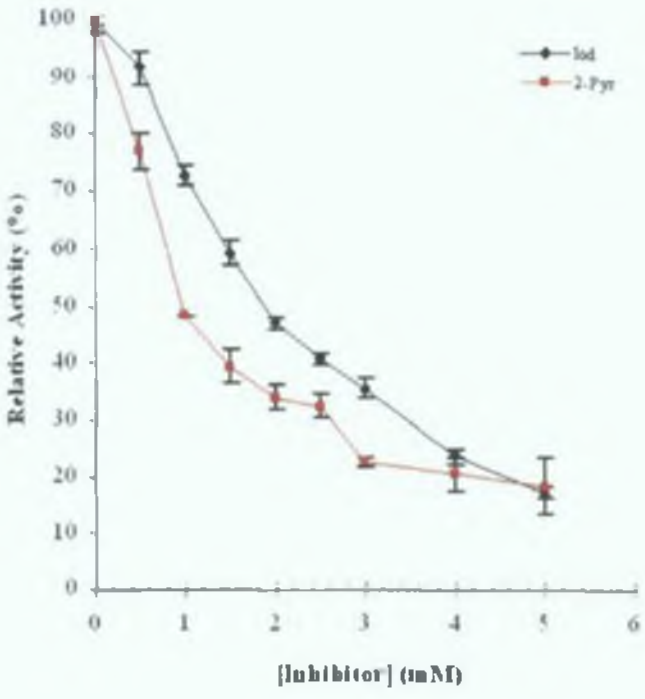

Figures 4.19 and 4.20 Inhibitor Profile Effects of Iodoacetamide and 2-Pyrrolidone on *rHsa*PAP1$_{6H}$ and *rHsa*PAP1_Δ3'$_{6H}$.

Plots of relative enzyme activity versus iodoacetamide and 2-pyrrolidone concentrations. Figure 4.19 shows the effect of these inhibitors on wild type *rHsa*PAP1$_{6H}$ activity, whereas Figure 4.20 illustrates the effect of inhibitors on *rHsa*PAP1_Δ3'$_{6H}$ activity. Enzyme activities are expressed as a percentage of uninhibited enzyme. Error bars represent the SD of triplicate readings.

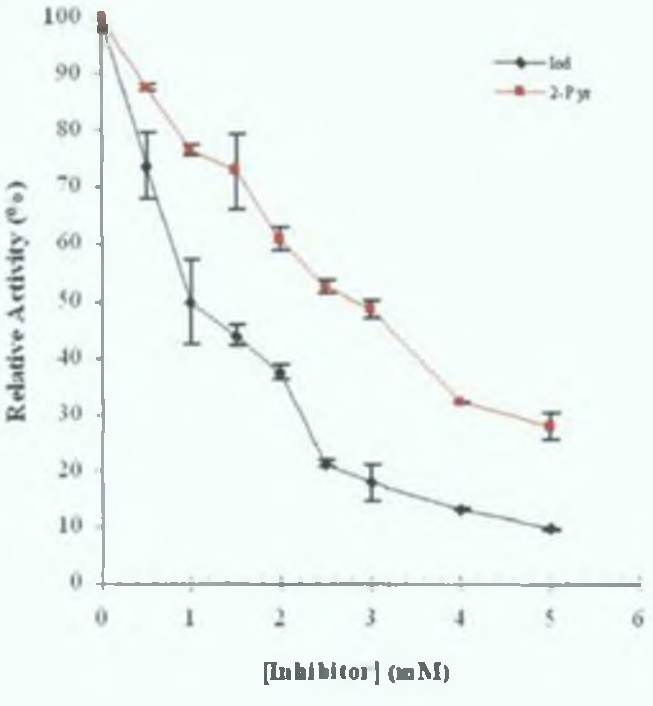

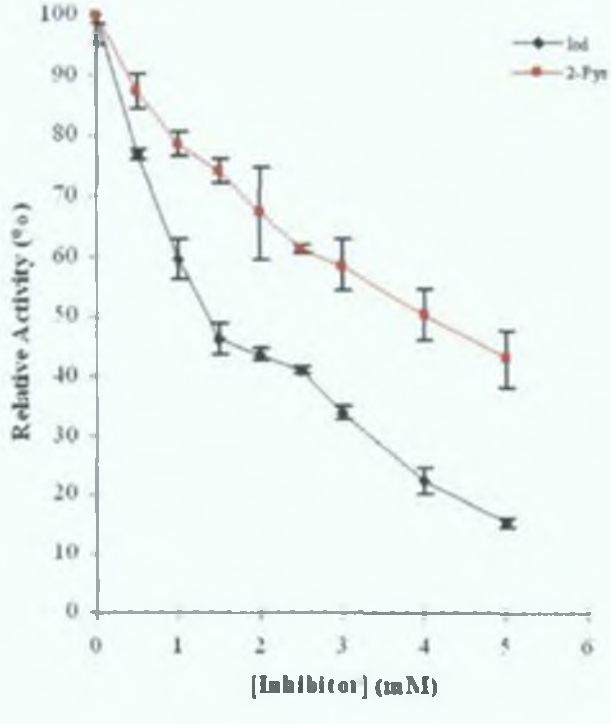

Figures 4.21 and 4.22 Inhibitor Profile Effects of Iodoacetamide and 2-Pyrrolidone on r*Hsa*PAP1_F13mY$_{6H}$ and r*Hsa*PAP1_F16mY$_{6H}$

Plots of relative enzyme activity versus iodoacetamide and 2-pyrrolidone concentrations. Figure 4.21 shows the effect of these inhibitors on r*Hsa*PAP1_F13mY$_{6H}$ activity, whereas Figure 4.22 illustrates the effect of inhibitors on r*Hsa*PAP1_F16mY$_{6H}$ activity. Enzyme activities are expressed as a percentage of uninhibited enzyme. Error bars represent the SD of triplicate readings.

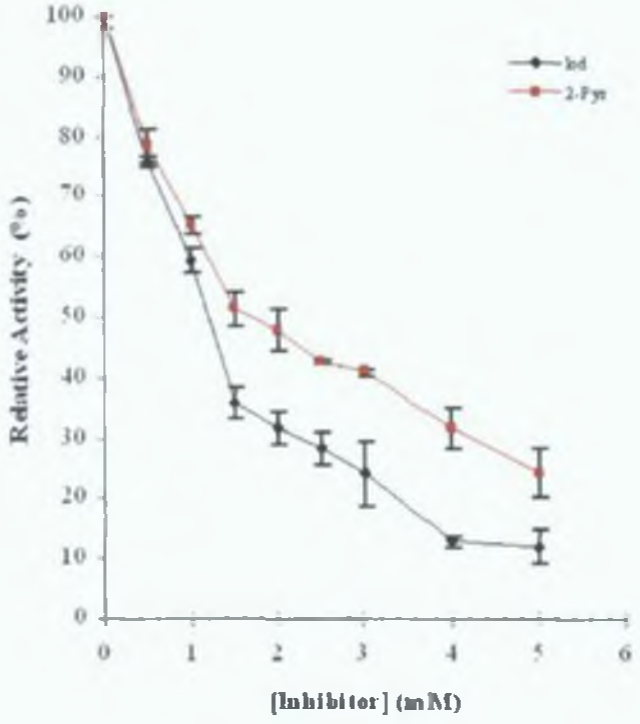

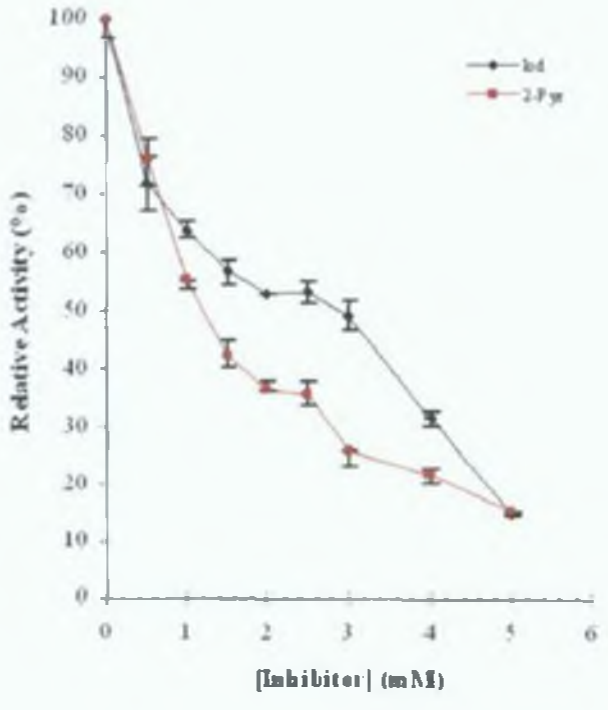

Figures 4.23 and 4.24 Inhibitor Profile Effects of Iodoacetamide and 2-Pyrrolidone r*Hsa*PAP1_N98mQ$_{6H}$ .and r*Hsa*PAP1_N98mV$_{6H}$. Plots of relative enzyme activity versus iodoacetamide and 2-pyrrolidone concentrations. Figure 4.23 shows the effect of these inhibitors on r*Hsa*PAP1_N98mQ$_{6H}$ activity, whereas Figure 4.24 illustrates the effect of inhibitors on r*Hsa*PAP1_N98mV$_{6H}$ activity. Enzyme activities are expressed as a percentage of uninhibited enzyme. Error bars represent the SD of triplicate readings.

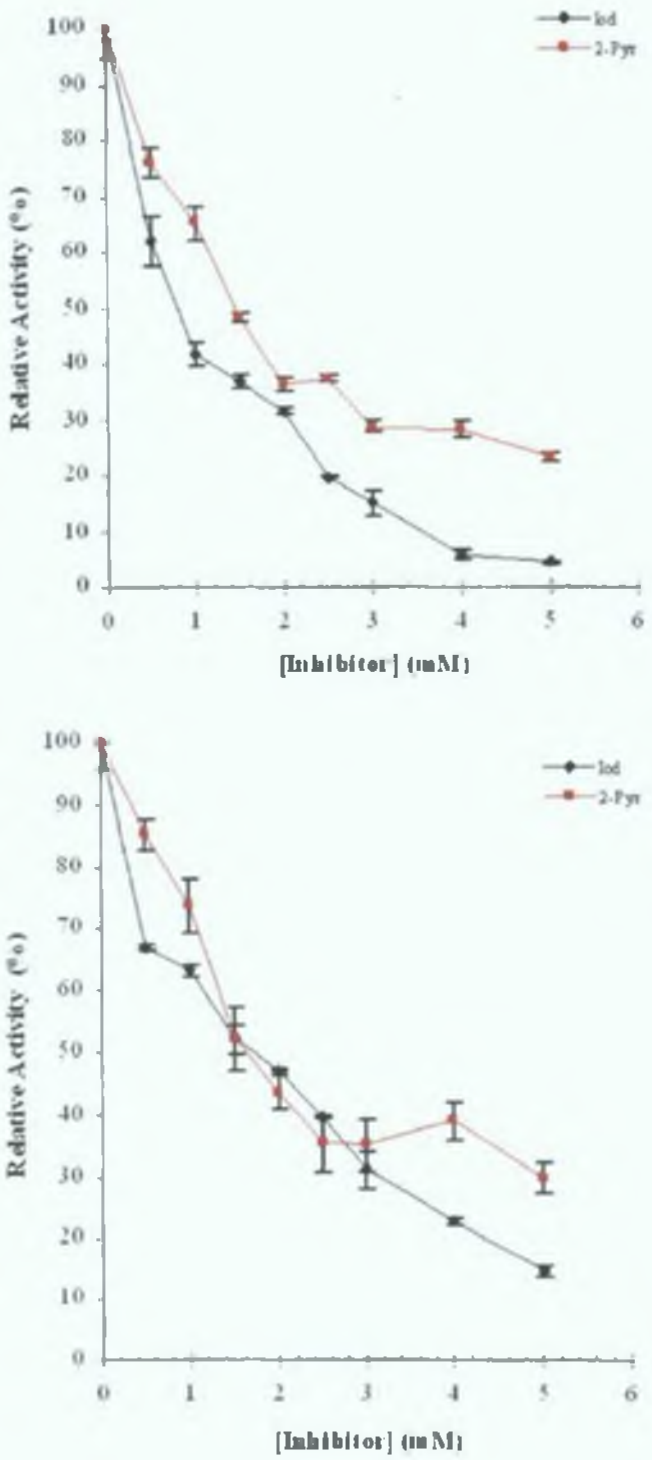

Figures 4.25 and 4.26 Inhibitor Profile Effects of Iodoacetamide and 2-Pyrrolidone on r*Hsa*PAP1_Q180mE$_{6H}$ .and r*Hsa*PAP1_Q180mE,N177mY$_{6H}$.

Plots of relative enzyme activity versus iodoacetamide and 2-pyrrolidinone concentrations. Figure 4.25 shows the effect of these inhibitors on r*Hsa*PAP1_Q180mE$_{6H}$ activity, whereas Figure 4.26 illustrates the effect of inhibitors on r*Hsa*PAP1_Q180mE,N177mY$_{6H}$ activity. Enzyme activities are expressed as a percentage of uninhibited enzyme. Error bars represent the SD of triplicate readings.

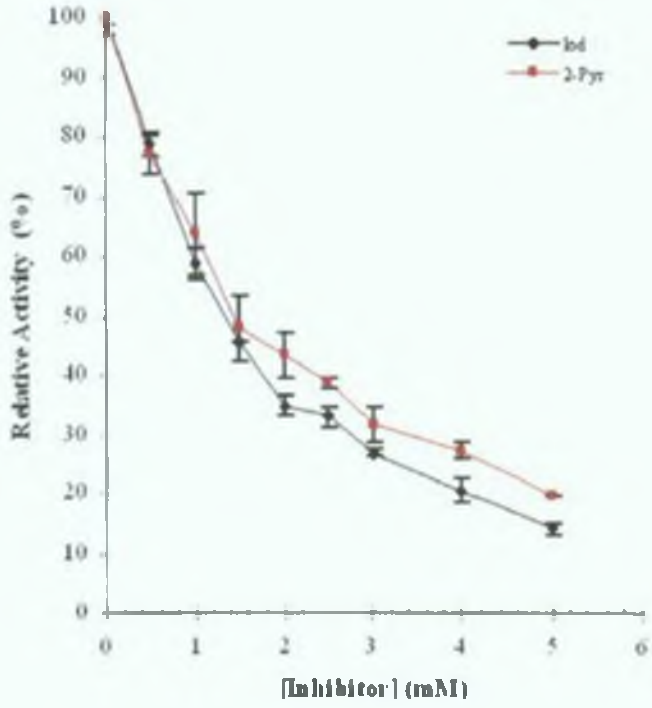

Figures 4.27 and 4.28 Inhibitor Profile Effects of Iodoacetamide and 2-Pyrrolidone on r*Hsa*PAP1_SID115AYF$_{6H}$ and r*Hsa*PAP1_Y147mF$_{6H}$.

Plots of relative enzyme activity versus iodoacetamide and 2-pyrrolidone concentrations. Figure 4.27 shows the effect of these inhibitors on r*Hsa*PAP1_SID115AYF$_{6H}$ activity, whereas Figure 4.28 illustrates the effect of inhibitors on r*Hsa*PAP1_Y147mF$_{6H}$ activity. Enzyme activities are expressed as a percentage of uninhibited enzyme. Error bars represent the SD of triplicate readings.

Table 4.3 Biochemical Properties of r*Hsa*PAP1$_{6H}$ Site-Directed Mutants

Mutant	Temp °C	pH	Iod IC_{50}	2-Pyr IC_{50}
r*Hsa*PAP1$_{6H}$ (wild type)	50	8.5	1.1	1.2
r*Hsa*PAP1_Δ3'$_{6H}$	50	8.0	2.0	1.0
r*Hsa*PAP1_F13mY$_{6H}$	37	9.0	1.0	2.8
r*Hsa*PAP1_F16mY$_{6H}$	50	8.5	1.4	4.1
r*Hsa*PAP1_N98mQ$_{6H}$	50	8.5	1.3	1.5
r*Hsa*PAP1_N98mV$_{6H}$	50	8.5	3.4	1.3
r*Hsa*PAP1_Q180mE$_{6H}$	37	8.5	0.8	1.5
r*Hsa*PAP1_Q180mE,N177mY$_{6H}$	50	9.5	1.8	1.6
r*Hsa*PAP1_SID115mAYF$_{6H}$	50	9.0	2.0	1.4
r*Hsa*PAP1_Y147mF$_{6H}$	37	8.5	1.2	1.5

4 4 Investigation of Human PAP1 Active-Site Residue Glutamic Acid

Site directed mutagenesis followed by functional characterisation is a widely used approach to obtain information on the structure-function relationship of proteins Active site residues Cys149 and His168 were investigated by Vaas, 2005, utilising a site-directed mutagenesis approach Cys149 and His168 were substituted with tryptophan and aspartic acid, respectively Both mutations caused a complete loss of PAP1 activity, supporting the catalytic significance of these residues in human PAP1

It is unknown whether or not the third active site residue Glu85 is required for human PAP1 activity or whether, like prokaryotic PAP1, its purpose is to help orientate the imidazolium ring of the histidine residue (Doran and Carey, 1996)

In this work, this residue was substituted individually with three differing amino acid residues The choice of amino acid replacements was based on altering amino acid properties Glu85 was substituted with aspartic acid, lysine and glutamine (see Figure 4 29) Codon changes were introduced on the expression plasmid pRV5 (see Figure 2 4) by the method described in Section 2 9 2, using primers listed in Table 2 2

Incorporation of diagnostic restriction sites into primers were considered for this work but similar work previously carried out in our laboratory reported that the use of silent codon mutations resulted in a significant drop in recombinant protein production (Vaas, 2005) As a result of this, diagnostic restriction sites were not utilised

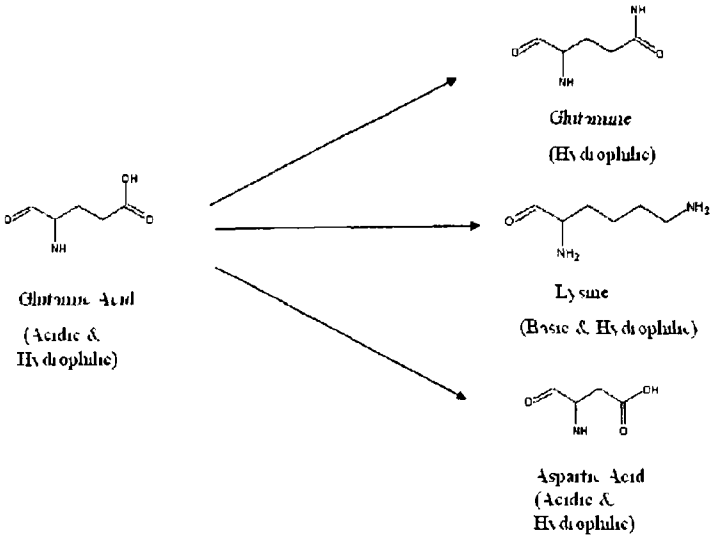

Figure 4 29 Substitution of r*Hsa*PAP1$_{6H}$ Active Site Residue Glu85 With Glutamine, Lysine and Aspartic Acid Amino acid side-chains of Glutamic Acid 85 which were substituted with Glutamine, Lysine and Aspartic Acid respectively For amino acid information see Appendix D Illustrated ing ChemSketch (see Section 2 11)

4 4 1 Analysis of Recombinant Human PAP1 Active Site Mutants

The mutant plasmid derivatives of pRV5 (see Table 4 4) were transformed into *E coli* XL10-Gold as described in Section 2 6 3 Expression cultures (100 ml) were prepared as outlined in Section 2 12 1 All mutants were purified using the IMAC procedure as described in Section 2 13 1 and were subsequently assayed for PAP1 activity (see Section 2 15 3 and 2 15 4) Increased activity was detected for r*Hsa*PAP1_E85mD$_{6H}$ while no activity was detected r*Hsa*PAP1_E85mK$_{6H}$ and r*Hsa*PAP1_E85mQ$_{6H}$ (see Figure 4 30, Table 4 5) SDS-PAGE analysis (see Section 2 16) shows that the purified mutants were expressed at levels comparable to r*Hsa*PAP1$_{6H}$ (see Figure 4 31) Purified samples were also analysed using Native-PAGE (see Section 2 17 1) Kinetic parameters were determined for r*Hsa*PAP1_E85mD$_{6H}$ (see Section 2 18 6, Table 4 7)

Table 4 4 pRV5 Active Site Mutant Derivatives

Mutation	Plasmid	Enzyme
Wild Type	pRV5	r*Hsa*PAP1$_{6H}$
E85 to D	pZK_E85mD	r*Hsa*PAP1_E85mD$_{6H}$
E85 to K	pZK_E85mK	r*Hsa*PAP1_E85mK$_{6H}$
E85 to Q	pZK_E85mQ	r*Hsa*PAP1_E85mQ$_{6H}$

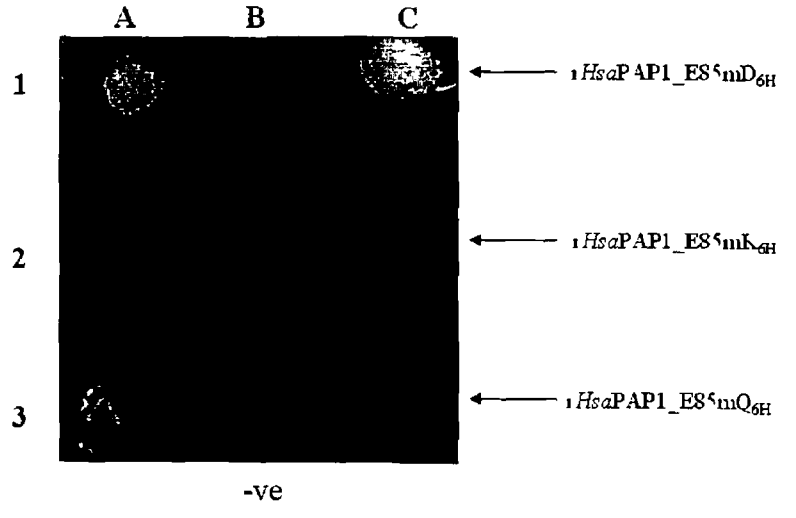

Figure 4 30 Agar Plate Activity Assay for PAP1 Activity
Agar plate assay (see Section 2 15 4) highlighted active mutant r*Hsa*PAP1_E85mD$_{6H}$ (1A & 1C) and inactive mutants r*Hsa*PAP1_E85mK$_{6H}$ (2A & 2C) and r*Hsa*PAP1_E85mQ$_{6H}$ (3A & 3C) Negative control is positioned in lane B

Table 4 5 Human PAP1 Active Site Mutant r*Hsa*PAP1_E85mD$_{6H}$

	Total Activity (Units)	Total Protein (mg)	Specific Activity (Units mg^{-1})
r*Hsa*PAP1$_{6H}$	2,656 98	0 55	4770 06
r*Hsa*PAP1_E85mD$_{6H}$	1,872 14	0 37	4,968 55

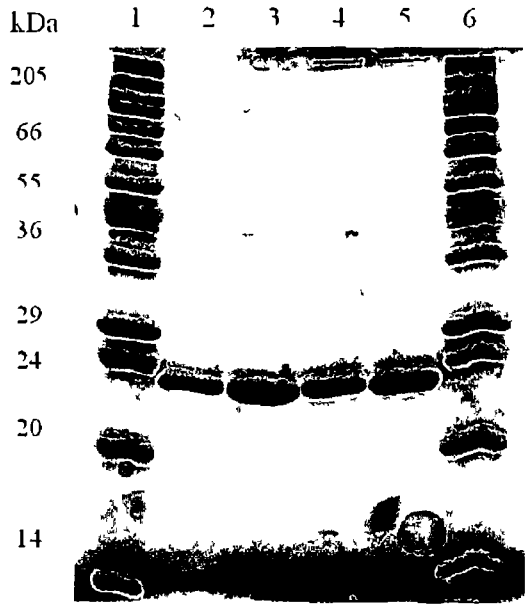

Figure 4 31 SDS-PAGE of Human PAP1 Active Site Mutants
Lane 1 & 6, protein molecular marker, lane 2, purified r*Hsa*PAP1$_{6H}$, lane 3, purified r*Hsa*PAP1_E85mD$_{6H}$, lane 4, r*Hsa*PAP1_E85mK$_{6H}$, lane 5, r*Hsa*PAP1_E85mQ$_{6H}$ The relevant sizes (kDa) of the protein marker are indicated

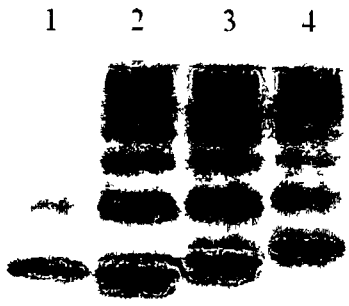

Figure 4 32 Native-PAGE of Human PAP1 Active Site Mutants.
Lane 1, purified r*Hsa*PAP1$_{6H}$, lane 2, purified r*Hsa*PAP1_E85mD$_{6H}$, lane 3, r*Hsa*PAP1_E85mK$_{6H}$ and lane 4, r*Hsa*PAP1_E85mQ$_{6H}$

Table 4 6 r*Hsa*PAP1_E85mD$_{6H}$ Biochemical and Kinetic Parameters

	Biochemical Parameters		Kinetic Parameters	
Enzyme	Temp °C	pH	K_m µM	K_{cat} s^{-1}
r*Hsa*PAP1$_{6H}$	50	8 5	53	3 75
r*Hsa*PAP1_E85mD$_{6H}$	50	9 5	109	1 7

4 5 Random Mutagenesis of Human PAP1

Random mutagenesis is another powerful tool for studying structure-function relationships and for modifying proteins to improve or alter their biochemical and kinetic properties The most commonly used random mutagenesis technique is error prone PCR (Leung, 1989) Error prone PCR generates random mutants of the target gene which are introduced under PCR conditions that reduce the fidelity of nucleotide incorporation (Yuan-zhi, 2006) Fidelity of DNA is reduced by use of error prone DNA polymerases and/or modifying PCR reaction conditions The mutated PCR products are then cloned into an expression vector, pPC225 (see Figure 2 3) and the resultant mutant libraries are screened for changes in enzyme activity Random mutagenesis enables researchers to identify interesting mutations in the absence of structural information and often yields unique mutations which could not have been predicted (Fujii, 2004)

4 5 1 PCR and Screening For Potential *Hsa*PAP1 Random Mutants

PCR reactions were set up as described in Section 2 9 3 using pRV5 (see Figure 2 4) plasmid DNA and primers PAPHsA and PAPHsB (see Table 2 2) The strategy in Figure 4 33 was utilised for random mutagenesis Vector pPC225 (see Figure 2 3) was used for this procedure Quantities of $MnCl_2$ included in the PCR reaction were varied from 0 05 to 2 0 mM PCR products were obtained when 0 05, 0 1 and 0 2 mM $MnCl_2$ were used (see Figure 4 34) However, when 2 mM $MnCl_2$ was utilised in the PCR reaction, a PCR product was not obtained An *Eco*RI/*Hind*III restriction enabled the PCR product to be ligated with pPC225, which had been opened with *Eco*RI/*Hind*III These ligations were subsequently transformed into *E coli* XL10-Gold (see Section 2 6 3) Screening for potential random mutants was done by *Eco*RI/*Hind*III restriction analysis (see Figure 4 35) and comparing wild-type PAP1 enzymatic activity to mutant activities This proved to be unsuccessful and a new approach was adopted It appeared

that the vector pPC225 was re-circularising and as a result failed to ligate with the restricted PCR products.

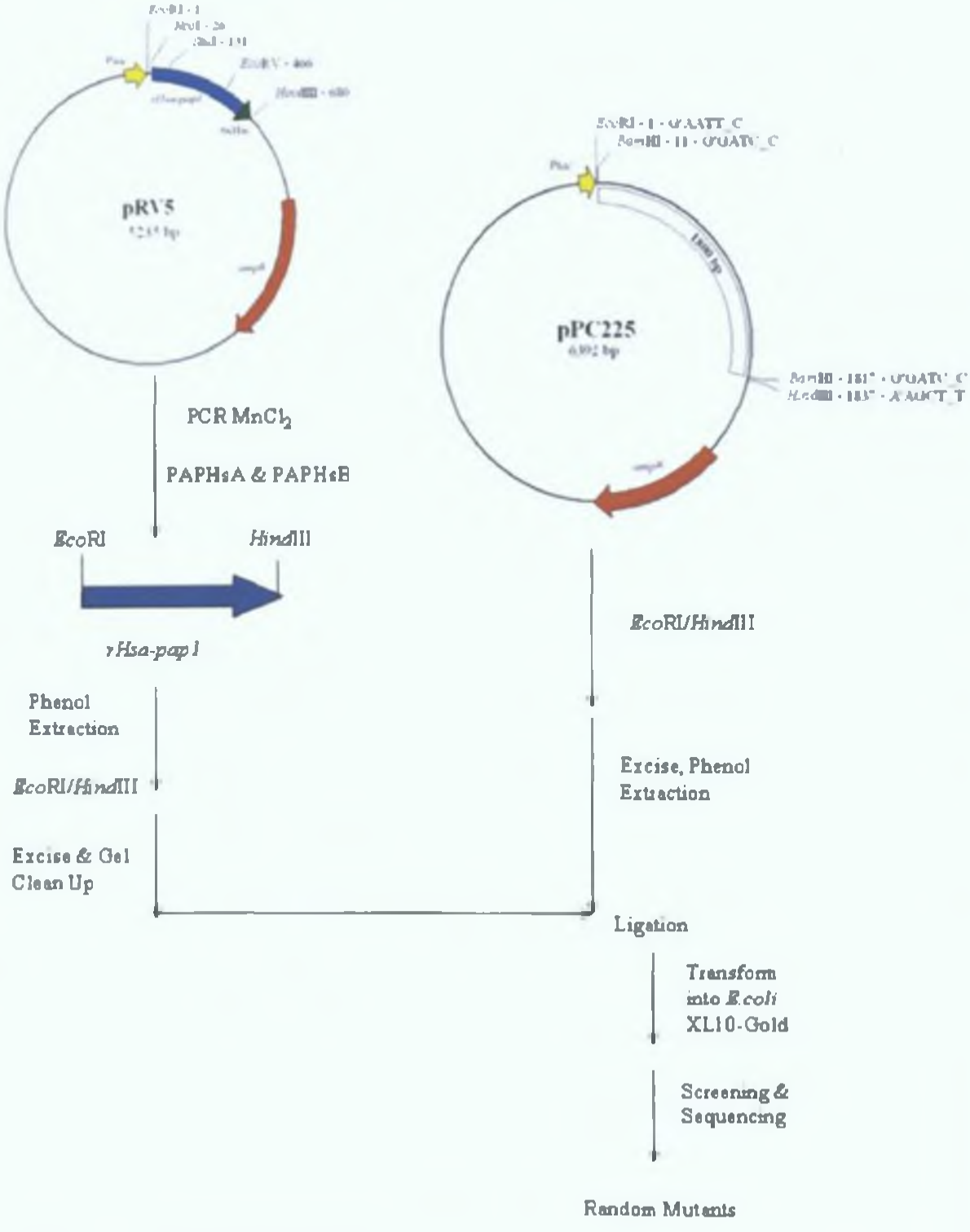

Figure 4.33 Strategy Used for r*Hsa*PAP1 Random Mutagenesis
PCR (see Section 2.9.3) on pRV5 using $MnCl_2$ and primers PAPHsA, PAPHsB (see Table 2.2) followed by phenol extraction and *Eco*RI/*Hind*III restriction generates product which is ligated into pPC225 (opened with *Eco*RI/*Hind*III. Ligation is transformed (see Section 2.6.3) into *E.coli* XL10-Gold and screened for random mutants. Illustrated using pDRAW32 (see Section 2.11).

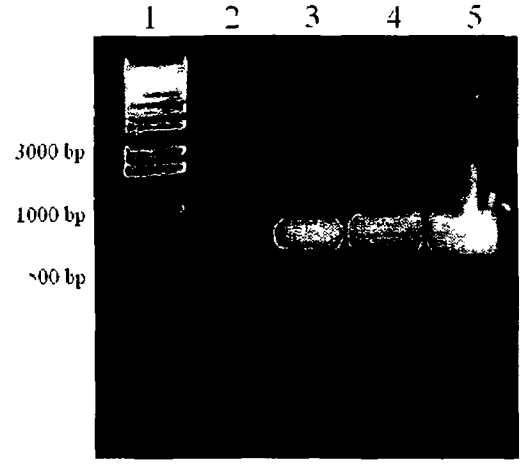

Figure 4 34 Random Mutagenesis PCR Products
1% agarose gel Lane 1, DNA Ladder (sizes as in Figure 2 6), Lane 2, PCR negative control, Lane 3, PCR product using 0 05 mM $MnCl_2$, Lane 4, PCR product using 0 1 mM $MnCl_2$, Lane 5, PCR product using 0 2 mM $MnCl_2$

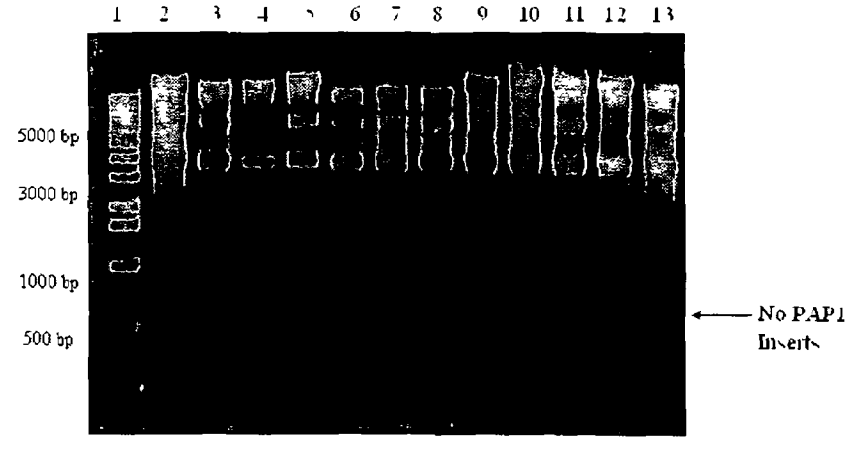

Figure 4 35 Restriction Analysis of Potential Random Mutants
*Eco*RI/*Hind*III restriction digest of potential random mutant clones analysed on 1% agarose gel (Section 2 5) Lane 1, DNA Ladder (sizes as in Figure 2 6), Lane 2 – 13, *Eco*RI/*Hind*III restriction analysis on all potential clones

Alkaline phosphatase treatment (see Section 2 8 3) was used as an intermediate step in this procedure Alkaline phosphatase catalyses the removal of 5' phosphate groups from DNA The CIP-treated fragments lack the 5' phosphoryl termini which are required by the ligases As a result, this treatment prevents self-ligation of the vector and thereby greatly facilitates ligation of other DNA fragments into the vector The modified strategy for random mutagenesis is shown in Figure 4 36

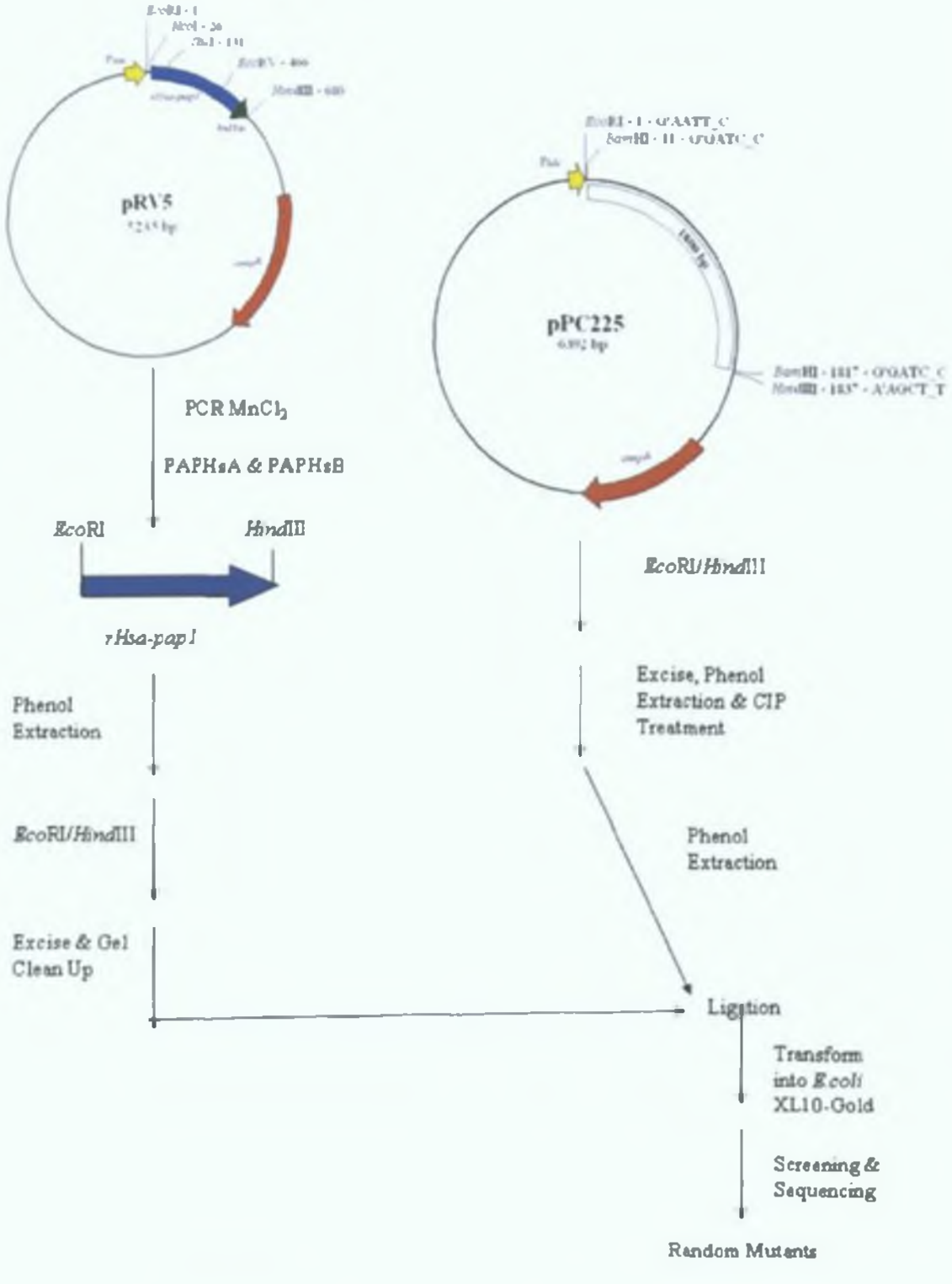

Figure 4.36 Modified Strategy for r*Hsa*PAP1 Random Mutagenesis
PCR (see Section 2.9.3) on pRV5 using $MnCl_2$ and primers PAPHsA, PAPHsB (see Table 2.2) followed by phenol extraction and *Eco*RI/*Hind*III restriction generates product which is ligated into pPC225 (opened with *Eco*RI/*Hind*III, and CIP Treated). Ligation is transformed (see Section 2.6.3) into *E.coli* XL10-Gold and screened for random mutants. Illustrated using pDRAW32 (see Section 2.11).

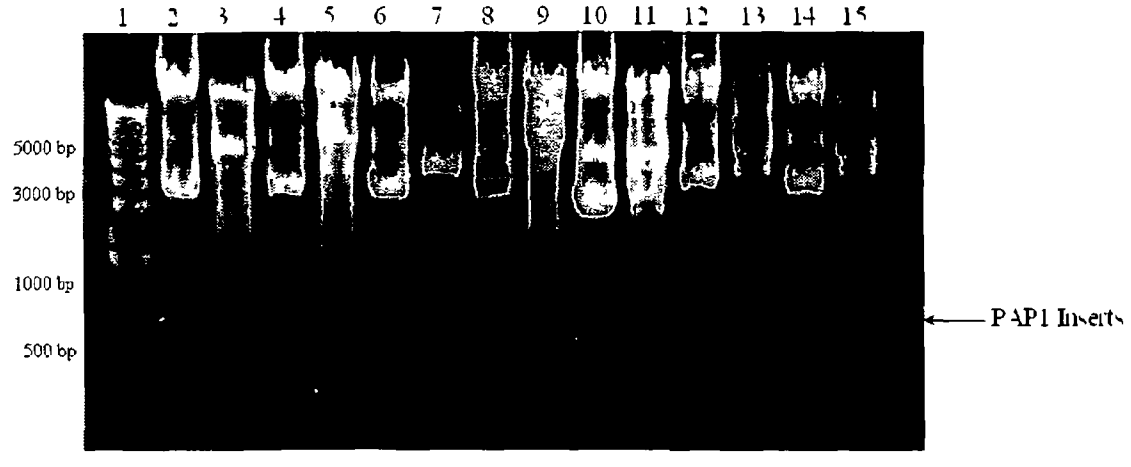

Figure 4 37 Restriction Analysis of Potential Random Mutants Using Modified Strategy *Eco*RI/*Hind*III restriction digest of potential random mutant clones analysed on 1% agarose gel (see Section 2 5) Lane 1, DNA Ladder (sizes as in Figure 2 6), Lane 2, Clone 1 uncut, Lane 3, Clone 1 *Eco*RI/*Hind*III cut, Lane 4, Clone 2 uncut, Lane 5, Clone 2 *Eco*RI/*Hind*III cut, Lane 6, Clone 3 uncut, Lane 7, Clone 3 *Eco*RI/*Hind*III I cut, Lane 8, Clone 4 uncut, Lane 9, Clone 4 *Eco*RI/*Hind*III cut, Lane 10, Clone 5 uncut, Lane 11, Clone 5 *Eco*RI/*Hind*III cut, Lane 12, Clone 6 uncut, Lane 13, Clone 6 *Eco*RI/*Hind*III cut, Lane 14, Clone 7 uncut, Lane 15, Clone 7 *Eco*RI/*Hind*III cut

A series of potential *Hsa*PAP1 random mutants were generated using this modified strategy *Eco*RI/*Hind*III restriction analysis show presence of the PAP1 680 bp fragment (see Figure 4 37) and varied PAP1 activity levels were also detected (see Section 2 15 3) The successful products of r*Hsa*PAP1 random mutants were confirmed by DNA sequencing (see Section 2 10) The sequencing data is given in Appendix B r*Hsa*PAP1 random mutants which were obtained from this work are listed in Table 4 8 and are also highlighted on *Hsa*PAP1 3D model (see Figure 4 38)

Table 4.7 Random Mutagenesis Plasmids and Enzymes

Mutation	Plasmid	Enzyme
G35 to T	pZK_G35mD	r*Hsa*PAP1_G35mD$_{6H}$
N90 to D	pZK_N90mD	r*Hsa*PAP1_N90mD$_{6H}$
M192 to T	pZK_M192mT	r*Hsa*PAP1_M192mT$_{6H}$
K94 to R	pZK_K94mR	r*Hsa*PAP1_K94mR$_{6H}$
A165 to V	pZK_A165mV	r*Hsa*PAP1_A165mV$_{6H}$
P48 to R	pZK_P48mR	r*Hsa*PAP1_P48mR$_{6H}$
A184 to P	pZK_A184mP	r*Hsa*PAP1_A184mP$_{6H}$
P48 to Q, D143 to H	pZK_P48mQ,D143mH	r*Hsa*PAP1_P48mQ,D143mH$_{6H}$
P67 to R	pZK_P67mR	r*Hsa*PAP1_M122mV$_{6H}$
M122 to V	pZK_M122mV	r*Hsa*PAP1_M122mV$_{6H}$
G77 to D	pZK_G77mD	r*Hsa*PAP1_G77mD$_{6H}$

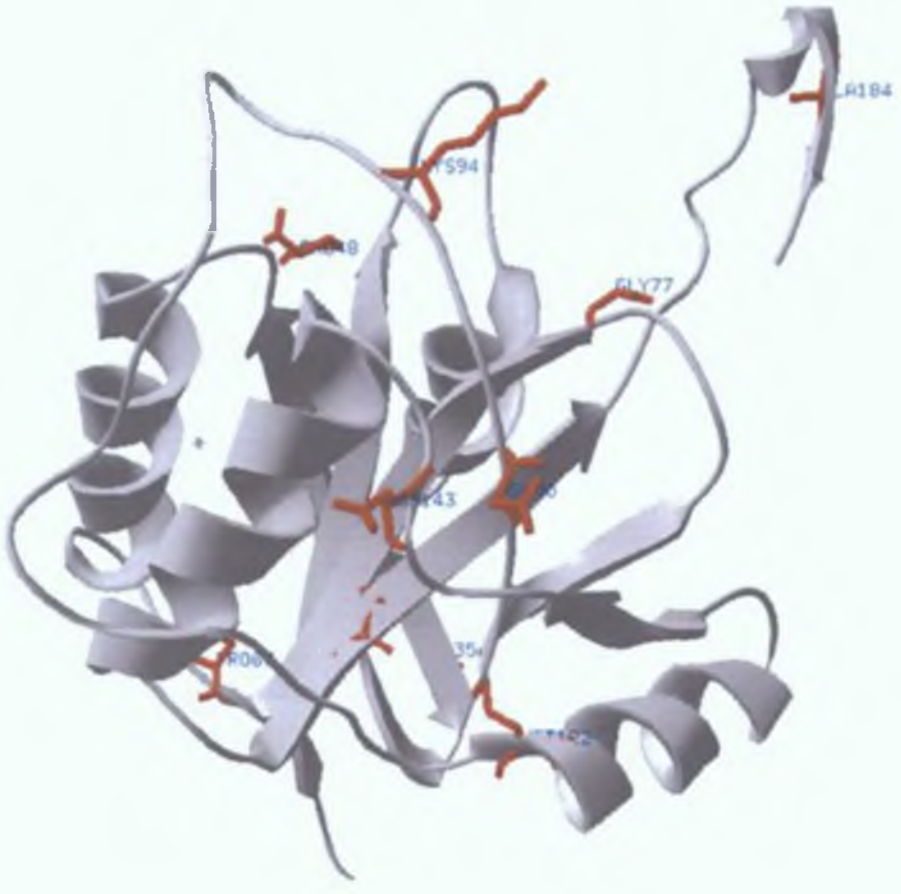

Figure 4.38 *Hsa*PAP1 Model Highlighting Targeted Residues During Random Mutagenesis Generated using DeepView (see Section 2.11).

4.5.2 Analysis of Recombinant Human PAP1 Random Mutants

Expression cultures (100 ml) were prepared as outlined in Section 2.12. All random mutants were purified using nickel-affinity chromatography (see Section 2.13.1). Mutants were assayed for PAP1 activity (see Section 2.15.3) and protein concentration (see Section 2.14.1). Figure 4.39 displays SDS-PAGE analysis (see Section 2.16) of purified random mutants.

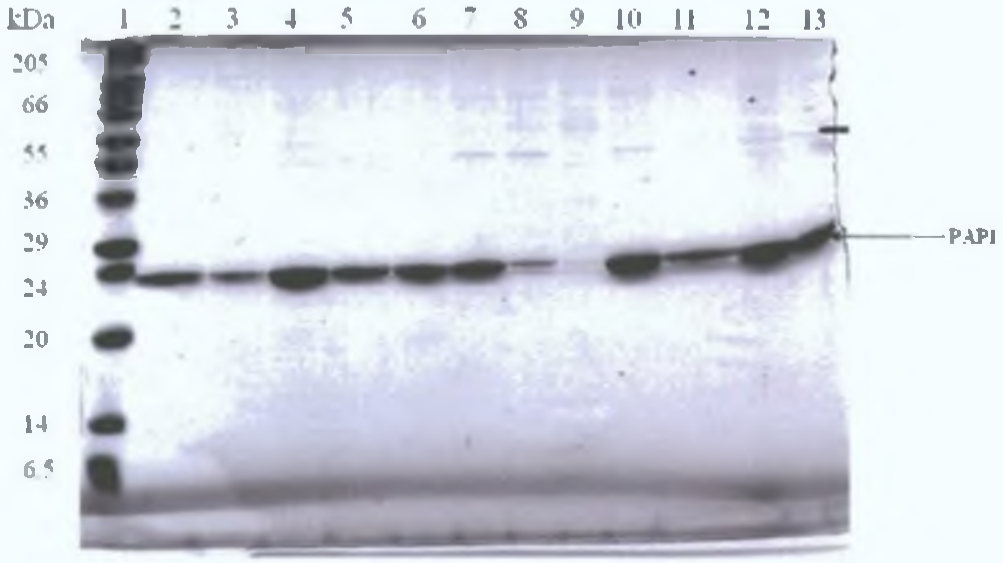

Figure 4.39 Purification of r*Hsa*PAP1$_{6H}$ Random Mutants

Lane 1, protein molecular marker; Lane 2, r*Hsa*PAP1$_{6H}$; Lane 3, r*Hsa*PAP1_A165mV$_{6H}$; Lane 4, r*Hsa*PAP1_G35mD$_{6H}$. Lane 5, r*Hsa*PAP1_G77mD$_{6H}$. Lane 6, r*Hsa*PAP1_K94mR$_{6H}$. Lane 7, r*Hsa*PAP1_P67mR$_{6H}$; Lane 8, r*Hsa*PAP1_M122mV$_{6H}$; Lane 9, r*Hsa*PAP1_M192mT$_{6H}$. Lane 10, r*Hsa*PAP1_P48mR$_{6H}$. Lane 11, r*Hsa*PAP1_P48mR,D143mH$_{6H}$,Lane 12, r*Hsa*PAP1_N90mD$_{6H}$; Lane 13, r*Hsa*PAP1_A184mT$_{6H}$.The relevant sizes (kDa) of the protein marker are indicated.

Table 4.8 Biochemical and Kinetic Parameters of r*Hsa*PAP1$_{6H}$ Random Mutants

Enzyme	pH	Temperature (°C)	Specific Activity (units mg^{-1})	K_m (μM)	K_{cat} (s^{-1})
r*Hsa*PAP1$_{6H}$	8 5	50	8770 3	53	2 07
r*Hsa*PAP1 _G35mD$_{6H}$	9 0	50	4257 7	67	0 31
r*Hsa*PAP1 _N90mD$_{6H}$	8 5	50	3063 2	76	0 44
r*Hsa*PAP1_M192mT$_{6H}$	8 5	50	1049 5	65	1 76
r*Hsa*PAP1_K94mR$_{6H}$	8 5	50	3492 3	85	0 78
r*Hsa*PAP1_A165mV$_{6H}$	8 0	60	2286 6	79	3 1
r*Hsa*PAP1_P48mR$_{6H}$	8 5	50	1334 4	71	1 5
r*Hsa*PAP1_A184mP$_{6H}$	9 0	50	3723 8	78	1 65
r*Hsa*PAP1_P48mQ,D143mH$_{6H}$	8 5	50	978 3	56	0 88
r*Hsa*PAP1_P67mR$_{6H}$	8 5	50	6615 37	52	0 77
r*Hsa*PAP1_M122mV$_{6H}$	9 0	50	9167 7	83	2 26
r*Hsa*PAP1_G77mD$_{6H}$	8 5	50	2617 7	64	1 55
r*Hsa*PAP1_N22mH$_{6H}$	8 5	50	1676 1	79	0 72

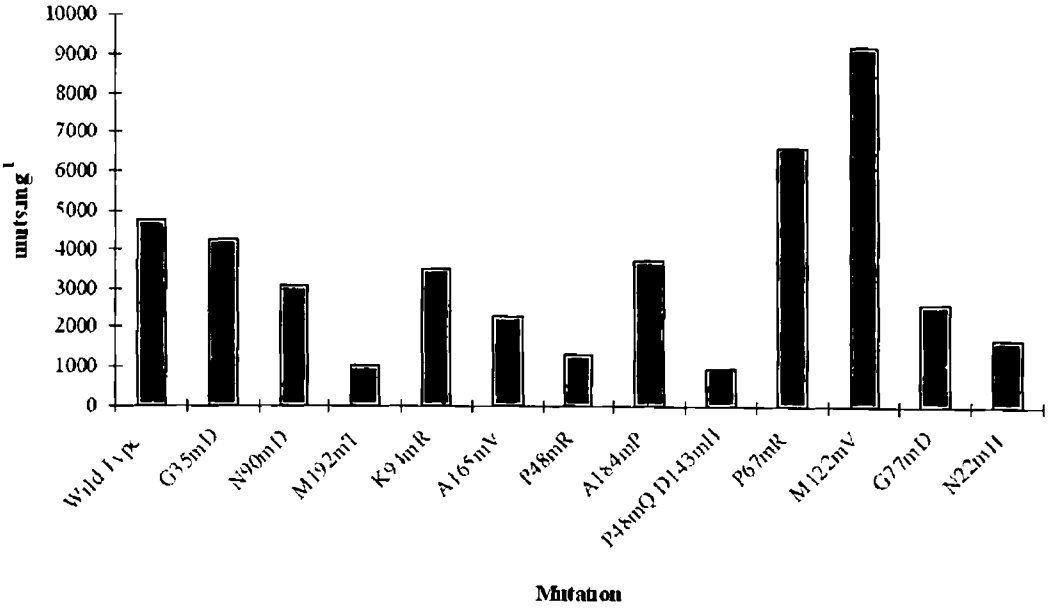

Figure 4 40 Effect of Mutations on Specific Activity

Values for specific activity (units mg^{-1}) taken from Table 4 8

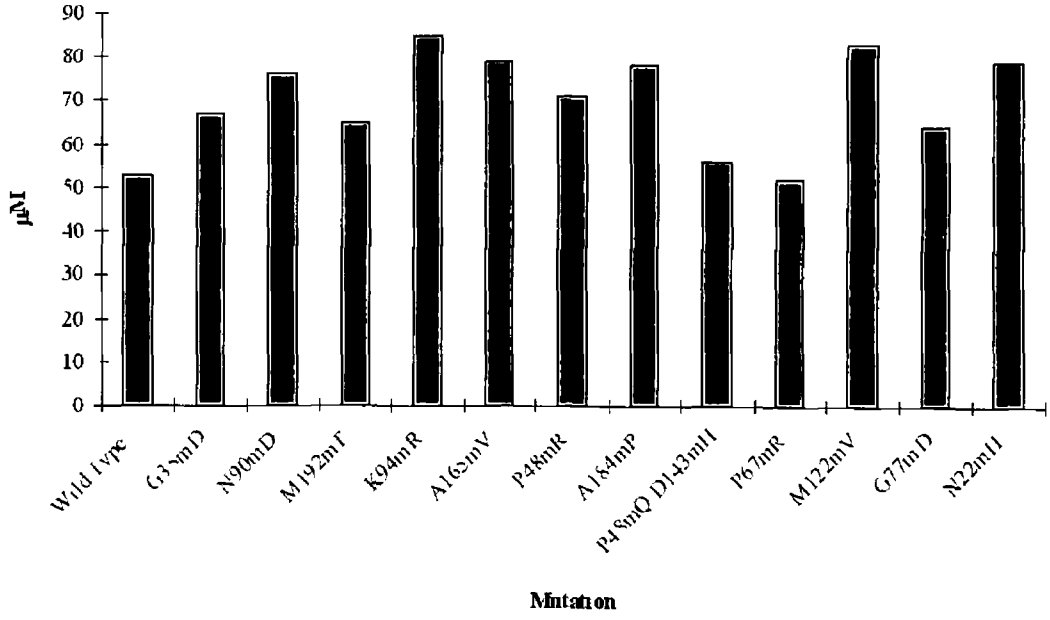

Figure 4 41 Effect of Mutations on K_m
Values for K_m (μM) taken from Table 4 8

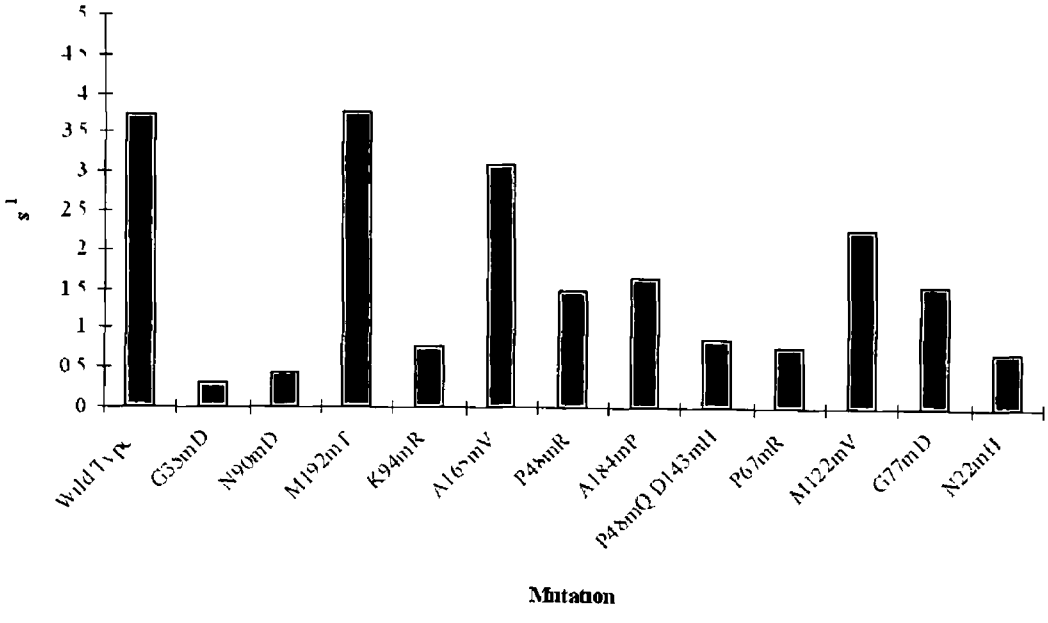

Figure 4 42 Effect of Mutations on K_{cat}
Values for K_{cat} (s^{-1}) taken from Table 4 8

4.6 Discussion

4.6.1 Human PAP1 Kinetics Using Pyroglutamyl Peptides

Kinetic analysis of a series of pyroglutamyl peptides has indicated that purified human PAP1 has a greater affinity for tripeptides over dipeptides (see Table 4.1). It is interesting to note that the same series of pyroglutamyl peptides were utilised to analyse purified bovine PAP1 and different effects have been observed for both enzymes.

A K_i value of 44 μM (see Figure 4.7) was determined for TRH showing the relative highest affinity for human PAP1. K_i values of 204 μM and 781 μM were determined for dipeptides pGlu-Ala and pGlu-Thr, respectively (see Table 4.1). Addition of an alanine residue to each of the aforementioned peptides resulted in a dramatic decrease of K_i values, indicating an increase of affinity for human PAP1. Tripeptides pGlu-Ala-Ala and pGlu-Thr-Ala yielded K_i values of 107 μM and 166 μM, respectively. Competitive inhibition was found for all four peptides (see Figures 4.2 – 4.9). The total opposite effect was found for bovine PAP1 (see Chapter 3.0). Uncompetitive inhibition was found for pGlu-Pro (see Figure 4.4), however a K_i value could not be determined.

Greatest affinity was shown for tripeptides pGlu-His-Pro-NH_2 (TRH) (44 μM) and pGlu-Glu-Ala (83 μM). When compared, both tripeptides have a hydrophilic residue in the P_2 position which agrees with results obtained for bovine PAP1 (see Chapter 3.0).

Amino acid residue in the P_3 position of a tripeptide also affects affinity of PAP1. This is clearly demonstrated with findings obtained using dipeptide pGlu-Thr and tripeptide pGlu-Thr-Ala (see Table 4.1). Overall, it can be concluded that greatest affinity is observed with tripeptides as opposed to dipeptides. However, the type of amino acid residue in both the P_2 and P_3 positions affect human PAP1 affinity for the peptide. From human, bovine and previous research (see Chapter 3.0), it appears that a hydrophilic residue is preferred at the P_2 position; however the preferred amino acid type at the P_3 position has yet to be determined.

4.6.2 Biochemical Analysis of Human PAP1 Mutants

A series of active mutants which were previously generated were biochemically characterised (see Table 4.2, Figure 4.10). Optimum temperature studies (see Section 2.18.3) found that the majority of the active mutants displayed an optimum temperature of 50°C, while three mutants, namely r*Hsa*PAP1_F13mY_{6H}, r*Hsa*PAP1_Q180mE_{6H} and r*Hsa*PAP1_Y147mF_{6H} were optimally active at 37°C (see Figures 4.11 – 4.13). As the temperature increases, the rate of most chemical reactions increases. However, due to

the instability of most protein molecules, the enzyme is inactivated at higher temperatures (Elliott and Elliott, 2005). Thermostability studies at 37°C (see Section 2.18.4) revealed that none of the nine active mutants display increased thermostability when compared to wild type PAP1 during the 0-90 minute period (see Figures 4.14 - 4.18). Mutants r*Hsa*PAP1_F13mY$_{6H}$ and r*Hsa*PAP1_N98mQ$_{6H}$ show increased stability during the 90 – 180 minute period. r*Hsa*PAP1_SID115AYF$_{6H}$ lost 60% enzyme activity after 15 minutes and rapidly declines thereafter showing poor thermostability at 37°C (see Figure 4.17).

Enzyme activity is influenced by pH in several ways. The stability of the protein is influenced by the state of its ionisable groups and on the function of the active site may be likewise dependent on this (Elliott and Elliott, 2005). Optimum pH for this series of active mutants was found to range between 8.0 and 8.5, while majority of mutants displayed an optimum pH of 8.5 (see Table 4.3).

IC_{50} values were determined (see Section 2.18.5) for these active mutants (see Table 4.3) using inhibitors iodacetamide and 2-pyrrolidone. IC_{50} values of 1.1 μM and 1.2 μM were determined for wild type PAP1 using the aforementioned inhibitors, respectively. Active mutants produced IC_{50} values ranging between 0.8 and 2.0 μM using thiol inhibitor iodacetamide. r*Hsa*PAP1_N98mV$_{6H}$ produced an IC_{50} value of 3.4 μM. Similar results were obtained with substrate analogue 2-pyrrolidone with two of the nine active mutants producing higher IC_{50} values than wild type PAP1 (see Figures 4.21 and 4.22, Table 4.3). Values of 2.8 and 4.1 μM were determined for mutants r*Hsa*PAP1_F13mY$_{6H}$ and r*Hsa*PAP1_F16mY$_{6H}$ respectively.

These differences could be due to structure of the substrate binding pocket being modified due to these mutations and as a result has increased IC_{50} values being determined signifying a reduced potency by these inhibitors towards pRV5 derivatives (see Table 4.3).

4.6.3 Investigation into the Active Site of Human PAP1

Investigation into human PAP1 active site residue Glu85 revealed that an acidic residue is required at this position to retain PAP1 activity. Substitution of Glu85 with another acidic residue, namely aspartic acid resulted in a slight increase in PAP1 specific activity. However, when basic amino acid glutamine and neutral amino acid lysine were substituted, complete loss of PAP1 activity was found for both pRV5 derivatives (see Figure 4.30, Table 4.5). SDS-PAGE analysis (see Section 2.16) shows that the purified

mutants were expressed at levels comparable to r*Hsa*PAP1$_{6H}$ (see Figure 4 31) Native-PAGE analysis highlights a gel shift for inactive mutants r*Hsa*PAP1_E85mK$_{6H}$ and r*Hsa*PAP1_E85mQ$_{6H}$ when compared to wild type PAP1 (see Figure 4 32) Mutation of this residue to either a lysine or glutamine residue likely results in some adjustment of its protein structure, influencing the hydrophobic pocket and as a result rendering r*Hsa*PAP1$_{6H}$ mutants inactive The native gel shows presence of multiple protein bands at the top of the gel are most probably due to protein aggregation due to overloading of sample

4 6 4 Human PAP1 Random Mutagenesis

Random mutagenesis PCR is a widely employed technique for the study of structure-function relationships Thermostable DNA polymerase from *Thermus aquaticus* (Taq-Pol) was chosen for random mutagenesis (see Section 2 9 3) Due to the relatively high fidelity of this polymerase, an additional component was included in the PCR reaction Various concentrations of $MnCl_2$ were included to reduce this high fidelity and as a result, generate a series of random mutants Other approaches which could have been taken to reduce fidelity of DNA polymerase include the variation of dNTP concentration in the PCR reaction (Yuan-zhi, 2006) Also, a low fidelity DNA polymerase could have been utilised as opposed to Taq-Pol, e g *Pyrococcus furiosus* (Pfu-Pol), where the proof-reading exonuclease has been disabled (Biles, 2004)

When analysing protein structure-function relationships, the desired mutation frequency is one amino acid change (1-2 nucleotide changes) per gene (Vartanian *et al,* 1996)

This mutation frequency was optimised by addition of $MnCl_2$ to PCR reaction The optimal $MnCl_2$ concentration for a single amino acid change was 0 05 mM Numerous amino acid changes were obtained when 0 1 and 0 2 mM $MnCl_2$ were utilised

The main problem which was encountered during random mutagenesis was the recircularisation of expression vector pPC225 (see Figure 2 3) which was resolved by including CIP treatment as an additional step (see Section 2 8 3) Problems of this nature have previously been reported during random mutagenesis (Fujii, 2006) Due to low ligation efficiencies during random mutagenesis, this group simplified steps of this method by using error prone rolling circle amplification (RCA) This method consists of a one RCA step followed by direct transformation of the host strain to generate random mutants

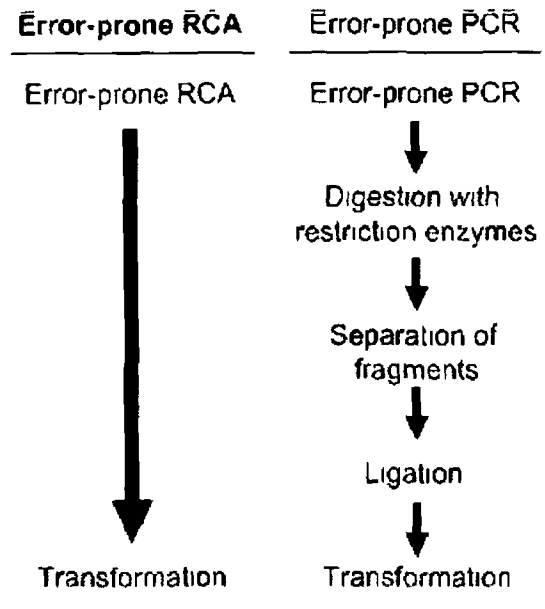

Figure 4 43 Schematic Diagram of Error-Prone RCA in Comparison With the Conventional Random Mutagenesis Method (Fujii, 2004).

In total, twelve human PAP1 random mutants were generated (see Table 4 7) Three silent mutants were also generated and it was interesting to note that in all three mutants, a cysteine residue was targeted

It has been reported that during random mutagenesis PCR, mutations of the type T/A – to- X occur far more frequently than others (Lin-Goerkr, 1997) However, this was not the case with the human PAP1 random mutants generated from this work as only 16% of the mutations are of this nature (see Table 4 7)

Due to availability of a 3-D model for *Hsa*PAP1 (see Figure 4 1) it was possible to visualise the positions of the targeted residues for random mutagenesis on the model (see Figure 4 38) Majority of the targeted residues reside within the hydrophobic pocket region which include N90, A165, D143, P67, N122 and G77 Both G35 and K94 are positioned on the outer loop of the pocket, while A184 is located at the edge of the hydrophobic pocket Although M192 is located at the C-terminal end, it was impossible to visualise it on the model due to the end twenty-four C-terminal amino acids being eliminated from the model

Table 4 8 shows that there is little variation in pH and temperature amongst the pRV5 derivatives All random mutants are within an 8 0-9 0 pH range An optimum temperature of 50°C was determined for mutants with the exception of

r*Hsa*PAP1_A165mV$_{6H}$ An optimum temperature of 60°C was obtained for this mutant As a result, residue substitution from an alanine to a valine was found to increase the thermostability of the enzyme Random mutant specific activity (see Figure 4 40) and protein expression (see Figure 4 39) levels vary considerably Lowest specific activity is observed for r*Hsa*PAP1_P48mQ,D143mH$_{6H}$ This dramatic decrease in specific activity of 978 3 units mg^{-1} suggests that this mutation is having a direct influence on the shape of the substrate binding pocket Due to the occurrence of two mutations it is unclear which substitution is actually causing the decrease Increased expression levels are observed for r*Hsa*PAP1_G35mD$_{6H}$, r*Hsa*PAP1_P48mR$_{6H}$ and r*Hsa*PAP1_N90mD$_{6H}$, while decreased levels are displayed for enzymes r*Hsa*PAP1_A165mV$_{6H}$, r*Hsa*PAP1_M122mV$_{6H}$ and r*Hsa*PAP1_M192mT$_{6H}$ (see Figure 4 39) It is interesting to note that in both cases of the latter two random mutants a methionine residue has been targeted Methionine residues are hydrophobic, non-polar residues that may play a role in the expression of human PAP1 protein Substitution of the methionine at position 122 with a valine residue does not have a major effect on specific activity (9,167 units mg^{-1}) However when methionine at position 192 was substituted with a threonine amino acid, specific activity is drastically reduced (1,049 units mg^{-1}), which may be due to the threonine residue causing a change in the hydrophobic pocket These differing levels of PAP1 protein expression and PAP1 activity are due to either position occupied by the methionine residues within the PAP1 amino acid sequence or properties of the amino acid residues used for substitution during random mutagenesis

Amino acid, valine, although smaller possesses similar properties to methionine being hydrophobic and non-polar This alone may cause or may result in specific activity remaining similar to wild type PAP1 The decrease in specific activity observed for r*Hsa*PAP1_M192mT$_{6H}$ may be due to the hydrophilic or polar nature of the threonine residue used for substitution It is interesting to observe that M192 is located at the C-terminal end which would agree with findings from PAP1 bovine study which has shown that residues at the C-terminal region are important for protein expression (see Chapter 3 0)

K_m values (see Figure 4 41) obtained for this series of mutants are in the range between 52 and 85 μM suggesting that the random mutants have resulted in little change occurring with regards to substrate affinity K_{cat} values (see Figure 4 42) vary considerably, majority of mutants have K_{cat} values between 1 0 and 2 0 There are only two mutants which possess a turnover number that is slightly higher than wild type

PAP1 Both r*Hsa*PAP1_P67mR$_{6H}$ and r*Hsa*PAP1_M122mV$_{6H}$ produced K_{cat} values of 2 77 and 2 26 s^{-1}, respectively

CHAPTER 5.0

Human PAP1 Crystallisation Study

5.1 Crystallography

Crystallography is the science of determining the arrangement of atoms, molecules or ions in solids. In older usage, it is the scientific study of crystals. A crystal is a homogenous solid formed by a repeating, three-dimensional pattern of atoms, ions or molecules and having fixed distances between constituent parts.

The crystallisation process is composed of two major events, **nucleation** and **crystal growth**. Nucleation is the stage when solute molecules dispersed in the solvent start to gather to create clusters. These stable clusters constitute the nuclei (consisting of 10^3 – 10^{15}). However when the clusters are not stable, they redissolve. Therefore, the clusters need to reach a critical size in order to become stable nuclei. It is at the stage of nucleation that the atoms arrange in a defined and periodic manner that defines the crystal structure.

The crystal growth is the subsequent growth of the nuclei that succeed in achieving the critical cluster size. Supersaturation is the driving force of the crystallisation, hence the rate of nucleation and growth is driven by the existing supersaturation in the solution. Depending upon the conditions, either nucleation or growth may be predominant over the other, and as a result, crystals with different sizes and shapes are obtained. Once the supersaturation is exhausted, the solid-liquid system reaches the equilibrium and the crystallisation process is complete (http://www.structmed.cirm.ac.uk).

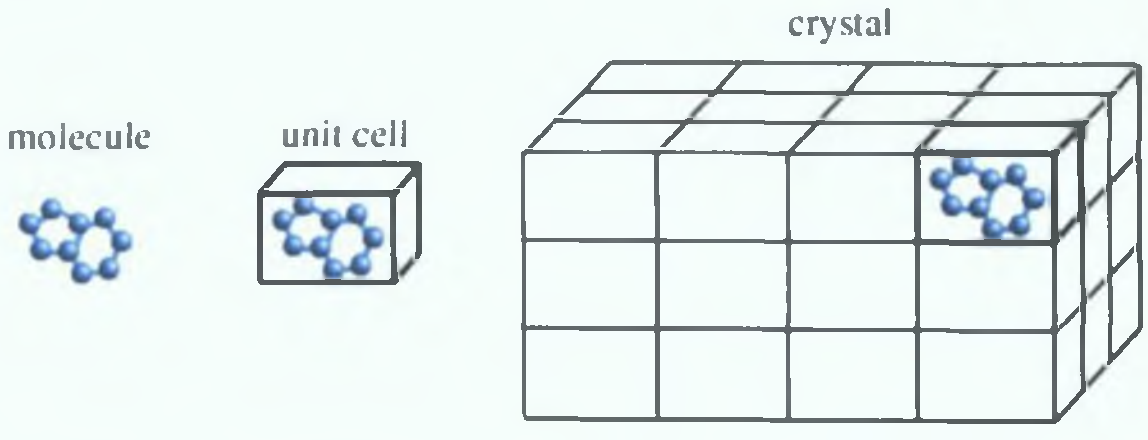

Figure 5.1 Crystal Formation
The unit cell is the basic building block for a crystal.The unit cell is a spatial arrangement of atoms which is tiled in three-dimensional space to the crystal (http://www.structurmed.cirm.cam.ac.uk).

5 1 1 Principles of X-ray Crystallography

X-ray diffraction is the major technique in crystallography in which the pattern produced by the diffraction of X-rays through the closely spaced lattice of atoms in a crystal is recorded and then analyzed to reveal the nature of that lattice This generally leads to an understanding of the material and molecular structure of a substance The spacing in the crystal lattice can be determined using Bragg's law The electrons that surround the atoms, rather than the atomic nuclei themselves, are the entities which physically interact with the incoming X-ray photons This technique is widely used in chemistry and biochemistry to determine the structures of an immense variety of molecules, including inorganic compounds, DNA and proteins X-ray diffraction is commonly carried out using single crystals of a material (Fersht, 2003)

5 1 2 Diffraction

Crystallographic methods now depend on the analysis of the diffraction patterns that emerge from a sample which is subjected to X-ray beams The beam is not always electromagnetic radiation, although X-rays are the most common choice Crystalline material has regularity in structure in 3-D form and it is this regularity that enables diffraction (http //www-structmed cirm ac uk) X-ray diffraction is an analytical technique which uses a beam of X-rays to probe repeating planes of atoms The reflection of X -rays of repeating planes of atoms creates a series of spots called a diffraction pattern The orientation of the X-ray and the crystal is of utmost importance As the angle between the X-ray beam and the crystal face is varied, the diffraction pattern will change as well By collecting data from a series of orientation angles (e g , 0°, 90°), the three dimensional atomic structure can be calculated In order to collect good X-ray diffraction data, chemists use only single crystals with minimum defects Modern methods, which employ automated diffractometers and high speed computers, have made diffraction studies a very powerful technique for determining the structure of crystalline solids A schematic of an X-ray diffractometer is shown in Figure 5 3 Once structural knowledge is known, function can then be resolved and at a later stage move onto designing specific therapeutic agents The Protein Data Bank (PDB) at http //www rcsb org is a freely accessible repository for the structures of proteins and other biological macromolecules

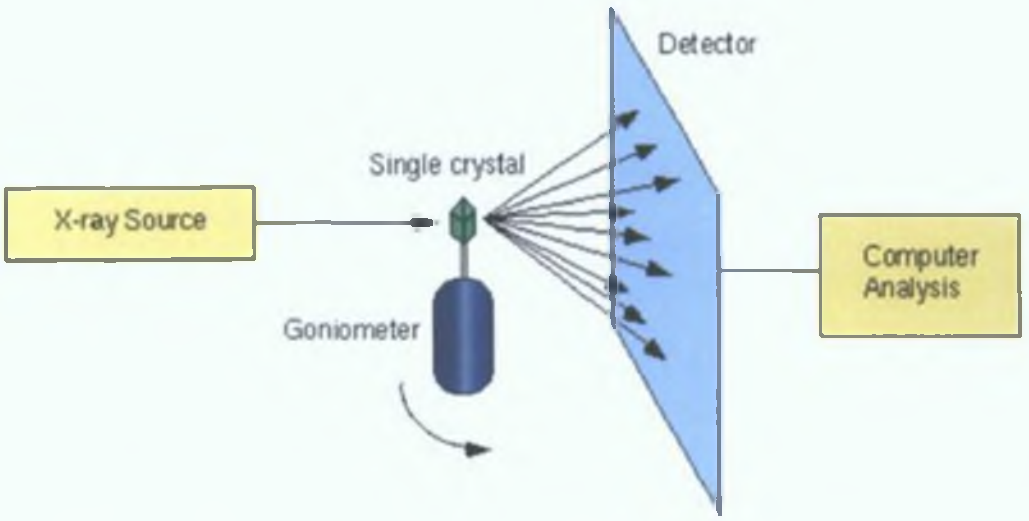

Figure 5.3 Schematic of X-Ray Diffractometer

The main components are an X-ray source, a goniometer (or crystal orientator), a detection system, and a computer control system. The X-ray source is a high-vacuum tube, and the X-ray beam passes out of the tube through a thin window. A single crystal is generally mounted on the end of a glass fiber. This fiber is then attached to a metal pin which is secured to the goniometer head. The goniometer precisely orients the sample in the X-ray beam. As the X-rays pass through the crystal, the detector collects information to generate a diffraction pattern. Finally, the computer control system processes the information from the detector, and the structure of the crystal is solved (http://www.chem.wisc.edu).

5.1.3 Protein Crystallography

More than a century ago, haemoglobin from the blood of various invertebrates and vertebrates were the first proteins to be crystallised. This was followed by the crystallisation of hen egg albumin and a series of plant proteins (Greige, *et al.*, 1995).

Proteins, like many molecules, can be prompted to form crystals when placed in the appropriate conditions as described above. The goal is usually to produce a well-ordered crystal that is lacking in contaminants and large enough to provide a diffraction pattern when hit with X-ray (http://www-structmed.cirm.ac.uk). This diffraction pattern can then be analyzed to discern the protein's three-dimensional structure.

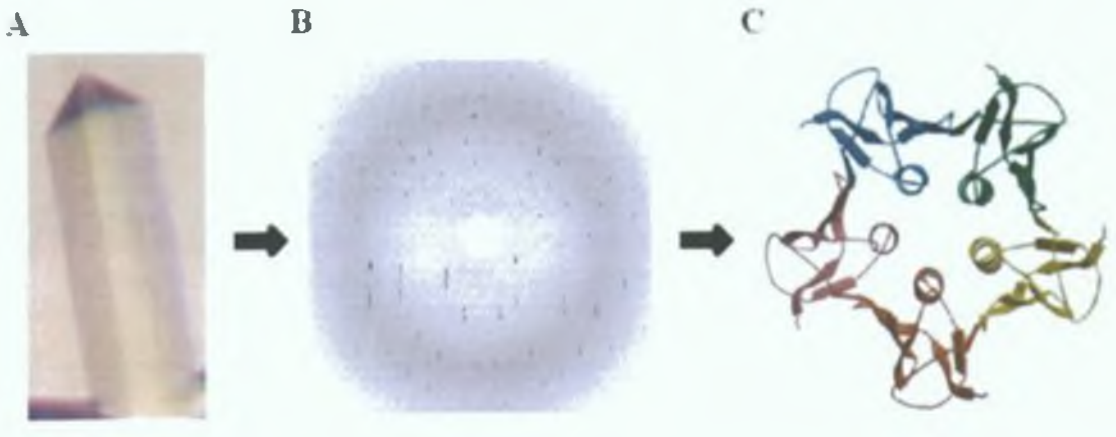

Figure 5.4 Overview of Protein Crystallography
The three key stages of protein crystallography are shown. **A**: Formation of single crystal; **B**: Protein diffraction pattern, **C**:3-D structure of protein (http://www-structmed.cimm.ac.uk).

Protein crystallisation is inherently difficult because of the fragile nature of protein crystals. Unlike most small molecule crystals which typically grow well and are hard, can be easily manipulated, the crystals of protein molecules are for the most part relatively brittle, soft and comprise on average 50% solvent although this may vary from system with extremes between 25 - 90% depending on the particular macromolecule and as a result require careful handling. The large size of the protein molecules and their water of hydration and solvation make them much more sensitive to distorting forces. The overall aim of protein crystallisation is to obtain a 3-D structure of protein of interest. 3-D structures allow one to understand biological processes at the most basic level: which molecules interact, how they interact and how enzymes catalyse reactions.

5.1.4 Protein Crystallisation Overview

Crystallization of biological macromolecules has often been considered unpredictable but follows the same principles as the crystallisation of small molecules. It is a similarly multi-parametric process. Differences arise from conventional crystal growth due to biochemical properties of proteins. In general, the crystallisation trials need more protein sample than conventional biochemical analyses as milligrams of sample are required. Highly purified (~99% purity) proteins are essential for protein crystallisation. Conventional chromatography in the past necessitated the use of up to a 5000-fold purification step unlike the typical 20 to 50 fold purification step used today. Expression systems now can facilitate the 5 – 10 mg sample needed to commence the crystallisation trials. The characterisation of the protein and assessment of the sample homogeneity is of utmost importance. Typically SDS-PAGE or isoelectric focusing are

commonly used for the determination of purity and homogeneity of the sample. The challenge of protein crystallography involves appropriate selection of experimental parameters. Manipulation of numerous variables is then carried out. Variables include protein sample concentration, crystallisation method, buffer concentration, temperature, pH and drop volume. Typically, concentrated solutions of protein are mixed with various solutions, which usually consist of a buffer to control the pH of the experiment, a precipitating agent to induce supersaturation and other salts or additives, such as detergents or co-factors. The process of crystallising macromolecules can be divided into three discrete stages. These are (1) screening for useful crystallization conditions; (2) optimisation of one or more initial conditions to produce single crystals suitable for X-ray diffraction analysis and (3) reproducible production of single crystals for X-ray data collection. Typically protein crystallographers can screen hundreds or thousands of conditions before a suitable condition is found that leads to a crystal of suitable quality.

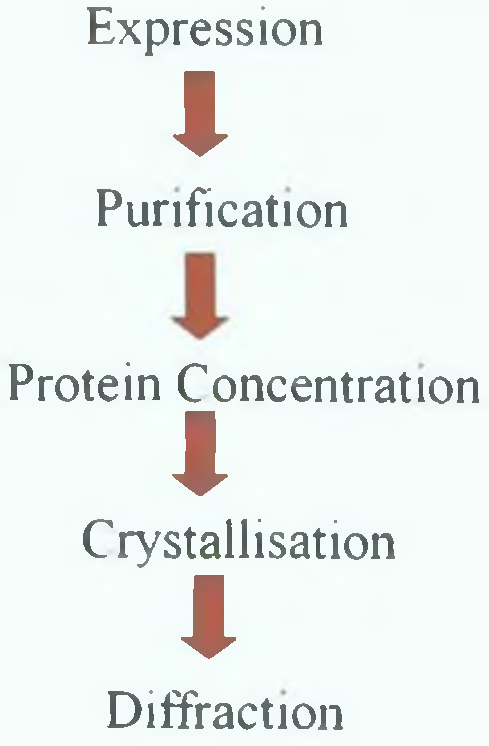

Figure 5.5 Processes Involved in Protein Crystallisation
Schematic diagram highlighting the various processes involved in protein crystallisation.

5.1.5 Protein Crystallisation Applications

The crystallisation of proteins currently has three major applications: (1) structural biology and drug design, (2) bioseparations, and (3) controlled drug delivery (http://www.che.utoledo.edu). In the first application, the protein crystals are used with

the techniques of protein crystallography to ascertain the three-dimensional structure of the molecule Obtaining high quality diffractive crystals is the bottleneck in protein structure determination This structure is indispensable for correctly determining the often-complex biological functions of these macromolecules The design of drugs is related to this, and involves designing a molecule that can exactly fit into a binding site of a macromolecule and block its function in the disease pathway Producing better quality crystals will result in more accurate 3D protein structures, which in turn means its biological function can be known more precisely, also resulting in improved drug design

Bioseparations refers to the downstream processing of the products of fermentation Typically the desired product of the fermentation process is a protein, which then needs to be separated from the biomass Crystallisation is one of the commonly employed techniques for separating the protein A majority of small molecular weight drugs are produced in crystalline form because of the high storage stability, purity, and reproducibility of the drug properties (Hanock and Zografi, 1997) There are hundreds of macromolecular therapeutic agents used in clinical trials or approved as drugs However, only insulin is produced and administered in a crystalline form (Jen and Merkle, 2001) The entire procedure is performed using yeast cells as a growth medium, as they secrete an almost complete human insulin molecule with perfect three dimensional structure This minimises the need for complex and costly purification procedures (http //www medicinenet com) According to Margolin and Navia (2000) the crystallization of macromolecular pharmaceuticals can offer significant advantages, such as a) protein purification by crystallization as mentioned above, b) high stability of the protein product compared with soluble forms, c) crystals are the most concentrated form of proteins, which is beneficial for storage, formulation, and for drugs that are needed in high doses *(e g ,* antibiotics)

The latest application of protein crystals is as a means of achieving controlled drug delivery Most drugs are cleared by the body rapidly following administration, making it difficult to achieve a constant desired level over a period of time When the drug is a protein (such as insulin), administering the drug in the crystalline form shows promise of achieving such controlled delivery and clinical trials are already underway to test it The challenge here is to produce crystals of relatively uniform sizes so that the dosage can be prescribed correctly

5.1.6 Problems with Protein Crystallisation

Many problems can be encountered during the crystallisation process. Protein storage is very important and processes such as oxidation, deamination, proteolysis and aggregation can lead to a general decrease in the quality of the overall protein sample. Storage under N_2 and at low temperature (-20°C or lower) can assist the long term storage. Proteins behave best at the pH and ionic strength of their host conditions and this usually means pH slightly above neutral and intermediate ionic strength. These may not be ideal for crystallization but dialysis can be performed prior to the crystallization trials. Anti-microbial agents such as NaN_3 can be used or filtration using 0.22 μm filters to stop the proliferation of microbes which can easily degrade the protein under study. Low temperature is advantageous as it helps stabilise the protein and also inhibit microbial growth. Freezing samples should only arise once as repeated freeze and thaw cycles are detrimental, but glycerol can help in the process.

Vibration can cause excess nucleation, leading to the formation of large numbers of low quality crystals. Protein to protein interactions are needed for nucleation, if this doesn't happen crystallisation will never occur. A number of factors can be responsible for the inability of protein to form proper contacts such as glycosylation, proteolytic degradation, aggregation, interference from N- or C-terminals and oxidation of cysteine residues (http://www.hamptonresearch.com).

Macromolecule crystals are much more sensitive to post-growth treatment, and this provides additional obstacles to structure determinations. For example, many proteins are very sensitive to radiation used in X-ray crystallography, which is an essential tool in the structure determination of proteins. In some cases the crystal sensitivity is unmanageable and the diffraction quality of crystals deteriorates rapidly and as a result can severely limit the amount of data that can be obtained from a single crystal. Quiocho and Richards initially described the concept of cross-linked protein crystals in 1964. They stabilized carboxypeptidase A crystals by glutaraldehyde treatment for X-ray structure analysis. There are only minor changes in the diffraction pattern of crosslinked protein crystals compared with that of the native crystals (Quiocho and Richards, 1964; Fitzpatrick *et al.*,1993; Lusty, 1999). Crosslinked crystals render it possible to study the protein structure in organic solvents, which cannot be done with native crystals (Fitzpatrick *et al.*, 1993). Lusty (1999) described the use of crystal cross-linking together with cryocrystallography, which is a common way to increase the stability of crystals towards the radiation. In cryocrystallography, crystals are treated

with a cryoprotectant (e g , sugar solutions, ethylene glycol, PEG, glycerol) and cooled rapidly to cryogenic temperatures (*e g* , with nitrogen gas around 100 K) However, the crystals often suffer damage on cooling Lusty proved that glutaraldehyde cross-linking protected the crystals from the damage on cooling without any effect on the diffraction properties

5 2 Human PAP1 Crystallisation

There are major gaps in our understanding of protein functions, in particular of those involved in development and in neurological function These proteins are very often involved in neuronal functions and the diseases concerned are some of the most prevalent in mankind A non-exhaustive list includes cerebrovascular disease, Parkinsons, epilepsy, schizophrenia, depression, manic depression, Alzheimers Drugs for neurological disorders are rare, the drug regimes are difficult to optimise and the commitment to follow a drug regime often for years and often with major side effects is a next to impossible in many cases New improved drugs are required and hence structure determinations of *molecules of the brain* are major scientific as well as medical challenges over the next few decades

Crystallography allows scientists, through the study of protein crystals, to determine the 3D molecular structures of proteins Such molecules will help shed light on some of the deepest mysteries of humanity, including memory, cognition and desire These structures will provide opportunities for treating those suffering from neurodegenerative disease due to ageing, genetic disposition, allergies, infection, traumas and combinations thereof Such CNS protein structures are one of the major challenges of biomacromolecular crystallography into the 21st century With an improved understanding of the molecular structures and interactions of proteins, drug designers may be able to develop new drug treatments that target specific human, diseases

At present, there is a varied view as to the exact physiological function of PAP1 and numerous researchers have suggested possible roles for PAP1 as discussed in Section 1 3 5 To date, the 3D structure of human or other eukaryotic PAP1 enzymes have not been solved The 3D structures of four prokaryotic PAP1 enzymes have been solved using X-ray crystallography as discussed in Section 1 3 11 With the availability of highly purified *Hsa*PAP1, an attempt to crystallise recombinant human PAP1 and obtain 3D structure was the main objective of this work

5 2 1 Human PAP1 Crystallisation Study Carried Out in DCU

5 2 1 1 PAP1 Expression and Purification

r*Hsa*PAP1$_{6H}$ was expressed in *E coli* XL10-Gold as outlined in Section 2 12 Cells were harvested from a 1 L expression culture and re-suspended in 100 ml 50 mM potassium phosphate buffer, pH 8 0 A purification scheme using nickel affinity chromatography was optimised for this study due to the requirement of highly purified protein sample for crystallisation (see Section 2 13 2) Seven (20 ml) washes were employed followed by three (5 ml) elutions as shown below in Figure 5 6

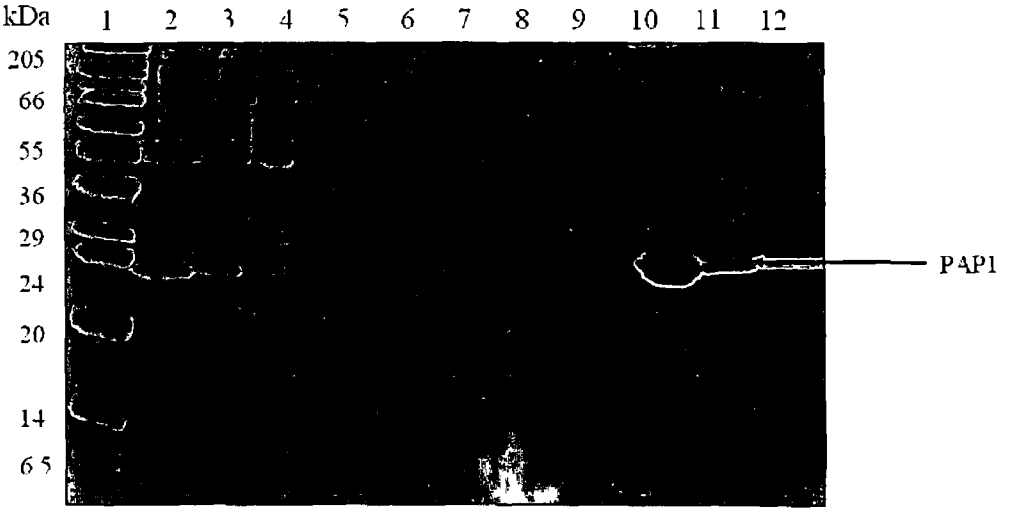

Figure 5 6 SDS-PAGE of Purified Human PAP1
Lane 1, protein molecular marker, lane 2, crude lysate, lane 3, flow through, lane 4, wash 1, lane 5, wash 2, lane 6, wash 3, lane 7, wash 4, lane 8, wash 5, lane 9, wash 6, lane 10, elution 1, lane 11, elution 2, lane 12, elution 3 The relevant sizes (kDa) of the protein marker are indicated

was dialysed against 3L of ultra pure water overnight at 4°C and concentrated using rotor vacuum until desired protein concentration was achieved Protein concentration was monitored using coomassie assay (see Section 2 14 2) Screening of crystallisation conditions for r*Hsa*PAP1$_{6H}$ was conducted by employing hanging drop vapor diffusion experiments Hampton Research kits utilised for screening included Crystal Screen 1 and 2 (see Table 2 8 and 2 9) Various temperatures used were 4, 20, 37 and 60°C and protein concentrations included 1 5, 3, 5, 6 5, 7 and 12 mg Crystal trays were stored in areas free from disturbance to avoid vibrations which could induce excess nucleation and result in formation of poor quality crystals

5.2.1.2 Crystals Obtained From DCU Study

Once crystallisation trials were set up, samples were monitored daily for the first week as majority of crystal nucleation and growth occurred during this time frame. Crystals were examined using a ZEISS-AXIOKOP microscope using 10x magnification in all cases. Protein crystal images obtained from this study are shown in Figures 5.6 – 5.9. All important information was recorded and tabulated (for example see Table 5.1) such as date, buffer, sample concentration, temperature, method utilised and status of each sample. For all data recorded during this crystallisation study see Appendix E.

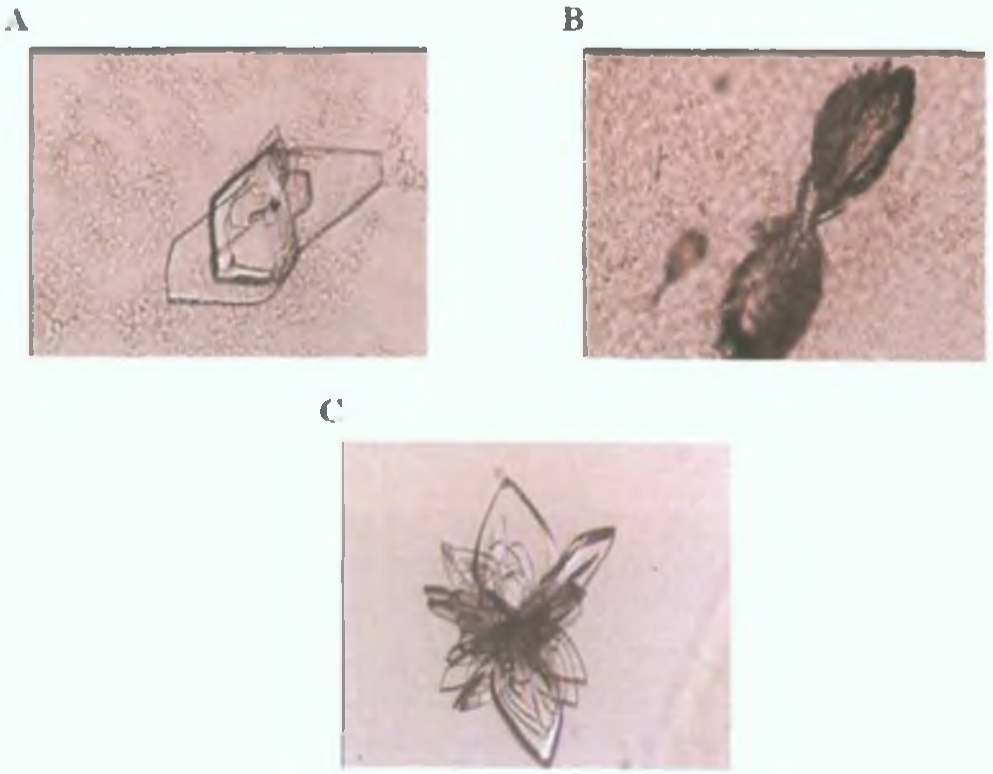

Figure 5.6 Images of Crystals Obtained for Human PAP1 Using a Protein Concentration of 1.5 mg.

All samples were set up at 24°C using Screen 1 and images were recorded using a 10x magnification. For components of Screen 1 see Table 2.8. Image A: Reagent 1, 172 hrs. Image B: Reagent 24, 172 hrs. Image C: Reagent 45, 360 hrs.

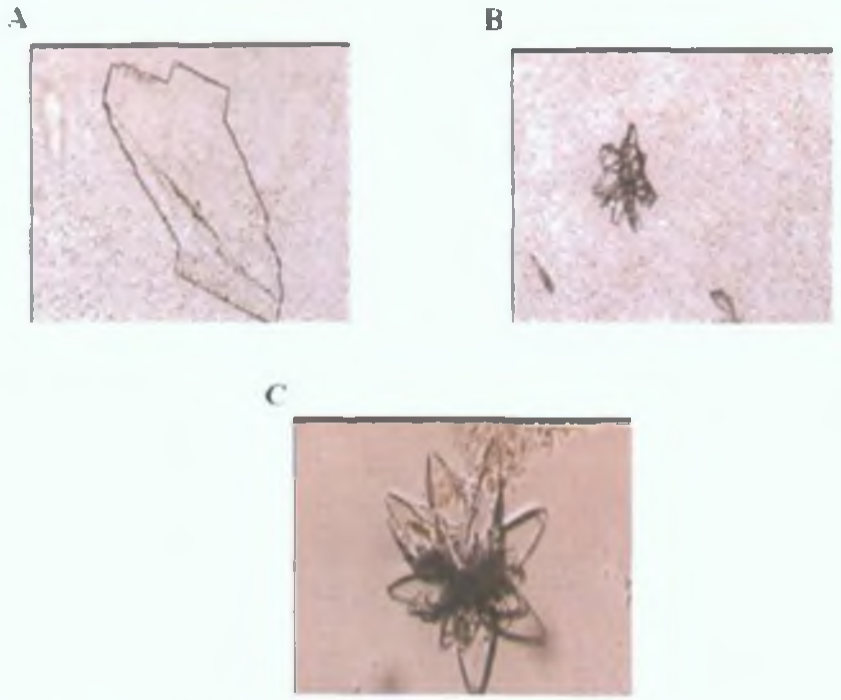

Figure 5.7 Images of Crystals Obtained for Human PAP1 Using a Protein Concentration of 3 mg.

All samples were set up at 24°C using Screen 1 and images were recorded using a 10x magnification. For components of Screen 1 see Table 2.8. Image A: Reagent 1, 144 hrs, Image B: Reagent 24, 72 hrs, Image C: Reagent 45, 240 hrs.

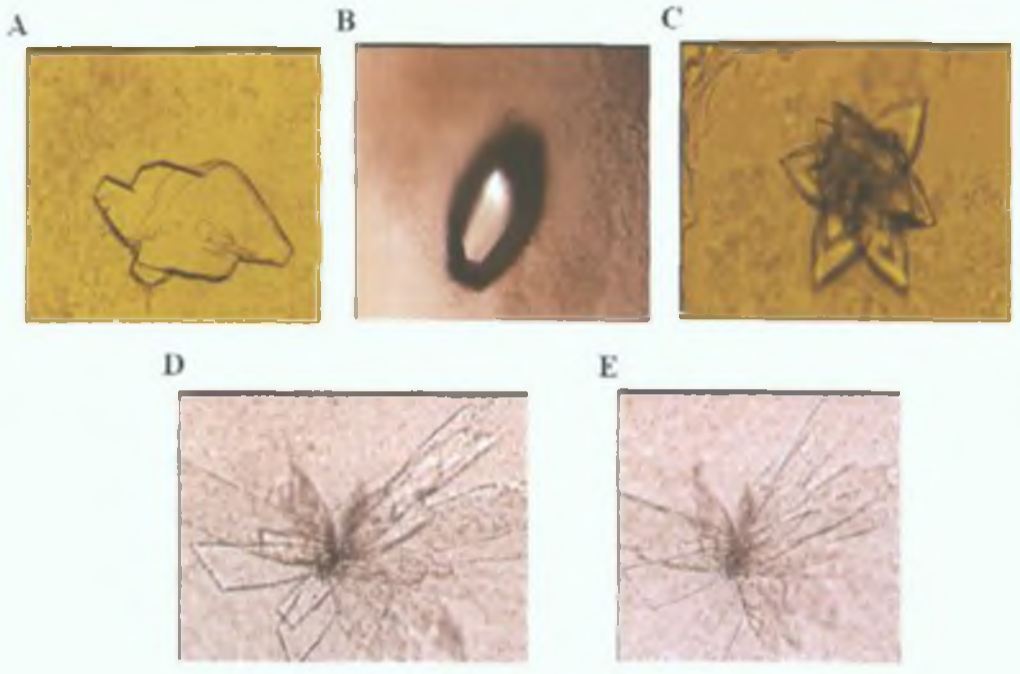

Figure 5.8 Images of Crystals Obtained for Human PAP1 Using a Protein Concentration of 5 mg.

All samples were set up at 24°C and images were recorded using a 10x magnification. For components of Screen 1 and 2 see Tables 2.8 and 2.9. Image A: Screen 1, Reagent 1, 42 hrs, Image B: Screen 1, Reagent 18, 480 hrs, Image C: Screen 1, Reagent 45, 66 hrs, Image D: Screen 2, Reagent 27, 72 hrs, Image E: Screen 2, Reagent 27, 144 hrs.

A

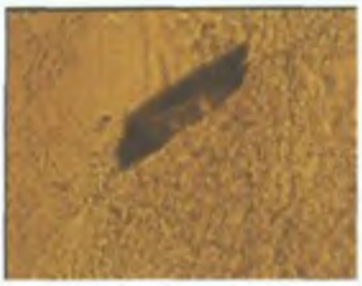

B

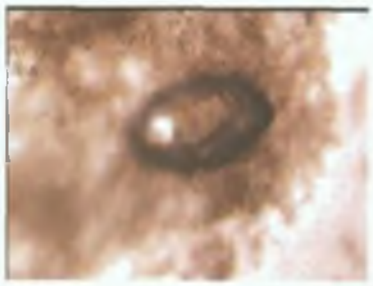

Figure 5.9 Images of Crystals Obtained for Human PAP1 Using a Protein Concentration of 12 mg.

All samples were set up at 24°C using Screen 1 and images were recorded using a 10x magnification. For components of Screen 1 see Table 2.8. Image A: Reagent 1, 48 hrs. Image B: Reagent 18, 144 hrs.

Table 5.1 Data Collection For Human PAP1 Crystallisation Study.
Crystal Screen 1 was utilised (see Table 2.8) and a PAP1 protein concentration of 5mg/ml was used. For further crystallisation data reports see Appendix E.

Stage 1 - Run 1				
Set up on the 16th of March 2004				
Sample	PAP 1 - 5mg/ml	1 Clear Drop		6 Needles 1D
Buffer	Screen 1	2 Mix of ppt		7 Plates 1D
Reservoir Volume	1ml	3 Light Precipitate		8 Stars
Drop	2ml sample + 2ul buffer	4 Medium - Heavy Precipitate		9 Rod >0.2 mm
Temperature	4+4 C	5 Spherulites		10 No Change
		Data (42 hrs)	Data (480hrs)	Data (530hrs)
HANGING DROP METHOD USED				
1	30% MPD, 0.1 M Na Acetate pH 4.6, 0.02 M Calcium Chloride	6	10	10
2	0.4 M K, Na Tartrate	3	10	10
3	0.4 M Ammonium Phosphate	3	10	10
4	2.0 M Ammonium Sulfate, 0.1 M Tris HCl pH 8.5	3	10	10
5	30% MPD, 0.1 M Na Hepes pH 7.5, 0.2 M Sodium Citrate	6	10	10
6	30% PEG 4000, 0.1 M Tris HCl pH 8.5, 0.2 M Magnesium Chloride	6	10	10
7	1.4 M Sodium Acetate, 0.1 M Na Cacodylate pH 6.5	6	10	10
8	30% Iso-Propanol, 0.1 M Na Cacodylate pH 6.5, 0.2 M Sodium Citrate	3	10	10
9	30% PEG 4000, 0.1 M Na Citrate pH 4.6, 0.2 M Ammonium Acetate	6	10	10
10	30% PEG 4000, 0.1 M Na Acetate pH 4.6, 0.2 M Ammonium Acetate	3	10	10
11	1.0 M Ammonium Phosphate, 0.1 M Na Citrate pH 5.6	6	10	10
12	30% Iso-Propanol, 0.1 M Na Hepes pH 7.5, 0.2 M Magnesium Chloride	6	10	10
13	30% PEG 400, 0.1 M Tris HCl pH 8.5, 0.2 M Sodium Citrate	3	10	10
14	30% PEG 400, 0.1 M Na Hepes pH 7.5, 0.2 M Calcium Chloride	6	10	10
15	30% PEG 8000, 0.1 M Na Cacodylate pH 6.5, 0.2 M Ammonium Sulfate	6	10	10
16	1.6 M Lithium Sulfate, 0.1 M Na Hepes pH 7.5	3	10	10
17	30% PEG 4000, 0.1 M Tris HCl pH 8.5, 0.2 M Lithium Sulfate	3	10	10
18	30% PEG 8000, 0.1 M Na Cacodylate pH 6.5, 0.2 M Magnesium Acetate	Something	Small Crystal, smooth edges, dark shadow underneath	10
19	30% Iso-Propanol, 0.1 M Tris HCl pH 8.5, 0.2 M Ammonium Acetate	3	10	10
20	25% PEG 4000, 0.1 M Na Acetate pH 4.6, 0.2 M Ammonium Sulfate	6	10	10
21	30% MPD, 0.1 M Na Cacodylate pH 6.5, 0.2 M Magnesium Acetate	dried up	10	10
22	30% PEG 4000, 0.1 M Tris HCl pH 8.5, 0.2 M Sodium Acetate	3	10	10
23	30% PEG 400, 0.1 M Na Hepes pH 7.5, 0.2 M Magnesium Chloride	3	10	10
24	30% Iso-Propanol, 0.1 M Na Acetate pH 4.6, 0.2 M Calcium Chloride	6	10	10
25	1.0 M Sodium Acetate, 0.1 M Imidazole pH 6.5	6	10	10
26	30% MPD, 0.1 M Na Citrate pH 5.6, 0.2 M Ammonium Acetate	3	10	10
27	30% Iso-Propanol, 0.1 M Na Hepes pH 7.5, 0.2 M Sodium Citrate	3	10	10
28	30% PEG 8000, 0.1 M Na Cacodylate pH 6.5, 0.2 M Sodium Acetate	3	10	Something new
29	0.8 M K, Na Tartrate, 0.1 M Na Hepes pH 7.5	3	10	10
30	30% PEG 8000, 0.2 M Ammonium Sulfate	3	10	10
31	30% PEG 4000, 0.2 M Ammonium Sulfate	3	10	10
32	2.0 M Ammonium Sulfate	3	10	10
33	4.0 M Sodium Formate	3	10	10
34	2.0 M Sodium Formate, 0.1 M Na Acetate pH 4.6	3	10	10
35	1.0 M Na, K Phosphate, 0.1 M Na Hepes pH 7.5	3	10	10
36	8% PEG 8000, 0.1 M Tris HCl pH 8.5	1	10	10
37	8% PEG 4000, 0.1 M Na Acetate pH 4.6	6	10	10
38	1.4 M Sodium Citrate, 0.1 M Na Hepes pH 7.5	3	10	10
39	2% PEG 400, 0.1 M Na Hepes pH 7.5, 2.0 M Ammonium Sulfate	3	10	10
40	30% Iso-Propanol, 0.1 M Na Citrate pH 5.6, 20% PEG 4000	6	10	10
41	10% Iso-Propanol, 0.1 M Na Hepes pH 7.5, 20% PEG 4000	3	10	10
42	20% PEG 8000, 0.05 M Potassium Phosphate	3	10	10
43	20% PEG 1600	3	10	10
44	0.2 M Magnesium Formate	6	10	10
45	18% PEG 8000, 0.1 M Na Cacodylate pH 6.5, 0.2 M Zinc Acetate	6	10	10
46	18% PEG 8000, 0.1 M Na Cacodylate pH 6.5, 0.2 M Calcium Acetate	6	10	10
47	2.0 M Ammonium Sulfate, 0.1 M Sodium Acetate pH 4.6	3	10	10
48	2.0 M Ammonium Phosphate, 0.1 M Tris HCl pH 8.5	3	10	10

Comments: No change was observed after 505 hrs, all controls remained clear.
No change was observed after 141 Hrs (13 May 04), and all controls remained clear
Results for 49 + 50 can be seen in run 2a

5 2 2 PAP1 Crystallisation Study at the University of Toronto, Canada.

As part of this research, a crystallisation study was carried out in the the University of Toronto, Canada (UTC) Wild type PAP1 and a range of PAP1 mutants listed in Table 5 2 were examined With access to a sophisticated diffractometer (Rigaku), it was possible to analyse promising crystals and progress one step further than previous work carried out in DCU

Table 5 2 List of Enzymes Which Were Subjected To Crystallisation Trials at the University of Toronto, Canada

Final protein concentration (mg) of each sample is also tabulated

Plasmid	Enzyme	Final Protein Concentration (mg)
pRV5	*HsaPAP1*$_{6H}$	18
pRV5_C149mW	*HsaPAP1_C149mW*$_{6H}$	12
pRV5_N98mQ	*HsaPAP1_N98mQ*$_{6H}$	29
pRV5_N98mV	*HsaPAP1_N98mV*$_{6H}$	39
pRV5_F16mY	*HsaPAP1_F16mY*$_{6H}$	9
pRV5_Y147mF	*HsaPAP1_Y147mF*$_{6H}$	20
pRV5_SID115mAYF	*HsaPAP1_SID115mAYF*$_{6H}$	27

5 2 2 1 PAP1 Protein Expression and Purification (UTC)

Wild type human PAP1 and a range of PAP1 mutants were expressed and purified by the methodology outlined in Sections 2 12 and 2 13 2 respectively Following overnight dialysis at 4°C in 3L ultrapure water, PAP1 protein samples were concentrated using Amicon Ultra centrifuge tubes from Millipore Concentrations ranged from 9 – 29 mg (see Table 5 2)

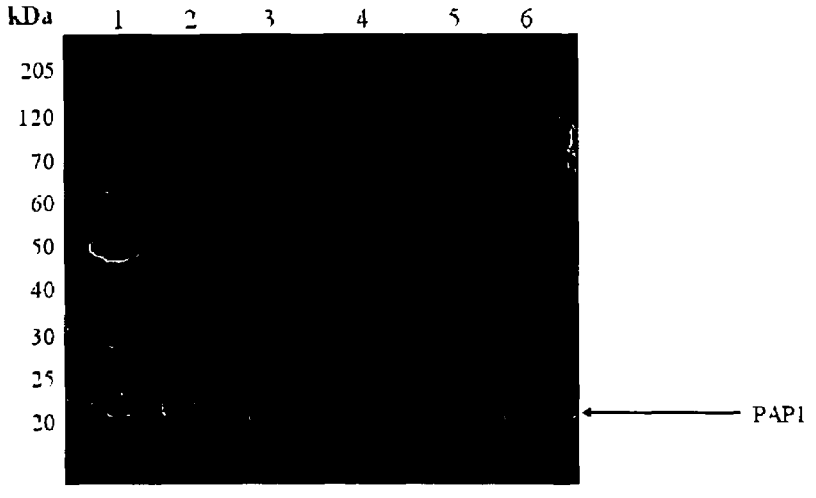

Figure 5 10 Purification of r*Hsa*PAP1$_{6H}$ Mutants for Crystallisation Study at the University of Toronto, Canada Lane 1, protein molecular marker, Lane 2, r*Hsa*PAP1$_{6H}$, Lane 3, r*Hsa*PAP1_C149mW$_{6H}$, Lane 4, r*Hsa*PAP1_N98mQ$_{6H}$, Lane5, r*Hsa*PAP1_F16mY$_{6H}$, Lane 6, r*Hsa*PAP1_Y147mF$_{6H}$ The relevant sizes (kDa) of the protein marker are indicated

5.2 2 2 Crystals Obtained From Study at the University of Toronto, Canada

Crystallisation kits used included Crystal Screen 1 and 2 and CryoScreen 1 and 2 (see Tables 2 8 – 2 11) All plates were set up at room temperature according to methodology in Section 2 19 2 As with DCU study samples were monitored, images and data were recorded and promising crystals were selected for latter diffraction

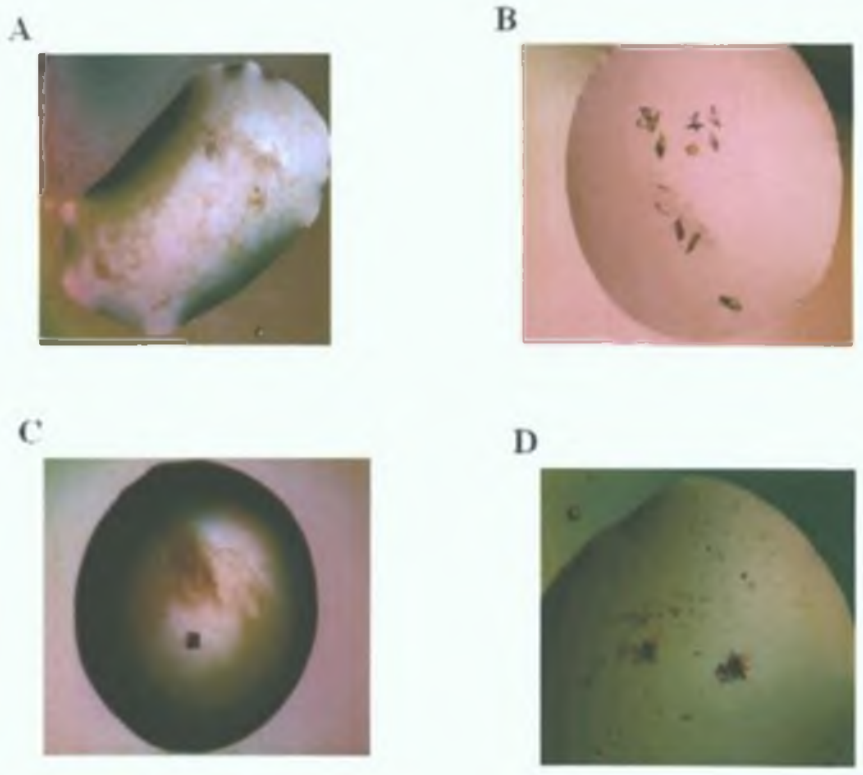

Figure 5.11 Images of Crystals Obtained for Wild Type Human PAP1 in UTC
All samples were set up at 24°C using Screen 1 and images were recorded using a 10x magnification. For components of Screen 1 see Table 2.8. Image A: Reagent 1, 50 hrs; Image B: Reagent 24, 78 hrs; Image C: Reagent 45, 68 hrs; Image D: Reagent 45, 100 hrs.

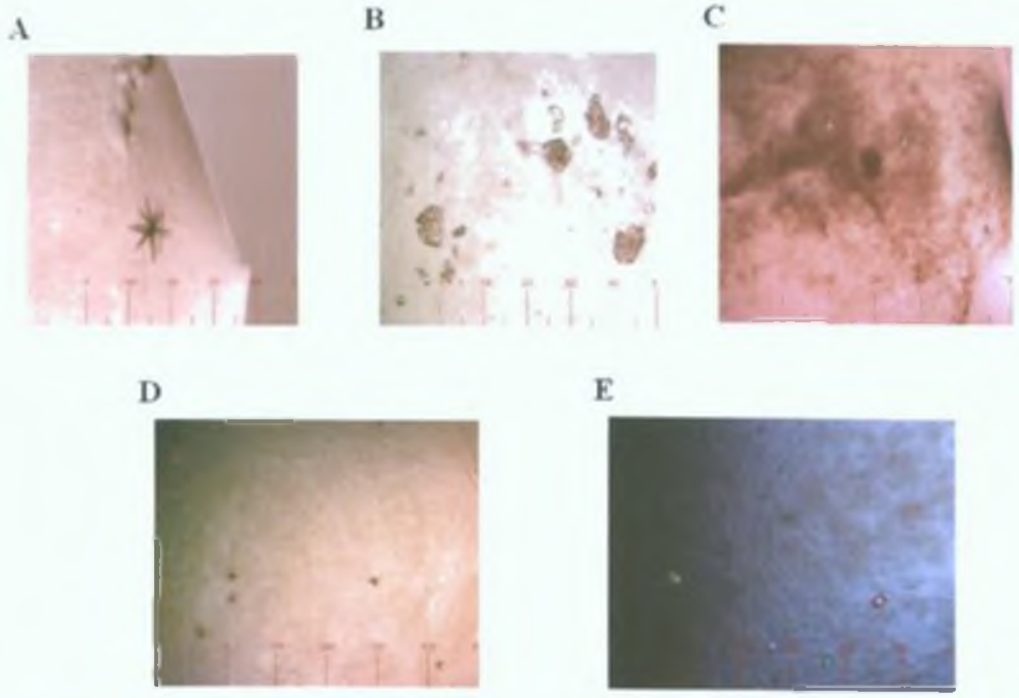

Figure 5.12 Images of Crystals Obtained for Mutant Forms of Human PAP1 in UTC. All samples were set up at 24°C and images were recorded using a 10x magnification. For components of Screen 1 and 2 see Table 2.9. Image A: r*Hsa*PAP1_C149mW_{6H}, Screen 1, Reagent 48, 48 hrs; Image B: r*Hsa*PAP1_C149mW_{6H}, Reagent 48, 78 hrs; Image C: r*Hsa*PAP1_Y147mF_{6H}, Screen 2,

Reagent 3, 68 hrs; Image D: r*Hsa*PAP1_Y147mF$_{6H}$, Screen 1, Reagent 3, 48 hrs; Image E: r*Hsa*PAP1_SID115AYF$_{6H}$, Screen 2, Reagent 48.

5.3 Diffraction Of Human PAP1 Crystals

A range of crystals were selected for diffraction analysis depending on size and morphology. Crystals which were flat edged and relatively large in size were chosen. These crystals were mounted using cryo-loops as described in Section 2.19.3, were exposed to X-rays and the following diffraction patterns were produced as a result.

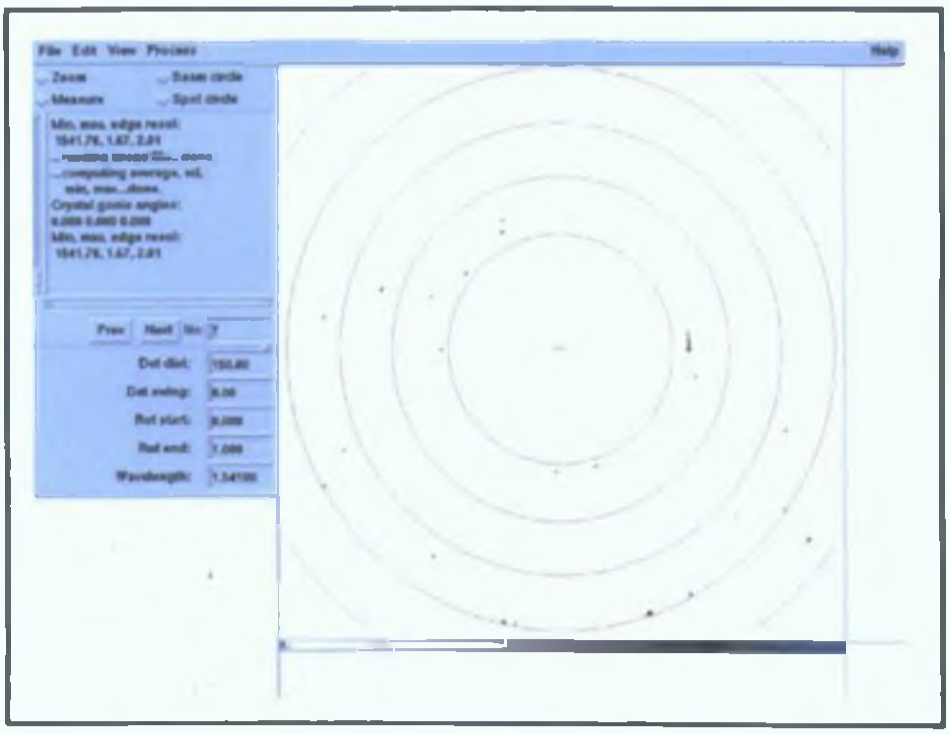

Figure 5.13 Wild Type PAP1 Diffraction Pattern Using 90° Angle
These crystals were obtained using reagent 45 from screen 1. An image of this crystal type is shown in Figure 5.11C.

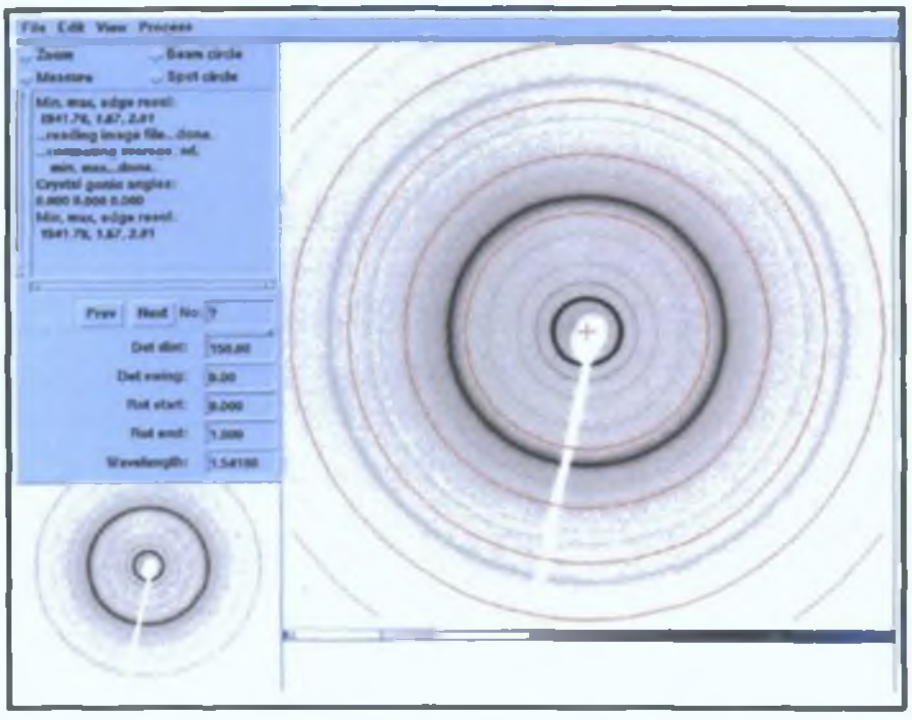

Figure 5.14 Wild Type PAP1 Diffraction Pattern Using 0° Angle
These crystals were obtained using reagent 24 from screen 1. An image of this crystal type is shown in Figure 5.11D.

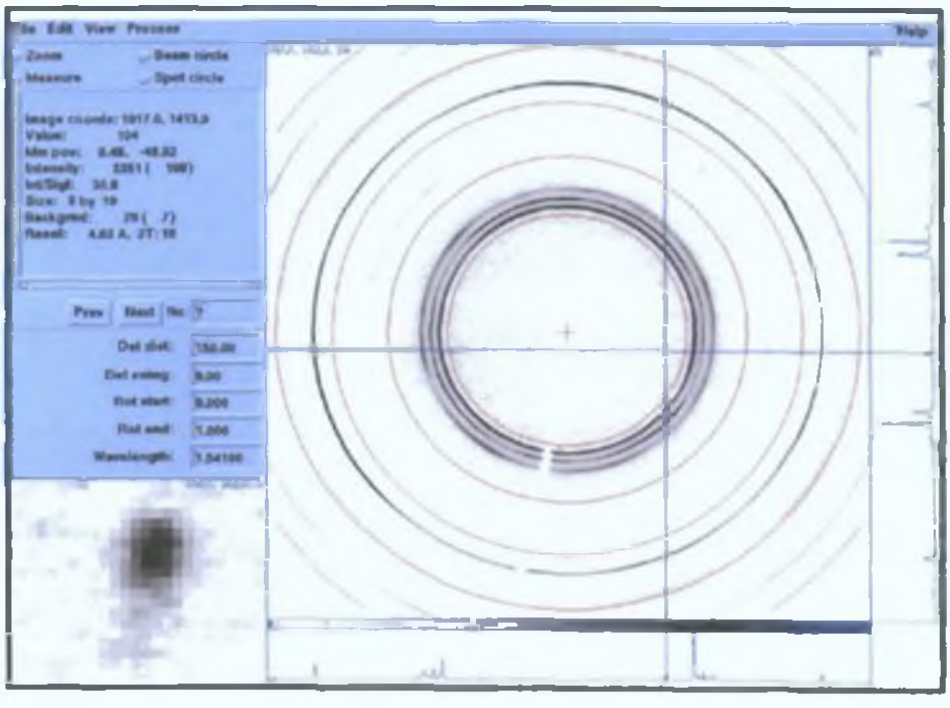

Figure 5.15 Wild Type PAP1 Diffraction Pattern Using 90° Angle
These crystals were obtained using reagent 24 from screen 1.An image of this crystal type is shown in Figure 5.11D.

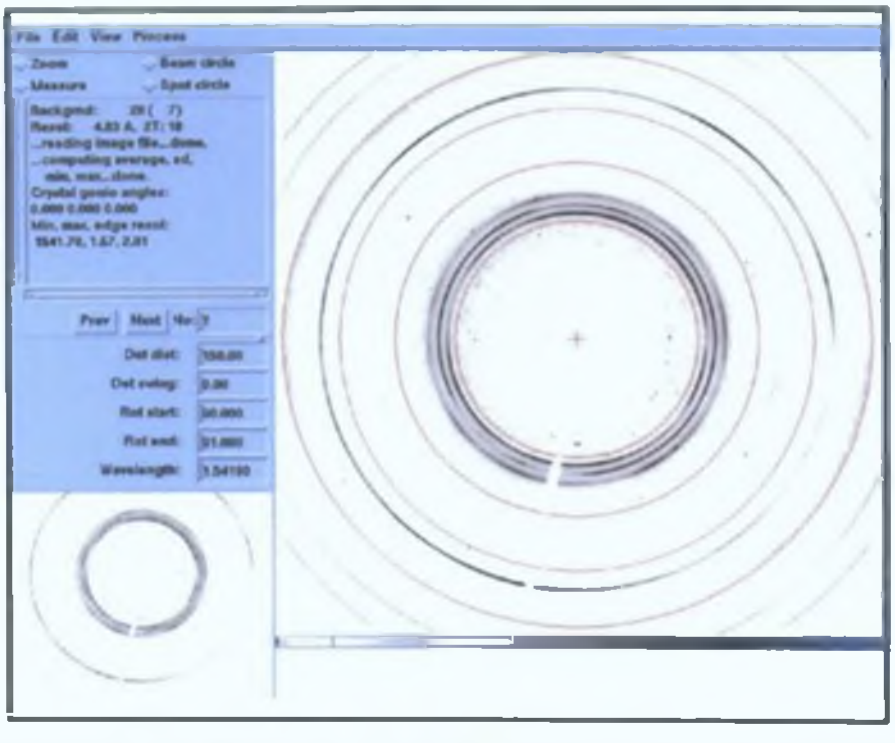

Figure 5.16 r*Hsa*PAP1_C149mW$_{6H}$ PAP1 Diffraction Pattern using a 90° Angle
These crystals were obtained using reagent 45 from screen 1. An image of this crystal type is shown in Figure 5.12A.

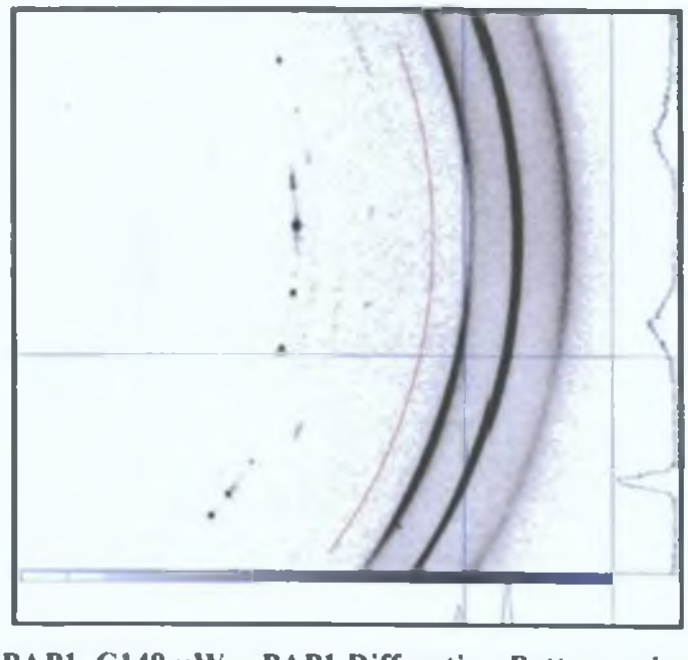

Figure 5.17 r*Hsa*PAP1_C149mW$_{6H}$ PAP1 Diffraction Pattern using a 90° Angle
This image was obtained by zooming in on the above Figure. These crystals were obtained using reagent 45 from screen 1. An image of this crystal type is shown in Figure 5.12A.

5.4 Discussion

Crystallisation of human PAP1 began with the optimisation of a purification scheme which could produce a highly purified sample of PAP1 protein. Figure 5.6 displays a prominent purified human PAP1 band in lane 10. Presence of a contaminant band is also visible at the 55 kDa region. Previous experiments carried out have indicated that presence of this band is strain dependent (data not shown). This band only appeared when PAP1 expression was performed using *E.coli* XL10-Gold, however did not appear when DH5α or BL21 cells were utilised. However, due to reduced PAP1 expression levels in the aforementioned *E.coli* strains, XL10-Gold was used throughout this work.

Once a purified PAP1 sample was obtained it was subsequently subjected to dialysis overnight to remove salts. A major problem at this stage was protein precipitating out of solution due to prolonged dialysis. After concentrating human PAP1 protein to the desired concentration crystallisation trials were set up as described in Section 2.19.2.

Various crystallisation conditions including reagent, temperature, protein concentration, drop volume, reservoir volume and pH were optimised. The hanging drop method was used throughout. This diffusion technique is the most popular method for the crystallisation of macromolecules. Typically the drop contains a lower reagent concentration than the reservoir. To achieve equilibrium, water vapour leaves the drop and eventually ends up in the reservoir. As the water leaves the drop, the sample undergoes an increase in supersaturation. Equilibration is reached when the reagent concentration in the drop is approximately the same as that in the reservoir.

A range of differing crystal types were obtained from this study (see Figure 5.6 – 5.9). Best quality crystals were produced at room temperature and using a PAP1 protein concentration of 5 mg. The most promising reagents which produced best quality crystals were 1, 18 and 45, all of which were part of Crystal Screen 1 (see Table 2.8). Flat slate-like and oval-shaped crystals were obtained using Reagent 1 (see Figures 5.8A) and Reagent 18 (see Figure 5.8B), respectively. Reagent 45, composed of 0.2 M zinc acetate dehydrate, 0.1 M sodium cacodylate pH 6.5 and 18% w/v polyethylene glycol 8000 appeared to be the most promising reagent which produced multiple floral shaped crystals with flat edges (see Figure 5.8C). It was interesting to note that *Bam*PAP1, which displays most homology with *Hsa*PAP1 from the four prokaryotic PAP1 forms, was successfully crystallised using similar crystallisation conditions (see Section 1.3.11.1). Pentagonal shaped crystals were obtained for *Bam*PAP1 using a

buffer which was composed of 0 05 M sodium cacodylate/KH_2PO_4, 0 1 M magnesium acetate, pH 6 5 and 10% w/v polyethylene glycol 4000 Focusing on Reagent 45, an attempt was made to alter each of the three components of the reagent by producing laboratory based reagent variants However, this proved to be unsuccessful as dagger-like crystals appeared in the controls This study could not progress any further due to a lack of resources in DCU

Later it was agreed that purified PAP1 samples of various concentrations would be sent to Dr John Gallagher (on sabbatical leave) in the University of Toronto, Canada Access to a diffractometer in HSC (a major resource lacking in DCU) would verify whether we were producing salt or protein crystals However, problems were encountered during transportation with PAP1 protein precipitating out of solution This occurred in all PAP1 samples with protein concentrations greater than 1 5 mg

Permission was granted to visit the HSC, Toronto to carry out the work in full there Agar slants of recombinant wild type PAP1 along with PAP1 mutants listed in Table 5 2 were sent to Toronto Figure 5 10 shows purified preparation from each PAP1 sample Higher protein concentrations were achieved in the UTC than previous work carried out in DCU, with protein concentrations reaching as high as 29 mg Approximately, one thousand samples were set up using various PAP1 protein samples and crystallisation screens Crystal Screen 1 and 2 along with CryoScreen 1 and 2 (see Tables 2 8 – 2 11) were used for this work

Various crystal morphologies were obtained from this study Figure 5 11 displays crystal images obtained for human wild type PAP1, many of which were very similar to those obtained from DCU study Floral-like crystal from Figure 5 11C was subjected to X-ray diffraction (see Section 2 19 3) Diffraction pattern for this crystal clearly demonstrates that this sample is in fact salt (see Figure 5 13) Salt unit cells are much smaller than protein unit cells, as a result a well dispersed pattern of dots is displayed for salt while a more clustered pattern of dots is typically obtained from protein crystals Results have also shown that crystals from figure 5 11D are also salt The diffraction image in Figure 5 14 displays presence of heavy ice rinks and a small number of well dispersed dots are visible in Figure 5 15 at the 90° angle Ice rinks are due to the crystallisation of water which is present in the protein sample Crystals obtained for PAP1 mutants are highlighted in Figure 5 12 Some crystals were too small in size for diffraction analysis The only PAP1 mutant which was subjected to

diffraction was r*Hsa*PAP1_C149mW$_{6H}$ (see Figure 5 12A) and diffraction patterns in Figures 5 16 and 5 17 prove that these crystals are also salt

Following lengthy discussions with protein crystallisation experts in Canada, it was suggested that the C-terminal His-tag of PAP1 may be causing the improper crystallisation of PAP1 to occur Interference from His-tags can be responsible for the inability of protein to form proper protein to protein interactions which are essential for protein crystallisation It is also possible that post-translational modifications of the His-tag are occurring leading to an increase in size and charge of the human PAP1 protein It is interesting to note that all four prokaryotic forms of PAP1 (see Section 1 3 11) which were successfully crystallised were purified using conventional chromatography as none of which possess any form of His-tag As a result, a new strategy for human PAP1 crystallisation was developed for future human PAP1 crystallisation studies involving the use of an N-terminal His-tag and a new protein expression vector, pQE30-Xa (see Chapter 6 0)

CHAPTER 6.0

Summary & Recommendations

In this research thesis, the gene for bovine PAP1 was cloned into an *E.coli* expression system, enabling expression and purification of the recombinant enzyme. Biochemical and kinetic characterisation of the enzyme was undertaken. Residues of the catalytic triad were investigated using site-directed mutagenesis for residue substitution. K_i values were determined using various pyroglutamyl peptides. With the availability of recombinant human PAP1 in our research group, a comparative study was carried out using both bovine and human recombinant PAP1 which revealed some interesting and significant differences at the molecular, biochemical and kinetic levels (see Chapter 3.0).

Kinetic analysis was carried out on recombinant human PAP1 using a range of pyroglutamyl peptides. Residues of the catalytic triad were also investigated. A structure/function relationship was investigated by generating a series of active mutants using random mutagenesis. All mutants were characterised both biochemically and kinetically (see Chapter 4.0).

An attempt to crystallise human PAP1 was carried out utilising sparse matrix screening method. Crystallisation studies were conducted in both DCU, Ireland and in the University of Toronto, Canada (see Chapter 5.0).

Additional studies on both recombinant human and bovine PAP1 could provide a further insight and deeper understanding of these two enzymes.

It would be interesting to continue kinetic research for bovine and human PAP1 using pyroglutamyl peptides (see Sections 3.8 and 4.6, respectively). The findings of this work and from previous PAP1 research (Cummins and O'Connor, 1996), it appears that a hydrophilic residue is the preferred type at the P_2 position, however, the preferred choice at the P_3 position has yet to be determined. A new range of pyroglutamyl tripeptides such as pGlu-His-Ala and pGlu-His-Met need to be synthesised for this study.

Random mutagenesis of human PAP1 has highlighted some interesting residues, in particular, two methionine residues which were mutated to valine and threonine, respectively as discussed in Section 4.6. There are four methionine residues in the human PAP1 amino acid sequence at positions 1, 78, 122 and 192. An interesting study for this area would comprise of each methionine residue being substituted with an alanine residue, thereby retaining the hydrophobic, non-polar properties of methionine to explore the significance of each methionine residue in PAP1 protein expression. Following mutagenesis, all resultant mutants including wild type PAP1 should be

subjected to native-PAGE to check if they possess differing mobilities which could suggest that they are folded differently.

Although numerous attempts were made, crystallisation of human PAP1 proved to be unsuccessful as discussed in Section 5.4. It is believed that the C-terminal 6xHis tag of PAP1 is causing improper crystallisation to occur. Consequently, a new method has been proposed to crystallise human PAP1 lacking the His_6 tag using expression vector pQE30-Xa (see Figure 6.1).

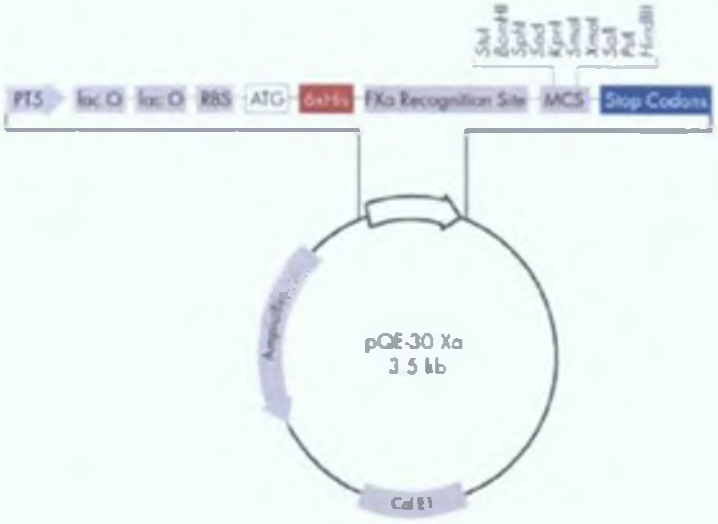

Figure 6.1 QE30-Xa Vector with N-terminal His-Tag
PT5: T5 promoter, **lac O**: lac operon, **RBS:** ribosomal binding site, **ATG:** start codon, **6xHis:** 6xHis tag sequence, **MSC:** multiple cloning site with restriction sites indicated, **Col E1**: Col E1 origin of replication, **Ampicillin:** ampicillin resistance gene, **Factor Xa Recognition Site:** factor Xa Protease recognition site (Qiagen, 2003).

The pQE30-Xa expression vector encodes a Factor-Xa Protease recognition site between the N-terminal His_6 tag sequence and the multiple cloning site. Factor Xa Protease recognises the amino acid sequence Ile-Glu-Gly-Arg and cleaves the peptide bond at the C-terminal of the arginine residue. If the human PAP1 gene is cloned blunt-ended at the 5' end using the *Stu*I restriction site of the vector, the subsequent Factor Xa cleavage of purified recombinant protein results in a PAP1 protein which is His-tag free (Qiagen, 2003). Human PAP1 crystallisation studies may prove to be more successful if this strategy is incorporated into the next PAP1 crystallisation study.

References

-A-

Abe, K , Fukada, K and Tokui, T (2004a) Marginal Involvement of Pyroglutamyl Aminopeptidase I in Metabolism of Thyrotropin-Releasing Hormone in Rat Brain *Biological & Pharmaceutical Bulletin* **27** 1197-1201

Abe, K , Saito, F , Yamada, M and Tokui, T (2004b) Pyroglutamyl Aminopeptidase I, as a Drug Metabolizing Enzyme, Recognises Xenobiotic Substrates Containing L-2-Oxothiazolidine-4-carboxylic Acid *Biological & Pharmaceutical Bulletin* **27** 113-116

Abe, K , Watanabe, N , Kosaka, T , Yamada, M , Tokui, T and Ikeda, T (2003) Hydrolysis of Synthetic Substrate, L-Pyroglutamyl p-Nitroanilide is Catalyzed Solely by Pyroglutamyl Aminopeptidase I in Rat Liver Cytosol *Biological & Pharmaceutical Bulletin* **26** 1528-1533

Albert, Z and Szewczuk, A (1972) Pyrrolidonyl Peptidase in Some Avian and Rodent Tissues Histochemical Localization and Biochemical Studies *ACTA Histochemica* **44** 98-105

Altschul, S F , Gish, W , Miller, W , Myers, E W and Lipman, D J (1990) Basic Local Alignment Search Tool *Journal of Molecular Biology* **215** 403-410

Aoyagi, T , Hatsu, M , Imada, C , Naganawa, H , Okami, Y and Takeuchi, T (1992b) Pyrizinostatin A New Inhibitor of Pyroglutamyl Peptidase *The Journal of Antibiotics* **45** 1795-1796

Aoyagi, T , Hatsu, M , Kojima, F , Hayashi, C , Hamada, M and Takeuchi, T (1992a) Benarthin A New Inhibitor of Pyroglutamyl Peptidase I Taxonomy, Fermentation, Isolation and Biological Activities *The Journal of Antibiotics* **45** 1079-1083

Armentrout, R W and Doolittle, R F (1969) Pyrrolidonecarboxylyl Peptidase Stabilization and Purification *Archives of Biochemistry and Biophysics* **132** 80-90

Armentrout, R W (1969) Pyrrolidonecarboxylyl Peptidase from Rat Liver *Biochimica et Biophysica ACTA* **191** 756-759

Awade, A , Cleuziat, Ph , Gonzales, Th and Robert-Baudouy, J (1994) Pyrrolidone Carboxyl Peptidase (Pcp) An Enzyme That Removes Pyroglutamic Acid (pGlu) From pGlu-Peptides and pGlu-Proteins *Proteins Structure, Function and Genetics* **20** 34-51

Awade, A , Cleuziat, Ph , Gonzales, Th and Robert-Baudouy, J (1992) Characterisation of the Pcp Gene Encoding the Pyrrolidone Carboxyl Peptidase of *Bacillus Subtilis Federation of European Biochemical Societies* **305** 67-73

Awade, A , Gonzalès, Th , Cleuziat, Ph and Robert-Baudouy, J (1992) One Step Purification and Characterisation of the Pyrrolidone Carboxyl Peptidase of *Streptococcus Pyogenes* Over-Expressed in *Escherischia coli Federation of European Biochemical Societies* **308** 70-74

-B-

Bairoch, A and Apweiler, R (1996) The SWISS-PROT Protein Sequence Data Bank and Its New Supplement TREMBL *Nucleic Acids Research* **24** 21-25

Barrett, A J and Rawlings, N D (2001) Evolutionary Lines of Cysteine Peptidases *Biological Chemistry* **382** 727-733

Barrett, A J , Rawlings, N D and Woessner, J F (1998) Handbook of Proteolytic Enzymes Academic Press, London

Bauer, K and Kleinkauf, H (1980) Catabolism of Thyroliberin by Rat Adenohypophyseal Tissue Extract *Journal of Biochemistry* **106** 107-117

Bauer, K , Nowak, P and Kleinkauf, H (1981) Specificity of a Serum Peptidase Hydrolysing Thyroliberin at the Pyroglutamyl-Histidine Bond *European Journal of Biochemistry* **118** 173-176

Bauer, K (1994) Purification and Characterisation of the Thyrotropin-Releasing-Hormone-Degrading Ectoenzyme *European Journal of Biochemistry* **224** 387-396

Benson, D A , Boguski, M ,Lipman, D J and Ostell, J (1996) GenBank *Nucleic Acids Research* **24** 1-5

Berman, H M , Westbrook, J , Feng, Z , Gilliland, G , Bhat, T N , Weissig, H , Shindyalov, I N and Bourne, P E (2000) The Protein Data Bank *Nucleic Acids Research* **28** 235-242

Biles, B D and Connolly B A (2004) Low-Fidelity *Pyrococcus Furiosus* DNA Polymerase Mutants Useful in Error-Prone PCR *Molecular Cell Biology* **25** 4602-14

Birnboim, H C and Doly, J (1979) A Rapid Alkaline Extraction Procedure for Screening Recombinant Plasmid DNA *Nucleic Acids Research* **7** 1513-1523

Bradford M M (1976) A Rapid and Sensitive Method for the Quantitation of Microgram Quantities of Protein Utilizing the Principle of Protein-Dye Binding *Analytical Biochemistry* **72** 248-254

Browne, P , Phelan, J and O'Cuinn, G (1981) TRH Pyroglutamate Aminopeptidase Activity In Two Different Subcellular Fractions of Guinea-Pig Brain *Irish Journal of Medical Sciences* **150** 348-349

Browne, P and O'Cuinn, G (1983) An Evaluation of the Role of a Pyroglutamyl Peptidase, a Post-Proline Cleaving Enzyme and a Post-Proline Dipeptidyl Amino Peptidase, Each Purified From the Soluble Fraction of Guinea-Pig Brain, in the Degradation of Thyroliberin *in vitro* *European Journal of Biochemistry* **137** 75-87

Brunetti, L , Cacciatore, I , Di Stefano, A , Dupre, S , Giorgi, A , Luisi, G , Michelotto, B , Orlando, G , Pinnen, F , Recinella, L , Sozio, P and Spirito, A (2002) Synthesis and Biological Evaluation of a Novel Pyroglutamyl-Modified TRH Analogue *Il Farmaco* **57** 479-486

Bujard, H , Gentz, R , Lanzer, M , Stueber, D , Mueller, M , Ibrahimi, I , Haeuptle, M-T , Dobberstein, B (1987) A T5 Promoter-Based Transcription-Translation System for the Analysis of Proteins *in vitro* and *in vivo* *Methods In Enzymology* **155** 416-433

-C-

Charli, JL, Mendez, M , Joseph-Bravo, P and Wilk, S (1987) Specific Inhibitors Of Pyroglutamyl Peptidase I And Prolyl Endopeptidase Do Not Change The *In Vitro* Release of TRH or Its Content in Rodent Brain *Neuropeptides* **9** 373-378

Chomczynski, P and Sacchi, N (1987) Single-Step Method of RNA Isolation by Acid Guanidinium Thiocyanate-Phenol-Chloroform Extraction *Analytical Biochemistry* **162** 156-159

Clarke, P (2000) PhD Thesis, Dublin City University, Ireland

Cleuziat, P , Awadé, A and Robert-Baudouy, J (1992) Molecular Characterisation of Pcp, the Structural Gene Encoding the Pyrrolidone Carboxylyl Peptidase from *Streptococcus pyogenes Molecular Microbiology* **6** 2051-2063

Corpet, F (1988) Multiple Sequence Alignment with Hierarchical Clustering *Nucleic Acids Research* **16** 10881-10890

Cruz, C , Charli, J-L , Vargas, M-A , Joseph-Bravo, P (1991) Neuronal Localisation of Pyroglutamate Aminopeptidase II in Primary Cultures of Fetal Mouse Brain *Journal of Neurochemistry* **56**(5) 1594-1601

Cudney, B and Patel, S (1994) Screening and Optimization Strategies for Macromolecular Crystal Growth *ACTA Crystallographica* **D50** 414-423

Cummins, P M and O'Connor, B (1996) Bovine Brain Pyroglutamyl Aminopeptidase (Type-1) Purification and Characterisation of a Neuropeptide-Inactivating Peptidase *The International Journal of Biochemistry and Cell Biology* **28** 883-893

Cummins, P M and O'Connor, B (1998) Pyroglutamyl Peptidase An Overview of the Three Known Enzymatic Forms *Biochimica et Biophysica ACTA* **1429** 1-17

Czekay, G and Bauer K (1993) Identification of the Thyrotropin-Releasing-Hormone-Degrading Ectoenzyme as a Metallopeptidase *Biochemical Journal* **290** 921-926

-D-

Dando, P M , Fortunato, M, Strand, G B , Smith, T S and Barrett, A J (2003) Pyroglutamyl-Peptidase I Cloning, Sequencing and Characterisation of the Recombinant Human Enzyme *Protein Expression and Purification* **28** 111-119

De Boer, H A , Comstock, L J and Vasser, M (1983) The *tac* Promoter A Functional Hybrid Derived From the *trp* and *lac* Promoters *Biochemistry* **80** 21-25

Dealler, S F , Campbell, L , Kerr, K G , McGoldrick, J , Flannigan, K A and Hawkey, P M (1989) Reliable Five-Minute Method for Identification of *Streptococcus pyogenes* *European Journal of Clinical Microbiology & Infectious Diseases* **8** 308-310

DeGandarias, J M De, Casis, O , Echevarria, E , Irazusta, J and Casis, L (1992) Pyroglutamyl-Peptidase I Activity in the Cortex of the Cat Brain During Development *International Journal of Developmental Biology* **36** 335-337

DeGandarias, J M , Irazusta, J , Fernandez, D , Varona, A and Casis, L (1994) Developmental Changes of Pyroglutamate-peptidase I Activity in Several Regions of the Female and Male Rat Brain *International Journal of Neuroscience* **77** 53-60

DeGandarias, J M , Irazusta, J , Gil, J , Varona, A , Ortega, F and Casis, L (2000) Subcellular Ontogeny of Brain Pyroglutamyl Peptidase I *Peptides* **21** 509-517

DeGandarias, J M , Irazusta, J , Silio, M , Gil, J , Saitua, N and Casis, L (1998) Soluble and Membrane-Bound Pyroglutamyl-Peptidase I Activity in the Developing Cerebellum and Brain Cortex *International Journal of Developmental Biology* **42** 103-106

Doolittle, R F and Armentrout, R W (1968) Pyrrolidonyl Peptidase An Enzyme for Selective Removal of Pyrrolidonecarboxylic Acid Residues from Polypeptides *Biochemistry* **7** 516-521

Doran, J D and Carey, P R (1996) α-Helix Dipoles and Catalysis Absorption and Raman Spectroscopic Studies of Acyl Cysteine Proteases *Biochemistry* **35** 12495-12502

-E-

Elliott, W H and Elliott, D C (2005) Biochemistry and Molecular Biology Third Edition *Oxford University Press New York*

Elmore, M A, Griffiths, E C, O'Connor, B and O'Cuinn, G (1990), Further Characterisation of the Substrate Specificity of TRH Hydrolysing Pyroglutamate Aminopeptidase from Guinea-Pig brain *Neuropeptides* **15** 31-36

Exterkate, F A (1977) Pyrrolidone Carboxylyl Peptidase in *Streptococcus cremoris* Dependence on an Interaction with Membrane Components *Journal of Bacteriology* **129** 1281-1288

-F-

Falkous, G, Shaw, P J, Ince, P G and Mantle, D Comparison of Cytoplasmic and Lysosomal Proteolytic Enzyme Levels in Spinal Cord Tissue From Motor Neurone Disease and Control Cases *6th International Symposium on ALS/MND*, 1995, Dublin, Ireland

Fersht, A Structure and Mechanism in Protein Science A Guide to Enzyme Catalysis and Protein Folding (2003) *Fifth Edition* W H Freeman and Company, New York

Fitzpatrick, P ,A, Steinmetz, A, C, U, Ringe, D and Klibanov, A M (1993) Enzyme Crystal Structure in a Neat Organic Solvent *Proc Natl Acad Sci* **90** 8653-8657

Fujii, R, Kitaoka, M and Hayashi, K (2004) One-Step Random Mutagenesis by Error-Prone Rolling Circle Amplification *Nucleic Acids Research* **32** 1-5

Fujiwara, K and Tsuru, D (1978) New Chromogenic and Fluorogenic Substrates for Pyrrolidonyl Peptidase *Journal of Biochemistry* **83** 1145-1149

Fujiwara, K, Kitagawa, T and Tsuru, D (1981a) Inactivation of Pyroglutamyl Aminopeptidase by L-Pyroglutamyl Chloromethyl Ketone *Biochimica et Biophysica ACTA* **655** 10-16

Fujiwara, K, Kobayashi, R and Tsuru, D (1979) The Substrate Specificity Of Pyrrolidone Carboxylyl Peptidase From *Bacillus Amyloliquefaciens Biochimica et Biophysica ACTA* **570** 140-148

Fujiwara, K, Matsumoto, E, Kitagawa, T and Tsuru, D (1981b) Inactivation of Pyroglutamyl Aminopeptidase by N^{α}-Carbobenzoxy-L-Pyroglutamyl Chloromethyl Ketone *Journal of Biochemistry* **90** 433-437

Fujiwara, K, Matsumoto, E, Kitagawa, T and Tsuru, D (1982) N-α-Carbobenzoxy Pyroglutamyl Diazomethyl Ketone As Active-Site-Directed Inhibitor For Pyroglutamyl Peptidase *Biochimica et Biophysica ACTA* **702** 149-154

-G-

Gallagher, S P and O'Connor, B (1998) A Study of a Highly Specific Pyroglutamyl Aminopeptidase Type-II From the Membrane Fraction of Bovine Brain, *Biochemistry & Cell Biology* **00**, 1-19

Gonzales, T and and Awade, A (1992) Purification and Characterisation of Recombinant Pyrrolidone Carboxyl Peptidase of *Bacillus subtilis Journal of Chromatography* **584** 101-107

Gonzales, T and Robert-Baudouy, J (1994) Characterisation of the Pcp Gene of *Pseudomonas fluorescens* and of Its Product, Pyrrolidone Carboxyl Peptidase (Pcp) *Journal of Bacteriology* **176** 2569-2576

Gonzales, T and Robert-Baudouy, J (1996) Bacterial Aminopeptidases Properties and Functions *FEMS Microbiology Reviews* **18** 319-344

Greige, R, Drenth J, Ducruix, A, McPherson, A and Saenger, W (1995) Crystallogenesis of Biological Macromolecules Biological, Microgravity and Other Physicochemical Aspects *Crystal Growth and Characterisation* **30** 237-281

-H-

Haitinger, L (1882) Vorlauge Mittheilung uber Glutaminsaure und Pyrrol *Monatshefte für Chemie* **3** 228-229

Hanahan, D (1985) Techniques for Transformation of E coli In DNA Cloning a Practical Approach, pp 109-135 Edited by D M Glover Oxford IRL Press

Hancock, B C and Zografi, G (1997) Characteristics and Significance of the Amorphous State in Pharmaceutical Systems *Journal of Pharmaceutical Sciences* **86** 1-12

-I-

Inoue, H, Nojima, H and Okayama, H (1990) High Efficiency Transformation of *Escherichia coli* with Plasmids *Gene* **96** 23-28

Ito, K, Inoue, T, Takahashi, T, Huang, H, Esumi, T, Hatakeyama, S, Tanaka, N, Nakamura, K T and Yoshimoto, T (2001) The Mechanism of Substrate Recognition of Pyroglutamyl-Peptidase I from *Bacillus amyloliquefaciens* as Determined by X-ray Crystallography and Site-directed Mutagenesis *The Journal of Biological Chemistry* **276** 18557-18562

-J-

Jackson, I M D (1982) Thyrotropin-Releasing Hormone *The New England Journal Of Medicine* **30** 145-155

Jancarik, J and Kim, S-H (1991) Sparse Matrix Sampling a Screening Method for Crystallization of Proteins *Journal of Applied Crystallography* **24** 409-411

Jen, A and Merkle, H P (2001) Diamonds In the Rough Protein Crystals From a Formulation Perspective *Pharmaceutical Research* **18** 1483-1488

-K-

Kabashima, T, Li, Y, Kanada, N, Ito, K and Yoshimoto, T (2001) Enhancement of the Thermal Stability of Pyroglutamyl Peptidase I by Introduction of an Intersubunit Disulfide Bond *Biochimica et Biophysica ACTA* **1547** 214-220

Kaufhold, A, Luttticken, R and Schwien, U (1989) Few-Minutes Test for the Identification of Group A Streptococci and Enterococci with Chromogenic Substrates *Zentralblatt für Bakteriologie* **272** 191-195

Kawarabayasi Y, Sawada M, Horikawa H, Haikawa Y, Hino Y, Yamamoto S, Sekine M, Baba S, Kosugi H, Hosoyama A, Nagai Y, Sakai M, Ogura K, Otsuka R, Nakazawa H, Takamiya M, Ohfuku Y, Funahashi T, Tanaka T, Kudoh Y, Yamazaki J, Kushida N, Oguchi A, Aoki K, Kikuchi H (1998) Complete Sequence and Gene Organization of the Genome of a Hyper-Thermophilic Archaebacterium, *Pyrococcus horikoshii* OT3 *DNA Research* **5** 55-76

Kim J K , Kim S J , Lee H G , Lim J S , Kim S J , Cho S H , Jeong W H , Choe I S , Chung T W , Paik S G , Choe Y K (2001) Molecular Cloning and Characterisation of *Mycobacterium bovis* BCG *pcp* Gene Encoding Pyrrolidone Carboxyl Peptidase *Molecules and Cells* **12** 347-352

Kwiatkowska, J , Torain, B and Glenner, G G (1974) A Pyrrolidonecarboxylate Peptidase from the Particulate Fraction of *Klebsiella cloacae* *The Journal of Biological Chemistry* **249** 7729-7736

-L-

Laemmli, U K (1970) Cleavage of Structural Proteins During the Assembly of the Head of Bacteriophage T4 *Nature* **227** 680-685

Lauffart, B and Mantle, D (1988) Rationalization of Aminopeptidase Activities in Human Skeletal Muscle Soluble Extract *Biochimica et Biophysica ACTA* **956** 300-306

Lauffart, B , McDermott, J R , Biggins, J A , Gibson, A M and Mantle, D (1989) Purification and Characterization of Pyroglutamyl Aminopeptidase from Human Cerebral Cortex *Biochemical Society Transactions* **17** 207-208

Le Saux, O , Gonzales, T and Robert-Baudouy, J (1996) Mutational Analysis of the Active Site of *Pseudomonas fluorescens* Pyrrolidone Carboxyl Peptidase *Journal of Bacteriology* **178** 3308-3313

Leung, D W , E Chen, and D V Goeddel (1989) A Method for Random Mutagenesis of a Defined DNA Segment Using a Modified Polymerase Chain Reaction *Technique* **1** 11-15

Lin-Goerke,J L , Robbins,D J and Burczak,J D (1997) PCR-Based Random Mutagenesis Using Manganese and Reduced dNTP Concentration *Biotechniques*, **23**, 409–412

Lusty C J (1999) A Gentle Vapor-Diffusion Technique for Cross-Linking of Protein Crystals for Cryocrystallography *Journal of Applied Crystallography* **32**, 106-112

-M-

Makrides, A C (1996) Strategies for Achieving High-Level Expression of Genes in *Escherichia coli Microbiological Reviews* **60** 512-538

Maniatis, T , Fritsch, E F and Sambrook, J (1982) Molecular Cloning, A Laboratory Manual Cold Spring Harbour Laboratory

Mantle, D , Lauffart, B and Gibson, A (1991) Purification and Characterisation of Leucyl Aminopeptidase and Pyroglutamyl Aminopeptidase from Human Skeletal Muscle *Clinica Chimica ACTA* **197** 35-46

Mantle, D , Lauffart, B , McDermot, J and Gibson, A (1990) Characterisation of Aminopeptidases in Human Kidney Soluble Fraction *Clinica Chimica ACTA* **187** 105-114

Margolin , A , L and Navia , M , A (2001) Protein Crystals as Novel Catalytic Materials *Angew Chem Int Ed* **40** 2204-2222

Mantle, D , Lauffart, B , Perry, E K and Perry, R H (1989) Comparison of Major Cortical Aminopeptidase Activity in Normal Brain and Brain from Patients with Alzheimer's Disease *Journal of the Neurological Sciences* **89** 227-234

Mineyama, R and Saito, K (1998) Partial Purification and Some Properties of Pyroglutamyl Peptidase from *Enterococcus faecalis Microbios* **94** 47-62

Mitchell, M J , Conville, P S and Gill, V J (1987) Rapid Identification of Enterococci by Pyrrolidonyl Aminopeptidase Activity (PyRase) *Diagnostic Microbiology and Infectious Disease* **6** 283-286

Monsuur AJ, Stepmak D, Diosdado B, Wapenaar MC, Mearin ML, Koning F and Wijmenga C (2006) Genetic and Functional Analysis of Pyroglutamyl-Peptidase I in Coeliac Disease *European Journal of Gastroenterology Hepatology* **18** 637-44

Morty,R E , Bulau,P , Pelle,R , Wilk,S and Abe,K (2006) Pyroglutamyl Peptidase Type I from *Trypanosoma brucei* a New Virulence Factor from African Trypanosomes that De-Blocks Regulatory Peptides in the Plasma of Infected Hosts *Biochemistry Journal* **394** 635-645

Mudge, A W and Fellows, R E (1973) Bovine Pituitary Pyrrolidonecarboxylyl Peptidase *Endocrinologia* **93** 1428-1434

Mulczyk, M and Szewczuk, A (1970) Pyrrolidonyl Peptidase in Bacteria A New Colrimetric Test for Differentiation of Enterobacteriaceae *Journal of General Microbiology* **61** 9-13

Mullis, K B and Faloona, F A (1987) Specific Synthesis of DNA *in Vitro* via a Polymerase-Catalyzed Chain Reaction *Methods in Enzymology* **155** 335-350

-N-

Nicholas, K B , Nicholas, H B Jr and Deerfield II, D W (1997) GeneDoc Analysis and Visualization of Genetic Variation *EMBnet News* **4** 14

-O-

O'Connor, B and O'Cuinn, G (1984) Localization of a Narrow-Specificity Thyroliberin Hydrolizing Pyroglutamate Aminopeptidase in Synaptosomal Membranes of Guinea-Pig Brain *European Journal of Biochemistry* **144** 271-278

O'Cuinn, G , O'Connor, B and Elmore, M (1990) Degradation of Thyrotropin-Releasing Hormone and Luteinising Hormone-Releasing Hormone by Enzymes of Brain Tissues *Journal of Neurochemistry* **54** 1-13

Odagaki, Y , Hayashi, A , Okada, K , Hirotsu, K , Kabashima, T , Ito, K , Yoshimoto, T , Tsuru, D , Sato, M and Clardy, J (1999) The Crystal Structure Of Pyroglutamyl

Peptidase I from *Bacillus amyloliquefaciens* Reveals a New Structure for a Cysteine Protease *Structure* **7** 399-411

O'Leary, R and O'Connor, B (1995) Thyrotropin-Releasing Hormone *Journal of Neurochemistry* **65** 953-963

Orlowski, M and Meister, A (1971), Enzymology of Pyrrolidone Carboxylic Acid, In *The Enzymes, IV Hydrolysis*, Boyer, P D (ed), Academic Press, New York 123-151

-P-

Pascual I , Gil-Parrado S , Cisneros M , Joseph-Bravo P , Diaz J , Possani L D , Charli J L and Chavez M (2004) Purification of a Specific Inhibitor of Pyroglutamyl Aminopeptidase II from the Marine Annelide *Hermodice carunculata in vivo* Effects in Rodent Brain *International Journal of Biochemistry Cell Biology* **36** 138–152

Patti, J M , Schneider, A , Garza, N and Boles, J O (1995) Isolation and Characterisation of Pcp, a Gene Encoding a Pyrrolidone Carboxyl Peptidase in *Staphylococcus aureus Gene* **166** 95-99

Perlman, J H , Laakkonen, L , Osman, R and Gershengorn, M C (1994b) A Model of the Thyrotropin-releasing Hormone (TRH) Receptor Binding Pocket *The Journal of Biological Chemistry* **269** 23383-23386

Perlman, J H , Thaw, C N , Laakkonen, L , Bowers, C Y , Osman, R and Gershengorn, M C (1994a) Hydrogen Bonding Interaction of Thyrotropin-releasing Hormone (TRH) with Transmembrane Tyrosine 106 of the TRH Receptor *The Journal of Biological Chemistry* **269** 1610-1613

Podell, D N and Abraham, G N (1978) A Technique For The Removal Of Pyroglutamic Acid From The Amino Terminus Of Proteins Using Calf Liver Pyroglutamate Amino Peptidase *Biochemical And Biophysical Research Communications* **81** 176-185

Prasad, C (1987) Activation/Inactivation Of Rat Tissue Pyroglutamate Aminopeptidase By Disulfide Bond-Reducing Agents *Neuropeptides* **9** 211-215

Prasad, C (1995) Bioactive Cyclic Dipeptides *Peptides* **16** 151-164

Prasad, C and Peterkofsky, A (1976) Demonstration of Pyroglutamylpeptidase and Amidase Activities Toward Thyrotropin-Releasing Hormone in Hamster Hypothalamus Extracts *The Journal of Biological Chemistry* **251** 3229-3234

Prasad, C , Mori, M , Wilber, J F , Pierson, W , Pegues, J and Jayaraman, A (1982) Distribution and Metabolism of Cyclo(His-Pro) A New Member of the Neuropeptide Family *Peptides* **3** 591-598

-Q-

Qiagen (2003) The QIAexpressionist A Handbook For High-Level Expression and Purification of 6xHis-Tagged Proteins Fifth Edition

Quiocho, F A and Richards, F M (1964) Intermolecular Cross Linking of a Protein In the Crystalline State Carboxypeptidase-A *Biochemistry* **52** 833-839

-R-

Ramirez, M , Sanchez, B , Arechaga, G , Garcia, S , Lardelli, P , Venzon D and De Gandarias, J M (1991) Diurnal Varaiation and Left-Right Distribution of Pyroglutamyl Peptidase I Activity in the Rat Brain and Retina *ACTA Endocrinologica* **125** 570-573

Rawlings, N D , Tolle, D P and Barrett, A J (2004) MEROPS the Peptidase Database *Nucleic Acids Research* **32** D160-D164

Russo, C , Violani, E , Salis, S , Venezia, V , Dolcini, V , Damonte, G , Benatti, U , D'Arrigo, C , Patrone, E , Carlo, P and Schettini, G (2002) Pyroglutamate-Modified Amyloid-α-Peptides AβN3(pE) Strongly Affect Cultured Neuron and Astrocyte Survival *Journal of Neurochemistry* **82** 1480-1489

-S-

Sanchez, B , Alba, F , de Dios Luna, J , Martinez, J M , Prieto, I And Ramirez, M (1996) Pyroglutamyl Peptidase I Levels and Their Left-Right Distribution in the Rat Retina and Hypothalamus are Influenced by Light-Dark Conditions *Brain Research* **731** 254-257

Schauder, B., Schomburg, L., Kohrle, J. and Bauer, K. (1994) Cloning of a cDNA Encoding an Ectoenzyme that Degrades Thyrotropin-Releasing Hormone. *Proceedings of the National Academy of Sciences of the United States of America* **91**: 9534-9538

Schmitmeier, S., Thole, H., Bader, A. and Bauer, K. (2002) Purification and Characterization of the Thyrotropin-Releasing Hormone (TRH)-Degrading Serum Enzyme and its Identification as a Product of Liver Origin. *European Journal of Biochemistry* **269**: 1278-1286

Schomburg, L., Turwitt, S., Prescher, G., Lohmann, D., Horsthemke, B. and Bauer, K. (1999) Human TRH-Degrading Ectoenzyme: cDNA Cloning, Functional Expression, Genomic Structure and Chromosomal Assignment. *European Journal of Biochemistry* **265**: 415-422

Schwede, T., Kopp, J., Guex, N. and Peitsch, M.C. (2003) SWISS-MODEL: an Automated Protein Homology-Modelling Server. *Nucleic Acids Research* **31**: 3381-3385

Singleton, M.R. and Littlechild, J.A. (2001) Pyrrolidone Carboxylpeptidase from *Thermococcus litoralis*. *Methods In Enzymology* **330**: 394-403

Singleton, M.R., Isupov, M.N. and Littlechild, J.A. (1999a) Crystallisation and Preliminary X-ray Diffraction Studies of Pyrrolidone Carboxyl Peptidase from the Hyperthermophilic Archaeon *Thermococcus litoralis*. *ACTA Crystallographica* **D55**: 702-703

Singleton, M.R., Isupov, M.N. and Littlechild, J.A. (1999b) X-ray Structure of Pyrrolidone Carboxyl Peptidase from the Hyperthermophilic Archaeon *Thermococcus litoralis*. *Structure* **7**: 237-244

Singleton, M.R., Taylor, S.J.C., Parrat, J.S. and Littlechild, J.A. (2000) Cloning, Expression and Characterization of Pyrrolidone Carboxyl Peptidase from the Archaeon *Thermococcus litoralis*. *Extremophiles* **4**: 297-303

Smith P.K., Krohn R.I., Hermanson G.T., Mallia A.K., Gartner F.H., Provenzano M.D., Fujimoto E.K., Goeke N.M., Olson B.J. and Klenk D.C. (1985) Measurement of Protein Using Bicinchoninic Acid. *Analytical Biochemistry* **150**: 76-85

Sokabe, M , Kawamura, T , Sakai, N , Yao, M , Watanabe, N and Tanaka, I (2002) X-Ray Crystal Structure of Pyrrolidone-Carboxylate Peptidase from Hyperthermophilic *Pyrococcus horikoshii Journal of Structural and Functional Genomics* **2** 145-154

Sullivan, J J , Muchnicky, E E , Davidson, B E and Jago, G R (1977) Purification and Properties of the Pyrrolidonecarboxylate Peptidase of *Stretococcus faecium Australian Journal of Biological Science* **30** 543-552

Szewczuk, A and Kwiatkowska, J (1970) Pyrrolidone Peptidase in Animal, Plant and Human Tissues Occurrence and Some Properties of the Enzyme *European Journal of Biochemistry* **15** 92-96

Szewczuk, A and Mulczyk, M (1969) Pyrrolidonyl Peptidase in Bacteria The Enzyme from *Bacillus subtilis European Journal of Biochemistry* **6** 63-67

-T-

Taylor, W L and Dixon, J E (1978) Characterization of a Pyroglutamate Aminopeptidase from Rat Serum that Degrades Thyrotropin-Releasing Hormone, *Journal of Biological Chemistry* **253**(19) 6934-6940

Tanaka, H , Chinami, M , Mizushima, T , Ogasahara, Ota, M , Tsukihara, T and Yutani, K (2001) X-Ray Crystalline Structures of Pyrrolidone Carboxyl Peptidase from a Hyperthermophile, *Pyrococcus furiosus*, and Its Cys-Free Mutant *Journal of Biochemistry* **130** 107-118

Tsunasawa, S , Nakura, S , Tanigawa, T and Kato, I (1998) Pyrrolidone Carboxyl Peptidase from the Hyperthermophilic Archaeon *Pyrococcus furiosus* Cloning and Overexpression in *Escherichia coli* of the Gene, and its Application to Protein Sequence Analysis *Journal of Biochemistry* **124** 778-783

Tsuru, D , Fujiwara, K and Kado, K (1978) Purification and Characterisation of L-Pyrrolidonecarboxylate Peptidase from *Bacillus amyloliquefaciens Journal of Biochemistry* **84** 467-476

Tsuru, D , Nakamura, K , Yoshimoto, T and Fujiwara, K (1984) Pyroglutamyl-Peptidase from *Bacillus amyloliquefaciens* An Improved Purification Method and Some Properties of the Enzyme *Biochimica et Biophysica ACTA* **791** 117-122

Tsuru, D , Sakabe, K , Yoshimoto, T and Fujiwara, K (1982) Pyroglutamyl Peptidase from Chicken Liver Purification and Some Properties *Journal of Pharmacobio-Dynamics* **5** 859-868

-U-

Uliana, J A and Doolittle, R F (1969) Pyrrolidonecarboxylyl Peptidase Studies on the Specificity of the Enzyme *Archives of Biochemistry and Biophysics* **131** 561-565

-V-

Vaas, R P (2005) PhD Thesis, Dublin City University, Ireland

Valdivia, A , Irazusta, J , Fernandez, D , Mugica, J , Ochoa, C and Casis, L (2004) Pyroglutamyl Peptidase I and Prolyl Endopeptidase in Human Semen Increased Activity in Necrozoospermia *Regulatory Peptides* **122** 79-84

Vartanain , J , henry , M and Wain-Hibson , S (1996) Hypermutagemc PCR Involving All Four Transitions and a Sizeable Proportion of Transversions *Nucleic Acids Research* **24** 2627-2631

-W-

Wilk, S , Friedman, T C and Kline, T B (1985) Pyroglutamyl Diazomethyl Ketone Potent Inhibitor of Mammalian Pyroglutamyl Peptide Hydrolase *Biochemical and Biophysical Research Communications* **130** 662-668

Wilk, S and Wilk, E K (1989) Pyroglutamyl Peptidase II, A Thyrotropin Releasing Hormone Degrading Enzyme Purification and Specificity Studies of the Rabbit Brain Enzyme, *Neurochemistry International* **15**(1) 81-89

-Y-

Yuan-zhı , Z , Guddat , L , Farlow , A and De Jersey , J (2006) Structure-Functıon Relatıonshıps ın Human Hypoxanthıne-Guamne Phosphorıbosyltransferase (HGPRT) by Random Mutagenesıs *Chemıcal Research Chınese* **22** 251-252

Yoshımoto, T , Shımoda, T , Kıtazono, A , Kabashıma, T , Ito, K and Tsuru, D (1993) Pyroglutamyl Peptıdase Gene from *Bacıllus amyloliquefacıens* Clonıng, Sequencıng, and Crystallısatıon of the Expressed Enzyme *Journal of Bıochemıstry* **113** 67-73

Internet Bıblıography

http //www chem wısc edu

http //www che utoledo edu

http //www hamptonresearch com

http //www medıcınenet com

http //www structmed cırm ac uk

Appendix A

Standard Curves

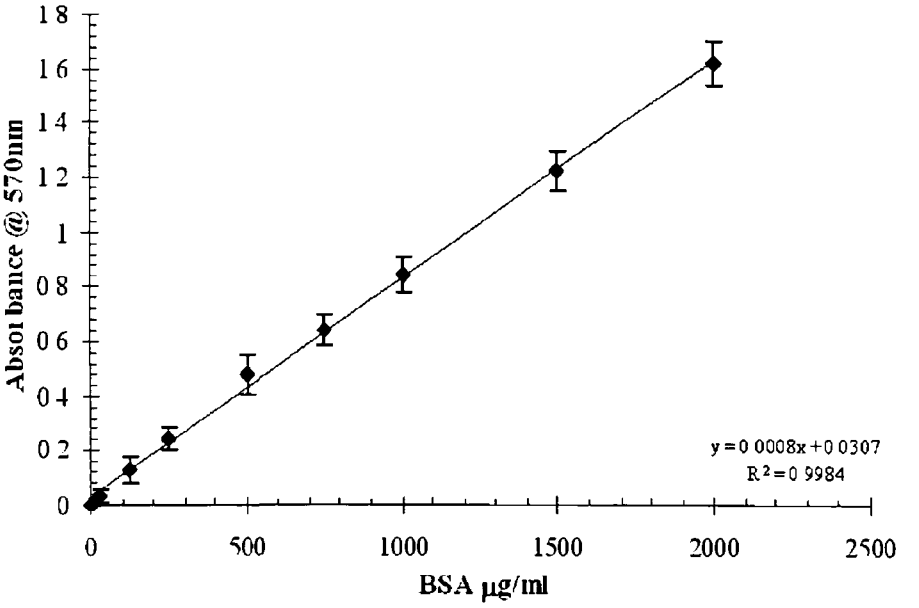

BSA standard curve for quantitative BCA assay

Standard curve of BSA (µg/ml) versus absorbance at 570 nm for the determination of protein concentration by the BCA assay described in Section 2 14 1

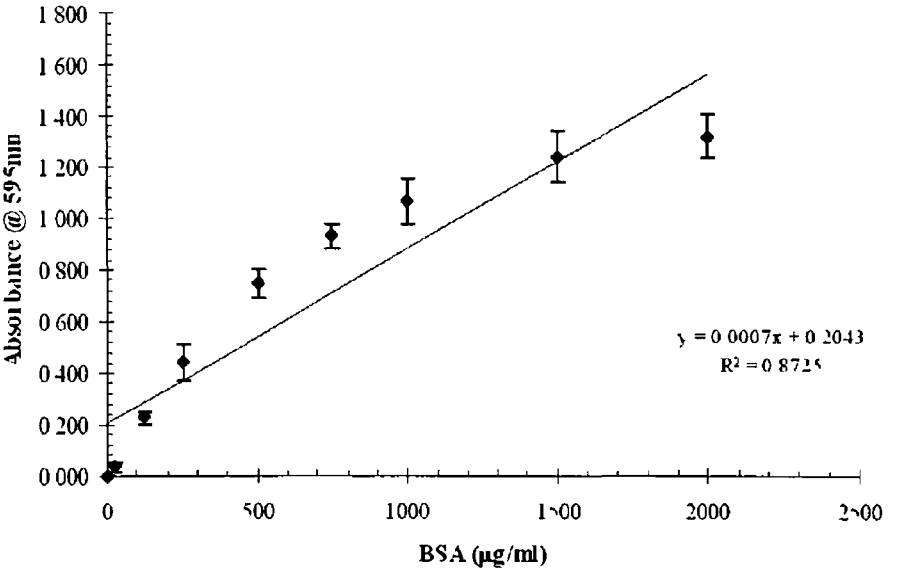

BSA standard curve for quantitative Coomassie assay

Standard curve of BSA (µg/ml) versus absorbance at 595 nm for the determination of protein concentration by the quantitative Coomassie assay described in Section 2 14 2

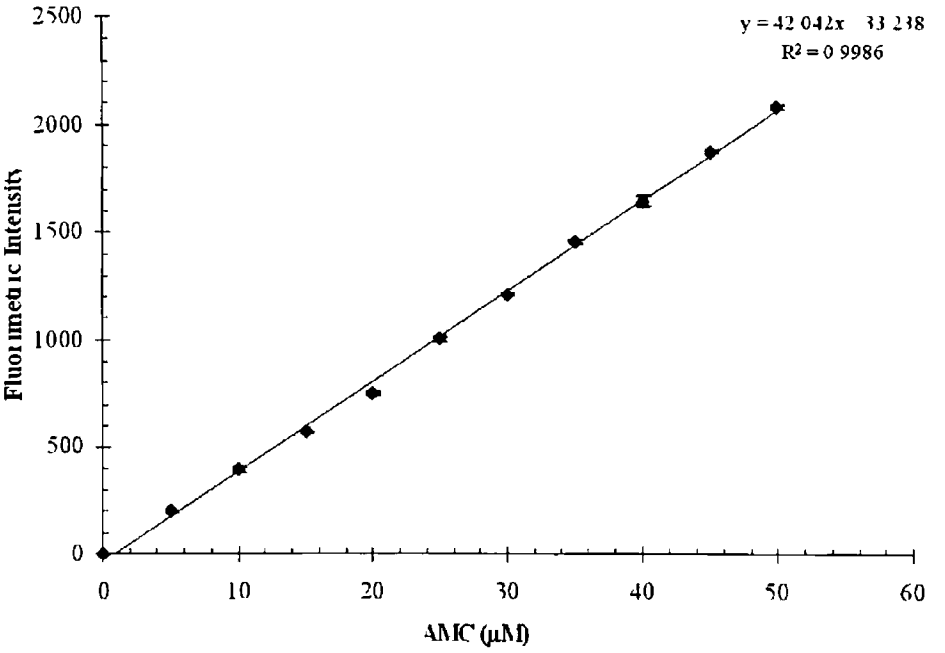

AMC standard curve

Standard curve of AMC (µM) versus fluorescence intensity as described in Section 2 15 1, for the determination of AMC released by PAP1 activity

Appendix B
Sequence Data

>pZK1_forward read, MWG
CCGCCAGTGTGCTGGAATTCGGCTTCAGCAAGGATCCGTGTTCATGGCAACAGTTGATTT
TGCCTTCTGACTGCTCTAGGAGGTCCAGCATCTCCTCAATGATGGCCCGAAGTGCCCGGC
CCAGCTGGTCTGCATTGTACGGCTTGCCCAGAGGGGGCACGTGAACAAAGGCTGAGCGGC
CGTGACTCTGGTACAGAGAGGTATAGTAGGTGAAGTCGCAGAGGTACCTGCCTGCATCTT
GTGAAATGGTCACTGACACATCTAAGCCCAGTGTAGTGACCCTCTTACACACAGCATCCA
TGTCGATGATGGAGTCAATGCTTTCCGGCCCGTCCTCCACACAGCACTGGGAGCCGGGGC
AGAATCGGCAGTTGTCCAGGCCCTTGTAACCCTTGTTGTGTCCACACTTCTCCAGTGTGA
CTGCGGTTGCCATGCCTGACACTCCTACGTGCACCACCAGCTGCGGACTGTGCTTCTCCC
ACAGGGCAGGGATGAGCCTCTGGACCGTCTGATACTCCACTGGAATCTCATACACATGTA
GGTCCACGCTGTCCCCAAGCCCTAGTTTCTCCAGCTCCTGGACCGCAATCCAGCTGGCAT
TCACAGTGTGTTCCCCAAAAGGGCCGAATGCCGTCACCACCACCGCCTTCCTGGGCTGCT
CCATGGCGGGTTCAAGCCGAATTCTGCAGATATCCATCACACTGGCGGCCGCTCGAGCAT
GCATCTAGAGGGCCCAATTCGCCCTATAGTGAGTCGTATTACAATTCACTGGCCGTCGTT
TTACAACGTCGTGACTGGGAAAACCCTGGCGTTACCCAACTTAATCGCCTTGCAGCACAT
CCCCCTTTCGCCAGCTGGCGTAATAGCGAAGAGGCCCGCACCGATTGCCCTTCCCAACAG
TTGCGCAGCCTGAATGGCGAATGGACGCGCCCTGTAGCGGCGCATTAGCGCGGCGGGGTG
TGGTGGTTACGCGCAGCGTGACCGCTACACTTGCCAGCGCCCTAGCGCCCGCTCCTTTCG
CTTTCTTCCCTTCTTTCTCGC

>pZK1_reverse read, MWG
CCCTCTAGATGCATGCTCGAGCGGCCGCCAGTGTGATGGATATCTGCAGAATTCGGCTTG
AACCCGCCATGGAGCAGCCCAGGAAGGCGGTGGTGGTGACGGCATTCGGCCCTTTTGGGG
AACACACTGTGAATGCCAGCTGGATTGCGGTCCAGGAGCTGGAGAAACTAGGGCTTGGGG
ACAGCGTGGACCTACATGTGTATGAGATTCCAGTGGAGTATCAGACGGTCCAGAGGCTCA
TCCCTGCCCTGTGGGAGAAGCACAGTCCGCAGCTGGTGGTGCACGTAGGAGTGTCAGGCA
TGGCAACCGCAGTCACACTGGAGAAGTGTGGACACAACAAGGGTTACAAGGGCCTGGACA
ACTGCCGATTCTGCCCCGGCTCCCAGTGCTGTGTGGAGGACGGGCCGGAAAGCATTGACT
CCATCATCGACATGGATGCTGTGTGTAAGAGGGTCACTACACTGGGCTTAGATGTGTCAG
TGACCATTTCACAAGATGCAGGCAGGTACCTCTGCGACTTCACCTACTATACCTCTCTGT
ACCAGAGTCACGGCCGCTCAGCCTTTGTTCACGTGCCCCCTCTGGGCAAGCCGTACAATG
CAGACCAGCTGGGCCGGGCACTTCGGGCCATCATTGAGGAGATGCTGGACCTCCTAGAGC
AGTCAGAAGGCAAAATCAACTGTTGCCATGAACACGGATCCTTGCTGAAGCCGAATTCCA
GCACACTGGCGGCCGTTACTAGTGGATCCGAGCTCGGTACCAAGCTTGGCGTAATCATGG
TCATAGCTGTTTCCTGTGTGAAATTGTTATCCGCTCACAATTCCACACAACATACGAGCC
GGAAGCATAAAGTGTAAAGCCTGGGGTGCCTAATGAGTGAGCTAACTCACATTAATTGCG
TTGCGCTCACTGCCCGCTTTCCAGTCGGGAAACCTGTCGTGCCAGCTGCATTAATGAATC
GGCAACGCGCGGGGAGAGGCGGTTTGCGTATGGGCGCTCTTCGGCTTCTCGCTCACTGAC
TCGCTGCGCTCGGTCGTTCGGCT

>pZK2_forward read, MWG
AATCATAAAAAATTTATTTGCTTTGTGAGCGGATAACAATTTCACACAGAATTCATTAAAGA
GGAGAAATTAACCATGGAGCAGCCGAGGAAGGCGGTGGTAGTGACGGGATTTGGCCCTTTT
GGGGAACACACCGTGAACGCCAGTTGGATTGCAGTTCAGGAGCTAGAAAAGCTAGGCCTTG
GCGACAGCGTGGACCTGCATGTGTACGAGATTCCGGTTGAGTACCAAACAGTCCAGAGACT
CATCCCCGCCCTGTGGGAGAAGCACAGTCCACAGCTGGTGGTGCATGTGGGGGTGTCAGGC
ATGGCGACCACAGTCACACTGGAGAAATGTGGACACAACAAGGGCTACAAGGGGCTGGACA
ACTGCCGCTTTTGCCCCGGCTCCCAGTGCTGCGTGGAGGACGGGCCTGAAAGCATTGACTCC
ATCATCGACATGGATGCTGTGTGCAAGCGAGTCACCACGTTGGGCCTGGATGTGTCGGTGAC
CATCTCGCAGGATGCCGGCAGATATCTCTGCGACTTTACCTACTACACCTCTTTGTACCAGAG
TCACGGTCGATCAGCCTTCGTCCACGTGCCCCCACTGGGGAAGCCGTACAACGCGGACCAGC
TGGGCAGGGCACTGAGAGCCATCATTGA

>pZK2_reverse read, MWG
AGCCGAGGAAGGCGGTGGTAGTGACGGAATTTGGCCCTTTTGGGGAACACACCGTGAACGC
CAGTTGGATTGCAGTTCAGGAGCTAGAAAAGCTAGGCCTTGGCGACAGCGTGGACCTGCAT
GTGTACGAGATTCCGGTTGAGTACCAAACAGTCCAGAGACTCATCCCCGCCCTGTGGGAGAA
GCACAGTCCACAGCTGGTGGTGCATGTGGGGGTGTCAGGCATGGCGACCACAGTCACACTG
GAGAAATGTGGACACAACAAGGGCTACAAGGGGCTGGACAACTGCCGCTTTTGCCCCGGCT
CCCAGTGCTGCGTGGAGGACGGGCCTGAAAGCATTGACTCCATCATCGACATGGATGCTGTG

TGCAAGCGAGTCACCACGTTGGGCCTGGATGTGTCGGTGACCATCTCGCAGGATGCCGGCAG
ATATCTCTGCGACTTTACCTACTACACCTCTTTGTACCAGAGTCACGGTCGATCAGCCTTCGT
CCACAGTGCCCCCACTGGGGAAGCCAGTACAACGCGGACCAGCTGGGCAGGGCACTGAGAG
CCATCATTGAGGAGATGTTGGACCTCCTGGAGCAGTCAGAGGGCAAAATCAACTATTGCCAC
AAACACGGATCTCATCACCATCACCATCACTAAGCTTAATTAGC

>pZK3_forward read, MWG
TTAGTGATGGTGATGGTGATGAGATCCGTGTTCATGGCAACAGTTGATTTTGCCTTCTGA
CTGCTCTAGGAGGTCCAGCATCTCCTCAATGATGGCCCGAAGTGCCCGGCCCAGCTGGTC
TGCATTGTACGGCTTGCCCAGAGGGGGCACGTGAACAAAGGCTGAGCGGCCGTGACTCTG
GTACAGAGAGGTATAGTAGGTGAAGTCGCAGAGGTACCTGCCTGCATCTTGTGAAATGGT
CACTGACACATCTAAGCCCAGTGTAGTGACCCTCTTACACACAGCATCCATGTCGATGAT
GGAGTCAATGCTTTCCGGCCCGTCCTCCACACAGCACTGGGAGCCGGGGCAGAATCGGCA
GTTGTCCAGGCCCTTGTAACCCTTGTTGTGTCCACACTTCTCCAGTGTGACTGCGGTTGC
CATGCCTGACACTCCTACGTGCACCACCAGCTGCGGACTGTGCTTCTCCCACAGGGCAGG
GATGAGCCTCTGGACCGTCTGATACTCCACTGGAATCTCATACACATGTAGGTCCACGCT
GTCCCCAAGCCCTAGTTTCTCCAGCTCCTGGACCGCAATCCAGCTGGCATTCACAGTGTG
TTCCCCAAAAGGGCCGAATGCCGTCACCACCACCGCCTTCCTGGGCTGCTCCATGGTTAA
TTTCTCCTCTTTAATGAATTCTGTTTCCTGTGTGAAATTGTTATCCGCTCACAATTCCAC
ACATTATACGAGCCGATGATTAATTGTCAACAGCTCATTTCAGAATATTTGCCAGAACCG
TTATGATGTCGGCGCAAAAAACATTATCCAGAACGGGAGTGCGCCTTGAGCGACACGAAT
TATGCAGTGATTTACGACCTGCACAGCCATACCACAGCTTCCGATGGCTGCCTGACGCCA
GAAGCATTGGTGCACCGTGCAGTCGATAAGCCCGGATCGCTCTAGAGCGATCCTCT

>pZK3_reverse read, MWG
GGTGGTGCACGTAGGAGTGTCAGGCATGGCAACCGCAGTCACACTGGAGAAGTGTGGACA
CAACAAGGGTTACAAGGGCCTGGACAACTGCCGATTCTGCCCCGGCTCCCAGTGCTGTGT
GGAGGACGGGCCGGAAAGCATTGACTCCATCATCGACATGGATGCTGTGTGTAAGAGGGT
CACTACACTGGGCTTAGATGTGTCAGTGACCATTTCACAAGATGCAGGCAGGTACCTCTG
CGACTTCACCTACTATACCTCTCTGTACCAGAGTCACGGCCGCTCAGCCTTTGTTCACGT
GCCCCCTCTGGGCAAGCCGTACAATGCAGACCAGCTGGGCCGGGCACTTCGGGCCATCAT
TGAGGAGATGCTGGACCTCCTAGAGCAGTCAGAAGGCAAAATCAACTGTTGCCATGAACA
CGGATCTCATCACCATCACCATCACTAAGCTTGGCTGTTTTGGCGGATGAGAGAAGATTT
TCAGCCTGATACAGATTAAATCAGAACGCAGAAGCGGTCTGATAAAACAGAATTTGCCTG
GCGGCAGTAGCGCGGTGGTCCCACCTGACCCCATGCCGAACTCAGAAGTGAAACGCCGTA
GCGCCGATGGTAGTGTGGGGTCTCCCCATG

>pZK3_E85mD_forward read, MWG
GGCCCAGTGTGCTGGAATTCGGCTTCAGCAAGGATCCGTGTTCATGGCAACAGTTGATTT
TGCCTTCTGACTGCTCTAGGAGGTCCAGCATCTCCTCAATGATGGCCCGAAGTGCCCGGC
CCAGCTGGTCTGCATTGTACGGCTTGCCCAGAGGGGGCACGTGAACAAAGGCTGAGCGGC
CGTGACTCTGGTACAGAGAGGTATAGTAGGTGAAGTCGCAGAGGTACCTGCCTGCATCTT
GTGAAATGGTCACTGACACATCTAAGCCCAGTGTAGTGACCCTCTTACACACAGCATCCA
TGTCGATGATGGAGTCAATGCTTTCCGGCCCGTCCTCCACACAGCACTGGGAGCCGGGGC
AGAATCGGCAGTTGTCCAGGCCCTTGTAACCCTTGTTGTGTCCACACTTCTCCAGTGTGA
CTGCGGTTGCCATGCCTGACACTCCTACGTGCACCACCAGCTGCGGACTGTGCTTCTCCC
ACAGGGCAGGGATGAGCCTCTGGACCGTCTGATACTCCACTGGAATCTCATACACATGTA
GGTCCACGCTGTCCCCAAGCCCTAGTTTCTCCAGCTCCTGGACCGCAATCCAGCTGGCAT
TCACAGTGTGTTCCCCAAAAGGGCCGAATGCCGTCACCACCACCGCCTTCCTGGGCTGCT
CCATGGCGGGTTCAAGCCGAATTCTGCAGATATCCATCACACTGGCGGCCGCTCGAGCAT
GCATCTAGAGGGCCCAATTCGCCCTATAGTGAGTCGTATTACAATTCACTGGCCGTCGTT
TTACAACGTCGTGACTGGGAAAACCCTGGCGTTACCCAACTTAATCGCCTTGCAGCACAT
CCCCCTTTCGCCAGCTGGCGTAATAGCGAAGAGGCCCGCACCGATTGCCCTTCCCAACAG
TTGCGCAGCCTGAATGGCGAATGGACGCGCCCTGTAGCGGCGCATTAGCGCGGCGGGGTG
TGGTGGTTACGCGCAGCGTGACCGCTACACTTGCCAGCGCCCTAGCGCCCGCTCCTTTCG
CTTTCTTCCCTTCTTTCTCGC

> pZK3_E85mD_reverse read, MWG
ACGTCTAGATGCATGCTCGAGCGGCCGCCAGTGTGATGGATATCTGCAGAATTCGGCTTG
AACCCGCCATGGAGCAGCCCAGGAAGGCGGTGGTGGTGACGGCATTCGGCCCTTTTGGGG

AACACACTGTGAATGCCAGCTGGATTGCGGTCCAGGAGCTGGAGAAACTAGGGCTTGGGG
ACAGCGTGGACCTACATGTGTATGAGATTCCAGTGGAGTATCAGACGGTCCAGAGGCTCA
TCCCTGCCCTGTGGGAGAAGCACAGTCCGCAGCTGGTGGTGCACGTAGGAGTGTCAGGCA
TGGCAACCGCAGTCACACTGGAGAAGTGTGGACACAACAAGGGTTACAAGGGCCTGGACA
ACTGCCGATTCTGCCCCGGCTCCCAGTGCTGTGTGGAGGACGGGCCGGAAAGCATTGACT
CCATCATCGACATGGATGCTGTGTGTAAGAGGGTCACTACACTGGGCTTAGATGTGTCAG
TGACCATTTCACAAGATGCAGGCAGGTACCTCTGCGACTTCACCTACTATACCTCTCTGT
ACCAGAGTCACGGCCGCTCAGCCTTTGTTCACGTGCCCCCTCTGGGCAAGCCGTACAATG
CAGACCAGCTGGGCCGGGCACTTCGGGCCATCATTGAGGAGATGCTGGACCTCCTAGAGC
AGTCAGAAGGCAAAATCAACTGTTGCCATGAACACGGATCCTTGCTGAAGCCGAATTCCA
GCACACTGGCGGCCGTTACTAGTGGATCCGAGCTCGGTACCAAGCTTGGCGTAATCATGG
TCATAGCTGTTTCCTGTGTGAAATTGTTATCCGCTCACAATTCCACACAACATACGAGCC
GGAAGCATAAAGTGTAAAGCCTGGGGTGCCTAATGAGTGAGCTAACTCACATTAATTGCG
TTGCGCTCACTGCCCGCTTTCCAGTCGGGAAACCTGTCGTGCCAGCTGCATTAATGAATC
GGCAACGCGCGGGGAGAGGCGGTTTGCGTATGGGCGCTCTTCGGCTTCTCGCTCACTGAC
TCGCTGCGCTCGGTCGTTCGGCT

>pZK3_C149mF_forward read, MWG
CCGCCAGTGTGCTGGAATTCGGCTTCAGCAAGGATCCGTGTTCATGGCAACAGTTGATTT
TGCCTTCTGACTGCTCTAGGAGGTCCAGCATCTCCTCAATGATGGCCCGAAGTGCCCGGC
CCAGCTGGTCTGCATTGTACGGCTTGCCCAGAGGGGGCACGTGAACAAAGGCTGAGCGGC
CGTGACTCTGGTACAGAGAGGTATAGTAGGTGAAGTCGCAGAGGTACCTGCCTGCATCTT
GTGAAATGGTCACTGACACATCTAAGCCCAGTGTAGTGACCCTCTTACACACAGCATCCA
TGTCGATGATGGAGTCAATGCTTTCCGGCCCGTCCTCCACACAGCACTGGGAGCCGGGGC
AGAATCGGCAGTTGTCCAGGCCCTTGTAACCCTTGTTGTGTCCACACTTCTCCAGTGTGA
CTGCGGTTGCCATGCCTGACACTCCTACGTGCACCACCAGCTGCGGACTGTGCTTCTCCC
ACAGGGCAGGGATGAGCCTCTGGACCGTCTGATACTCCACTGGAATCTCATACACATGTA
GGTCCACGCTGTCCCCAAGCCCTAGTTTCTCCAGCTCCTGGACCGCAATCCAGCTGGCAT
TCACAGTGTGTTCCCCAAAAGGGCCGAATGCCGTCACCACCACCGCCTTCCTGGGCTGCT
CCATGGCGGGTTCAAGCCGAATTCTGCAGATATCCATCACACTGGCGGCCGCTCGAGCAT
GCATCTAGAGGGCCCAATTCGCCCTATAGTGAGTCGTATTACAATTCACTGGCCGTCGTT
TTACAACGTCGTGACTGGGAAAACCCTGGCGTTACCCAACTTAATCGCCTTGCAGCACAT
CCCCCTTTCGCCAGCTGGCGTAATAGCGAAGAGGCCCGCACCGATTGCCCTTCCCAACAG
TTGCGCAGCCTGAATGGCGAATGGACGCGCCCTGTAGCGGCGCATTAGCGCGGCGGGGTG
TGGTGGTTACGCGCAGCGTGACCGCTACACTTGCCAGCGCCCTAGCGCCCGCTCCTTTCG
CTTTCTTCCCTTCTTTCTCGC

> pZK3_C149mF_reverse read, MWG
TGCATGCTCGAGCGGCCGCCAGTGTGATGGATATCTGCAGAATTCGGCTTGAACCCGCCATG
GAGCAGCCCAGGAAGGCGGTGGTGGTGACGGCATTCGGCCCTTTTGGGGAACACACTGTGA
ATGCCAGCTGGATTGCGGTCCAGGAGCTGGAGAAACTAGGGCTTGGGGACAGCGTGGACCT
ACATGTGTATGAGATTCCAGTGGAGTATCAGACGGTCCAGAGGCTCATCCCTGCCCTGTGGG
AGAAGCACAGTCCGCAGCTGGTGGTGCACGTAGGAGTGTCAGGCATGGCAACCGCAGTCAC
ACTGGAGAAGTGTGGACACAACAAGGGTTACAAGGGCCTGGACAACTGCCGATTCTGCCCC
GGCTCCCAGTGCTGTGTGGAGGACGGGCCGGAAAGCATTGACTCCATCATCGACATGGATG
CTGTGTGTAAGAGGGTCACTACACTGGGCTTAGATGTGTCAGTGACCATTTCACAAGATGCA
GGCAGGTACCTCTGCGACTTCACCTACTATACCTCTCTGTACCAGAGTCACGGCCGCTCAGC
CTTTGTTCACGTGCCCCCTCTGGGCAAGCCGTACAATGCAGACCAGCTGGGCCGGGCACTTC
GGGCCATCATTGAGGAGATGCTGGACCTCCTAGAGCAGTCAGAAGGCAAAATCAACTGTTG
CCATGAACACGGATCCTTGCTGAAGCCGAATTCCAGCACACTGGCGGCCGTTACTAGTGGAT
CCGAGCTCGGTACCAAGCTTGGCGTAATCATGGTCATAGCTGTTTCCTGTGTGAAATTGTTAT
CCGCTCACAATTCCACACAACATACGAGCCGGAAGCATAAAGTGTAAAGCCTGGGGTGCCT
AATGAGTGAGCTAACTCACATTAATTGCGTTGCGCTCACTGCCCGCTTTCCAGTCGGGAAAC
CTGTCGTGCCAGCTGCATTAATGAATCGGCAACGCGCGGGGAGAGGCGGTTTGCGTATGGG
CGCTCTTCGGCTTCTCGCTCACTGACTCG

>pZK3_H168mD_forward read MWG
GCCAGTGTGCTGGAATTCGGCTTCAGCAAGGATCCGTGTTCATGGCAACAGTTGATTT
TGCCTTCTGACTGCTCTAGGAGGTCCAGCATCTCCTCAATGATGGCCCGAAGTGCCCGGC
CCAGCTGGTCTGCATTGTACGGCTTGCCCAGAGGGGGCACGTGAACAAAGGCTGAGCGGC

CGTGACTCTGGTACAGAGAGGTATAGTAGGTGAAGTCGCAGAGGTACCTGCCTGCATCTT
GTGAAATGGTCACTGACACATCTAAGCCCAGTGTAGTGACCCTCTTACACACAGCATCCA
TGTCGATGATGGAGTCAATGCTTTCCGGCCCGTCCTCCACACAGCACTGGGAGCCGGGGC
AGAATCGGCAGTTGTCCAGGCCCTTGTAACCCTTGTTGTGTCCACACTTCTCCAGTGTGA
CTGCGGTTGCCATGCCTGACACTCCTACGTGCACCACCAGCTGCGGACTGTGCTTCTCCC
ACAGGGCAGGGATGAGCCTCTGGACCGTCTGATACTCCACTGGAATCTCATACACATGTA
GGTCCACGCTGTCCCCAAGCCCTAGTTTCTCCAGCTCCTGGACCGCAATCCAGCTGGCAT
TCACAGTGTGTTCCCCAAAAGGGCCGAATGCCGTCACCACCACCGCCTTCCTGGGCTGCT
CCATGGCGGGTTCAAGCCGAATTCTGCAGATATCCATCACACTGGCGGCCGCTCGAGCAT
GCATCTAGAGGGCCCAATTCGCCCTATAGTGAGTCGTATTACAATTCACTGGCCGTCGTT
TTACAACGTCGTGACTGGGAAAACCCTGGCGTTACCCAACTTAATCGCCTTGCAGCACAT
CCCCCTTTCGCCAGCTGGCGTAATAGCGAAGAGGCCCGCACCGATTGCCCTTCCCAACAG
TTGCGCAGCCTGAATGGCGAATGGACGCGCCCTGTAGCGGCGCATTAGCGCGGCGGGGTG
TGGTGGTTACGCGCAGCGTGACCGCTACACTTGCCAGCGCCCTAGCGCCCGCTCCTTTCG
CTTTCTTCCCTTCTTTC

> pZK3_H168mD_reverse read, MWG
TCTAGATGCATGCTCGAGCGGCCGCCAGTGTGATGGATATCTGCAGAATTCGGCTTGAAC
CCGCCATGGAGCAGCCCAGGAAGGCGGTGGTGGTGACGGCATTCGGCCCTTTTGGGG
AACACACTGTGAATGCCAGCTGGATTGCGGTCCAGGAGCTGGAGAAACTAGGGCTTGGGG
ACAGCGTGGACCTACATGTGTATGAGATTCCAGTGGAGTATCAGACGGTCCAGAGGCTCA
TCCCTGCCCTGTGGGAGAAGCACAGTCCGCAGCTGGTGGTGCACGTAGGAGTGTCAGGCA
TGGCAACCGCAGTCACACTGGAGAAGTGTGGACACAACAAGGGTTACAAGGGCCTGGACA
ACTGCCGATTCTGCCCCGGCTCCCAGTGCTGTGTGGAGGACGGGCCGGAAAGCATTGACT
CCATCATCGACATGGATGCTGTGTGTAAGAGGGTCACTACACTGGGCTTAGATGTGTCAG
TGACCATTTCACAAGATGCAGGCAGGTACCTCTGCGACTTCACCTACTATACCTCTCTGT
ACCAGAGTCACGGCCGCTCAGCCTTTGTTCACGTGCCCCCTCTGGGCAAGCCGTACAATG
CAGACCAGCTGGGCCGGGCACTTCGGGCCATCATTGAGGAGATGCTGGACCTCCTAGAGC
AGTCAGAAGGCAAAATCAACTGTTGCCATGAACACGGATCCTTGCTGAAGCCGAATTCCA
GCACACTGGCGGCCGTTACTAGTGGATCCGAGCTCGGTACCAAGCTTGGCGTAATCATGG
TCATAGCTGTTTCCTGTGTGAAATTGTTATCCGCTCACAATTCCACACAACATACGAGCC
GGAAGCATAAAGTGTAAAGCCTGGGGTGCCTAATGAGTGAGCTAACTCACATTAATTGCG
TTGCGCTCACTGCCCGCTTTCCAGTCGGGAAACCTGTCGTGCCAGCTGCATTAATGAATC
GGCAACGCGCGGGGAGAGGCGGTTTGCGTATGGGCGCTCTTCGGCTTCTCGCTCACTGAC
TCGCTGCGCTCGGTCGTTCG

>pZK3_A91mT_forward read, MWG
CAAACAGCCAAGCTTAGTGATGGTGATGGTGATGAGATCCGTGTTCATGGCAACAGTTGA
TTTTGCCTTCTGACTGCTCTAGGAGGTCCAGCATCTCCTCAATGATGGCCCGAAGTGCCC
GGCCCAGCTGGTCTGCATTGTACGGCTTGCCCAGAGGGGGCACGTGAACAAAGGCTGAGC
GGCCGTGACTCTGGTACAGAGAGGTATAGTAGGTGAAGTCGCAGAGGTACCTGCCTGCAT
CTTGTGAAATGGTCACTGACACATCTAAGCCCAGTGTAGTGACCCTCTTACACACAGCAT
CCATGTCGATGATGGAGTCAATGCTTTCCGGCCCGTCCTCCACACAGCACTGGGAGCCGG
GGCAGAATCGGCAGTTGTCCAGGCCCTTGTAACCCTTGTTGTGTCCACACTTCTCCAGTG
TGACTGTGGTTGCCATGCCTGACACGCCTACGTGCACCACCAGCTGCGGACTGTGCTTCT
CCCACAGGGCAGGGATGAGCCTCTGGACCGTCTGATACTCCACTGGAATCTCATACACAT
GTAGGTCCACGCTGTCCCCAAGCCCTAGTTTCTCCAGCTCCTGGACCGCAATCCAGCTGG
CATTCACAGTGTGTTCCCCAAAAGGGCCGAATCCCGTCACCACCACCGCCTTCCTGGGCT
GCTCCATGGTTAATTTCTCCTCTTTAATGAATTCTGTTTCCTGTGTGAAATTGTTATCCG
CTCACAATTCCACACATTATACGAGCCGATGATTAATTGTCAACAGCTCATTTCAGAATA
TTTGCCAGAACCGTTATGATGTCGGCGCAAAAAACATTATCCAGAACGGGAGTGCGCCTT
GAGCGACACGAATTATGCAGTGATTTACGACCTGCACAGCCATACCACAGCTTCCGATGG
CTGCCTGACGCCAGAAGCATTGGTGCACCGTGCAGTCGATAAGCCCGGATCGCTCTAGAG
CGATCCTCTACGCCGGACGCATCGTGGCC

> pZK3_A91mT_revere read, MWG
GAATTAACCATGGAGCAGCCCAGGAAGGCGGTGGTGGTGACGGGATTCGGCCCTTTTGGG
GAACACACTGTGAATGCCAGCTGGATTGCGGTCCAGGAGCTGGAGAAACTAGGGCTTGGG
GACAGCGTGGACCTACATGTGTATGAGATTCCAGTGGAGTATCAGACGGTCCAGAGGCTC
ATCCCTGCCCTGTGGGAGAAGCACAGTCCGCAGCTGGTGGTGCACGTAGGCGTGTCAGGC

ATGGCAACCACAGTCACACTGGAGAAGTGTGGACACAACAAGGGTTACAAGGGCCTGGAC
AACTGCCGATTCTGCCCCGGCTCCCAGTGCTGTGTGGAGGACGGGCCGGAAAGCATTGAC
TCCATCATCGACATGGATGCTGTGTGTAAGAGGGTCACTACACTGGGCTTAGATGTGTCA
GTGACCATTTCACAAGATGCAGGCAGGTACCTCTGCGACTTCACCTACTATACCTCTCTG
TACCAGAGTCACGGCCGCTCAGCCTTTGTTCACGTGCCCCCTCTGGGCAAGCCGTACAAT
GCAGACCAGCTGGGCCGGGCACTTCGGGCCATCATTGAGGAGATGCTGGACCTCCTAGAG
CAGTCAGAAGGCAAAATCAACTGTTGCCATGAACACGGATCTCATCACCATCACCATCAC
TAAGCTTGGCTGTTTTGGCGGATGAGAGAAGATTTTCAGCCTGATACAGATTAAATCAGA
ACGCAGAAGCGGTCTGATAAAACAGAATTTGCCTGGCGGCAGTAGCGCGGTGGTCCCACC
TGACCCCATGCCGAACTCAGAAGTGAAACGCCGTAGCGCCGATGGTAGTGTGGGGTCTCC
CCATGCGAGAGTAGGGAACTGCCAGGCATCAAATAAAACGAAAGGCTCAGTCGAAAGACT
GGGCCTTTCGTTTTATCTGTTGTTTGTCGGTGAACGCTCTCCTGAGTAGGACAAATCCGC
CGGGAGCGGATTTGAACGTTGCGAAGCAACGGCCC

>pZK3_C205mY_forward read, MWG
CAAACAGCCAAGCTTAGTGATGGTGATGGTGATGAGATCCGTGTTCATGGCAATAGTTGA
TTTTGCCTTCTGACTGCTCTAGGAGGTCCAGCATCTCCTCAATGATGGCCCGAAGTGCCC
GGCCCAGCTGGTCTGCATTGTACGGCTTGCCCAGAGGGGGCACGTGAACAAAGGCTGAGC
GGCCGTGACTCTGGTACAGAGAGGTATAGTAGGTGAAGTCGCAGAGGTACCTGCCTGCAT
CTTGTGAAATGGTCACTGACACATCTAAGCCCAGTGTAGTGACCCTCTTACACACAGCAT
CCATGTCGATGATGGAGTCAATGCTTTCCGGCCCGTCCTCCACACAGCACTGGGAGCCGG
GGCAGAATCGGCAGTTGTCCAGGCCCTTGTAACCCTTGTTGTGTCCACACTTCTCCAGTG
TGACTGCGGTTGCCATGCCTGACACGCCTACGTGCACCACCAGCTGCGGACTGTGCTTCT
CCCACAGGGCAGGGATGAGCCTCTGGACCGTCTGATACTCCACTGGAATCTCATACACAT
GTAGGTCCACGCTGTCCCCAAGCCCTAGTTTCTCCAGCTCCTGGACCGCAATCCAGCTGG
CATTCACAGTGTGTTCCCCAAAAGGGCCGAATCCCGTCACCACCACCGCCTTCCTGGGCT
GCTCCATGGTTAATTTCTCCTCTTTAATGAATTCTGTTTCCTGTGTGAAATTGTTATCCG
CTCACAATTCCACACATTATACGAGCCGATGATTAATTGTCAACAGCTCATTTCAGAATA
TTTGCCAGAACCGTTATGATGTCGGCGCAAAAAACATTATCCAGAACGGGAGTGCGCCTT
GAGCGACACGAATTATGCAGTGATTTACGACCTGCACAGCCATACCACAGCTTCCGATGG
CTGCCTGACGCCAGAAGCATTGGTGCACCGTGCAGTCGATAAGCCCGGATCGCTCTAGAG
CGATCCTCTACGCCGGACGCATCGTGGCCGGCATCACCGGCGCA

> pZK3_C205mY_reverse read, MWG
GGAGAATTAACCATGGAGCAGCCCAGGAAGGCGGTGGTGGTGACGGGATTCGGCCCTTTT
GGGGAACACACTGTGAATGCCAGCTGGATTGCGGTCCAGGAGCTGGAGAAACTAGGGCTT
GGGGACAGCGTGGACCTACATGTGTATGAGATTCCAGTGGAGTATCAGACGGTCCAGAGG
CTCATCCCTGCCCTGTGGGAGAAGCACAGTCCGCAGCTGGTGGTGCACGTAGGCGTGTCA
GGCATGGCAACCGCAGTCACACTGGAGAAGTGTGGACACAACAAGGGTTACAAGGGCCTG
GACAACTGCCGATTCTGCCCCGGCTCCCAGTGCTGTGTGGAGGACGGGCCGGAAAGCATT
GACTCCATCATCGACATGGATGCTGTGTGTAAGAGGGTCACTACACTGGGCTTAGATGTG
TCAGTGACCATTTCACAAGATGCAGGCAGGTACCTCTGCGACTTCACCTACTATACCTCT
CTGTACCAGAGTCACGGCCGCTCAGCCTTTGTTCACGTGCCCCCTCTGGGCAAGCCGTAC
AATGCAGACCAGCTGGGCCGGGCACTTCGGGCCATCATTGAGGAGATGCTGGACCTCCTA
GAGCAGTCAGAAGGCAAAATCAACTATTGCCATGAACACGGATCTCATCACCATCACCAT
CACTAAGCTTGGCTGTTTTGGCGGATGAGAGAAGATTTTCAGCCTGATACAGATTAAATC
AGAACGCAGAAGCGGTCTGATAAAACAGAATTTGCCTGGCGGCAGTAGCGCGGTGGTCCC
ACCTGACCCCATGCCGAACTCAGAAGTGAAACGCCGTAGCGCCGATGGTAGTGTGGGGTC
TCCCCATGCGAGAGTAGGGAACTGCCAGGCATCAAATAAAACGAAAGGCTCAGTCGAAAG
ACTGGGGCCTTTCGTTTTATCTGTTGTTTGTCGGTGAACGCTCTCCTGAGTAGGACAAAT
CCGCCGGGAGCGGATTTGAACGTTGCGAAGCAACGGCCCGGAAGGT

>pZK3_E208mK_forward read, MWG
CATCCGCCAAAACAGCCAAGCTTAGTGATGGTGATGGTGATGAGATCCGTGTTTATGGCA
ACAGTTGATTTTGCCTTCTGACTGCTCTAGGAGGTCCAGCATCTCCTCAATGATGGCCCG
AAGTGCCCGGCCCAGCTGGTCTGCATTGTACGGCTTGCCCAGAGGGGGCACGTGAACAAA
GGCTGAGCGGCCGTGACTCTGGTACAGAGAGGTATAGTAGGTGAAGTCGCAGAGGTACCT
GCCTGCATCTTGTGAAATGGTCACTGACACATCTAAGCCCAGTGTAGTGACCCTCTTACA
CACAGCATCCATGTCGATGATGGAGTCAATGCTTTCCGGCCCGTCCTCCACACAGCACTG
GGAGCCGGGGCAGAATCGGCAGTTGTCCAGGCCCTTGTAACCCTTGTTGTGTCCACACTT

CTCCAGTGTGACTGCGGTTGCCATGCCTGACACGCCTACGTGCACCACCAGCTGCGGACT
GTGCTTCTCCCACAGGGCAGGGATGAGCCTCTGGACCGTCTGATACTCCACTGGAATCTC
ATACACATGTAGGTCCACGCTGTCCCCAAGCCCTAGTTTCTCCAGCTCCTGGACCGCAAT
CCAGCTGGCATTCACAGTGTGTTCCCCAAAAGGGCCGAATCCCGTCACCACCACCGCCTT
CCTGGGCTGCTCCATGGTTAATTTCTCCTCTTTAATGAATTCTGTTTCCTGTGTGAAATT
GTTATCCGCTCACAATTCCACACATTATACGAGCCGATGATTAATTGTCAACAGCTCATT
TCAGAATATTTGCCAGAACCGTTATGATGTCGGCGCAAAAAACATTATCCAGAACGGGAG
TGCGCCTTGAGCGACACGAATTATGCAGTGATTTACGACCTGCACAGCCATACCACAGCT
TCCGATGGCTGCCTGACGCCAGAAGCATTGGTGCACCGTGCAGTCGATAAGCCCGGATCG
CTCTAGAGCGATCCTCTACGCCGGACGCATCGTGGCCGGCATCACCGGCGCCA

>pZK3_E208mK_reverse read, MWG
AGAGGAGAATTAACCATGGAGCAGCCCAGGAAGGCGGTGGTGGTGACGGGATTCGGCCCT
TTTGGGGAACACACTGTGAATGCCAGCTGGATTGCGGTCCAGGAGCTGGAGAAACTAGGG
CTTGGGGACAGCGTGGACCTACATGTGTATGAGATTCCAGTGGAGTATCAGACGGTCCAG
AGGCTCATCCCTGCCCTGTGGGAGAAGCACAGTCCGCAGCTGGTGGTGCACGTAGGCGTG
TCAGGCATGGCAACCGCAGTCACACTGGAGAAGTGTGGACACAACAAGGGTTACAAGGGC
CTGGACAACTGCCGATTCTGCCCCGGCTCCCAGTGCTGTGTGGAGGACGGGCCGGAAAGC
ATTGACTCCATCATCGACATGGATGCTGTGTGTAAGAGGGTCACTACACTGGGCTTAGAT
GTGTCAGTGACCATTTCACAAGATGCAGGCAGGTACCTCTGCGACTTCACCTACTATACC
TCTCTGTACCAGAGTCACGGCCGCTCAGCCTTTGTTCACGTGCCCCCTCTGGGCAAGCCG
TACAATGCAGACCAGCTGGGCCGGGCACTTCGGGCCATCATTGAGGAGATGCTGGACCTC
CTAGAGCAGTCAGAAGGCAAAATCAACTGTTGCCATAAACACGGATCTCATCACCATCAC
CATCACTAAGCTTGGCTGTTTTGGCGGATGAGAGAAGATTTTCAGCCTGATACAGATTAA
ATCAGAACGCAGAAGCGGTCTGATAAAACAGAATTTGCCTGGCGGCAGTAGCGCGGTGGT
CCCACCTGACCCCATGCCGAACTCAGAAGTGAAACGCCGTAGCGCCGATGGTAGTGTGGG
GTCTCCCCATGCGAGAGTAGGGAACTGCCAGGCATCAAATAAAACGAAAGGCTCAGTCGA
AAGACTGGGGCCTTTCGTTTATCTGTTGTTTGTCGGTGAACGCTCTCCTGAGTAGGACAA
ATCCGCCGGGAGCGGATTTGAACGTTGCGAAGCAACGGCCCGG

>pZK_E85mD_forward read, MWG
CAAACAGCCAAGCTTAGTGATGGTGATGGTGATGAGATCCGTGTTTGTGGCAATAGTTGA
TTTTGCCCTCTGACTGCTCCAGGAGGTCCAACATCTCCTCAATGATGGCTCTCAGTGCCC
TGCCCAGCTGGTCCGCGTTGTACGGCTTCCCCAGTGGGGGCACGTGGACGAAGGCTGATC
GACCGTGACTCTGGTACAAAGAGGTGTAGTAGGTAAAGTCGCAGAGATATCTGCCGGCAT
CCTGCGAGATGGTCACCGACACATCCAGGCCCAACGTGGTGACTCGCTTGCACACAGCAT
CCATGTCGATGATGGAGTCAATGCTTTCAGGCCCGTCCTCCACGCAGCACTGGGAGCCGG
GGCAAAAGCGGCAGTTGTCCAGCCCCTTGTAGCCCTTGTTGTGTCCACATTTATCCAGTG
TGACTGTGGTCGCCATGCCTGACACCCCCACATGCACCACCAGCTGTGGACTGTGCTTCT
CCCACAGGGCGGGGATGAGTCTCTGGACTGTTTGGTACTCAACCGGAATCTCGTACACAT
GCAGGTCCACGCTGTCGCCAAGGCCTAGCTTTTCTAGCTCCTGAACTGCAATCCAACTGG
CGTTCACGGTGTGTTCCCCAAAAGGGCCAAATCCCGTCACTACCACCGCCTTCCTCGGCT
GCTCCATGGTTAATTTCTCCTCTTTAATGAATTCTGTTTCCTGTGTGAAATTGTTATCCG
CTCACAATTCCACACATTATACGAGCCGATGATTAATTGTCAACAGCTCA

> pZK_E85mD_reverse read, MWG
ATGGAGCAGCCGAGGAAGGCGGTGGTAGTGACGGGATTTGGCCCTTTTGGGGAACACACC
GTGAACGCCAGTTGGATTGCAGTTCAGGAGCTAGAAAAGCTAGGCCTTGGCGACAGCGTG
GACCTGCATGTGTACGAGATTCCGGTTGAGTACCAAACAGTCCAGAGACTCATCCCCGCC
CTGTGGGAGAAGCACAGTCCACAGCTGGTGGTGCATGTGGGGGTGTCAGGCATGGCGACC
ACAGTCACACTGGATAAATGTGGACACAACAAGGGCTACAAGGGGCTGGACAACTGCCGCT
TTTGCCCCGGCTCCCAGTGCTGCGTGGAGGACGGGCCTGAAAGCATTGACTCCATCATC
GACATGGATGCTGTGTGCAAGCGAGTCACCACGTTGGGCCTGGATGTGTCGGTGACCATC
TCGCAGGATGCCGGCAGATATCTCTGCGACTTTACCTACTACACCTCTTTGTACCAGAGT
CACGGTCGATCAGCCTTCGTCCACGTGCCCCCACTGGGGAAGCCGTACAACGCGGACCAG
CTGGGCAGGGCACTGAGAGCCATCATTGAGGAGATGTTGGACCTCCTGGAGCAGTCAGAG
GGCAAAATCAACTATTGCCACAAACACGGATCTCATCACCATCACCATCACTAAGCTTGG
CTGTTTTGGCGGATGAGAGAAGATTTTCAGCCTGATACAGATTAAATCAGAACGCAGAAG
CGGTCTGATAAAACAGAATTTGCCTGGCGG

>pZK_E85mQ_forward read, MWG
GATGGTGATGGTGATGAGATCCGTGTTTGTGGCAATAGTTGATTTTGCCCTCTGACTGCTCCA
GGAGGTCCAACATCTCCTCAATGATGGCTCTCAGTGCCCTGCCCAGCTGGTCCGCGTTGTAC
GGCTTCCCCAGTGGGGGCACGTGGACGAAGGCTGATCGACCGTGACTCTGGTACAAAGAGG
TGTAGTAGGTAAAGTCGCAGAGATATCTGCCGGCATCCTGCGAGATGGTCACCGACACATCC
AGGCCCAACGTGGTGACTCGCTTGCACACAGCATCCATGTCGATGATGGAGTCAATGCTTTC
AGGCCCGTCCTCCACGCAGCACTGGGAGCCGGGGCAAAAGCGGCAGTTGTCCAGCCCCTTG
TAGCCCTTGTTGTGTCCACATTTCTGCAGTGTGACTGTGGTCGCCATGCCTGACACCCCCACA
TGCACCACCAGCTGTGGACTGTGCTTCTCCCACAGGGCGGGGATGAGTCTCTGGACTGTTTG
GTACTCAACCGGAATCTCGTACACATGCAGGTCCACGCTGTCGCCAAGGCCTAGCTTTTCTA
GCTCCTGAACTGCAATCCAACTGGCGTTCACGGTGTGTTCCCCAAAAGGGCCAAATCCCGTC
ACTACCACCGCCTTCCTCGGCTGCTCCATGGTTAATTTCTCCTCTTTAATGAATTCTGTTTCCT
GTGTGAAATTGTTATCCGCTCACAATTCCACACATTATACGAGCCGATGATTAATTGTCAAC
AGCTCATTTCAGAATATTTGCCAGAACCGTTATGATGTCGGCGCAAAAAACATTATCCAGAA
CGGGAGTGCGCCTTGAGCGACACGAATTATGCAGTGATTTACGACCTGCACAGCCATACCAC
AGCTTTCGATGGCTGCCTGACGCCAGAAGCATTGGTGCA

> pZK_E85mQ_reverse read, MWG
AGCCGAGGAAGGCGGTGGTAGTGACGGGATTTGGCCCTTTTGGGGAACACACCGTGAACGC
CAGTTGGATTGCAGTTCAGGAGCTAGAAAAGCTAGGCCTTGGCGACAGCGTGGACCTGCAT
GTGTACGAGATTCCGGTTGAGTACCAAACAGTCCAGAGACTCATCCCCGCCCTGTGGGAGAA
GCACAGTCCACAGCTGGTGGTGCATGTGGGGGTGTCAGGCATGGCGACCACAGTCACACTG
CAGAAATGTGGACACAACAAGGGCTACAAGGGGCTGGACAACTGCCGCTTTTGCCCCGGCT
CCCAGTGCTGCGTGGAGGACGGGCCTGAAAGCATTGACTCCATCATCGACATGGATGCTGTG
TGCAAGCGAGTCACCACGTTGGGCCTGGATGTGTCGGTGACCATCTCGCAGGATGCCGGCAG
ATATCTCTGCGACTTTACCTACTACACCTCTTTGTACCAGAGTCACGGTCGATCAGCCTTCGT
CCACGTGCCCCCACTGGGGAAGCCGTACAACGCGGACCAGCTGGGCAGGGCACTGAGAGCC
ATCATTGAGGAGATGTTGGACCTCCTGGAGCAGTCAGAGGGCAAAATCAACTATTGCCACA
AACACGGATCTCATCACCATCACCATCACTAAGCTTGGCTGTTTTGGCGGATGAGAGAAGAT
TTTCAGCCTGATACAGATTAAATCAGAACGCAGAAGCGGTCTGATAAAACAGAATTTGCCTG
GCGGCAGTAGCGCGGTGGTCCCACCTGACCCCATGCCGAACTCAGAAGTGAAACGCCGTAG
CGCCGATGGTAGTGTGGGGTCTCCCCATGCGAGAGTAGGGGAACTGCCAGGCATCAAATAA
AACGAAAAGGCTCAGTCGAAAGACTGGGGCCTTTCGTTTTATCTGTTGTTTGTCGGTGAACG
CTCTCCTGAGTAGGACAAAT

>pZK_E85mK_forward read, MWG
GATGGTGATGGTGATGAGATCCGTGTTTGTGGCAATAGTTGATTTTGCCCTCTGACTGCTCCA
GGAGGTCCAACATCTCCTCAATGATGGCTCTCAGTGCCCTGCCCAGCTGGTCCGCGTTGTAC
GGCTTCCCCAGTGGGGGCACGTGGACGAAGGCTGATCGACCGTGACTCTGGTACAAAGAGG
TGTAGTAGGTAAAGTCGCAGAGATATCTGCCGGCATCCTGCGAGATGGTCACCGACACATCC
AGGCCCAACGTGGTGACTCGCTTGCACACAGCATCCATGTCGATGATGGAGTCAATGCTTTC
AGGCCCGTCCTCCACGCAGCACTGGGAGCCGGGGCAAAAGCGGCAGTTGTCCAGCCCCTTG
TAGCCCTTGTTGTGTCCACATTTCTTCAGTGTGACTGTGGTCGCCATGCCTGACACCCCCACA
TGCACCACCAGCTGTGGACTGTGCTTCTCCCACAGGGCGGGGATGAGTCTCTGGACTGTTTG
GTACTCAACCGGAATCTCGTACACATGCAGGTCCACGCTGTCGCCAAGGCCTAGCTTTTCTA
GCTCCTGAACTGCAATCCAACTGGCGTTCACGGTGTGTTCCCCAAAAGGGCCAAATCCCGTC
ACTACCACCGCCTTCCTCGGCTGCTCCATGGTTAATTTCTCCTCTTTAATGAATTCTGTTTCCT
GTGTGAAATTGTTATCCGCTCACAATTCCACACATTATACGAGCCGATGATTAATTGTCAAC
AGCTCATTTCAGAATATTTGCCAGAACCGTTATGATGTCGGCGCAAAAAACATTATCCAGAA
CGGGAGTGCGCCTTGAGCGACACGAATTATGCAGTGATTTACGACCTGCACAGCCATACCAC
AGCTTCCGATGGCTGCCTGACGCCAGAAG

> pZK_E85mK_reverse read, MWG
AGCAGCCGAGGAGGCGGTGGTAGTGACGGGATTTGGCCCTTTTGGGGAACACACCGTGAAC
GCCAGTTGGATTGCAGTTCAGGAGCTAGAAAAGCTAGGCCTTGGCGACAGCGTGGACCTGC
ATGTGTACGAGATTCCGGTTGAGTACCAAACAGTCCAGAGACTCATCCCCGCCCTGTGGGAG
AAGCACAGTCCACAGCTGGTGGTGCATGTGGGGGTGTCAGGCATGGCGACCACAGTCACAC
TGAAGAAATGTGGACACAACAAGGGCTACAAGGGGCTGGACAACTGCCGCTTTTGCCCCGG
CTCCCAGTGCTGCGTGGAGGACGGGCCTGAAAGCATTGACTCCATCATCGACATGGATGCTG
TGTGCAAGCGAGTCACCACGTTGGGCCTGGATGTGTCGGTGACCATCTCGCAGGATGCCGGC

AGATATCTCTGCGACTTTACCTACTACACCTCTTTGTACCAGAGTCACGGTCGATCAGCCTTC
GTCCACGTGCCCCCACTGGGGAAGCCGTACAACGCGGACCAGCTGGGCAGGGCACTGAGAG
CCATCATTGAGGAGATGTTGGACCTCCTGGAGCAGTCAGAGGGCAAAATCAACTATTGCCAC
AAACACGGATCTCATCACCATCACCATCACTAAGCTTGGCTGTTTTGGCGGATGAGAGAAGA
TTTTCAGCCTGATACAGATTAAATCAGAACGCAGAAGCGGTCTGATAAAACAGAATTTGCCT
GGCGGCAGTAGCGCGGTGGTCCCACCTGACCCCATGCCGA
ACTCAGAAGTGAAACGCCGTAGCGCCGATGGTAGTGTGGGGTCTCCCCATGCGAGAGTAGG
GAACTGCCAGGCATCAAATAAAACGAAAGGCTCAGTCGAAAGACTGGGCCTTTTCGTTTTAT
CTGTTGTTTGTCGGTGAACGCTCTCCTGAGTAGGACAAATCCGCCGGGAGCGGGAT

>pZK_G35mD_forward read, MWG
GTTGATTTTGCCCTCTGACTGCTCCAGGAGGTCCAACATCTCCTCAATGATGGCTCTCAG
TGCCCTGCCCAGCTGGTCCGCGTTGTACGGCTTCCCCAGTGGGGGCACGTGGACGAAGGC
TGATCGACCGTGACTCTGGTACAAAGAGGTGTAGTAGGTAAAGTCGCAGAGATATCTGCC
GGCATCCTGCGAGATGGTCACCGACACATCCAGGCCCAACGTGGTGACTCGCTTGCACAC
AGCATCCATGTCGATGATGGAGTCAATGCTTTCAGGCCCGTCCTCCACGCAGCACTGGGA
GCCGGGGCAAAAGCGGCAGTTGTCCAGCCCCTTGTAGCCCTTGTTGTGTCCACATTTCTC
CAGTGTGACTGTGGTCGCCATGCCTGACACCCCCACATGCACCACCAGCTGTGGACTGTG
CTTCTCCCACAGGGCGGGGATGAGTCTCTGGACTGTTTGGTACTCAACCGGAATCTCGTA
CACATGCAGGTCCACGCTGTCGCCAAGGTCTAGCTTTTCTAGCTCCTGAACTGCAATCCA
ACTGGCGTTCACG

> pZK_G35mD_reverse read, MWG
GGAGCAGCCGAGGAAGGCGGTGGTAGTGACGGGATTTGGCCCTTTTGGGGAACACACCGT
GAACGCCAGTTGGATTGCAGTTCAGGAGCTAGAAAAGCTAGGCCTTGGCGACAGCGTGGA
CCTGCATGTGTACGAGATTCCGGTTGAGTACCAAACAGTCCAGAGACTCATCCCCGCCCT
GTGGGAGAAGCACAGTCCACAGCTGGTGGTGCATGTGGGGGTGTCAGGCATGGCGACCAC
AGTCACACTGGAGAAATGTGGACACAACAAGGGCTACAAGGGGCTGGACAACTGCCGCTT
TTGCCCCGGCTCCCAGTGCTGCGTGGAGGACGGGCCTGAAAGCATTGACTCCATCATCGA
CATGGATGCTGTGTGCAAGCGAGTCACCACGTTGGGCCTGGATGTGTCGGTGACCATCTC
GCAGGATGCCGGCAGATATCTCTGCGACTTTACCTACTACACCTCTTTGTACCAGAGTCA
CGGTCGATCAGCCTTCGTCCACGTGCCCCCACTGGGGAAGCCGTACAACGCGGACCAGCT
GGGCAGGGCACTGAGAGCCATCATTGAGGAGATGTTGGACCTCCTGGAGCAGTCAGAGGG
CAAAATCAACTATTGCCACAAACACGGATCTCATCACCATCACCATCACTAAGCTTGGCT
GTTTTTGGCGGATGAGAGAAGATTTTCAGCCTGATACAGATTAAATCAGAACGCAGAAGC
GGTCTGATAAAACAGAATTTGCC

>pZK_N90mD_forward read, MWG
TTAGTGATGGTGATGGTGATGAGATCCGTGTTTGTGGCAATAGTTGATTTTGCCCTCTGA
CTGCTCCAGGAGGTCCAACATCTCCTCAATGATGGCTCTCAGTGCCCTGCCCAGCTGGTC
CGCGTTGTACGGCTTCCCCAGTGGGGGCACGTGGACGAAGGCTGATCGACCGTGACTCTG
GTACAAAGAGGTGTAGTAGGTAAAGTCGCAGAGATATCTGCCGGCATCCTGCGAGATGGT
CACCGACACATCCAGGCCCAACGTGGTGACTCGCTTGCACACAGCATCCATGTCGATGAT
GGAGTCAATGCTTTCAGGCCCGTCCTCCACGCAGCACTGGGAGCCGGGGCAAAAGCGGCA
GTTGTCCAGCCCCTTGTAGCCCTTGTCGTGTCCACATTTCTCCAGTGTGACTGTGGTCGC
CATGCCTGACACCCCCACATGCACCACCAGCTGTGGACTGTGCTTCTCCCACAGGGCGGG
GATGAGTCTCTGGACTGTTTGGTACTCAACCGGAATCTCGTACACATGCAGGTCCACGCT
GTCGCCAAGGCCTAGCTTTTCTAGCTCCTGAACTGCAATCCAACTGGCGTTCACGGTGTG
TTCCCCAAAAGGGCCAAATCCCGTCACTACCACCGCCTTCCTCGGCTGCTCCATGGTTAA
TTTCTCCTCTTTAATGAATTCTGTTTCCTGTGTGAAATTGTTATCCGCTCACAATTCCAC
ACATTATACGAGCCGATGATTAATTGTCAACAGCTCATTTCAGAATATTTGCCAGAACCG
TTATGATGTCGGCGCAAAAAACATTATCCAGAACGGGAGTGCGCCTTGAGCGACA

> pZK_N90mD_reverse read, MWG
GGAGCAGCCGAGGAAGGCGGTGGTAGTGACGGGATTTGGCCCTTTTGGGGAACACACCGT
GAACGCCAGTTGGATTGCAGTTCAGGAGCTAGAAAAGCTAGGCCTTGGCGACAGCGTGGA
CCTGCATGTGTACGAGATTCCGGTTGAGTACCAAACAGTCCAGAGACTCATCCCCGCCCT
GTGGGAGAAGCACAGTCCACAGCTGGTGGTGCATGTGGGGGTGTCAGGCATGGCGACCAC
AGTCACACTGGAGAAATGTGGACACGACAAGGGCTACAAGGGGCTGGACAACTGCCGCTT
TTGCCCCGGCTCCCAGTGCTGCGTGGAGGACGGGCCTGAAAGCATTGACTCCATCATCGA

CATGGATGCTGTGTGCAAGCGAGTCACCACGTTGGGCCTGGATGTGTCGGTGACCATCTC
GCAGGATGCCGGCAGATATCTCTGCGACTTTACCTACTACACCTCTTTGTACCAGAGTCA
CGGTCGATCAGCCTTCGTCCACGTGCCCCCACTGGGGAAGCCGTACAACGCGGACCAGCT
GGGCAGGGCACTGAGAGCCATCATTGAGGAGATGTTGGACCTCCTGGAGCAGTCAGAGGG
CAAAATCAACTATTGCCACAAACACGGATCTCATCACCATCACCATCACTAAGCTTGGCT
GTTTTGGCGGATGAGAGAAGATTTTCAGCCTGATACAGATTAAATCAGAACGCAGAAGCG
GTCTGATAAAACAGAATTTGCCTGGCGGCAGTAGCGCGGTGGTCCCACCTGACCCCATGC
CGAACTCAGAAGTGAAACGCCGTAGCGCCGATGGTAGTGTGGGGTCTCCCCATGCGAGAG
TAGGGAACTGCCAGGCATCAAATAAAAACGAAAGGCTCAGTCGAAAGACTGGGCCTTTCG
TTTTATCTGTTGTTTGTCGGTGAACGCTCTCCTGAGTAGGACAAATCCGCCGGGAG

>pZK_M192mT_forward read, MWG
GCCAAGCTTAGTGATGGTGATGGTGATGAGATCCGTGTTTGTGGCAATAGTTGATTTTGC
CCTCTGACTGCTCCAGGAGGTCCAACGTCTCCTCAATGATGGCTCTCAGTGCCCTGCCCA
GCTGGTCCGCGTTGTACGGCTTCCCCAGTGGGGGCACGTGGACGAAGGCTGATCGACCGT
GACTCTGGTACAAAGAGGTGTAGTAGGTAAAGTCGCAGAGATATCTGCCGGCATCCTGCG
AGATGGTCACCGACACATCCAGGCCCAACGTGGTGACTCGCTTGCACACAGCATCCATGT
CGATGATGGAGTCAATGCTTTCAGGCCCGTCCTCCACGCAGCACTGGGAGCCGGGGCAAA
AGCGGCAGTTGTCCAGCCCCTTGTAGCCCTTGTTGTGTCCACATTTCTCCAGTGTGACTG
TGGTCGCCATGCCTGACACCCCCACATGCACCACCAGCTGTGGACTGTGCTTCTCCCACA
GGGCGGGGATGAGTCTCTGGACTGTTTGGTACTCAACCGGAATCTCGTACACATGCAGGT
CCACGCTGTCGCCAAGGCCTAGCTTTTCTAGCTCCTGAACTGCAATCCAACTGGCGTTCA
CGGTGTGTTCCCCAAAAGGGCCAAATCCCGTCACTACCACCGCCTTCCTCGGCTGCTCCA
TGGTTAATTTCTCCTCTTTAATGAATTCTGTTTCCTGTGTGAAATTGTTATCCGCTCACA
ATTCCACACATTATACGAGCCGATGATTAATTGTCAACAGCTCATTTCAGAATATTTGCC
AGAACCGTTATGATGTCGGCGCAAAAAACATTATCCAGAACGGGAGTGCGCCTTGAGCGA
CACGAATTATGCAGTGATTTACGACCTGCA

>pZK_M192mT_reverse read, MWG
TGGAGCAGCCGAGGAAGGCGGTGGTAGTGACGGGATTTGGCCCTTTTGGGGAACACACCG
TGAACGCCAGTTGGATTGCAGTTCAGGAGCTAGAAAAGCTAGGCCTTGGCGACAGCGTGG
ACCTGCATGTGTACGAGATTCCGGTTGAGTACCAAACAGTCCAGAGACTCATCCCCGCCC
TGTGGGAGAAGCACAGTCCACAGCTGGTGGTGCATGTGGGGGTGTCAGGCATGGCGACCA
CAGTCACACTGGAGAAATGTGGACACAACAAGGGCTACAAGGGGCTGGACAACTGCCGCT
TTTGCCCCGGCTCCCAGTGCTGCGTGGAGGACGGGCCTGAAAGCATTGACTCCATCATCG
ACATGGATGCTGTGTGCAAGCGAGTCACCACGTTGGGCCTGGATGTGTCGGTGACCATCT
CGCAGGATGCCGGCAGATATCTCTGCGACTTTACCTACTACACCTCTTTGTACCAGAGTC
ACGGTCGATCAGCCTTCGTCCACGTGCCCCCACTGGGGAAGCCGTACAACGCGGACCAGC
TGGGCAGGGCACTGAGAGCCATCATTGAGGAGACGTTGGACCTCCTGGAGCAGTCAGAGG
GCAAAATCAACTATTGCCACAAACACGGATCTCATCACCATCACCATCACTAAGCTTGGC
TGTTTTGGCGGATGAGAGAAGATTTTCAGCCTGATACAGATTAAATCAGAACGCAGAAGC
GGTCTGATAAAACAGAATTTGCCTGGCGGCAGTAGCGCGGTGGTCCCACCTGACCCCATG
CCGAACTCAGAAGTGAAACGCCGTAGCGCCGATGGTAGTGTGGGGTCTCCCCATGCGAGA
GTAGGGAACTGCCAGGCATCAAATAAAACGAAAGGCTCAGTCGAAAGACTGGGCCTTTCG
TTTTATCTGTTGTTTGTCGGTGAACGCTCTCCTG

>pZK_K94mR_forward read, MWG
CAAACAGCCAAGCTTAGTGATGGTGATGGTGATGAGATCCGTGTTTGTGGCAATAGTTGA
TTTTGCCCTCTGACTGCTCCAGGAGGTCCAACATCTCCTCAATGATGGCTCTCAGTGCCC
TGCCCAGCTGGTCCGCGTTGTACGGCTTCCCCAGTGGGGGCACGTGGACGAAGGCTGATC
GACCGTGACTCTGGTACAAAGAGGTGTAGTAGGTAAAGTCGCAGAGATATCTGCCGGCAT
CCTGCGAGATGGTCACCGACACATCCAGGCCCAACGTGGTGACTCGCTTGCACACAGCAT
CCATGTCGATGATGGAGTCAATGCTTTCAGGCCCGTCCTCCACGCAGCACTGGGAGCCGG
GGCAAAAGCGGCAGTTGTCCAGCCCCCTGTAGCCCTTGTTGTGTCCACATTTCTCCAGTG
TGACTGTGGTCGCCATGCCTGACACCCCCACATGCACCACCAGCTGTGGACTGTGCTTCT
CCCACAGGGCGGGGATGAGTCTCTGGACTGTTTGGTACTCAACCGGAATCTCGTACACAT
GCAGGTCCACGCTGTCGCCAAGGCCTAGCTTTTCTAGCTCCTGAACTGCAATCCAACTGG
CGTTCACGGTGTGTTCCCCAAAAGGGCCAAATCCCGTCACTACCACCGCCTTCCTCGGCT
GCTCCATGGTTAATTTCTCCTCTTTAATGAATTCTGTTTCCTGTGTGAAATTGTTATCCG
CTCACAATTCCACACATTATACGAGCCGATGATTAATTGTCAACAGCTCATTTCAGAATA

TTTGCCAGAACCGTTATGATGTCGGCGCAAAAAACATTATCCAGAACGGGAGTGCGCCTT
GAGCGACACGAATTATGCA

>pZK_ K94mR _reverse read, MWG
ATGGAGCAGCCGAGGAAGGCGGTGGTAGTGACGGGATTTGGCCCTTTTGGGGAACACACC
GTGAACGCCAGTTGGATTGCAGTTCAGGAGCTAGAAAAGCTAGGCCTTGGCGACAGCGTG
GACCTGCATGTGTACGAGATTCCGGTTGAGTACCAAACAGTCCAGAGACTCATCCCCGCC
CTGTGGGAGAAGCACAGTCCACAGCTGGTGGTGCATGTGGGGGTGTCAGGCATGGCGACC
ACAGTCACACTGGAGAAATGTGGACACAACAAGGGCTACAGGGGGCTGGACAACTGCCGC
TTTTGCCCCGGCTCCCAGTGCTGCGTGGAGGACGGGCCTGAAAGCATTGACTCCATCATC
GACATGGATGCTGTGTGCAAGCGAGTCACCACGTTGGGCCTGGATGTGTCGGTGACCATC
TCGCAGGATGCCGGCAGATATCTCTGCGACTTTACCTACTACACCTCTTTGTACCAGAGT
CACGGTCGATCAGCCTTCGTCCACGTGCCCCCACTGGGGAAGCCGTACAACGCGGACCAG
CTGGGCAGGGCACTGAGAGCCATCATTGAGGAGATGTTGGACCTCCTGGAGCAGTCAGAG
GGCAAAATCAACTATTGCCACAAACACGGATCTCATCACCATCACCATCACTAAGCTTGG
CTGTTTTGGCGGATGAGAGAAGATTTTCAGCCTGATACAGATTAAATCAGAACGCAGAAG
CGGTCTGATAAAACAGAATTTGCCTGGCGGCAGTAGCGCGGTGGTCCCACCTGACCCCAT
GCCGAACTCAGAAGTGAAACGCCGTAGCGCCGATGGTAGTGTGGGGTCTCCCCATGCGAG
AGTAGGGAACTGCCAGGCATCAAATAAAAACGAAAAG

>pZK_A165mV_forward read, MWG
CCAAGCTTAGTGATGGTGATGGTGATGAGATCCGTGTTTGTGGCAATAGTTGATTTTGCC
CTCTGACTGCTCCAGGAGGTCCAACATCTCCTCAATGATGGCTCTCAGTGCCCTGCCCAG
CTGGTCCGCGTTGTACGGCTTCCCCAGTGGGGGCACGTGGACGAAGACTGATCGACCGTG
ACTCTGGTACAAAGAGGTGTAGTAGGTAAAGTCGCAGAGATATCTGCCGGCATCCTGCGA
GATGGTCACCGACACATCCAGGCCCAACGTGGTGACTCGCTTGCACACAGCATCCATGTC
GATGATGGAGTCAATGCTTTCAGGCCCGTCCTCCACGCAGCACTGGGAGCCGGGGCAAAA
GCGGCAGTTGTCCAGCCCCTTGTAGCCCTTGTTGTGTCCACATTTCTCCAGTGTGACTGT
GGTCGCCATGCCTGACACCCCCACATGCACCACCAGCTGTGGACTGTGCTTCTCCCACAG
GGCGGGGATGAGTCTCTGGACTGTTTGGTACTCAACCGGAATCTCGTACACATGCAGGTC
CACGCTGTCGCCAAGGCCTAGCTTTTCTAGCTCCTGAACTGCAATCCAACTGGCGTTCAC
GGTGTGTTCCCCAAAAGGGCCAAATCCCGTCACTACCACCGCCTTCCTCGGCTGCTCCAT
GGTTAATTTCTCCTCTTTAATGAATTCTGTTTCCTGTGTGAAATTGTTATCCGCTCACAA
TTCCACACATTATACGAGCCGATGATTAATTGTCAACAGCTCATTTCAGAATATTTGCCA
GAACCGTTATGATGTCGGCGCAAAAAACATTATCCAGAACGGGAGTGCGCCTTGAGCGAC
ACGAATTATGCAGTGATTTACGACCTGCACAGCCATACCACAGCTTCC

>pZK_ A165mV _reverse read, MWG
GAGCAGCCGAGGAAGGCGGTGGTAGTGACGGGATTTGGCCCTTTTGGGGAACACACCGTG
AACGCCAGTTGGATTGCAGTTCAGGAGCTAGAAAAGCTAGGCCTTGGCGACAGCGTGGAC
CTGCATGTGTACGAGATTCCGGTTGAGTACCAAACAGTCCAGAGACTCATCCCCGCCCTG
TGGGAGAAGCACAGTCCACAGCTGGTGGTGCATGTGGGGGTGTCAGGCATGGCGACCACA
GTCACACTGGAGAAATGTGGACACAACAAGGGCTACAAGGGGCTGGACAACTGCCGCTTT
TGCCCCGGCTCCCAGTGCTGCGTGGAGGACGGGCCTGAAAGCATTGACTCCATCATCGAC
ATGGATGCTGTGTGCAAGCGAGTCACCACGTTGGGCCTGGATGTGTCGGTGACCATCTCG
CAGGATGCCGGCAGATATCTCTGCGACTTTACCTACTACACCTCTTTGTACCAGAGTCAC
GGTCGATCAGTCTTCGTCCACGTGCCCCCACTGGGGAAGCCGTACAACGCGGACCAGCTG
GGCAGGGCACTGAGAGCCATCATTGAGGAGATGTTGGACCTCCTGGAGCAGTCAGAGGGC
AAAATCAACTATTGCCACAAACACGGATCTCATCACCATCACCATCACTAAGCTTGGCTG
TTTTGGCGGATGAGAGAAGATTTTCAGCCTGATACAGATTAAATCAGAACGCAGAAGCGG
TCTGATAAAACAGAATTTGCCTGGCGGCAGT

>pZK_A27mT_forward read, MWG
GATGGTGATGGTGATGAGATCCGTGTTTGTGGCAATAGTTGATTTTGCCCTCTGACTGCT
CCAGGAGGTCCAACATCTCCTCAATGATGGCTCTCAGTGCCCTGCCCAGCTGGTCCGCGT
TGTACGGCTTCCCCAGTGGGGGCACGTGGACGAAGGCTGATCGACCGTGACTCTGGTACA
AAGAGGTGTAGTAGGTAAAGTCGCAGAGATATCTGCCGGCATCCTGCGAGATGGTCACCG
ACACATCCAGGCCCAACGTGGTGACTCGCTTGCACACAGCATCCATGTCGATGATGGAGT
CAATGCTTTCAGGCCCGTCCTCCACGCAGCACTGGGAGCCGGGGCAAAAGCGGCAGTTGT
CCAGCCCCTTGTAGCCCTTGTTGTGTCCACATTTCTCCAGTGTGACTGTGGTCGCCATGC
CTGACACCCCCACATGCACCACCAGCTGTGGACTGTGCTTCTCCCACAGGGCGGGGATGA

GTCTCTGGACTGTTTGGTACTCAACCGGAATCTCGTACACATGCAGGTCCACGCTGTCGC
CAAGGCCTAGCTTTTCTAGCTCCTGAACTGTAATCCAACTGGCGTTCACGGTGTGTTCCC
CAAAAGGGCCAAATCCCGTCACTACCACCGCCTTCCTCGGCTGCTCCATGGTTAATTTCT
CCTCTTTAATGAATTCTGTTTCCTGTGTGA AATTGTTATCCGCTCACAATTCCACACATT
ATACGAGCCGATGATTAATTGTCAACAGCTCATTTCAGAATATTTGCCAGAACCGTTATG
ATGTCGGCGCAAAAAACATTATCCAGAACGGGAGTGCGCCTTGAGCGACACGAATTATGC
AGTGATTTACGACCTGCACAGCCATACCACAGCTTCCGATGGCTGCCTGACGCCAGAAGC
ATTGGTGCACCGTGCAGTCGATAACCCGGATCGCT

>pZK_A27mT_reverse read. MWG
AGCCGAGGAAGGCGGTGGTAGTGACGGGATTTGGCCCTTTTGGGGAACACACCGATGAAC
GCCAGTTGGATTACAGTTCAGGAGCTAGAAAAGCTAGGCCTTGGCGACAGCGTGGACCTG
CATGTGTACGAGATTCCGGTTGAGTACCAAACAGTCCAGAGACTCATCCCCGCCCTGTGG
GAGAAGCACAGTCCACAGCTGGTGGTGCATGTGGGGGTGTCAGGCATGGCGACCACAGTC
ACACTGGAGAAATGTGGACACAACAAGGGCTACAAGGGGCTGGACAACTGCCGCTTTTGC
CCCGGCTCCCAGTGCTGCGTGGAGGACGGGCCTGAAAGCATTGACTCCATCATCGACATG
GATGCTGTGTGCAAGCGAGTCACCACGTTGGGCCTGGATGTGTCGGTGACCATCTCGCAG
GATGCCGGCAGATATCTCTGCGACTTTACCTACTACACCTCTTTGTACCAGAGTCACGGT
CGATCAGCCTTCGTCCACGTGCCCCCACTGGGGAAGCCGTACAACGCGGACCAGCTGGGC
AGGGCACTGAGAGCCATCATTGAGGAGATGTTGGACCTCCTGGAGCAGTCAGAGGGCAAA
ATCAACTATTGCCACAAACACGGATCTCATCACCATCACCATCACTAAGCTTGGCTGTTT
TGGCGGATGAGAGAAGATTTTCAGCCTGATACAGATTAAATCAGAACGCAGAAGCGGTCT
GATAAAACAGAATTTGCCTGGCGGCAGTAGCGCGGTGGTCCCACCTGACCCCATGCCGAA
CTCAGAAGTGAAACGCCGTAGCGCCGATGGTAGTGTGGGGTCTCCCCATGCGAGAGTAGG
GAACTGCCAGGCATCAAATAAAACGAAAGGCTCAGTCGAAAGACTGGGCCCTTTCGTTTT
ATCTGTTGTTTGT

>pZK_G77mD_forward read. MWG
TCCCCAGTGGGGGCACGTGGACGAAGGCTGATCGACCGTGACTCTGGTACAAAGAGGTGT
AGTAGGTAAAGTCGCAGAGATATCTGCCGGCATCCTGCGAGATGGTCACCGACACATCCA
GGCCCAACGTGGTGACTCGCTTGCACACAGCATCCATGTCGATGATGGAGTCAATGCTTT
CAGGCCCGTCCTCCACGCAGCACTGGGAGCCGGGGCAAAAGCGGCAGTTGTCCAGCCCCT
TGTAGCCCTTGTTGTGTCCACATTTCTCCAGTGTGACTGTGGTCGCCATGTCTGACACCC
CCACATGCACCACCAGCTGTGGACTGTGCTTCTCCCACAGGGCGGGGATGAGTCTCTGGA
CTGTTTGGTACTCAACCGGAATCTCGTACACATGCAGGTCCACGCT

>pZK_G77mD_reverse read. MWG
TGAGTACCAAACAGTCCAGAGACTCATCCCCGCCCTGTGGGAGAAGCACAGTCCACAGCT
GGTGGTGCATGTGGGGGTGTCAGGCATGGCGACCACAGTCACACTGGAGAAATGTGGACA
CAACAAGGGCTACAAGGGGCTGGACAACTGCCGCTTTTGCCCCGGCTCCCAGTGCTGCGT
GGAGGACGGGCCTGAAAGCATTGACTCCATCATCGACATGGATGCTGTGTGCAAGCGAGT
CACCACGTTGGGCCTGGATGTGTCGGTGACCATCTCGCAGGATGCCGGCAGATATCTCTG

>pZK_P67mR_forward read. MWG
GCCAAGCTTAGTGATGGTGATGGTGATGAGATCCGTGCTTTGTGGCAATAGTTGATTTTG
CCCTCTGACTGCTCCAGGAGGTCCAACATCTCCTCAATGATGGCTCTCAGTGCCCTGCCC
AGCTGGTCCGCGTTGTACGGGTTCCCCAGTGGGGGCACGTGGACGAAGGCTGATCGACCG
TGACTCTGGTACAAAGAGGTGTAGTAGGTAAAGTCGCAGAGATATCTGCCGGCATCCTGC
GAGATGGTCACCGACACATCCAGGCCCAACGTGGTGACTCGCTTGCACACAGCATCCATG
TCGATGATGGAGTCAATGCTTTCAGGCCCGTCCTCCACGCAGCACTGGGAGCCGGGGCAA
AAGCGGCAGTTGTCCAGCCCCTTGTAGCCCTTGTTGTGTCCACATTTCTCCAGTGTGACT
GTGGTCGCCATGCCTGACACCCCCACATGCACCACCAGCTGCGGACTGTGCTTCTCCCAC
AGGGCGGGGATGAGTCTCTGGACTGTTTGGTACTCAACCGGAATCTCGTACACATGCAGG
TCCACGCTGTCGCCAAGGCCTAGCTTTTCTAGCTCCTGAACTGCAATCCAACTGGCGTTC
ACGGTGTGTTCCCCAAAAGGGCCAAATCCCGTCACTACCACCGCCTTCCTCGGCTGCTCC
ATGGTTAATTTCTCCTCTTTAATGAATTCTGTTTCCTGTGTGAAATTGTTATCCGCTC

>pZK_P67mR_forward read. MWG
AGCCGAGGAAGGCGGTGGTAGTGACGGGATTTGGCCCTTTTGGGGAACACACCGTGAACG
CCAGTTGGATTGCAGTTCAGGAGCTAGAAAAGCTAGGCCTTGGCGACAGCGTGGACCTGC
ATGTGTACGAGATTCCGGTTGAGTACCAAACAGTCCAGAGACTCATCCCCGCCCTGTGGG
AGAAGCACAGTCCGCAGCTGGTGGTGCATGTGGGGGTGTCAGGCATGGCGACCACAGTCA

CACTGGAGAAATGTGGACACAACAAGGGCTACAAGGGGCTGGACAACTGCCGCTTTTGCC
CCGGCTCCCAGTGCTGCGTGGAGGACGGGCCTGAAAGCATTGACTCCATCATCGACATGG
ATGCTGTGTGCAAGCGAGTCACCACGTTGGGCCTGGATGTGTCGGTGACCATCTCGCAGG
ATGCCGGCAGATATCTCTGCGACTTTACCTACTACACCTCTTTGTACCAGAGTCACGGTC
GATCAGCCTTCGTCCACGTGCCCCCACTGGGGAAGCCGTACAACGCGGACCAGCTGGGCA
GGGCACTGAGAGCCATCATTGAGGAGATGTTGGACCTCCTGGAGCAGTCAGAGGGCAAAA
TCAACTATTGCCACAAACACGGATCTCATCACCATCACCATCACTAAGCTTGGCTGTTTT
GGCGGATGAGAGAAGATTTTCAGCCTGATACAGATTAAATCAGAACGCAGAAGCGGTCTG
ATAAAACAGAATTTGCCTGGCGGCAGTAGCGCGGTGGTCCCACCTGACCCCATGCCGAAC
TCAGAAGTGAAACGCCGTAGCGCCGATGGTAGTG

>pZK_N22mH_forward read, MWG
GATGGTGATGAGATCCGTGTTTGTGGCAATAGTTGATTTTGCCCTCTGACTGCTCCAGGA
GGTCCAACATCTCCTCAATGATGGCTCTCAGTGCCCTGCCCAGCTGGTCCGCGTTGTACG
GCTTCCCCAGTGGGGGCACGTGGACGAAGGCTGATCGACCGTGACTCTGGTACAAAGAGG
TGTAGTAGGTAAAGTCGCAGAGATATCTGCCGGCATCCTGCGAGATGGTCACCGACACAT
CCAGGCCCAACGTGGTGACTCGCTTGCACACAGCATCCATGTCGATGATGGAGTCAATGC
TTTCAGGCCCGTCCTCCACGCAGCACTGGGAGCCGGGGCAAAAGCGGCAGTTGTCCAGCC
CCTTGTAGCCCTTGTTGTGTCCACATTTCTCCAGTGTGACTGTGGTCGCCATGCCTGACA
CCCCCACATGCACCACCAGCTGTGGACTGTGCTTCTCCCACAGGGCGGGGATGAGTCTCT
GGACTGTTTGGTACTCAACCGGAATCTCGTACACATGCAGGTCCACGCTGTCGCCAAGGC
CTAGCTTTTCTAGCTCCTGAACTGCAATCCAACTGGCGTTCACGGTGTGTTCCCCAAAAG
GGCCAAATCCCGTCACTACCACCGCCTTCCTCGGCTGCTCCATGGTTAATTTCTCCTCTT
TAATGAATTCTGTTTCCTGTGTGAAATTGTTATCCGCTCACAATTCCACACATTATACGA
GCCGATGATTAATTGTCAACAGCTCATTTCAGAATATTTGCCAGAACCGTTATGAT

>pZK_N22mH_reverse read, MWG
CGAGGAAGGCGGTGGTAGTGACGGGATTTGGCCCTTTTGGGGAACACACCGTGCACGCCA
GTTGGATTGCAGTTCAGGAGCTAGAAAAGCTAGGCCTTGGCGACAGCGTGGACCTGCATG
TGTACGAGATTCCGGTTGAGTACCAAACAGTCCAGAGACTCATCCCCGCCCTGTGGGAGA
AGCACAGTCCACAGCTGGTGGTGCATGTGGGGGTGTCAGGCATGGCGACCACAGTCACAC
TGGAGAAATGTGGACACAACAAGGGCTACAAGGGGCTGGACAACTGCCGCTTTTGCCCCG
GCTCCCAGTGCTGCGTGGAGGACGGGCCTGAAAGCATTGACTCCATCATCGACATGGATG
CTGTGTGCAAGCGAGTCACCACGTTGGGCCTGGATGTGTCGGTGACCATCTCGCAGGATG
CCGGCAGATATCTCTGCGACTTTACCTACTACACCTCTTTGTACCAGAGTCACGGTCGAT
CAGCCTTCGTCCACGTGCCCCCACTGGGGAAGCCGTACAACGCGGACCAGCTGGGCAGGG
CACTGAGAGCCATCATTGAGGAGATGTTGGACCTCCTGGAGCAGTCAGAGGGCAAAATCA
ACTATTGCCACAAACACGGATCTCATCACCATCACCATCACTAAGCTTGGCTGTTTTGGC
GGATGAGAGAAGATTTTCAGCCTGATACAGATTAAATCAGAACGCAGAAGCGGTCTGATA
AAACAGAATTTGCCTGGCGGCAGTAGCGCGGTGGTCCCACCTGACCCCATGCCGAACTCA
GAAGTGAAACGC

>pZK_P48mR_forward read, MWG
TGGGGTCAGGTGGGACCACCGCGCTACTGCCGCCAGGCAAATTCTGTTTTATCAGACCGC
TTCTGCGTTCTGATTTAATCTGTATCAGGCTGAAAATCTTCTCTCATCCGCCAAAACAGC
CAAGCTTAGTGATGGTGATGGTGATGAGATCCGTGTTTGTGGCAATAGTTGATTTTGCCC
TCTGACTGCTCCAGGAGGTCCAACATCTCCTCAATGATGGCTCTCAGTGCCCTGCCCAGC
TGGTCCGCGTTGTACGGCTTCCCCAGTGGGGGCACGTGGACGAAGGCTGATCGACCGTGA
CTCTGGTACAAAGAGGTGTAGTAGGTAAAGTCGCAGAGATATCTGCCGGCATCCTGCGAG
ATGGTCACCGACACATCCAGGCCCAACGTGGTGACTCGCTTGCACACAGCATCCATGTCG
ATGATGGAGTCAATGCTTTCAGGCCCGTCCTCCACGCAGCACTGGGAGCCGGGGCAAAAG
CGGCAGTTGTCCAGCCCCTTGTAGCCCTTGTTGTGTCCACATTTCTCCAGTGTGACTGTG
GTCGCCATGCCTGACACCCCCACATGCACCACCAGCTGTGGACTGTGCTTCTCCCACAGG
GCGGGGATGAGTCTCTGGACTGTTTGGTACTCAACCCGAATCTCGTACACATGCAGGTCC
ACGCTGTCGCCAAGGCCTAGCTTTTCTAGCTCCTGAACTGCAATCCAACTGGCGTTCACG
GTGTGTTCCCCAAAAGGGTACAAATCCCGTCACTACCACCGCCTTCCTCGGCTGCTCC

>pZK_P48mR_reverse read, MWG
GGAGCAGCCGAGGAAGGCGGTGGTAGTGACGGGATTTGTACCCTTTTGGGGAACACACCG
TGAACGCCAGTTGGATTGCAGTTCAGGAGCTAGAAAAGCTAGGCCTTGGCGACAGCGTGG
ACCTGCATGTGTACGAGATTCGGGTTGAGTACCAAACAGTCCAGAGACTCATCCCCGCCC
TGTGGGAGAAGCACAGTCCACAGCTGGTGGTGCATGTGGGGGTGTCAGGCATGGCGACCA
CAGTCACACTGGAGAAATGTGGACACAACAAGGGCTACAAGGGGCTGGACAACTGCCGCT
TTTGCCCCGGCTCCCAGTGCTGCGTGGAGGACGGGCCTGAAAGCATTGACTCCATCATCG
ACATGGATGCTGTGTGCAAGCGAGTCACCACGTTGGGCCTGGATGTGTCGGTGACCATCT
CGCAGGATGCCGGCAGATATCTCTGCGACTTTACCTACTACACCTCTTTGTACCAGAGTC
ACGGTCGATCAGCCTTCGTCCACGTGCCCCCACTGGGGAAGCCGTACAACGCGGACCAGC
TGGGCAGGGCACTGAGAGCCATCATTGAGGAGATGTTGGACCTCCTGGAGCAGTCAGAGG
GCAAAATCAACTATTGCCACAAACACGGATCTCATCACCATCACCATCACTAAGCTTGGC
TGTTTTGGCGGATGAGAGAAGATTTTCAGCCTGATACAGATTAAATCAGAACGCAGAAGC
GGTCTGATAAAACAGAATTTGCCTGGCGGCAGTAGCGCGGTGGTCCCACCTGACCCCA

>pZK_P48mQ,D143mH_forward read, MWG
TACGGCTTCCCCAGTGGGGGCACGTGGACGAAGGCTGATCGACCGTGACTCTGGTACAAA
GAGGTGTAGTAGGTAAAGTCGCAGAGATATCTGCCGGCATGCTGCGAGATGGTCACCGAC
ACATCCAGGCCCAACGTGGTGACTCGCTTGCACACAGCATCCATGTCGATGATGGAGTCA
ATGCTTTCAGGCCCGTCCTCCACGCAGCACTGGGAGCCGGGGCAAAAGCGGCAGTTGTCC
AGCCCCTTGTAGCCCTTGTTGTGTCCACATTTCTCCAGTGTGACTGTGGTCGCCATGCCT
GACACCCCCACATGCACCACCAGCTGTGGACTGTGCTTCTCCCACAGGGCGGGGATGAGT
CTCTGGACTGTTTGGTACTCAACCTGAATCTCGTACACATGCAGGTCCACGCTGTCGCCA
AGGCCTAGCTTT

>pZK_P48mQ,D143mH_reverse read, MWG
AAAGCTAGGCCTTGGCGACAGCGTGGACCTGCATGTGTACGAGATTCAGGTTGAGTACCA
AACAGTCCAGAGACTCATCCCCGCCCTGTGGGAGAAGCACAGTCCACAGCTGGTGGTGCA
TGTGGGGGTGTCAGGCATGGCGACCACAGTCACACTGGAGAAATGTGGACACAACAAGGG
CTACAAGGGGCTGGACAACTGCCGCTTTTGCCCCGGCTCCCAGTGCTGCGTGGAGGACGG
GCCTGAAAGCATTGACTCCATCATCGACATGGATGCTGTGTGCAAGCGAGTCACCACGTT
GGGCCTGGATGTGTCGGTGACCATCTCGCAGCATGCCGGCAGATATCTCTGCGACTTTAC
CTACTACACCTCTTTGTACCAGAGTCACGGTCGATCAGCCTTCGTCCACGTGCCCCCACT
GGGGAAGCCGTA

>pZK_P4mS, S164mP_forward read, MWG
ATGGTGATGGTGATGAGATCCGTGTTTGTGGCAATAGTTGATTTTGCCCTCTGACTGCTC
CAGGAGGTCCAACATCTCCTCAATGATGGCTCTCAGTGCCCTGCCCAGCTGGTCCGCGTT
GTACGGCTTCCCCAGTGGGGGCACGTGGACGAAGGCTGGTCGACCGTGACTCTGGTACAA
AGAGGTGTAGTAGGTAAAGTCGCAGAGATATCTGCCGGCATCCTGCGAGATGGTCACCGA
CACATCCAGGCCCAACGTGGTGACTCGCTTGCACACGGCATCCATGTCGATGATGGAGTC
AATGCTTTCAGGCCCGTCCTCCACGCAGCACTGGGAGCCGGGGCAAAAGCGGCAGTTGTC
CAGCCCCTTGTAGCCCTTGTTGTGTCCACATTTCTCCAGTGTGACTGTGGTCGCCATGCC
TGACACCCCCACATGCACCACCAGCTGTGGACTGTGCTTCTCCCACAGGGCGGGGATGAG
TCTCTGGACTGTTTGGTACTCAACCGGAATCTCGTACACATGCAGGTCCACGCTGTCGCC
AAGGCCTAGCTTTTCTAGCTCCTGAACTGCAATCCAACTGGCGTTCACGGTGTGTTCCCC
AAAAGGGCCAAATCCCGTCACTACCACCGCCTTCCTCGACTGCTCCATAGTTAATTTCTC
CTCTTTAATGAATTCTGTTTCCTGTGTGAAATTGTTATCCGCTCACAATTCCACACATTA
TACGAGCCGATGATTAATTGTCAACAGCTCATTTCAGAATATTTGCCAGAACCGTTATGA
TGTCGGCGCAAAAAACATTATCCAGAACGGGAGTGCGCCTTGAGCGACACGAATTATGCA
GTGATTTACGACCTGCACAGCCATACCACAGCTTCCGATGGCTGCCTGACG

>pZK_P4mS, S164mP_reverse read, MWG
GAGCAGTCGAGGAAGGCGGTGGTAGTGACGGGATTTGGCCCTTTTGGGGAACACACCGCT
GAACGCCAGTTGGATTGCAGTTCAGGAGCTAGAAAAGCTAGGCCTTGGCGACAGCGTGGA
CCTGCATGTGTACGAGATTCCGGTTGAGTACCAAACAGTCCAGAGACTCATCCCCGCCCT
GTGGGAGAAGCACAGTCCACAGCTGGTGGTGCATGTGGGGGTGTCAGGCATGGCGACCAC
AGTCACACTGGAGAAATGTGGACACAACAAGGGCTACAAGGGGCTGGACAACTGCCGCTT
TTGCCCCGGCTCCCAGTGCTGCGTGGAGGACGGGCCTGAAAGCATTGACTCCATCATCGA
CATGGATGCCGTGTGCAAGCGAGTCACCACGTTGGGCCTGGATGTGTCGGTGACCATCTC

GCAGGATGCCGGCAGATATCTCTGCGACTTTACCTACTACACCTCTTTGTACCAGAGTCA
CGGTCGACCAGCCTTCGTCCACGTGCCCCCACTGGGGAAGCCGTACAACGCGGACCAGCT
GGGCAGGGCACTGAGAGCCATCATTGAGGAGATGTTGGACCTCCTGGAGCAGTCAGAGGG
CAAAATCAACTATTGCCACAAACACGGATCTCATCACCATCACCATCACTAAGCTTGGCT
GTTTTGGCGGATGAGAGAAGATTTTCAGCCTGATACAGATTAAATCAGAACGCAGAAGCG
GTCTGATAAAACAGAATTTGCCTGGCGGCAGTAGCGCGGTGGTCCCACCTGACCCCATGC
CGAACTCAGAAGTGAAACGCCGTAGCGCCGATGGTAGTGTGGGGTCTCCCCATGCGAGAG
TAGGGAACTGCCAGGCATCAAATAAAACGAAAGGCTCAGTCGAAAGACTGGGCCTTTCGT
TTTATCTGTTGTTTGTC

Appendix C

Activity & Kinetics

Quantification of PAP1 activity

One unit of activity is defined as the amount of enzyme, which releases 1 nanomole of AMC per minute at 37°C (unit = nmoles min^{-1})

Derivation

AMC released (X) is defined as fluorescent intensity (F_1) divided by the slope of the appropriate AMC standard curve (Appendix A)

$$\frac{F_1}{m} = X\ \mu M$$
$$= \mu moles\ L^{-1}$$

The reaction volume is $125x10^{-6}$ L and duration is 15 min

$$\text{AMC released} = \frac{X(125x10^{-6})}{15}\ \mu moles\ L^{-1}\ L\ min^{-1}$$

Reaction uses $25x10^{-6}$ L enzyme

$$\text{AMC released by enzyme} = \frac{X(125\ x10^{-6})}{15(25\ x10^{-6})}\ \mu moles\ min^{-1}\ L^{-1}$$
$$= \frac{X(125\ x10^{-6})(1000)}{15(25\ x10^{-6})(1000)}\ nmoles\ min^{-1}\ ml^{-1}$$
$$= \frac{X}{3}\ units\ ml^{-1}$$
$$= \frac{F_1}{3m}\ units\ ml^{-1}$$

From AMC standard curve, m = 42 042

$$\text{Enzyme activity} = \frac{F_1}{126\ 12}\ units\ ml^{-1}$$

Determination of K_m and V_{max}

The Michaelis constant (K_m) of an enzyme, for a particular substrate, is defined as the substrate concentration which gives rise to half the maximal enzyme velocity (V_{max}) This constant can be determined by measuring reaction velocity at various concentrations of substrate, giving rise to the Michaelis-Menten hyperbola curve In the case of PAP1, activity is determined by measuring fluorescent intensity (F_I) resulting at various concentrations of the substrate pGlu-AMC, as described in Section 2 18 6 1 A plot of F_I versus [pGlu-AMC] yields the Michaelis-Menten curve Once an enzyme-catalysed reaction follows normal Michaelis-Menten kinetics, data can be applied to a choice of kinetic models

Lineweaver-Burk Plot of $1/F_I$ versus 1/[pGlu-AMC] The intercept of the line on the x-axis gives $-1/K_m$ and the intercept of the line on the y-axis gives $1/V_{max}$

Eadie-Hofstee Plot of F_I versus F_I/[pGlu-AMC] The slope is $-K_m$ and the intercept on the y-axis represents V_{max}

Hanes-Woolf Plot of [pGlu-AMC]/F_I versus [pGlu-AMC] The intercept on the x-axis gives $-K_m$, and the slope is $1/V_{max}$

Determination of k_{cat}

The turnover constant (k_{cat}) of an enzyme can be determined if the V_{max} and total enzyme (E_t) are known

$$k_{cat} = \frac{V_{max}}{E_t} \qquad \frac{nmoles\ min^{-1}\ ml^{-1}}{nmoles\ ml^{-1}} = min^{-1}\ (s^{-1})$$

In the case of PAP1, V_{max} (nmoles min^{-1} ml^{-1} or units ml^{-1}) is determined experimentally as described above E_t (nmoles ml^{-1}) can be calculated from the molecular weight (g mole^{-1}) and amount of enzyme used (g ml^{-1}) The molecular weight of His-tagged recombinant human PAP1 (r*Hsa*PAP1$_{6H}$) is 24,105 g mole^{-1}, as deduced from the amino acid sequence

Determination of K_i

The inhibition constant (K_i), or dissociation constant for the enzyme-inhibitor complex, can be determined by measuring the apparent K_m (K_m^{app}) observed in the presence of an inhibitor at a specific concentration ([I]), as described in Section 2 18 6 2 and applied to the following equation

$$K_i = \frac{K_m[I]}{K_m^{app} - K_m}$$

Appendix D
Amino Acids

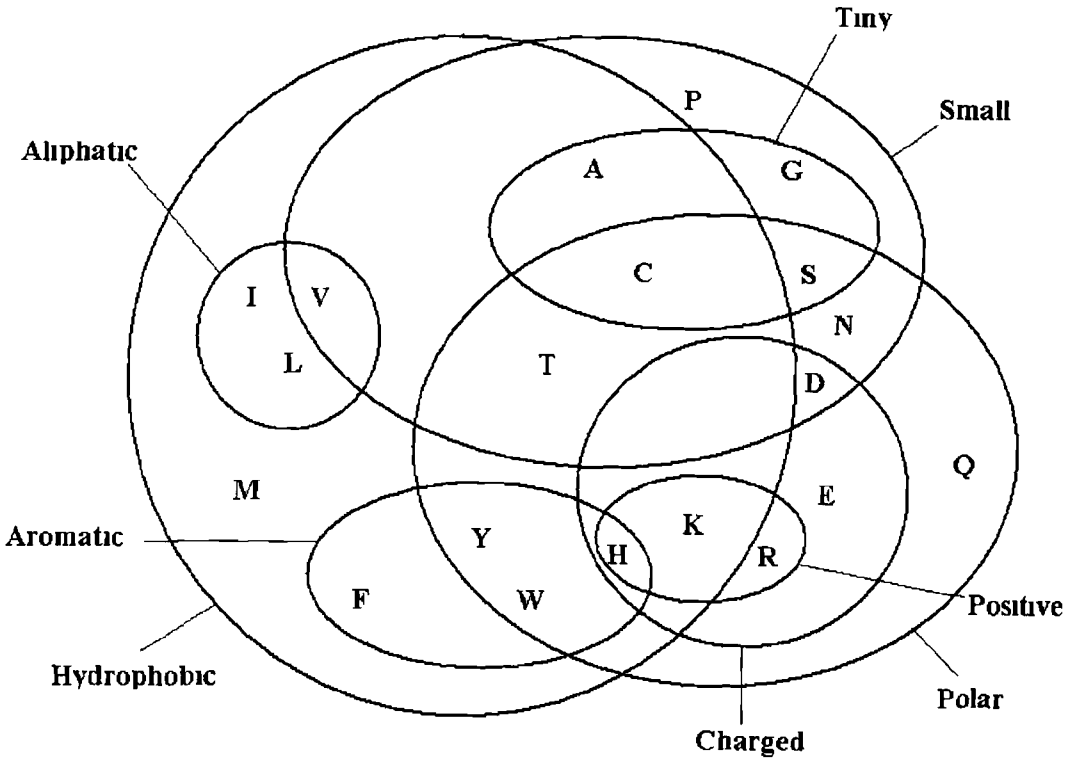

Amino acid properties
Venn diagram presenting properties of the 20 amino acids

Alanine	Ala	A	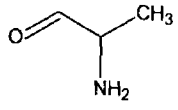
Arginine	Arg	R	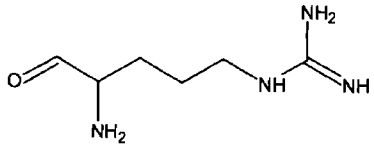
Asparagine	Asn	N	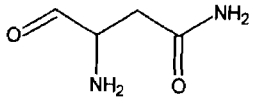
Aspartic acid	Asp	D	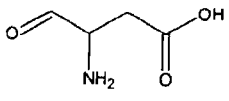
Cysteine	Cys	C	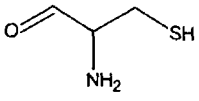
Glutamic acid	Glu	E	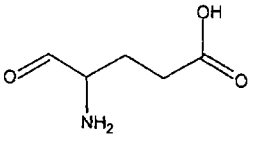
Glutamine	Gln	Q	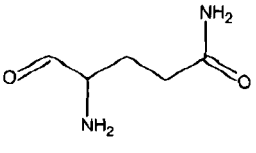

Glycine	Gly	G	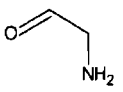
Histidine	His	H	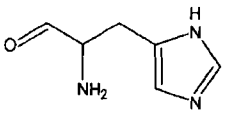
Isoleucine	Ile	I	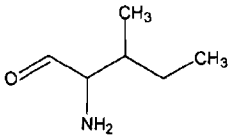
Leucine	Leu	L	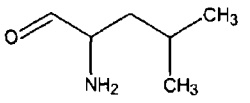
Lysine	Lys	K	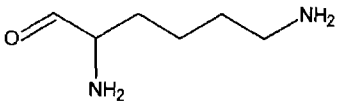
Methionine	Met	M	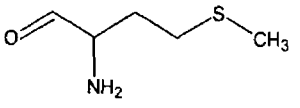
Phenylalanine	Phe	F	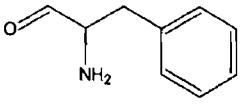
Proline	Pro	P	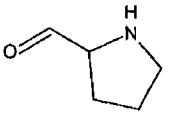
Serine	Ser	S	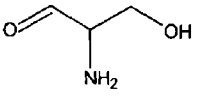
Threonine	Thr	T	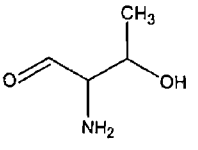
Tryptophan	Trp	W	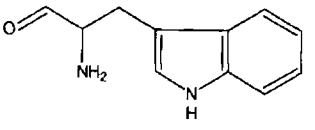
Tyrosine	Tyr	Y	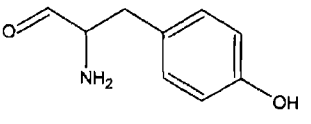
Valine	Val	V	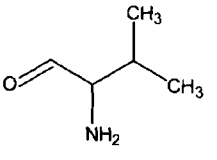

First Position	Second Position: U	Second Position: C	Second Position: A	Second Position: G	Third Position
U	**UUU** Phe	**UCU** Ser	**UAU** Tyr	**UGU** Cys	U
	UUC Phe	**UCC** Ser	**UAC** Tyr	**UGC** Cys	
	UUA Leu	**UCA** Ser	**UAA** Stop	**UGA** Stop	
	UUG Leu	**UCG** Ser	**UAG** Stop	**UGG** Trp	
C	**CUU** Leu	**CCU** Pro	**CAU** His	**CGU** Arg	C
	CUC Leu	**CCC** Pro	**CAC** His	**CGC** Arg	
	CUA Leu	**CCA** Pro	**CAA** Gln	**CGA** Arg	
	CUG Leu	**CCG** Pro	**CAG** Gln	**CGG** Arg	
A	**AUU** Ile	**ACU** Thr	**AAU** Asn	**AGU** Ser	A
	AUC Ile	**ACC** Thr	**AAC** Asn	**AGC** Ser	
	AUA Ile	**ACA** Thr	**AAA** Lys	**AGA** Arg	
	AUG Met	**ACG** Thr	**AAG** Lys	**AGG** Arg	
G	**GUU** Val	**GCU** Ala	**GAU** Asp	**GGU** Gly	G
	GUC Val	**GCC** Ala	**GAC** Asp	**GGC** Gly	
	GUA Val	**GCA** Ala	**GAA** Glu	**GGA** Gly	
	GUG Val	**GCG** Ala	**GAG** Glu	**GGG** Gly	

Genetic code

Amino acid codons applicable to both *H. sapiens* and *E. coli*.

Appendix E

Crystallisation Data Sheets

Data Collection For Human PAP1 Crystallisation Study.

Crystal Screen 1 was utilised (see Table 2.8) and a PAP1 protein concentration of 12 mg/ml was used.

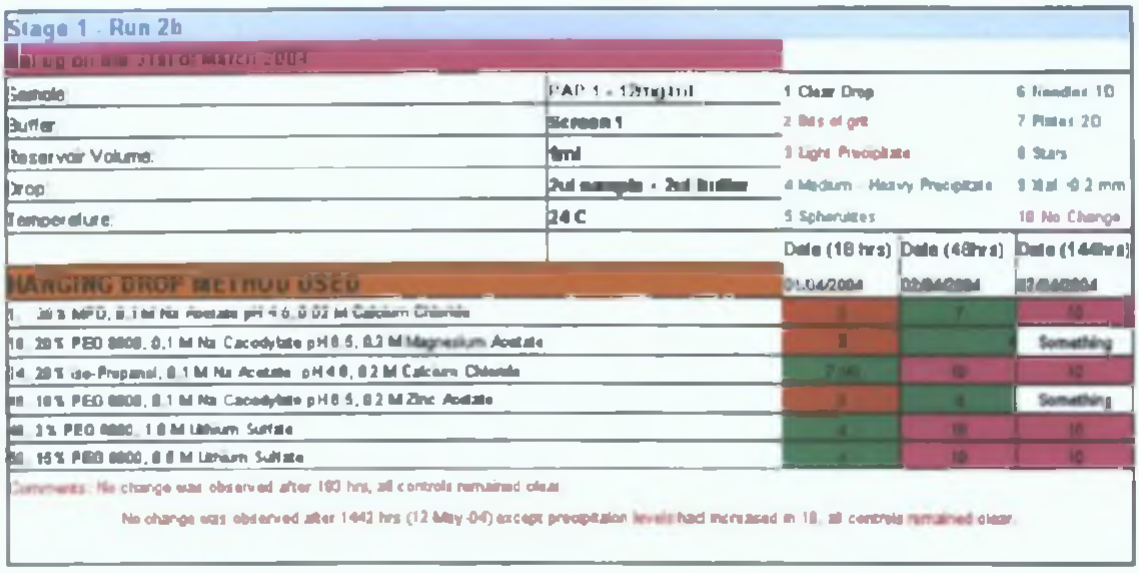

Stage 1 - Run 2b

Set up on the 31st of March 2004

Sample	PAP 1 - 12mg/ml	1 Clear Drop	6 Needles 1D
Buffer	Screen 1	2 Bits of grit	7 Plates 2D
Reservoir Volume:	1ml	3 Light Precipitate	8 Stars
Drop	2ul sample + 2ul buffer	4 Medium - Heavy Precipitate	9 Xtal >0.2 mm
Temperature:	24 C	5 Spherulites	10 No Change

HANGING DROP METHOD USED	Date (18 hrs) 01.04.2004	Date (48hrs) 03.04.2004	Date (144hrs) 07.04.2004
1. 30 % MPD, 0.1 M Na Acetate pH 4.6, 0.02 M Calcium Chloride	3	7	10
10. 20% PEG 8000, 0.1 M Na Cacodylate pH 6.5, 0.2 M Magnesium Acetate	3		Something
24. 20% iso-Propanol, 0.1 M Na Acetate pH 4.6, 0.2 M Calcium Chloride	7 (4)	10	10
86. 10% PEG 8000, 0.1 M Na Cacodylate pH 6.5, 0.2 M Zinc Acetate	3	4	Something
46. 2% PEG 6000, 1.0 M Lithium Sulfate	4	10	10
50. 15% PEG 6000, 0.6 M Lithium Sulfate	4	10	10

Comments: No change was observed after 180 hrs, all controls remained clear.

No change was observed after 1442 hrs (12 May-04) except precipitation levels had increased in 10, all controls remained clear.

Data Collection For Human PAP1 Crystallisation Study.

Crystal Screen 1 was utilised (see Table 2.8) and a PAP1 protein concentration of 1.5 mg/ml was used.

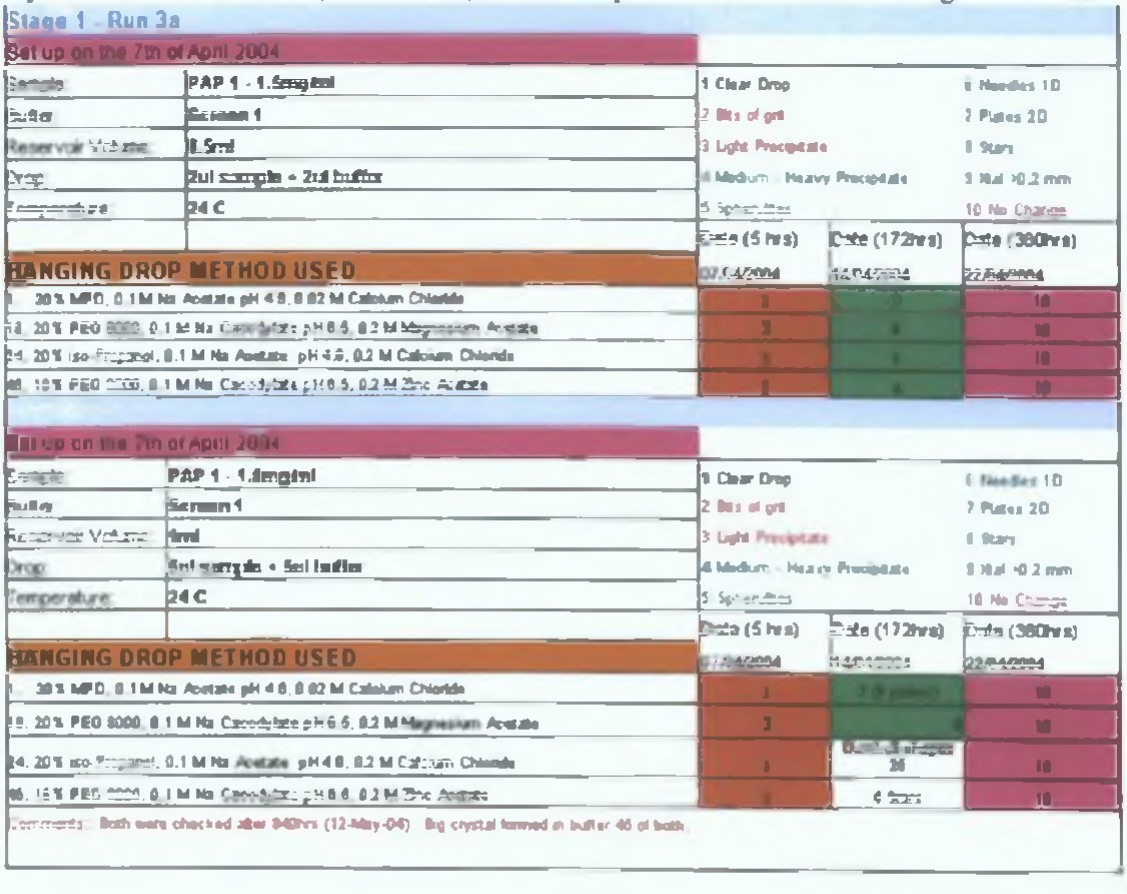

Stage 1 - Run 3a

Set up on the 7th of April 2004

Sample	PAP 1 - 1.5mg/ml	1 Clear Drop	6 Needles 1D
Buffer	Screen 1	2 Bits of grit	7 Plates 2D
Reservoir Volume:	1.5ml	3 Light Precipitate	8 Stars
Drop	2ul sample + 2ul buffer	4 Medium - Heavy Precipitate	9 Xtal >0.2 mm
Temperature:	24 C	5 Spherulites	10 No Change

HANGING DROP METHOD USED	Date (5 hrs) 07.04.2004	Date (172hrs) 14.04.2004	Date (360hrs) 22.04.2004
1. 30 % MPD, 0.1 M Na Acetate pH 4.6, 0.02 M Calcium Chloride	3	7	10
10. 20% PEG 8000, 0.1 M Na Cacodylate pH 6.5, 0.2 M Magnesium Acetate	3	4	10
24. 20% iso-Propanol, 0.1 M Na Acetate pH 4.6, 0.2 M Calcium Chloride	3	7	10
86. 10% PEG 8000, 0.1 M Na Cacodylate pH 6.5, 0.2 M Zinc Acetate	3	4	10

Set up on the 7th of April 2004

Sample	PAP 1 - 1.0mg/ml	1 Clear Drop	6 Needles 1D
Buffer	Screen 1	2 Bits of grit	7 Plates 2D
Reservoir Volume:	1ml	3 Light Precipitate	8 Stars
Drop	2ul sample + 2ul buffer	4 Medium - Heavy Precipitate	9 Xtal >0.2 mm
Temperature:	24 C	5 Spherulites	10 No Change

HANGING DROP METHOD USED	Date (5 hrs) 07.04.2004	Date (172hrs) 14.04.2004	Date (360hrs) 22.04.2004
1. 30 % MPD, 0.1 M Na Acetate pH 4.6, 0.02 M Calcium Chloride	3	7 (3 spikes)	10
10. 20% PEG 8000, 0.1 M Na Cacodylate pH 6.5, 0.2 M Magnesium Acetate	3	4	10
24. 20% iso-Propanol, 0.1 M Na Acetate pH 4.6, 0.2 M Calcium Chloride	3	5 (Small Crystals 2d)	10
86. 10% PEG 8000, 0.1 M Na Cacodylate pH 6.5, 0.2 M Zinc Acetate	3	4 Stars	10

Comments: Both were checked after 840hrs (12-May-04) Big crystal formed in buffer 46 of both.

Data Collection For Human PAP1 Crystallisation Study.

Crystal Screen 1 was utilised (see Table 2.8) and a PAP1 protein concentration of 3 and 8 mg/ml were used.

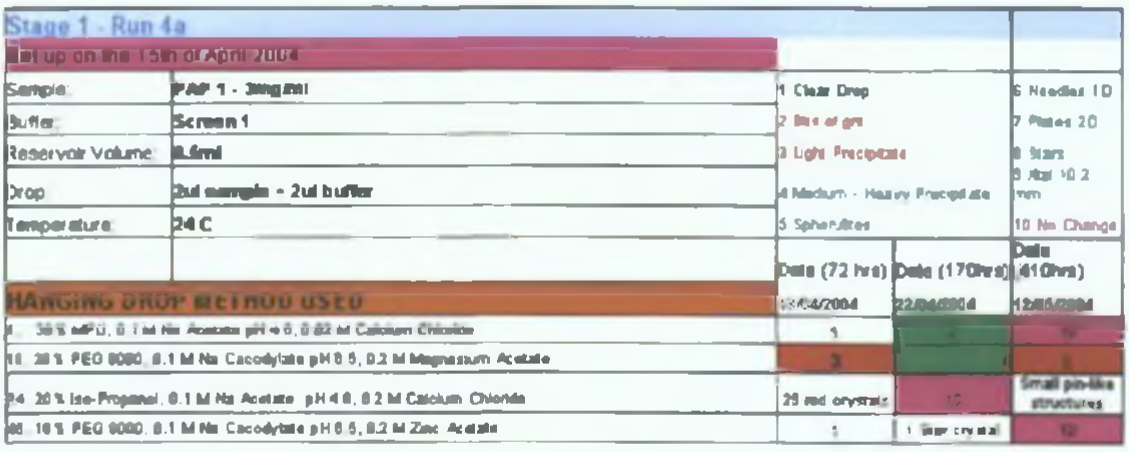

Stage 1 - Run 4a				
Set up on the 15th of April 2004				
Sample:	PAP 1 - 3mg/ml	1 Clear Drop		6 Needles 1D
Buffer:	Screen 1	2 Bits of grit		7 Plates 2D
Reservoir Volume:	0.5ml	3 Light Precipitate		8 Stars
Drop:	2ul sample + 2ul buffer	4 Medium - Heavy Precipitate		9 Xtal >0.2 mm
Temperature:	24 C	5 Spherulites		10 No Change
		Date (72 hrs)	Date (170hrs)	Date (410hrs)
HANGING DROP METHOD USED		13/04/2004	22/04/2004	12/05/2004
1 30% MPD, 0.1 M Na Acetate pH 4.6, 0.02 M Calcium Chloride		1	1	10
16 20% PEG 8000, 0.1 M Na Cacodylate pH 6.5, 0.2 M Magnesium Acetate		3	4	8
24 20% Iso-Propanol, 0.1 M Na Acetate pH 4.6, 0.2 M Calcium Chloride		25 red crystals	10	Small pin-like structures
48 10% PEG 8000, 0.1 M Na Cacodylate pH 6.5, 0.2 M Zinc Acetate		1	1 star crystal	10

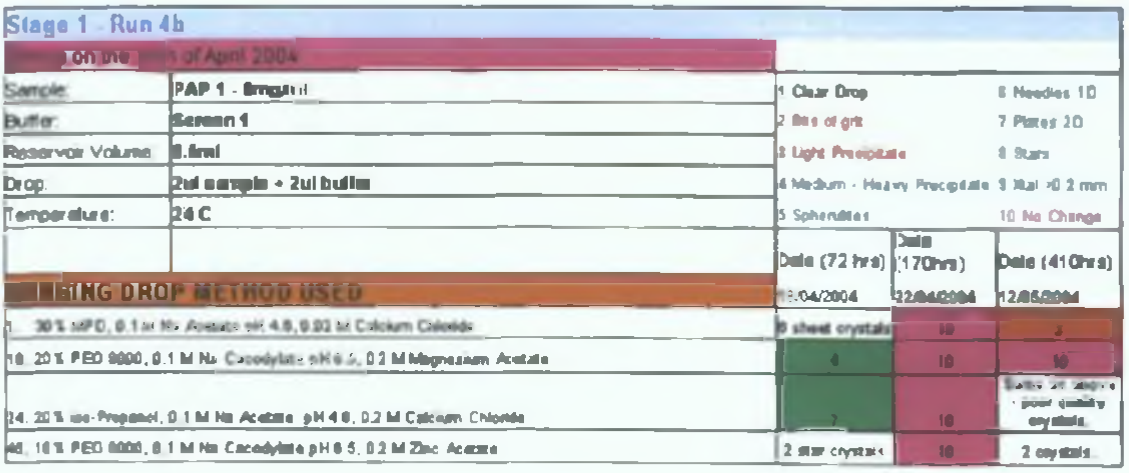

Stage 1 - Run 4b				
Set up on the 15th of April 2004				
Sample:	PAP 1 - 8mg/ml	1 Clear Drop		6 Needles 1D
Buffer:	Screen 1	2 Bits of grit		7 Plates 2D
Reservoir Volume:	0.5ml	3 Light Precipitate		8 Stars
Drop:	2ul sample + 2ul buffer	4 Medium - Heavy Precipitate		9 Xtal >0.2 mm
Temperature:	24 C	5 Spherulites		10 No Change
		Date (72 hrs)	Date (170hrs)	Date (410hrs)
HANGING DROP METHOD USED		13/04/2004	22/04/2004	12/05/2004
1 30% MPD, 0.1 M Na Acetate pH 4.6, 0.02 M Calcium Chloride		9 sheet crystals	10	2
16 20% PEG 8000, 0.1 M Na Cacodylate pH 6.5, 0.2 M Magnesium Acetate		4	10	10
24 20% Iso-Propanol, 0.1 M Na Acetate pH 4.6, 0.2 M Calcium Chloride		2	10	Some of drops - poor quality crystals
48 10% PEG 8000, 0.1 M Na Cacodylate pH 6.5, 0.2 M Zinc Acetate		2 star crystals	10	2 crystals

Data Collection For Human PAP1 Crystallisation Study.

Crystal Screen 2 was utilised (see Table 2.9) and a PAP1 protein concentration of 5 mg/ml was used.

Stage 1 - Run 5				
Set up on the 15th of April 2004				
Sample	PAP 1 Sugund	1 Clear Drop		6 Needles 1D
Buffer	Screen 2	2 Bits of grit		7 Plates 2D
Reservoir Volume	0.5ml	3 Light Precipitate		8 Xtal <0.2 mm
Drop	2ul reservoir + 2ul buffer	4 Medium-Heavy Precipitate		9 Xtal >0.2 mm
Temperature	24C	5 Stars		10 No Change
		Date (72 hrs) 18/04/2004	Date (17 days) 22/04/2004	Date (650) 12/05/2004
HANGING DROP METHOD				
1	10% PEG 8000, 2.0 M Sodium Chloride	3	10	10
2	0.5 M Sodium Chloride, 0.01 M CTAB, 0.01 M Magnesium Chloride	1	10	10
3	25% Ethylene Glycol	3	10	10
4	30% Dioxane	1	3	10
5	5% iso-Propanol, 2.0 M Ammonium Sulfate	3	3	10
6	1.0 M Imidazole pH 7.0	3	4	10
7	10% PEG 1000, 10% PEG 8000	1	10	Dried Up
8	10% Ethanol, 1.5 M Sodium Chloride	3	10	4
9	2.0 M Sodium Chloride, 0.1 M Na Acetate pH 4.6	3	10	10
10	30% MPD, 0.1 M Na Acetate pH 4.6, 0.2 M Sodium Chloride	3	3	10
11	1.0 M 1,6 Hexanediol, 0.1 M Na Acetate pH 4.6, 0.01 M Cobalt Chloride	3	10	Dried Up
12	30% PEG 400, 0.1 M Na Acetate pH 4.6, 0.1 M Cadmium Chloride	3	10	10
13	30% PEG MME 2000, 0.1 M Na Acetate pH 4.6, 0.2 M Ammonium Sulfate	3	10	4
14	2.0 M Ammonium Sulfate, 0.1 M Na Citrate pH 5.6, 0.2 M K/Na Tartrate	3	3	10
15	1.0 M Lithium Sulfate, 0.1 M Na Citrate pH 5.6, 0.5 M Ammonium Sulfate	3	3	4
16	2% Polyethyleneimine, 0.1 M Na Citrate pH 5.6, 0.5M Sodium Chloride	3	4	4
17	30% Iso-Propanol, 0.1 M Na Citrate pH 5.6	Buffer Dried Up	10	10
18	10% Jeffamine M-600, 0.1 M Na Citrate pH 5.6, 0.01 M Ferric Chloride	3	4	Dried Up
19	2.5 M 1,6 Hexanediol, 0.1 M Na Citrate pH 5.6	1	4	10
20	1.8 M Magnesium Sulfate, 0.1 M MES pH 6.5	3	4	Fungal Growth
21	2.0 M Sodium Chloride, 0.1 M MES pH 6.5, 0.2 M Na/K Phosphate	3	4	4
22	12% PEG 20,000, 0.1 M MES pH 6.5	3	4	10
23	10% Dioxane, 0.1 M MES pH 6.5, 1.0 M Ammonium Sulfate	3	4	Dried Up
24	30% Jeffamine M-600, 0.1 M MES pH 6.5, 0.05 M Cesium Chloride	1	3	Dispersed
25	1.0 M Ammonium Sulfate, 0.1 M MES pH 6.5, 0.01 M Cobalt Chloride	3	3	10
26	30% PEG MME 5000, 0.1 M MES pH 6.5, 0.2 M Ammonium Sulfate	3	4	Filamentous Growth
27	25% PEG MME 550, 0.1 M MES pH 6.5, 0.01 M Zinc Sulfate	2 Heavy precipitate	10	10 - Additional filamentous growth
28	1.0 M Sodium Citrate pH 6.5	3	3	10
29	30% MPD, 0.1 M Hepes pH 7.5, 0.5 M Ammonium Sulfate	1	10	10
30	10% PEG 8000, 0.1 M Hepes pH 7.5, 5% MPD	1	10	Bubble dispersed
31	20% Jeffamine M-600, 0.1 M Hepes pH 7.5	1	3	10
32	1.0 M Ammonium Sulfate, 0.1 M Hepes pH 7.5, 0.1 M Sodium Chloride	3	4	10
33	2.0 M Ammonium Formate, 0.1 M Hepes pH 7.5	3	4	10
34	1.0 M Sodium Acetate, 0.1 M Hepes pH 7.5, 0.05 M Cadmium Sulfate	3	4	10
35	70% MPD, 0.1 M Hepes pH 7.5	Blank	10	10
36	4.3 M Sodium Chloride, 0.1 M Hepes pH 7.5	3	4	4
37	10% PEG 8000, 0.1 M Hepes pH 7.5, 8% Ethylene Glycol	3	3	10
38	20% PEG 10,000, 0.1 M Hepes pH 7.5	3	10	Dried Up
39	3.4 M 1,6 Hexanediol, 0.1 M Tris pH 8.5, 0.2 M Magnesium Chloride	3	10	10
40	25% tert-Butanol, 0.1 M Tris pH 8.5	1	dried up	10
41	1.0 M Lithium Sulfate, 0.1 M Tris pH 8.5, 0.01 M Nickel (II) Chloride	1	3	4
42	12% Glycerol, 0.1 M Tris pH 8.5, 1.5 M Ammonium Sulfate	1	3	10
43	40% MPD, 0.1 M Tris pH 8.5, 0.2 M Ammonium Phosphate	3	dried up	10
44	20% Ethanol, 0.1 M Tris pH 8.5	1	10	Dried Up
45	20% PEG MME 2000, 0.1 M Tris pH 8.5, 0.01 M Nickel (II) Chloride	1	3	10
46	20% PEG MME 550, 0.1 M Bicine pH 9.0, 0.1 M Sodium Chloride	1	10	Filamentous Growth
47	2.0 M Magnesium Chloride, 0.1 M Bicine pH 9.0	1	3	4
48	10% PEG 20,000, 0.1 M Bicine pH 9.0, 2% Dioxane	1	10	Bubble dispersed

Data Collection For Human PAP1 Crystallisation Study.

Crystal Screen 2 was utilised (see Table 2.9) and a PAP1 protein concentration of 12 mg/ml was used.

Stage 1 - Run 2

Set up on the 31st of March 2004

Sample:	PAP 1 12mg/ml	1 Clear Drop		6 Needles 1D
Buffer:	Screen 2	2 Bits of grit		7 Plates 2D
Reservoir Volume:	0.5ml	3 Light Precipitate		8 Xtal >0.2 mm
Drop:	2ul sample + 2ul buffer	4 Medium-Heavy Precipitate		9 Xtal >0.2 mm
Temperature:	24C	5 Stars		10 No Change
		Date (16 hrs)	Date (48hrs)	Date (144hrs)
HANGING DROP METHOD		01/04/2004	02/04/2004	06/04/2004
1. 10% PEG 6000, 2.0 M Sodium Chloride		4	10	10
2. 0.5 M Sodium Chloride, 0.01 M CTAB, 0.01 M Magnesium Chloride		4	10	10
3. 25% Ethylene Glycol		3	10	10
4. 35% Dioxane		3	4	10
5. 5% Iso-Propanol, 2.0 M Ammonium Sulfate		3	4	10
6. 1.0 M Imidazole pH 7.0		4	10	10
7. 10% PEG 1000, 10% PEG 8000		1	10	10
8. 10% Ethanol, 1.5 M Sodium Chloride		4	10	10
9. 2.0 M Sodium Chloride, 0.1 M Na Acetate pH 4.0		4	10	10
10. 30% MPD, 0.1 M Na Acetate pH 4.6, 0.2 M Sodium Chloride		4	9	10
11. 1.0 M 1,6 Hexanediol, 0.1 M Na Acetate pH 4.6, 0.01 M Cobalt Chloride		4	10	10
12. 30% PEG 400, 0.1 M Na Acetate pH 4.6, 0.1 M Cadmium Chloride		3	4	10
13. 30% PEG MME 2000, 0.1 M Na Acetate pH 4.6, 0.2 M Ammonium Sulfate		4	10	10
14. 2.0 M Ammonium Sulfate, 0.1 M Na Citrate pH 5.6, 0.2 M K/Na Tartrate		4	10	10
15. 1.0 M Lithium Sulfate, 0.1 M Na Citrate pH 5.6, 0.5 M Ammonium Sulfate		3	10	10
16. 2% Polyethyleneimine, 0.1 M Na Citrate pH 5.6, 0.6 M Sodium Chloride		3	4	10
17. 35% tert-Butanol, 0.1 M Na Citrate pH 5.6		3	4	10
18. 10% Jeffamine M-600, 0.1 M Na Citrate pH 5.6, 0.01 M Ferric Chloride		Something	10	10
19. 2.5 M 1,6 Hexanediol, 0.1 M Na Citrate pH 5.6		3	10	10
20. 1.6 M Magnesium Sulfate, 0.1 M MES pH 6.5		Something	10	10
21. 2.0 M Sodium Chloride, 0.1 M MES pH 6.5, 0.2 M Na/K Phosphate		4	10	10
22. 12% PEG 20,000, 0.1 M MES pH 6.5		4	10	10
23. 10% Dioxane, 0.1 M MES pH 6.5, 1.6 M Ammonium Sulfate		4	10	10
24. 30% Jeffamine M-600, 0.1 M MES pH 6.5, 0.05 M Cesium Chloride		3	10	10
25. 1.8 M Ammonium Sulfate, 0.1 M MES pH 6.5, 0.01 M Cobalt Chloride		4	10	10
26. 30% PEG MME 5000, 0.1 M MES pH 6.5, 0.2 M Ammonium Sulfate		4	4	10
27. 25% PEG MME 550, 0.1 M MES pH 6.5, 0.01 M Zinc Sulfate		3	10	10
28. 1.6 M Sodium Citrate pH 6.5		3	4	10
29. 30% MPD, 0.1 M Hepes pH 7.5, 0.5 M Ammonium Sulfate		3	10	10
30. 10% PEG 6000, 0.1 M Hepes pH 7.5, 5% MPD		Something	10	10
31. 20% Jeffamine M-600, 0.1 M Hepes pH 7.5		3	4	10
32. 1.6 M Ammonium Sulfate, 0.1 M Hepes pH 7.5, 0.1 M Sodium Chloride		4	10	10
33. 2.0 M Ammonium Formate, 0.1 M Hepes pH 7.5		4	10	10
34. 1.0 M Sodium Acetate, 0.1 M Hepes pH 7.5, 0.05 M Cadmium Sulfate		4	10	10
35. 70% MPD, 0.1 M Hepes pH 7.5		Buffer Empty	10	10
36. 4.3 M Sodium Chloride, 0.1 M Hepes pH 7.5		4	10	10
37. 10% PEG 8000, 0.1 M Hepes pH 7.5, 8% Ethylene Glycol		3	10	10
38. 20% PEG 10,000, 0.1 M Hepes pH 7.5		3	Something	Nothing Here
39. 3.4 M 1,6 Hexanediol, 0.1 M Tris pH 8.5, 0.2 M Magnesium Chloride		3	4	10
40. 25% tert-Butanol, 0.1 M Tris pH 8.5		3	10	10
41. 1.0 M Lithium Sulfate, 0.1 M Tris pH 8.5, 0.01 M Nickel (II) Chloride		4	10	10
42. 12% Glycerol, 0.1 M Tris pH 8.5, 1.5 M Ammonium Sulfate		4	10	10
43. 50% MPD, 0.1 M Tris pH 8.5, 0.2 M Ammonium Phosphate		Something	10	Star Crystals
44. 20% Ethanol, 0.1 M Tris pH 8.5		3	Something	10
45. 20% PEG MME 2000, 0.1 M Tris pH 8.5, 0.01 M Nickel (II) Chloride		3	4	10
46. 20% PEG MME 550, 0.1 M Bicine pH 9.0, 0.1 M Sodium Chloride		1	3	10
47. 2.0 M Magnesium Chloride, 0.1 M Bicine pH 9.0		4	10	10
48. 10% PEG 20,000, 0.1 M Bicine pH 9.0, 2% Dioxane		1	10	10
49. Control		1	1	1

Comments: No change after 184 hrs and 672 hrs. All controls remained clear.
No change was observed after 1416hrs (12-May-04) except increase in precipitation in some buffers, all controls remained clear.

Data Collection For Human PAP1 Crystallisation Study.

Crystal Screen 2 was utilised (see Table 2.9) and a PAP1 protein concentration of 1.5 mg/ml was used.

Stage 1 - Run 3b

Set up on the 7th of April 2004

Sample:	PAP 1 1.5mg/ml
Buffer:	Screen 2
Reservoir Volume:	1.0ml
Drop:	2ul sample + 2ul buffer
Temperature:	24C

1 Clear Drop — 6 Needles 1D
2 Bits of grit — 7 Plates 2D
3 Light Precipitate — 8 Xtal <0.2 mm
4 Medium Heavy Precipitate — 9 Xtal >0.2 mm
5 Stars — 10 No Change

HANGING DROP METHOD

	Date (5 hrs) 01/04/2004	Date (172hrs) 08/04/2004	Date (840hrs) 12/05/2004
18. 10% Jeffamine M-600, 0.1 M Na Citrate pH 5.6, 0.01 M Ferric Chloride	2	4	2
39. 1.6 M Magnesium Sulfate, 0.1 M MES pH 6.5	1	4	10
28. 10% PEG 8000, 0.1 M Hepes pH 7.5, 5% MPD	2	2	1
40. 50% MPD, 0.1 M Tris pH 8.5, 0.2 M Ammonium Phosphate	2	4	1
44. 20% Ethanol, 0.1 M Tris pH 8.5	1	2	1

Data Collection For Human PAP1 Crystallisation Study.

Crystal Screen 2 was utilised (see Table 2.9) and a PAP1 protein concentration of 3 and 8 mg/ml were used.

Stage 1 - Run 4c

Set up on the 15th of April 2004

Sample	PAP 1 3mg/ml
Buffer	Screen 2
Reservoir Volume	1.0ml
Drop	2ul sample + 2ul buffer
Temperature	24C

1 Clear Drop — 6 Needles 1D
2 Bits of grit — 7 Plates 2D
3 Light Precipitate — 8 Xtal <0.2 mm
4 Medium-Heavy Precipitate — 9 Xtal >0.2 mm
5 Stars — 10 No Change

HANGING DROP METHOD

	Date (72 hrs) 18/04/2004	Date (170hrs) 22/04/2004	Date (410hrs) 12/05/2004
18. 10% Jeffamine M-600, 0.1 M Na Citrate pH 5.6, 0.01 M Ferric Chloride	1	2	10
39. 1.6 M Magnesium Sulfate, 0.1 M MES pH 6.5	2	4	Filamentous Growth
28. 10% PEG 8000, 0.1 M Hepes pH 7.5, 5% MPD	1	2	Dried Up
40. 50% MPD, 0.1 M Tris pH 8.5, 0.2 M Ammonium Phosphate	1	Dried up	Dried Up
44. 20% Ethanol, 0.1 M Tris pH 8.5	1	10	1

Stage 1 - Run 4d

Set up on the 15th of April 2004

Sample	PAP 1 8mg/ml
Buffer	Screen 2
Reservoir Volume	1.0ml
Drop	2ul sample + 2ul buffer
Temperature	24C

1 Clear Drop — 6 Needles 1D
2 Bits of grit — 7 Plates 2D
3 Light Precipitate — 8 Xtal <0.2 mm
4 Medium-Heavy Precipitate — 9 Xtal >0.2 mm
5 Stars — 10 No Change

HANGING DROP METHOD

	Date (5 hrs) 01/04/2004	Date (172hrs) 08/04/2004	Date (410hrs) 12/05/2004
18. 10% Jeffamine M-600, 0.1 M Na Citrate pH 5.6, 0.01 M Ferric Chloride	2	4	10
39. 1.6 M Magnesium Sulfate, 0.1 M MES pH 6.5	2	4	Filamentous growth
28. 10% PEG 8000, 0.1 M Hepes pH 7.5, 5% MPD	1	2	1
40. 50% MPD, 0.1 M Tris pH 8.5, 0.2 M Ammonium Phosphate	Buffer Dried Up	10	Dried Up
44. 20% Ethanol, 0.1 M Tris pH 8.5	1	10	Dried Up